THE ROLE OF MOLECULAR CHAPERONES IN YEAST CELL WALL INTEGRITY AND IDENTIFICATION OF CHAPERONE MODULATORS THAT INTERFERE WITH SIMIAN VIRUS 40 REPLICATION

by

Christine Marion Wright

B.S., Clemson University, 2001

Submitted to the Graduate Faculty of

Arts and Sciences in partial fulfillment

of the requirements for the degree of

Doctor of Philosophy

University of Pittsburgh

2007

UNIVERSITY OF PITTSBURGH

FACULTY OF ARTS AND SCIENCES

This dissertation was presented

by

Christine Marion Wright

It was defended on

April 20, 2007

and approved by

Karen Arndt, Ph.D., Associate Professor

Roger Hendrix, Ph.D., Professor

Saleem Khan, Ph.D., Professor

James Pipas, Ph.D., Professor

Dissertation Advisor: Jeffrey Brodsky, Ph.D., Professor

THE ROLE OF MOLECULAR CHAPERONES IN YEAST CELL WALL INTEGRITY AND IDENTIFICATION OF CHAPERONE MODULATORS THAT INTERFERE WITH SIMIAN VIRUS 40 REPLICATION

Christine Marion Wright, Ph.D.

University of Pittsburgh, 2007

Hsp70 molecular chaperones play critical roles in the pathogenesis of many human diseases, including cancer and viral replication. Hsp70s bind polypeptides and couple ATP hydrolysis to alter substrate conformation and function. However, ATP hydrolysis by Hsp70 is weak, but can be stimulated by J domain-protein chaperones. To identify new targets of chaperone action, I performed a multi-copy suppressor screen for genes that improved the slow growth defect of yeast lacking *YDJ1* but expressing a defective *YDJ1* chimera. Among the genes identified were *MID2*, which regulates cell wall integrity, and *PKC1*, which encodes protein kinase C, which is also linked to cell wall biogenesis. Consistent with these data, I found that *ydj1Δ* yeast and yeast with temperature sensitive mutations in Hsp90 exhibit phenotypes consistent with cell wall defects but these phenotypes were improved by Mid2p or Pkc1p over-expression. Mid2p over-expression thickened the *ydj1Δ* cell wall, which is likely the basis for suppression of the *ydj1Δ* growth defect. These data provide the first link between cytoplasmic chaperones and cell wall integrity, and suggest that chaperones orchestrate the biogenesis of this structure.

Another J domain-protein is the Large Tumor Antigen (TAg) in the polyomavirus Simian Virus 40 (SV40). TAg is required for viral replication and cellular transformation, and binds Hsp70. Because of their roles in cancer and SV40 function, small molecule modulators that

inhibit Hsp70 or J-protein activity might represent novel anti-cancer and/or anti-viral agents. To identify such agents, I screened a bank of small molecules and identified a compound, MAL3-101, that had no effect on endogenous Hsp70 ATPase activity, but inhibited TAg stimulation of Hsp70 ATPase activity and reduced breast cancer cell proliferation. Forty-two derivatives of MAL3-101 were then synthesized and twelve compounds inhibited breast cancer cell proliferation at lower concentrations than MAL3-101. Reduction of cell proliferation correlated with reduced TAg stimulation of Hsp70 *in vitro*. Intriguingly, one compound, MAL2-11B, also inhibited the ATPase activity of TAg. This compound inhibited viral replication almost five-fold and SV40 DNA replication *in vitro*. These data show that J-protein inhibitors may be viable treatments for breast cancer and polyomavirus infection.

TABLE OF CONTENTS

PREFACE ..... **XVI**

1.0 INTRODUCTION **1**

1.1 CLASSES OF MOLECULAR CHAPERONES **2**

1.2 STRUCTURE AND FUNCTION OF SELECT CYTOSOLIC CHAPERONES AND COCHAPERONES **4**

1.2.1 Hsp70/Hsc70 ..... **4**

1.2.1.1 Structure of Hsp70 ..... **4**

1.2.1.2 Mechanism of action **9**

1.2.2 Hsp40 ..... **13**

1.2.2.1 Structure and types of Hsp40s **13**

1.2.2.2 Mechanism of action **16**

1.2.2.3 Hsp70/Hsp40 specificity **20**

1.2.3 Nucleotide exchange factors (NEFs) **21**

1.2.3.1 GrpE **22**

1.2.3.2 BAG-1 ..... **22**

1.2.3.3 HspBP1 ..... **25**

1.2.3.4 Sse1p **28**

1.2.4 Hsp90/Hsc90 ..... **29**

1.2.4.1 Structure of Hsp90 30

1.2.4.2 Mechanism of action 30

1.3 THE FUNCTIONS OF SELECT CHAPERONES IN *SACCHAROMYCES CEREVISIAE* 36

1.3.1 Protein folding and refolding 37

1.3.2 Protein translocation across membranes 38

1.3.3 Activation of receptors/kinases 38

1.3.4 Multiprotein complex rearrangement 39

1.4 CHAPERONES AND DISEASE 40

1.4.1 Aggregation diseases 40

1.4.2 Cancer 41

1.4.3 Small molecule modulators of molecular chaperones 42

1.5 VIRUSES AND CHAPERONES 44

1.5.1 General characteristics of polyomaviruses 45

1.5.1.1 BK Virus (BKV) 48

1.5.1.2 JC Virus (JCV) 48

1.5.1.3 KI Virus (KIPyV) and WU virus (WUV) 49

1.5.1.4 Simian Virus 40 (SV40) 50

1.5.2 Functional domains of SV40 Large Tumor Antigen (TAg) 50

1.5.2.1 The TAg J domain 51

1.5.2.2 The N-terminal flexible linker domain 54

1.5.2.3 Origin binding domain 58

1.5.2.4 Zinc binding domain 59

1.5.2.5 ATPase and p53 binding domain 59

1.5.2.6 Linker domain and host range domain 60

1.5.3 SV40 replication 61

1.5.4 Screen for novel TAg J domain mutants 62

1.6 DISSERTATION OVERVIEW 65

2.0 THE HSP40 MOLECULAR CHAPERONE YDJ1P, ALONG WITH THE PROTEIN KINASE C PATHWAY, AFFECTS CELL-WALL INTEGRITY IN THE YEAST SACCHAROMYCES CEREVISIAE 67

2.1 INTRODUCTION 67

2.2 MATERIALS AND METHODS 73

2.2.1 Yeast strains and methods 73

2.2.2 Molecular techniques 75

2.2.3 Low-copy suppressor screen in *ydj1-151* 83

2.2.4 High-copy suppressor screen in *ydj1Δ* 83

2.2.5 Biochemical and immunological methods 86

2.2.6 Lyticase digestion assays 87

2.2.7 Immunoprecipitations 88

2.2.8 Subcellular fractionation 88

2.2.9 Immunofluorescence 89

2.2.10 Electron microscopy 89

2.3 RESULTS 90

2.3.1 Identification of the known *ydj1-151* multi-copy suppressor, *SSE1* 90

2.3.2 Identification of suppressors of *T(K53R)-YDJ1* and *ydj1Δ* yeast 93

2.3.3 *PKC1* and constitutively activated components of the PKC pathway improve the *ydj1Δ* slow-growth phenotype 102

2.3.4 *MID2* and *PKC1* partially suppress the temperature sensitive phenotype of *hsp82* mutant strains 110

2.3.5 The *ydj1Δ* and *hsp82* temperature sensitive strains show phenotypes consistent with cell wall defects 124

2.3.6 Mid2p is not dramatically mislocalized or aggregated in *ydj1Δ* yeast . 129

2.3.7 *MID2-HA* over-expression thickens the cell wall of *ydj1Δ* yeast 139

2.3.8 Directed screening does not identify "factor X" 144

2.3.9 HopI1 contains a *bona fide* J domain 145

3.0 IDENTIFICATION OF HSP70 MODULATORS THAT INHIBIT BREAST CANCER CELL PROLIFERATION 153

3.1 INTRODUCTION 153

3.2 MATERIALS AND METHODS 154

3.2.1 Materials 154

3.2.2 Single turnover ATPase assay 155

3.2.3 ATPase assay 156

3.2.4 Assays for interactions between Hlj1p and Ssa1p 157

3.2.5 Cell proliferation assays 158

3.3 RESULTS 158

3.3.1 The identification of Hsp70/J-domain modulators 158

3.3.2 Characterization of MAL3-101 166

3.3.3 Identification of a putative, minimal pharmocophore 171

3.3.4 MAL3-101 inhibits breast cancer cell proliferation 178

3.3.5 Some MAL3-101 derivatives inhibit breast cancer cell proliferation .. 180

3.3.6 Novel Hsp70 modulators inhibit mammalian Hsp70 ATP hydrolysis . 185

4.0 A NOVEL SMALL MOLECULE INHIBITS SV40 PRODUCTION BY PREVENTING VIRAL DNA SYNTHESIS 191

4.1 INTRODUCTION 191

4.2 MATERIALS AND METHODS 194

4.2.1 Reagents 194

4.2.2 Single turnover ATPase assay and ATPase assay 194

4.2.3 Viral plaque assay 195

4.2.4 *In vitro* DNA replication assays 195

4.3 RESULTS 198

4.3.1 Modulators of TAg J domain stimulation of Hsp70 differentially affect the activities of other molecular chaperones 198

4.3.2 MAL2-11B drastically inhibits the AAA+ ATPases SV40 TAg and MCM2-7 203

4.3.3 MAL2-11B inhibits SV40 replication 209

4.3.4 MAL-11B inhibits SV40 DNA replication *in vitro* 213

5.0 DISCUSSION 222

5.1 A MULTI-COPY YEAST SUPPRESSOR SCREEN IDENTIFIES A ROLE FOR MOLECULAR CHAPERONES IN THE YEAST CELL WALL 223

5.2 MAL3-101 AND RELATED COMPOUNDS INHIBIT BREAST CANCER CELL PROLIFERATION 232

5.3 MAL2-11B INHIBITS SV40 REPLICATION AND SV40 DNA SYNTHESIS..... 240

BIBLIOGRAPHY 247

LIST OF TABLES

Table 1: Select examples of specific chaperone families 5

Table 2: Yeast strains utilized during this study 74

Table 3: Plasmids used in this study 76

Table 4: Primers used in this study 82

Table 5: Initial screening conditions tested 91

Table 6: Summary of the results obtained from the screen. 94

Table 7: The effect of the DSG and R/1 analogs on Ssa1p ATPase activity 162

Table 8: The effect of the DSG and R/1 analogs on TAg stimulation of Ssa1p ATP hydrolysis 163

Table 9: The effects of the compounds with a "putative minimal pharmocophore" on Ssa1p stimulated ATP hydrolysis and TAg stimulation of Ssa1p ATP hydrolysis. 177

Table 10: The effect of the compounds on SK-BR-3 cell proliferation. 179

Table 11: MAL3-101 inhibits cell proliferation. 179

Table 12: Select MAL3-101 derivatives inhibit SK-BR-3 cell proliferation. 181

Table 13: The SW compounds have little effect on DnaK ATP hydrolysis. 189

Table 14: The effect of MAL2-11B, MAL3-51, and MAL3-101 on various ATPases..... 200

LIST OF FIGURES

Figure 1: The crystal structures of the Hsp70 ATPase, substrate binding, and lid domains. 7

Figure 2: The Hsp70 ATPase cycle. 10

Figure 3: Key features of the Hsp40 class of molecular chaperones. 14

Figure 4: Space-filling and ribbon representations of amino acids 110-337 of the Ydj1p substrate binding domain. 18

Figure 5: Crystal structures of the three classes of nucleotide exchange factors..... 23

Figure 6: A representation of the interaction of Hsp70 with either HspBP1 or BAG-1..... 26

Figure 7: The crystal structure of a dimer of Hsp90, bound to AMPPNP. 31

Figure 8: Hsp90 folding cycle for the Progesterone Receptor (PR). 34

Figure 9: Genome map for the SV40 polyomavirus. 46

Figure 10: Structural representation of the TAg monomer. 52

Figure 11: The chaperone model for E2F release from Rb. 56

Figure 12: A yeast screen uncovers novel TAg J domain mutations. 63

Figure 13: The canonical PKC signaling pathway. 69

Figure 14: *HSP82* A493T can support cell growth as the only Hsp90 in the yeast cell. 79

Figure 15: T-Ydj1p and T(K53R)-Ydj1p are expressed in the both the *ydj1-151* and *ydj1Δ* strains. 84

Figure 16: *pCMS154* in multiple copies moderately rescues the *T(K53R)-YDJ1* growth defect at 35°. 95

Figure 17: *SSA1* improves the growth of strains possessing the *T(K53R)-YDJ1* thermosensitive phenotype. 98

Figure 18: *MID2* suppresses the thermosensitive growth defect of *ydj1Δ* yeast. 100

Figure 19: *MID2* and *PKC1* improve the growth of the *ydj1Δ* yeast expressing T(H42R)-Ydj1p. 103

Figure 20: Introduction of a high-copy *PKC1* containing vector and over-expression of constitutively active components in the PKC pathway improve the slow growth phenotype of the *ydj1Δ* strain. 105

Figure 21: Over-expression of *BCK1* and *MPK1* do not restore growth of the *ydj1Δ* strain..... 108

Figure 22: Over-expression of SVG and HOG pathway members do not improve the growth of *ydj1Δ* yeast. 111

Figure 23: Multi-copy *MID2* and *PKC1*-containing plasmids do not improve the temperature-sensitive growth defects of *ssa1-45* temperature sensitive mutants. 113

Figure 24: Over-expression of *MID2* and *PKC1* suppress the growth defect of the *hsp82* G170D and *hsp82* G313N strains. 115

Figure 25: Over-expression of *MID2* or *PKC1* does not restore growth in the *sti1Δsse1Δ* yeast strain..... 118

Figure 26: Introduction of a high-copy *HSP82* containing vector does not improve the temperature sensitive phenotype of *T(K53R)-YDJ1* or the slow growth phenotype of the *ydj1Δ* strain 120

Figure 27: Hsp82p and Ssa1p are upregulated in the *ydj1Δ* strain. 122

Figure 28: The cell wall in the *ydj1Δ* yeast strain is not preferentially sensitive to lyticase. 125

Figure 29: The *ydj1Δ* and *hsp82* temperature sensitive mutant strains have phenotypes consistent with defects in cell wall synthesis. 127

Figure 30: Mid2p or Pkc1p over-expression, coupled with growth on 1 M sorbitol, restores growth of the *ydj1Δ* strain to 37°. 130

Figure 31: Over-expression of *MID2* and *PKC1* can partially restore growth of the *ydj1Δ* strain in the presence of calcofluor white (CW). 132

Figure 32: Only a modest increase in Mid2p aggregation is evident in *ydj1Δ* yeast. 134

Figure 33: Mid2p does not co-immunoprecipitate with molecular chaperones. 137

Figure 34: The actin cytoskeleton is not perturbed in the *ydj1Δ* yeast strain. 140

Figure 35: Over-expression of Mid2p thickens the cell wall of *ydj1Δ* yeast. 142

Figure 36: HspBP1, BAG-1S and Cul7 do not improve growth in the *ydj1Δ* strain expressing T(K53R)-Ydj1p 146

Figure 37: HspBP1, BAG-1S and Cul7 do not improve growth in the *ydj1Δ* strain. 148

Figure 38: The introduction of an *I-YDJ1*-containing vector improves the growth of *ydj1Δ* yeast at 30°. 151

Figure 39: Structure of select chaperone modulators, including parental compounds 15-Deoxyspergualin (DSG) and NSC 630668-R/1 (R/1). 160

Figure 40: MAL3-38 and MAL3-90 stimulate the ATPase activity of Ssa1p, but inhibit J-protein stimulation of Ssa1p ATP hydrolysis in single turnover assays. 164

Figure 41: MAL3-39 and MAL3-101 selectively inhibit J-protein stimulation of Ssa1p. 167

Figure 42: Concentration dependence of MAL3-101 and TAg in the single turnover assays. . 169

Figure 43: MAL3-101 does not interfere with Ssa1p binding to GST-Hlj1p-His. 172

Figure 44: Structures of compounds that were proposed to contain the putative minimal pharmocophore. 174

Figure 45: Two classes of compounds identified with a minimal pharmocophore. 176

Figure 46: Representative members from each of the classes of MAL3-101 derivatives. 183

Figure 47: SW02 and SW03 inhibit Hsp70 ATP hydrolysis, but do not alter the total J-protein stimulated ATP hydrolysis. 186

Figure 48: Viral replication is monitored by a viral plaque assay. 196

Figure 49: MAL2-11B slightly inhibits the ATPase activity of Hsp70 and Hsp90. 201

Figure 50: MAL2-11B does not inhibit Ydj1p stimulation of Ssa1p. 204

Figure 51: MAL2-11B dramatically inhibits the ATPase activity of TAg and MCM. 206

Figure 52: Cidofovir inhibits SV40 replication in a concentration dependent manner. 211

Figure 53: MAL2-11B inhibits SV40 replication. 214

Figure 54: MAL2-11B inhibits *in vitro* DNA replication. 217

Figure 55: MAL2-11B related compounds in the Biginelli acid class also inhibit *in vitro* DNA replication. 219

PREFACE

My passion for science was ignited by Mrs. Palko's 3rd grade science class. With a classroom filled with animals, microscopes, and other equipment, she taught us how to write hypotheses, perform experiments, and interpret the data. My graduate advisor, Jeff Brodsky helped me become a true scientist who could design, perform, interpret experiments, and then repeat the process. Jeff always had his door open and was always available to discuss any experiment and help plan the next one. He was always supportive of my ideas, even when they didn't work. I am the scientist that I am today because of Jeff, and I thank him for it. I would also like to thank Jim Pipas, who allowed me to become a surrogate lab member even when my work focused more on the yeast cell wall than tumorigenesis. Jim was always willing to answer any question about SV40, and I always felt welcome in the Pipas lab. I would like to thank my committee members Karen Arndt, Roger Hendrix, and Saleem Khan. In science, it is so easy to lose focus of the big picture. My committee ensured that I focused on how my results fit in with the big picture. I must also thank Susan Gilbert, who was on my committee during the comprehensive exams, and has spent hours helping me interpret the kinetic data presented in this work.

Many members of the Brodsky and Pipas labs were invaluable to this work. Sheara Fewell was an amazing mentor during my first four years of graduate school. She spent countless hours teaching me how to DO science, and she taught me the importance of collaboration, which made the projects presented in this dissertation possible. I need to thank

Raj Chovatiya, Nora Jameson, and Fengfeng Xu who performed numerous single turnover assays and made screening through all the compounds possible. In addition, thanks to Paul Cantalupo who always helped with new protocols, and provided much advice and reagents.

Science today requires collaboration with people from many disciplines including biology, chemistry, and pharmacology. These projects would not have been possible without our numerous collaborators, who each bring their individual expertise, but also communicate their knowledge and allow science to happen. I would like to thank Billy Day, Ellen Fanning, Jason Gestwicki, Michael Lyons, Mara Sullivan, Stefan Werner, Peter Wipf, and Guangyu Zhu for their invaluable assistance. I would also like to thank the entire chaperone, yeast, and tumor-virus community who have provided reagents, plasmids, and advice.

The Brodsky lab has been an amazing place to work the past 5+ years, and I would like to thank all current and previous members for all the advice, help with experiments, and support when an experiment went horribly wrong. I would like to thank the lab manager (and so much more), Jen Goeckeler, the post-docs Teresa Buck, Annette Chiang, Chris Coughlan, Nancy Kaufmann, and Kunio Nakatsukasa, and the graduate students, Annette Ahner, Stacy Hrizo, Craig Scott, Shruthi Vembar, and Bob Youker. I would especially like to thank Stacy Hrizo, Shruthi Vembar, and Nancy Kaufmann for their friendship.

Finally, none of this work would have been possible without the love and support of my friends and family. A big thanks to my friends Dava, Sarah, and Stephanie and numerous family members including Mom, Dad, C.J., Uncle Cliff, Aunt Helen, and Jack and Maureen Wright for all their support now and through the years. Finally, I must thank my amazing husband, John. He has been by my side since my second year of graduate school, and was loving throughout all of the ups and downs. Thank you John, for everything.

1.0 INTRODUCTION

Protein biogenesis is a complex process and newly synthesized proteins face many obstacles before they fully mature. The proteins must properly fold, localize, and often be activated before they can properly function. However, in the concentrated cellular milieu, these processes are difficult without assistance. In addition, improperly folded proteins may aggregate or be targeted for degradation --- both processes have been found to be linked to disease. To deal with this issue, cells have evolved complex molecular chaperone machinery to aid in protein maturation and localization. Molecular chaperones aid in most aspects of protein maturation including: folding, assembly into multi-protein complexes, protein activation, and membrane translocation. In addition, chaperones help refold misfolded or aggregated proteins and aid in protein degradation. Thus, chaperones are essential to process proteins responsible for most cellular pathways.

The importance of molecular chaperones is highlighted by their roles in disease and disease prevention (BARRAL *et al.* 2004; JOLLY and MORIMOTO 2000). For example a point mutation in a mitochondrial Hsp60 chaperone leads to the disease spastic paraplegia, probably due to misfolding of Hsp60 substrates (HANSEN *et al.* 2002). Other diseases such as cystic fibrosis (AMARAL 2004) and Alzheimer's disease (SMITH *et al.* 2005) are characterized by misfolded or aggregated proteins, and changes in chaperone levels can either aggravate or alleviate disease symptoms. Finally, chaperones are upregulated in both cancerous and viral

infected cells and may serve a protective function for the diseased cells (CALDERWOOD *et al.* 2006; SULLIVAN and PIPAS 2001). Unfortunately, few drugs that target chaperones have been identified, leaving a vast medicinal target untapped.

Despite the ubiquitous roles of chaperones in cells, I have uncovered a novel link between cytosolic chaperones and yeast cell wall integrity. Because the cell wall is considered a prime target for anti-fungals (GEORGOPAPADAKOU and WALSH 1996), this link suggests that cytosolic chaperones could be viable targets for new anti-fungal drugs. Secondly, I have identified small molecule modulators that inhibit breast cancer cell proliferation and viral replication. In turn, these could be the precursors to viable treatment options for many other diseases.

1.1 CLASSES OF MOLECULAR CHAPERONES

Many molecular chaperones were initially characterized as proteins upregulated in response to heat shock and other cellular stresses. These proteins are traditionally named according to their size. For example, Heat Shock Protein 70 (Hsp70) is a 70 kDa protein upregulated by stress. In addition, some heat shock proteins have constitutively expressed counterparts, the Heat Shock Cognate (Hsc) proteins that properly fold "housekeeping" proteins in the absence of stress. Hsc70 is essential for growth under normal conditions and accounts for up to 1% of total cellular protein. Hsp70 and Hsc70 have high sequence identity and are virtually identical in biochemical assays, but differ primarily in regulation (BRODSKY and CHIOSIS 2006). Unless otherwise stated, the Hsp prefix will be used to describe characteristics common to both Hsp and Hsc family members.

Some molecular chaperones were independently discovered as *Escherichia coli* proteins required for λ phage replication. Prior to replication, the origin of λ phage replication contains a complex of two λ phage proteins (λO and λP) and one bacterial protein (DnaB). The activity of DnaB, a DNA helicase, is inhibited by the interaction with λP. DnaK (Hsp70) and DnaJ (Hsp40) act in concert to rearrange this multi-protein complex at the phage origin in order to remove λP from DnaB and allow λ replication to begin (TAYLOR and WEGRZYN 1995). DnaK and DnaJ are the best studied members of the Hsp70 and Hsp40 families and are considered the "prototypal" examples of their respective classes.

Many classes of chaperones have been identified which bind diverse substrates and alter their conformations via ATP hydrolysis. Under normal cellular conditions, chaperones fold newly synthesized proteins or aid in other maturation processes via this conformation change (HARTL and HAYER-HARTL 2002). In hindsight, it is not surprising that molecular chaperones are required during times of stress or are corrupted during cancer and viral replication. Under stressful conditions, properly folded proteins become misfolded and increased chaperone levels compensate by using ATP catalyzed conformational changes to unfold misfolded proteins or disrupt protein aggregates before aiding in protein refolding (MAYER and BUKAU 2005; WEIBEZAHN *et al.* 2005). Thus, in the stressful environment of a tumor, chaperones play a protective role (BRODSKY and CHIOSIS 2006; JOLLY and MORIMOTO 2000). Also, viruses like λ phage can commandeer the chaperone machine to allow viral replication by rearranging inhibitory subunits.

1.2 STRUCTURE AND FUNCTION OF SELECT CYTOSOLIC CHAPERONES AND COCHAPERONES

This section focuses on four main classes of molecular chaperone: Hsp40, Hsp70, Hsp90, and the Hsp70 nucleotide exchange factors (NEFs). All chaperones discussed in this study are listed in Table 1.

1.2.1 Hsp70/Hsc70

Members of the Hsp70/Hsc70 class of molecular chaperones are essential for a vast majority of the chaperone dependent processes already discussed, including protein folding, membrane translocation, disrupting protein aggregates, and rearranging multiprotein complexes (DESHAIES *et al.* 1988; GLOVER and LINDQUIST 1998; SZABO *et al.* 1994; UNGEWICKELL *et al.* 1995). These highly conserved chaperones are found in all organisms. To date, three Hsp70s have been identified in *E. coli* and this number increases to ~10 in higher organisms (MAYER and BUKAU 2005). Hsp70 function and specificity is highly regulated by cochaperones such as Hsp40s and nucleotide exchange factors (NEFs), which will be discussed in detail in Section 1.2.3.

1.2.1.1 Structure of Hsp70

All Hsp70s are composed of three domains, an ~44 kDa N-terminal ATPase domain, an ~15 kDa substrate binding domain, and an ~10 kDa C-terminal lid domain (FLAHERTY *et al.* 1990; WANG *et al.* 1993; ZHU *et al.* 1996). The extreme C-terminus contains an EEVD motif that interacts with cochaperones that contain several degenerate 34 amino acid repeats, called tetratricopeptide repeats (TPRs). Crystallographic studies of bovine Hsc70 show that the ATPase domain

Table 1: Select examples of specific chaperone families

Family	Type	Organism	Protein	Location
Hsp70	N/A	*E. coli*	DnaK	Cytosol
		S. cerevisiae	Ssa1-4p	Cytosol
		S. cerevisiae	Ssb1-2p	Cytosol
		S. cerevisiae	Kar2p	ER
		H. sapiens	Hsc70	Cytosol
		H. sapiens	Hsp70	Cytosol
		BYV	p65	Nucleus/Cytosol
Hsp40	I	*E. coli*	DnaJ	Cytosol
	I	*S. cerevisiae*	Ydj1p	Cytosol
	II	*S. cerevisiae*	Sis1p	Cytosol
	III	*S. cerevisiae*	Swa2p	Cytosol
	III	*S. cerevisiae*	Sec63p	ER
	I	*S. cerevisiae*	Scj1p	ER
	III	*S. cerevisiae*	Jem1p	ER
	I	*S. cerevisiae*	Mdj1p	Mitochondria
	II	*H. sapiens*	HSJ1	Cytosol
	I	*H. sapiens*	DNAJ2	Cytosol
	III	SV40	TAg	Nucleus/Cytosol
	III	BKV	TAg	Nucleus/Cytosol
	III	JCV	TAg	Nucleus/Cytosol
NEF	N/A	*E. coli*	GrpE	Cytosol
		S. cerevisiae	Snl1p	ER
		S. cerevisiae	Fes1p	Cytosol
		S. cerevisiae	Sse1p	Cytosol
		H. sapiens	BAG-1	Cytosol
		H. sapiens	HspBP1	Cytosol
		H. sapiens	BAP	ER
Hsp90	N/A	*S. cerevisiae*	Hsp82p	Cytosol
		S. cerevisiae	Hsc82p	Cytosol
		H. sapiens	Hsp90α	Cytosol
		H. sapiens	Hsp90β	Cytosol

contains two globular domains which are separated by a deep cleft which binds ATP (Figure 1A). These two globular domains have been further divided into subdomain IA, IB, IIA, and IIB (FLAHERTY *et al.* 1990). Little change in the tertiary structure is seen by crystallography when ATP or ADP is bound in the active site (FLAHERTY *et al.* 1994), although more recent NMR analyses have uncovered some changes in conformation (REVINGTON *et al.* 2004; REVINGTON *et al.* 2005; ZHANG and ZUIDERWEG 2004). The structure of the ATPase domain shows structural similarity to two proteins with little sequence identity, hexokinase and actin (FLAHERTY *et al.* 1990; FLAHERTY *et al.* 1991).

The structure of the substrate binding domain has been determined for DnaK (Figure 1B) and is composed of mostly β sheets, upon which hydrophobic peptides bind (ZHU *et al.* 1996). This peptide is sequestered by, but does not interact with, an α helical lid domain at the C-terminus (ZHU *et al.* 1996). The peptide interacts with the substrate binding domain in an extended conformation and several Hsp70 amino acids directly interact with the peptide. A glutamine at position 433 forms a hydrogen bond to the peptide and appears critical to position the peptide. This glutamine is found in at least 30 other Hsp70 sequences (ZHU *et al.* 1996). Most of the other residues that interact with the peptide are hydrophobic in nature. While these residues are less conserved in other Hsp70s, they remain hydrophobic (ZHU *et al.* 1996). The substrate binding domain and lid domain dictate substrate specificity via relative affinities for peptide sequences. The Bukau lab determined that the preferred DnaK peptide contains a core sequence containing 4-5 hydrophobic residues flanked by 2 basic residues and strongly disfavors acidic residues (RUDIGER *et al.* 1997). The best DnaK binding peptide discovered by the Bukau lab interacted with DnaK with very high affinity (K_D=~100 nM), (RUDIGER *et al.* 1997) though

Figure 1: The crystal structures of the Hsp70 ATPase, substrate binding, and lid domains.

All β-sheets are shown in orange and all α helices are shown in pink. (A) The bovine Hsp70 ATPase domain, which binds and hydrolyzes ATP. The two domains, I and II, form the cleft in which ATP binds. The subdomains are labeled. Figure adapted from FLAHERTY *et al*. 1990. (B) The DnaK substrate binding domain and lid domain crystallized in the presence of a peptide. The peptide, shown in white, binds in the β-sheet rich substrate binding domain and the α helical lid domain aids in high affinity peptide binding. Figure adapted from ZHU *et al*. 1996.

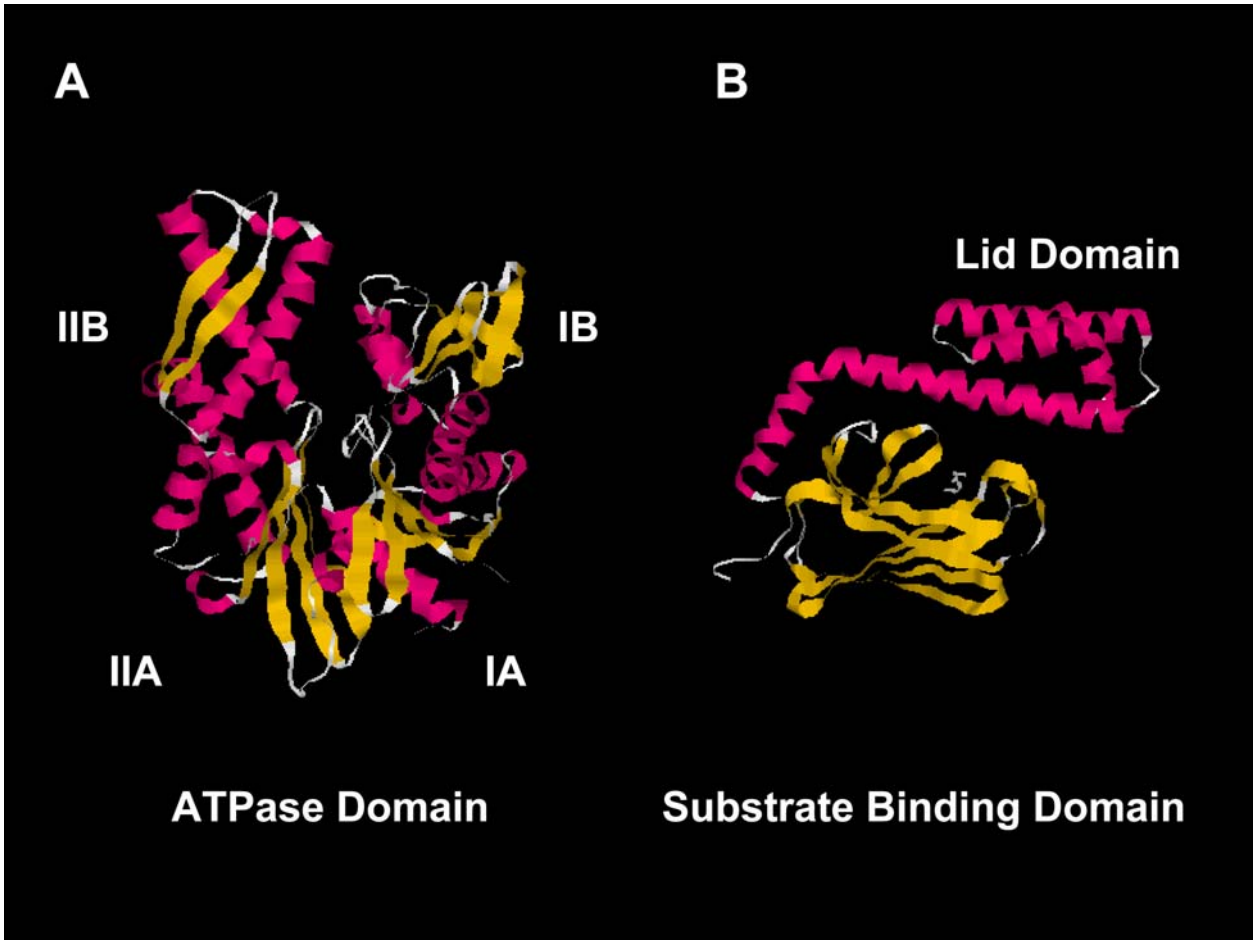
A
B
Lid Domain
IIB
IB
IIA
IA
ATPase Domain
Substrate Binding Domain

this is higher than previously reported for other Hsp70s (BLOND-ELGUINDI *et al.* 1993; FLYNN *et al.* 1989).

A flexible linker between the ATPase domain and substrate binding domain has made crystallization of the full length protein difficult. The Sousa lab recently crystallized a bovine Hsc70 protein that contained both the ATPase domain and the substrate binding domain, but lacked the lid domain (JIANG *et al.* 2005). In order to obtain high-quality crystals, they also mutated two charged residues on the surface of the ATPase domain and crystallized the proteins in conditions that contained high concentrations of the osmolyte, trimethylamine oxide (TMAO). In the final structure, the substrate binding domain folds onto the ATPase domain and interacts in a groove between domains IA and IIA. Also, the substrate binding domain is partially unfolded, and some of the residues adjacent to the lid domain occupy the peptide binding site. However because of chosen construct and crystallization conditions, and because nucleotide was absent from the nucleotide binding site, this structure is difficult to interpret.

1.2.1.2 Mechanism of action

Hsp70s function by binding substrates and using the energy from ATP hydrolysis to influence substrate binding (Figure 2). The unstimulated rate of ATP hydrolysis ranges from 0.02 to 0.2 min^{-1} (HA and MCKAY 1994; MCCARTY *et al.* 1995; THEYSSEN *et al.* 1996). When Hsp70 is found in the ATP bound state, the lid domain is open and substrates have a low affinity for the peptide binding domain, resulting in a high on/off rate. However, peptide binding can stimulate Hsp70 ATP hydrolysis 2-10 fold and cause the lid domain to clamp down onto the substrate (FLYNN *et al.* 1989; JORDAN and MCMACKEN 1995). In ADP-bound Hsp70, the substrate interacts with the peptide binding domain with high affinity and thus has a low on/off rate (MCCARTY *et al.* 1995; RUSSELL *et al.* 1999). After ADP is released, the Hsp70 rebinds ATP,

Figure 2: The Hsp70 ATPase cycle.

In the ATP bound state, the lid domain of Hsp70 is open and peptide associates with high on/off rate. Often, substrate (S) is delivered to Hsp70 by a J-protein, though this is not required. The J domain and substrate stimulate Hsp70 ATPase activity and leads to an Hsp70 conformational change in which the lid domain closes and the peptide has high affinity for Hsp70. Nucleotide exchange factors (NEF) bind to the ATPase domain and stimulate nucleotide release to allow ATP rebinding to Hsp70. Some components in this process are known to function as dimers, but monomers are shown for simplicity.

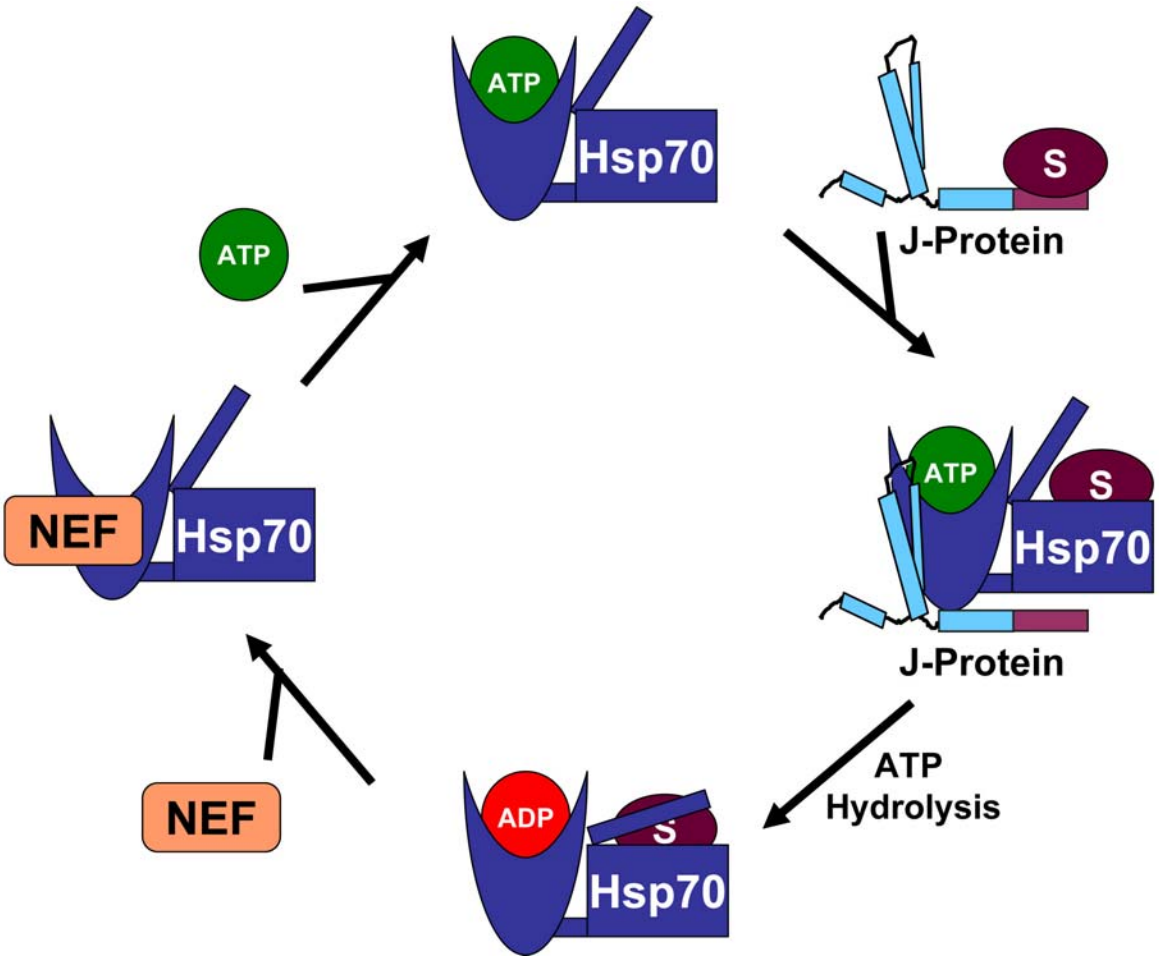
ATP
Hsp70
S
J-Protein
ATP
NEF
Hsp70
ATP
S
Hsp70
J-Protein
ATP
Hydrolysis
NEF
ADP
S
Hsp70

the lid domain opens, and peptide dissociation rates increase by 2-3 orders of magnitude and peptide affinity decreases by a factor of 10 (GISLER *et al.* 1998; MAYER *et al.* 2000).

The conformation changes in Hsp70 are becoming better defined and in one recent example it was shown to require a proline at residue 143 and an arginine at residue 151 in the DnaK ATPase domain (proline 147 and arginine 155 in bovine Hsp70) (VOGEL *et al.* 2006). When ATP is bound to the ATPase domain, ATP binding is relayed to the substrate binding domain via a proline, potentially by cis-trans isomerization of the proline, which shifts the arginine toward the peptide binding domain. When substrate binds to the peptide binding domain and Hsp40 interacts with the ATPase domain, the arginine is moved inward and the conformation of the proline is altered. This conformation positions the ATP catalyzing residues in the ATPase domain in correct proximity to ATP and facilitates ATP hydrolysis. As might be anticipated, mutation of the proline residue prevents the ATPase and substrate binding domains from communicating and accelerates the switch between the two conformations (VOGEL *et al.* 2006). Also, even a conserved mutation of arginine to lysine nearly abolishes allosteric cross-talk between the domains and substrate binding stimulates ATP hydrolysis to only 6% of wild type levels (VOGEL *et al.* 2006).

For most Hsp70 chaperones ATP hydrolysis is very weak and represents the rate-limiting step (MCCARTY *et al.* 1995; THEYSSEN *et al.* 1996). In addition to stimulation by peptide, the Hsp70 ATPase cycle is stimulated by cochaperones such as Hsp40 and NEFs. Hsp40s stimulate ATP hydrolysis directly (CHEETHAM and CAPLAN 1998; GASSLER *et al.* 1998; SUH *et al.* 1998) whereas NEFs aid in the release of ADP from Hsp70 to accelerate the ATPase cycle (ALBERTI *et al.* 2003; HARRISON 2003); these factors will be discussed in Sections 1.2.2 and 1.2.3. Hsp40 stimulation can increase ATP hydrolysis 2-10 fold (CYR and DOUGLAS 1994; WALL *et al.* 1994)

and the bacterial NEF GrpE can stimulate ADP release from DnaK by 5000 fold (PACKSCHIES *et al.* 1997). These cofactors and peptide function together to regulate Hsp70 function. In fact, DnaK ATPase activity can be stimulated >1000 fold when both DnaJ and substrate are present (LAUFEN *et al.* 1999; LIBEREK *et al.* 1991)

1.2.2 Hsp40

Members of the Hsp40 class of chaperones are obligate cochaperones of Hsp70s. The primary role of Hsp40s is to stimulate Hsp70 ATP hydrolysis, though some Hsp40s also have a substrate binding domain and are responsible for delivering substrates to Hsp70s (HAN and CHRISTEN 2003; LANGER *et al.* 1992; RUDIGER *et al.* 2001; SZABO *et al.* 1996; WICKNER *et al.* 1991). All Hsp40s contain a J domain, named for its presence in DnaJ, so these proteins are often called J domain containing proteins or J-proteins. There are six J-proteins in *E. coli* and between 20 and 40 in yeast and higher organisms (QIU *et al.* 2006; WALSH *et al.* 2004). The large number of J-proteins, relative to Hsp70, is probably because they help define Hsp70 specificity.

1.2.2.1 Structure and types of Hsp40s

As noted above, the defining feature of Hsp40s is the J domain (Figure 3A). The structures of seven J domains have been solved and show that the J domain is comprised of four alpha helices (HENNESSY *et al.* 2005). Helices II and III interact to form a finger-like projection and hydrophobic interactions between these helices are critical to maintain the structure of the J domain. The loop between Helix II and III contains an invariant HPD motif which is essential for stimulating Hsp70 ATP hydrolysis. Conserved residues in the J domain are seen on all four

Figure 3: Key features of the Hsp40 class of molecular chaperones.

(A) The structures of 7 J domains have been determined. These include NMR structures from three *E. coli* DnaJ proteins (1XBL, 1BQZ, 1BQ0), human HDJ1 (1HDJ), and murine polyomavirus (1FAF) and crystal structures of *E. coli* Hsc20 (1FPO), SV40 TAg (1GH6), and bovine auxilin (1NZ6). Figure adapted from HENNESSY *et al*. 2005. (B) J-proteins are defined by their homology to DnaJ. Type I J-proteins are exemplified by DnaJ and contain an N-terminal J domain, a glycine/phenylalanine (G/F) rich region, and a cysteine rich domain that coordinates zinc atoms. Type II J-proteins do not contain a cysteine rich domain and generally have an elongated G/F domain. Type III J-proteins only contain the J domain which can be localized throughout the protein.

A

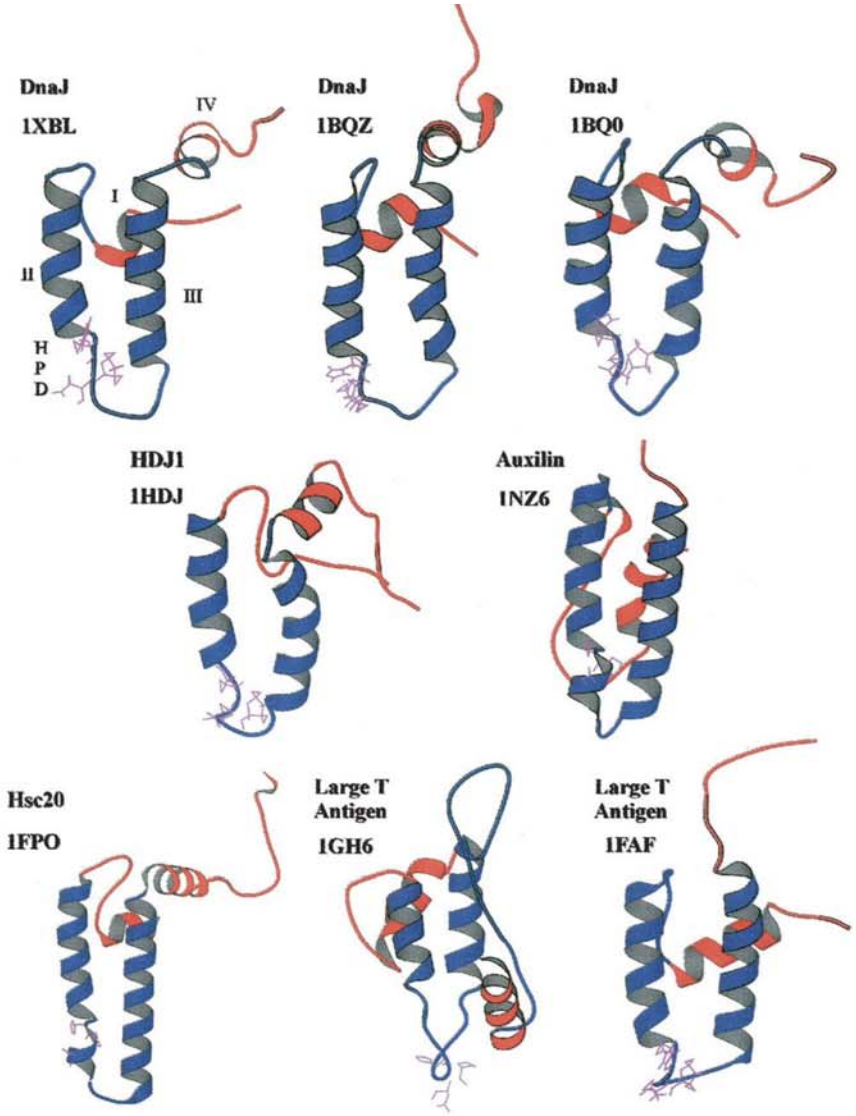
DnaJ
1XBL
IV
I
II
III
H
P
D
DnaJ
1BQZ
DnaJ
1BQ0
HDJ1
1HDJ
Auxilin
1NZ6
Hsc20
1FPO
Large T
Antigen
1GH6
Large T
Antigen
1FAF

B

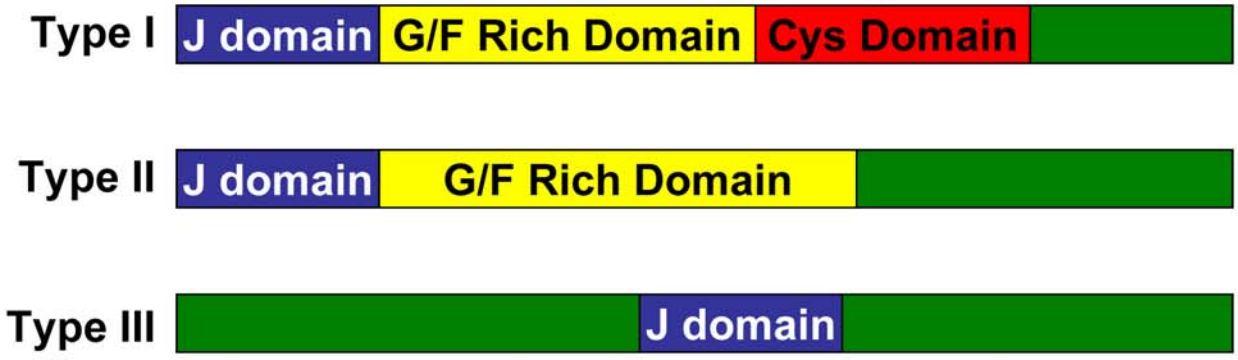
Type I
J domain
G/F Rich Domain
Cys Domain
Type II
J domain
G/F Rich Domain
Type III
J domain

helices, though the importance of many of these residues has not been thoroughly investigated (HENNESSY *et al.* 2000).

The prototypical Hsp40 is the *E. coli* DnaJ and all Hsp40s are defined by their similarity to DnaJ (Figure 3B) (CHEETHAM and CAPLAN 1998). DnaJ is a type I Hsp40, and contains an N-terminal J domain, a glycine/phenylalanine rich domain (G/F), and a cysteine rich domain. In contrast, type II Hsp40s do not have a cysteine rich domain, and generally have a longer glycine/phenylalanine rich domain. Finally, type III proteins only have the J domain which is not restricted to the N-terminus. Type I and II Hsp40s bind to substrate through the G/F and cysteine rich domain and are *bona fide* Hsp40 chaperones. The differences between type I and type II Hsp40s help dictate substrate specificity (FAN *et al.* 2004). Type III J-proteins (e.g. TAg discussed in detail in Section 1.5.2.1) are not involved in protein folding and are not considered molecular chaperones.

1.2.2.2 Mechanism of action

Many J domain containing proteins bind peptide substrate and deliver it to Hsp70 through a poorly characterized mechanism (HAN and CHRISTEN 2003; LANGER *et al.* 1992; RUDIGER *et al.* 2001; SZABO *et al.* 1996; WICKNER *et al.* 1991). Peptide binding and the J domain are required for maximal stimulation of Hsp70 ATPase activity. The J domain binds the Hsp70 ATPase domain with a relatively low affinity [K_D=20μM for DnaK/DnaJ, though a higher affinity (544 nM) was determined by Biocore (RUSSELL *et al.* 1999; SUH *et al.* 1999)] primarily through helix II and the HPD motif as shown by DnaJ NMR perturbation studies (GREENE *et al.* 1998). However, recent studies using a mouse polyomavirus Type III J domain containing protein have shown that residues in helices III may also be important for Hsp70 interaction (GARIMELLA *et al.* 2006). However the J domain alone is sometimes insufficient for stimulating Hsp70 ATPase

activity, suggesting that for some J-proteins C-terminal regions of the protein are essential for Hsp70 interaction (SUH *et al.* 1999). J domains stimulate Hsp70 through the proline switch and arginine relay (VOGEL *et al.* 2006) previously discussed in Section 1.2.1.2. Mutations in the HPD loop and in some residues in helix II abrogate the ability of Hsp40s to stimulate ATP hydrolysis (GENEVAUX *et al.* 2002; HENNESSY *et al.* 2005; TSAI and DOUGLAS 1996; WALL *et al.* 1994).

The interaction of the J domain may also be mediated through domain IA in the Hsp70 ATPase domain. To identify Hsp70 residues important for an interaction with the J domain HPD motif, the Gross lab screened for mutants of DnaK that suppress two phenotypes associated with HPD mutations in DnaJ. A DnaK R167H mutation, localized to domain IA, was discovered that suppresses the growth defect of cells containing DnaJ D35N and allows productive λ phage infections. Surface plasmon resonance experiments indicated the DnaK R167H mutation restores a functional interaction with DnaJ D35N (SUH *et al.* 1998). In fact, DnaK R167H bound 3 fold better to DnaJ D35N than wild type DnaJ (SUH *et al.* 1998). Further supporting the role of this residue in the J domain interaction, mutation of this residue in DnaK prevented a functional interaction with a wild type J domain (SUH *et al.* 1998). At this point, it is uncertain whether the J domain directly binds the cleft near DnaK R167 or if this residue is indirectly involved in the stimulation of Hsp70.

In addition to their role in stimulating Hsp70 ATP hydrolysis, many J-proteins also bind substrates. The peptide binding domain of the yeast Type I Hsp40 Ydj1p bound to peptide has been crystallized (Figure 4) (LI *et al.* 2003b). Three subdomains in the peptide binding domain are readily identified. Domains I and III form an extended region of mostly β sheets and domain I binds to peptide. Zinc binding in domain I and II allow domain II to extend from the end of

Figure 4: Space-filling and ribbon representations of amino acids 110-337 of the Ydj1p substrate binding domain.

The space-filling model indicates surface potential, and blue residues are positively charged and red residues are negatively charged. The red box surrounds the peptide that was cocrystallized with Ydj1p. The ribbon diagram labels the zinc binding domains (ZBDI and ZBDII) and the cysteines that coordinate the zinc molecules (orange spheres). The C terminal domains (CTDI and CTDII) and the cocrystallized peptide (red ribbon) are also shown. Figure adapted from LI *et al*. 2003.

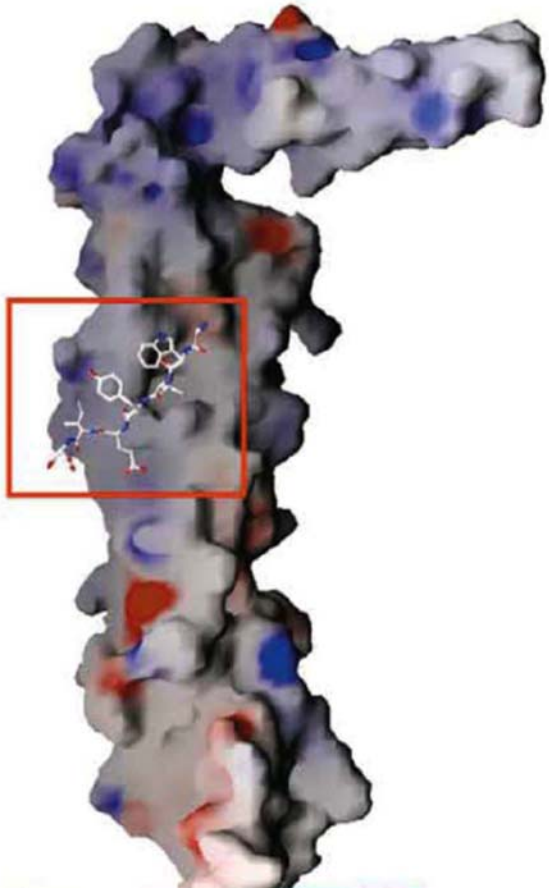

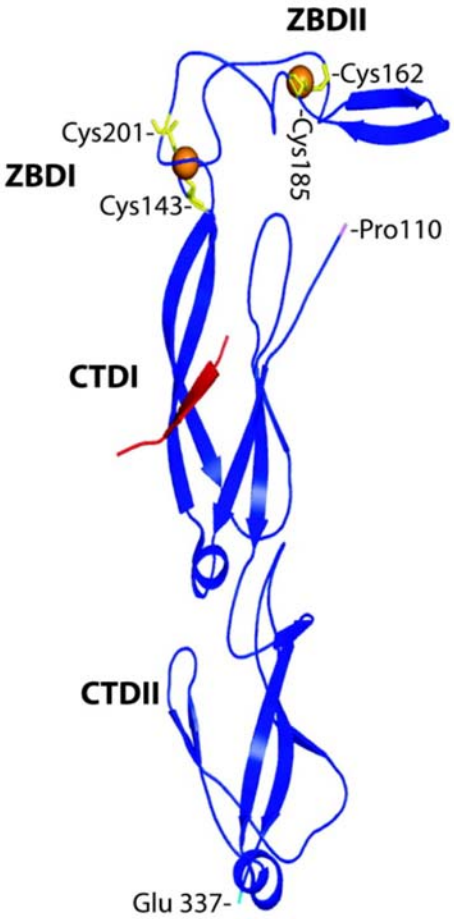
ZBDII
-Cys162
Cys201-
-Cys185
ZBDI
Cys143-
-Pro110
CTDI
CTDII
Glu 337-

domain I to form an structure that looks like a capital "L" (LI *et al.* 2003b). Modeling of the Ydj1p dimer shows interactions between the tips of domain III create a central pocket between the two dimers. The previously crystallized Type II Hsp40 Sis1p looked virtually identical (SHA *et al.* 2000). As with DnaK, the preferred peptide binding residues of DnaJ were identified by the Bukau lab and contain eight aromatic or hydrophobic residues (RUDIGER *et al.* 2001). While the DnaJ peptide preferences are slightly different than DnaK, which prefers 4-5 hydrophobic residues flanked by 2 basic residues (RUDIGER *et al.* 1997), most peptides that bind to DnaJ also bind to DnaK. The Bukau lab proposed two hypotheses for substrate transfer from DnaJ to DnaK (RUDIGER *et al.* 2001). The "handover" mechanism suggests that since DnaJ and DnaK bind similar peptides, DnaK displaces DnaJ from the substrate and binds the same residues. A second hypothesis proposes that since the preferred residues are different, DnaJ and DnaK bind residues in close proximately and each protein occupies discrete positions on the substrate at the same time.

1.2.2.3 Hsp70/Hsp40 specificity

There has been much debate about how substrate-specific interactions with individual Hsp70 and Hsp40 are created. Some specificity is certainly created simply by differential localization of proteins. Membrane enclosed compartments such as the endoplasmic reticulum and mitochondria have dedicated Hsp70s and Hsp40s which are physically separated from the cytosolic chaperones. However, specificity is also seen within a single compartment. For example yeast Hsp70, Ssa1p, is stimulated 6.1 fold by a cytosolic partner, Ydj1p, but only 1.5 fold by GST-63J (a chimeric protein containing GST fused to the J domain of Sec63p which resides in the ER lumen). Similarly, Kar2p is stimulated 13.1 fold by its the J domain found in GST-63J, but only 1.4 fold by Ydj1p (MCCLELLAN *et al.* 1998). J domain swapping experiments

have also been performed to address Hsp70/Hsp40 specificity (HENNESSY *et al.* 2005). These studies have shown that not all J domains can functionally substitute for each other and that J domains must code for some interaction specificity. J domain swaps between the yeast cytosolic J-protein Sis1p, mitochondrial J-protein Mdj1p, and ER luminal J-proteins Scj1p with Sec63p were performed in the Silver lab (SCHLENSTEDT *et al.* 1995). The J domains of mitochondrial Mdj1p and cytosolic Sis1p do not substitute for the ER luminal Sec63p J domain. However, ER luminal Scj1p functionally substituted for Sec63p, which is perhaps not surprising since both proteins interact with the same Hsp70, Kar2p. In some J-proteins the J domain appears sufficient to dictate specificity. For example, the exposed regions of some type III J-proteins [e.g. polyomavirus tiny tumor antigen (tAg) and Sec63p] are extremely short and contain little other sequence information. Despite this lack of additional sequences, residues in the Sec63p J domain allow productive interactions with BiP, but not Ssa1p (MCCLELLAN *et al.* 1998). However, none of these studies rule out the possibility that residues beyond the J domain play an additional role in determining specificity.

1.2.3 Nucleotide exchange factors (NEFs)

In the presence of a J domain containing protein, the rate-limiting step of the Hsp70 cycle becomes the release of ADP (BUKAU and HORWICH 1998). Cells have evolved NEFs to remove ADP from the ATPase domain. ATP then rebinds with high efficiency since it is found in high cytosolic concentrations. Interestingly, three structurally distinct NEFs have been identified, GrpE in bacteria, and BAG-1 and HspBP1 in eukaryotes. Also, recent studies have shown that the yeast Hsp110 homologue, Sse1p, acts as a NEF for Ssa1p (DRAGOVIC *et al.* 2006a; RAVIOL *et al.* 2006). Each of these factors is considered in detail below.

1.2.3.1 GrpE

GrpE was the first Hsp70 NEF identified and exchanges nucleotide on *E. coli* DnaK. GrpE homologues have only been identified in bacteria and eukaryotic organelles of prokaryotic origin such as the mitochondria (HARRISON 2003). GrpE was initially discovered as a protein required for λ phage replication (SAITO and UCHIDA 1977) and can remove both ADP and ATP from DnaK (BREHMER *et al.* 2001), though the affinity of GrpE for DnaK is decreased in the presence of ATP (ZYLICZ *et al.* 1987) In fact, GrpE reduces the affinity of ADP for DnaK 200 fold and stimulates nucleotide exchange 5000 fold (PACKSCHIES *et al.* 1997).

GrpE has been crystallized as a dimer and consistent with this observation, previous experiments suggest that the ratio of DnaK to GrpE is 1:2 (HARRISON *et al.* 1997; SCHONFELD *et al.* 1995). The monomer of GrpE consists of a long α helix, a small α helix and a C-terminal β sheet region. In the dimer the α helices are aligned to form a four helix bundle with two β sheet protrusions. The β sheets interact with domain IIB of DnaK and shift the domain outward by 14°, which prevents high affinity nucleotide binding in the binding pocket (HARRISON *et al.* 1997). Thus, GrpE interferes with ATP binding by changing the conformation of the ATPase domain and does not directly interact with the ATP binding pocket (Figure 5A). Overall, the GrpE/DnaK interaction increases protein folding by accelerating the DnaK ATP hydrolysis cycle (SZABO *et al.* 1994). GrpE has also been reported to directly accelerate peptide release from DnaK (MALLY and WITT 2001), but this was disputed in a more recent study (BREHMER *et al.* 2004).

1.2.3.2 BAG-1

BAG-1 was first identified as a Bcl-2 associated athanogene, which binds anti-apoptotic Bcl-2 (TAKAYAMA *et al.* 1995) and was then discovered to associate with many others proteins,

Figure 5: Crystal structures of the three classes of nucleotide exchange factors.

(A) Two representations of the GrpE NEF, which was crystallized as a dimer. The monomers of GrpE are shown in yellow and blue, and the ATPase domain of Hsp70 is shown in red. On the right, the 14° shift in the Hsp70 ATPase domain can be observed. Figure adapted from HARRISON 2003. (B) The BAG domain of BAG-1 (red) is cocrystallized with the Hsp70 ATPase domain (green). Figure adapted from SONDERMANN *et al*. 2001. (C) Two representations of the HspBP1 core domain (green) are shown with the IIA and IIB subdomains of the Hsp70 ATPase domain (left) or a model of the entire Hsp70 ATPase domain (right). Figure adapted from SHOMURA *et al*. 2005.

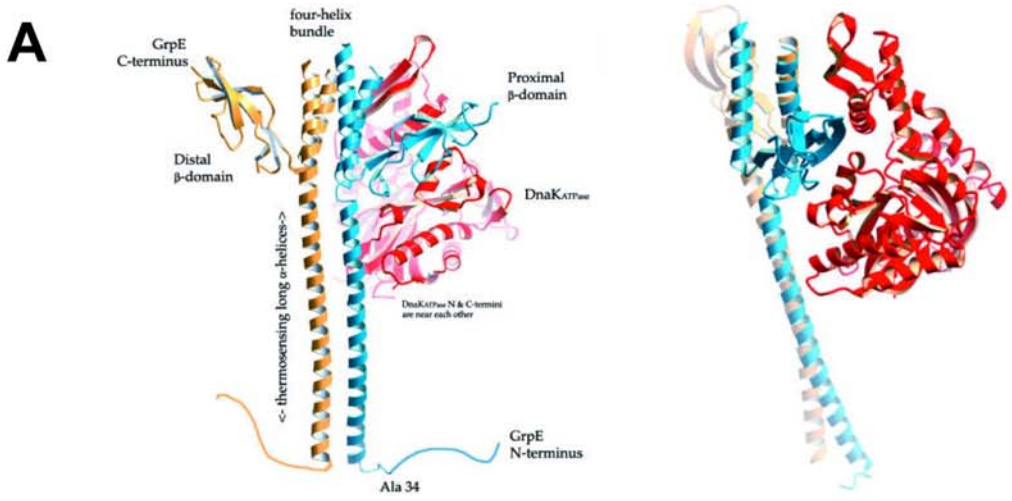
A
four-helix bundle
GrpE C-terminus
Proximal β-domain
Distal β-domain
DnaKATPase
<- thermosensing long α-helices ->
DnaKATPase N & C-termini are near each other
GrpE N-terminus
Ala 34

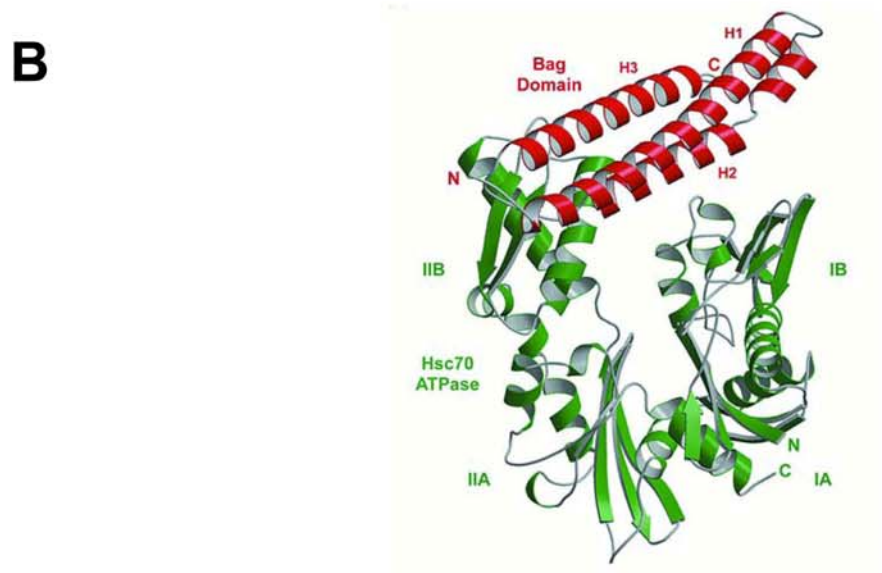
B
H1
Bag Domain
H3
C
N
H2
IIB
IB
Hsc70 ATPase
N
C
IIA
IA

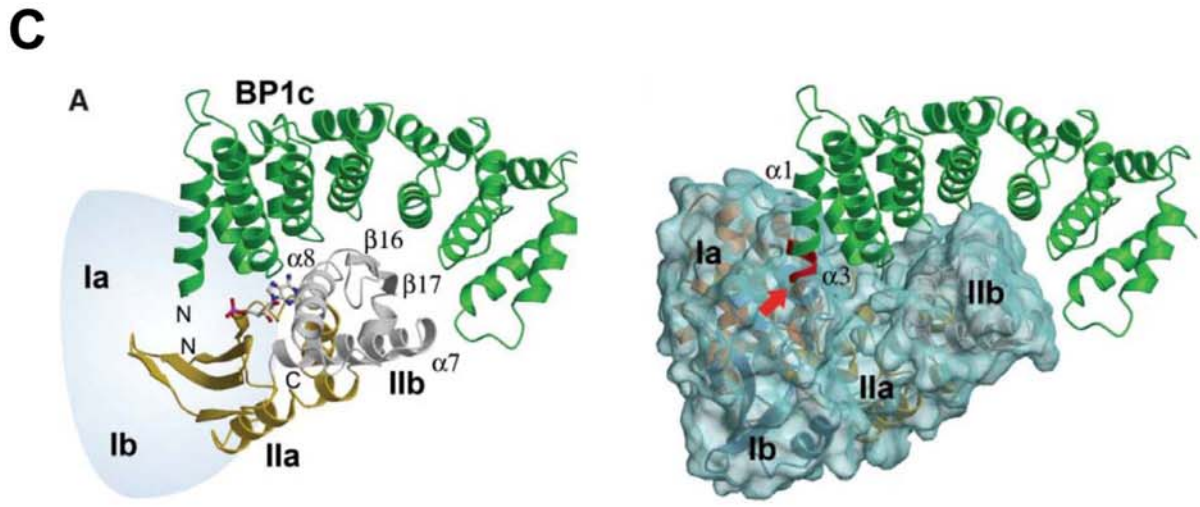
C
A
BP1c
Ia
α8
β16
β17
N
N
C
IIb
α7
Ib
IIa
α1
Ia
α3
IIb
IIa
Ib

including Hsp70 (TAKAYAMA *et al.* 1997). The complete role of BAG-1 in the cell is currently unclear, but it has been shown conclusively to be a NEF for Hsp70 (HOHFELD and JENTSCH 1997). The BAG-1 mRNA codes for 4 isoforms, BAG-1L, BAG-1M, BAG-1, BAG-1S, which differ in length and sequence at the N-terminus. All isoforms contain a C-terminal BAG domain which is essential for the interaction with the Hsp70 ATPase domain (ALBERTI *et al.* 2003). A BAG-1 homologue, Snl1p, has been identified in *S. cerevisiae* (SONDERMANN *et al.* 2002). Snl1p interacts with Ssa1p, Ssa4p, and Ssb1 as shown by yeast two hybrid and coimmunoprecipitation and stimulates nucleotide release by mammalian Hsc70 (SONDERMANN *et al.* 2002). *SNL1* is a multi-copy suppressor of growth defects seen in strains with mutations in nuclear pore associated proteins (HO *et al.* 1998) and Snl1p interaction with Hsp70 is required for this activity (SONDERMANN *et al.* 2002). Based on these results, the Hartl lab proposed Hsp70 folds the nuclear pore associated proteins and over-expression of *SNL1* increased the folding rate.

The BAG domain consists of a 3 helix bundle that interacts with Hsp70 ATPase domains Ib and IIb (Figure 5B). While the BAG domain is structurally very different from GrpE, it disrupts nucleotide in a similar fashion by rotating domain IIb 14°, and releases ADP from the nucleotide binding pocket (Figure 6) (SONDERMANN *et al.* 2001). Unlike GrpE, BAG-1 is selective for ADP and only releases ADP from Hsp70 (BREHMER *et al.* 2001). BAG-1 can stimulate the steady state ATPase activity of Hsp70, and has differing effects on Hsp70 substrate folding depending on stoichiometry between Hsp70 and BAG-1 (GASSLER *et al.* 2001).

1.2.3.3 HspBP1

A third class of NEF is the Hsp Binding Protein 1, HspBP1 which was first identified as an inhibitor of Hsp70 refolding at high concentrations of HspBP1 (RAYNES and GUERRIERO 1998).

Figure 6: A representation of the interaction of Hsp70 with either HspBP1 or BAG-1.

HspBP1 interacts with the Hsp70 ATPase subdomains IB and IIB and rotates them relative to each other. BAG-1 also interacts with both domains, but only changes the conformation of subdomain IIB. Figure adapted from SHOMURA *et al*. 2005.

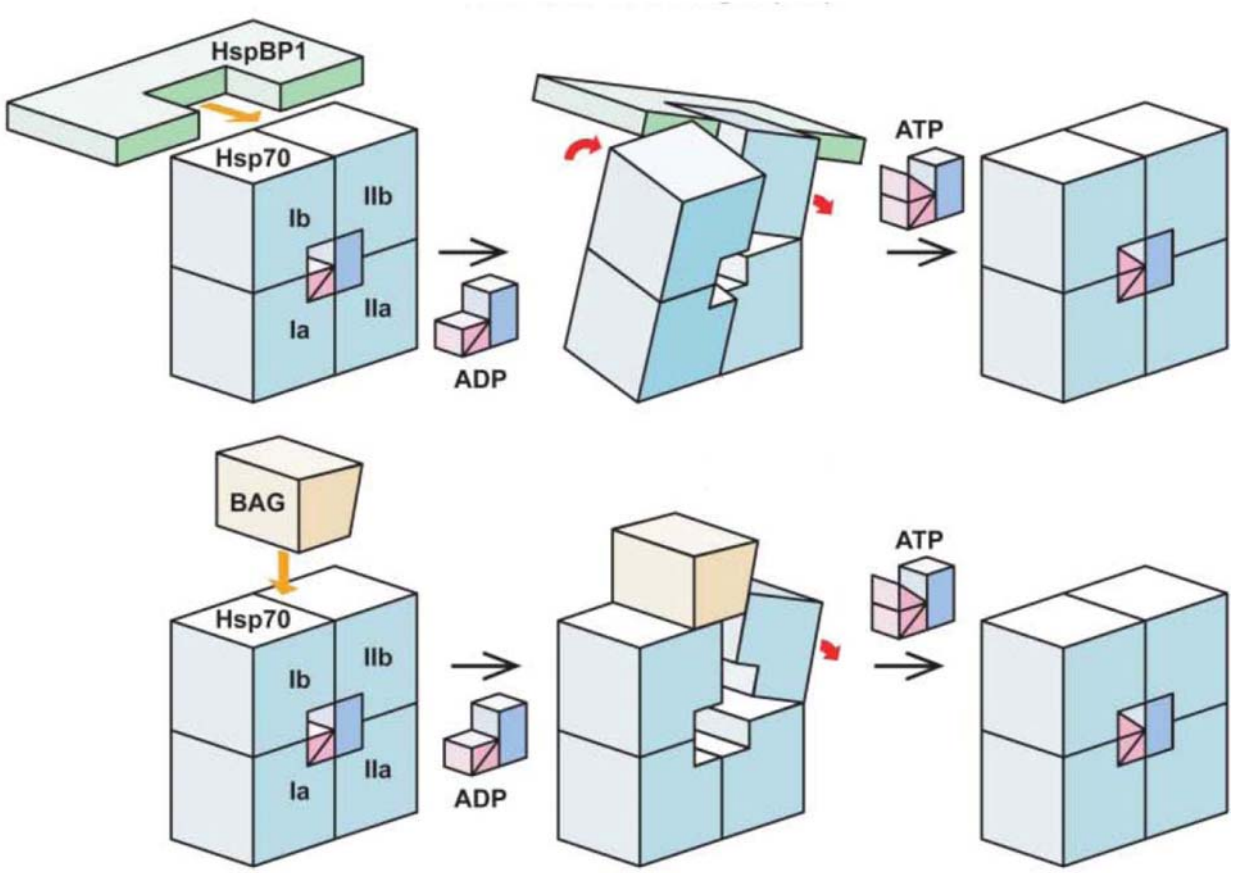
HspBP1
Hsp70
Ib
IIb
Ia
IIa
ADP
ATP
BAG
Hsp70
Ib
IIb
Ia
IIa
ADP
ATP

Two HspBP1 homologues have been identified, Fes1p in yeast cytosol and BAP in the mammalian ER (CHUNG *et al.* 2002; KABANI *et al.* 2002a). HspBP1 is a NEF for Hsp70 and facilitates luciferase folding *in vivo* (AHNER *et al.* 2005; KABANI *et al.* 2002b). Interestingly, Fes1p is a NEF for two yeast cytosolic chaperones, Ssa1p and the ribosome-associated Ssb1p (DRAGOVIC *et al.* 2006b; KABANI *et al.* 2002a). Also, *fes1Δ* cells are sensitive to cycloheximide, an inhibitor of protein translation, and contain increased levels of 80s ribosomes relative to wild type cells (KABANI *et al.* 2002a). Taken together, these results suggest that Fes1p is important for folding newly synthesized polypeptides as they exit the ribosome.

HspBP1 is structurally distinct from GrpE and BAG-1 and has a unique mechanism for nucleotide exchange. The core domain of HspBP1 was crystallized and was composed entirely of α helices. The arrangement of the helices leads to a slightly concave face of the molecule. The most closely related structure to HspBP1 is the Armadillo repeat, which is found in β catenin and importin-α (CONTI *et al.* 1998; HUBER *et al.* 1997). The core domain of HspBP1 was also crystallized in association with lobe II of Hsp70. (Figure 5C) While HspBP1 has a similar overall binding affinity for the Hsp70 ATPase domain as BAG-1, it binds Hsp70 domain IIb with higher affinity than BAG-1, and does not interact with Ib very well (SHOMURA *et al.* 2005). Instead of simply disrupting domain IIb by 14°, HspBP1 disrupts lobes I and II relative to each other to release ADP (Figure 6) (SHOMURA *et al.* 2005).

1.2.3.4 Sse1p

Recently, the yeast Hsp110 molecular chaperone, Sse1p, was shown to exhibit nucleotide exchange activity (DRAGOVIC *et al.* 2006a; RAVIOL *et al.* 2006). Hsp110s are distantly related to Hsp70s and have similar N-terminal ATPase domains, but the C-terminal putative substrate binding domain is not homologous to Hsp70. In addition, Hsp110s also have extended regions

between the ATPase and C-terminal domains and at the extreme C-terminus. Sse1p acts as a holdase, and prevents protein aggregation but cannot induce protein folding (BRODSKY *et al.* 1999). Sse1p is found in chaperone complexes with Hsp82p and the two yeast Hsp70s, Ssa1p and Ssb1p (LIU *et al.* 1999; SHANER *et al.* 2005). A role in Hsp70 function was first hinted at by the discovery of Sse1p as a multi-copy suppressor of the *ydj1-151* thermosensitive allele of the yeast Hsp40, *YDJ1* (GOECKELER *et al.* 2002). This suggested Sse1p, like Ydj1p, stimulates the Ssa1p ATP hydrolysis cycle.

Sse1p stimulates steady state ATPase activity of Ssa1p, but does not stimulate Ssa1p in single turnover ATPase assays, suggesting that it is involved in nucleotide binding or release (RAVIOL *et al.* 2006). Fluorescent ADP release assays show that Sse1p stimulates nucleotide release of Ssa1p by 150 fold and Ssb1p by 80 fold (RAVIOL *et al.* 2006) and stimulates Ssa1p peptide release (DRAGOVIC *et al.* 2006a). While Sse1p cannot fold luciferase independently, it can stimulate luciferase folding by Ssa1p *in vivo* and *in vitro* (DRAGOVIC *et al.* 2006a; RAVIOL *et al.* 2006).

1.2.4 Hsp90/Hsc90

Hsp90s, like Hsp70s, bind and release substrate proteins concomitant with ATP hydrolysis. However, unlike Hsp70 and Hsp40 which are involved in folding newly synthesized polypeptides, Hsp90 folds a specific set of client proteins that have neared their native conformation (TERASAWA *et al.* 2005; ZHAO and HOURY 2005). A list of known Hsp90 clients is available on Didier Picard's website, http://www.picard.ch/downloads/Hsp90interactors.pdf. Specifically, Hsp90 is responsible for activating proteins or holding them in a conformation conducive for interaction with required hormones or proteins. For example, most Hsp90 clients

are hormone binding receptors, kinases, and transcription factors (PRATT and TOFT 2003). Two Hsp90 homologues have been identified in S. *cerevisiae* (Hsp82p and Hsc82p) and 4 Hsp90s are found in human cells, including the cytoplasmic forms Hsp90α and Hsp90β, and single mitochondrial and ER forms (ZHAO and HOURY 2005).

1.2.4.1 Structure of Hsp90

Hsp90 contains an ~25 kDa N-terminal ATP binding domain, which is usually connected to the ~35 kDa middle domain through a highly charged region and a C-terminal ~12 kDa dimerization domain (Figure 7). The ATP binding domain contains an ATP binding pocket, which also binds the competitive inhibitor, geldanamycin (see details below) (PRODROMOU *et al.* 1997; STEBBINS *et al.* 1997). The Hsp90 ATPase domain shows structural similarity to the GHKL family of ATPases, which include type II topoisomerases and the mutL mismatch repair enzyme (DUTTA and INOUYE 2000). Hsp90, like other GHKL family members, contains a split ATPase domain, since optimal ATPase activity requires the adjacent middle domain. The middle domain contains an acceptor site for the γ phosphate of ATP and may aid in the removal of the γ phosphate during ATP hydrolysis (MEYER *et al.* 2003). The middle domain also contains a large hydrophobic patch that is responsible for client protein binding (MEYER *et al.* 2003). The C-terminal dimerization domain is responsible for Hsp90 dimerization, which is required for client binding and optimal ATP hydrolysis (HARRIS *et al.* 2004; PRODROMOU *et al.* 2000).

1.2.4.2 Mechanism of action

In the nucleotide free state, the Hsp90 dimer exists in the "open" conformation in which the N-terminal ATP binding domains are separated and client proteins interact freely in the region between the two dimers. However, upon ATP binding, the N-terminal domains interact and

Figure 7: The crystal structure of a dimer of Hsp90, bound to AMPPNP.

The crystal structure on the left is colored to show the orientation of the domains of the two monomers. The crystal structure on the right colors the monomers blue and orange to show the orientation of the monomers. Figure adapted from PEARL *et al*. 2006.

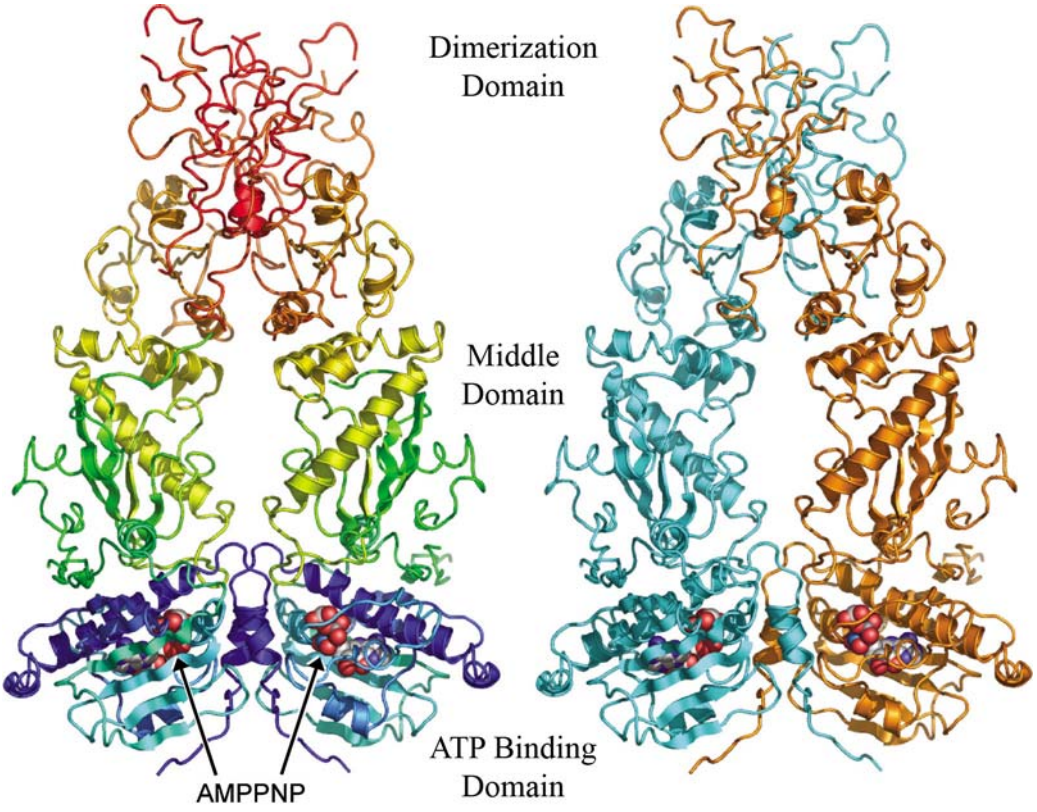
Dimerization
Domain
Middle
Domain
ATP Binding
Domain
AMPPNP

form a "closed" state around the client protein. Hsp90 is a relatively weak ATPase activity (0.44 min^{-1} for yeast Hsp82p) (GRENERT *et al.* 1999; OBERMANN *et al.* 1998; PANARETOU *et al.* 1998) and many cochaperones including Hsp70 and Hsp40 are required for Hsp90 function. After ATP hydrolysis, client proteins are released and Hsp90 is recycled for future folding cycles.

The Hsp90 folding complex contains a large number of cochaperones, which differ somewhat depending on the substrate. Hsp90 folding has been well characterized *in vitro* for progesterone receptor (PR) and this mechanism of action is probably very similar for the folding of other hormone receptors (DITTMAR and PRATT 1997; SMITH *et al.* 1992). Hsp90 binds inactive hormone receptors and folds them into a hormone binding competent state until the hormone binds (Figure 8). First, Hsp40 binds PR and delivers it to Hsp70 (HERNANDEZ *et al.* 2002) where it stimulates Hsp70 ATPase activity to allow Hsp70 to clamp down on PR. Hsp70/Hsp40/PR then forms an intermediate complex with Hsp90 and Hsp Organizing Protein, HOP. HOP simultaneously links Hsp70 to Hsp90 via two different TPR motifs (SCHEUFLER *et al.* 2000) and may transfer substrate from Hsp70 to Hsp90 (WEGELE *et al.* 2006). HOP preferentially binds ADP bound Hsp70 (JOHNSON *et al.* 1998) and yeast HOP, Sti1p, stimulates Hsp70 ATP hydrolysis and inhibits Hsp90 ATPase activity (RICHTER *et al.* 2003; WEGELE *et al.* 2003). Interestingly, mammalian HOP does not directly regulate Hsp70 or Hsp90 ATPase activity, instead acting as a passive linker between the two (JOHNSON *et al.* 1998; WEGELE *et al.* 2003). The mature complex is formed when p23 replaces Hsp70/HOP and ATP binds to Hsp90. p23 only binds ATP bound Hsp90 and is thought to stabilize the complex (DITTMAR *et al.* 1997)). The final complex contains ATP bound Hsp90, Hsp40, p23 and PR. The exact role of Hsp40 in the Hsp90 complex is currently unclear, but it appears to differ depending on the type of Hsp40 and the client protein (CINTRON and TOFT 2006; MURPHY *et al.* 2003).

Figure 8: Hsp90 folding cycle for the Progesterone Receptor (PR).

Ydj1p first binds and delivers PR to Hsp70 in the ATP bound state. PR and Ydj1p stimulate Hsp70 ATP hydrolysis and substrate is transferred to Hsp70. The intermediate complex is formed by the addition of Hsp90 (90) and HOP/Sti1p. HOP serves as a linker between Hsp70 and Hsp90. The substrate is transferred to Hsp90 from Hsp70, which together with HOP leaves the complex. ATP and p23/Sba1p bind to Hsp90 to stabilize the final "mature" complex. Some components of this process are known to be dimers, but only the monomer is shown for simplicity.

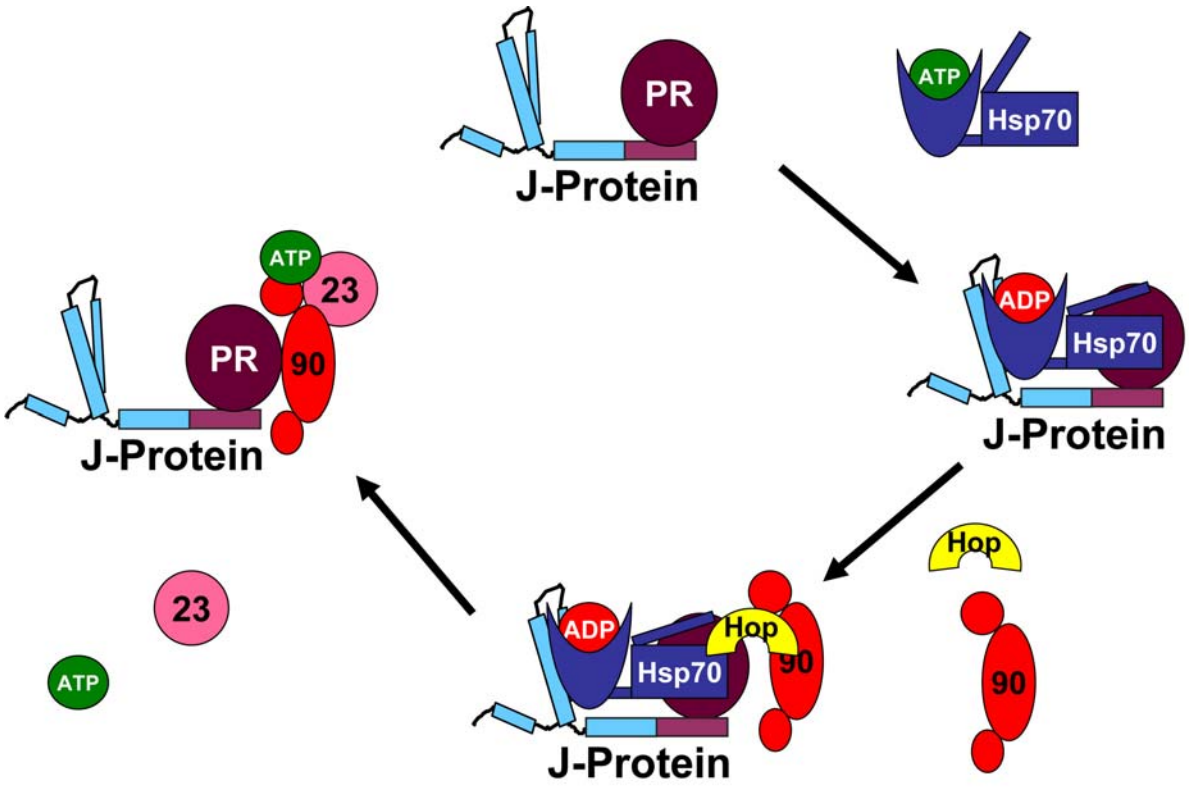
PR
J-Protein
ATP
Hsp70
ADP
Hsp70
J-Protein
Hop
90
ADP
Hop
Hsp70
90
J-Protein
23
ATP
ATP
23
PR
90
J-Protein

The Hsp90 cochaperone requirement is very different for the activation of protein kinases, such as Chk1 (ARLANDER *et al.* 2006). Unlike hormone receptors, kinases only transiently associate with Hsp90 and represent a different class of Hsp90 client proteins. Chk1 requires Hsp70, Hsp40, and Hsp90 for activation, suggesting that these chaperones are essential for all Hsp90 client proteins (ARLANDER *et al.* 2006). However, Chk1 also requires the kinase chaperone, Cdc37, and the kinase CK1 for complete activation. Cdc37 has been shown to bind both Hsp90 and client proteins and may be used to recruit Hsp90 to the client (HUNTER and POON 1997). CK1 phosphorylates Cdc37, which is required for Cdc37 function, and it is unclear if CK1 also phosphorylates Chk1. While HOP and p23 are required for PR folding, they are not required for Chk1 activation. In fact, addition of HOP enhances Chk1 activation but addition of p23 has no effect on activation, suggesting that these proteins are not required for all Hsp90 clients.

1.3 THE FUNCTIONS OF SELECT CHAPERONES IN *SACCHAROMYCES CEREVISIAE*

Many chaperones, including Ssa1p (Hsp70) and Hsp82 (Hsp90), are essential for the growth of the yeast *Saccharomyces cerevisiae*. This section will describe a few examples of chaperone function in *S. cerevisiae* to illustrate how the chaperone mechanisms described earlier are utilized in the cell. Also, examples of *S. cerevisiae* as a model system to study chaperone function are given.

1.3.1 Protein folding and refolding

As mentioned previously, Hsp70s are required to fold newly synthesized peptides. Hsp70s bind hydrophobic exposed residues in newly synthesized proteins and maintain their solubility by preventing unwanted hydrophobic interactions and aggregation. Then, through successive ATPase cycles the proteins are bound and released from the Hsp70 substrate binding domain. The energy of ATP hydrolysis induces conformational changes that lead to proper folding of the substrate. Hsp70s do not directly fold protein substrate; instead they prevent protein misfolding and maintain their solubility until they fold.

Firefly luciferase has become a model substrate for chaperone-dependant folding *in vitro*. Specifically, once firefly luciferase is folded, it can act on the substrate luciferin and produce a fluorescent readout directly related to the amount of active luciferase. This system has been adapted to probe the role of yeast chaperones during protein folding. For example, cytosol containing Ssa1p is sufficient to refold denatured luciferase. However, when cytosols immunodepleted for Ssa1p/Ssa2p are added to denatured luciferase, folding is impaired (BUSH and MEYER 1996). Hsp40 cochaperones are also important for luciferase folding. When using purified proteins, addition of Ssa1p to denatured luciferase has little effect on luciferase folding. However, addition of purified Ssa1p and Ydj1p stimulates luciferase refolding 20 fold (LU and CYR 1998a). Interestingly, Sis1p, a second Ssa1p cochaperone, does not stimulate Ssa1p folding to the same extent as Ydj1p (LU and CYR 1998b). This system has also been used to show that Hsp110 chaperones, like Sse1p, do not refold luciferase, but can act as a "holdase" to retain the substrate in a folding competent state (GOECKELER *et al.* 2002).

1.3.2 Protein translocation across membranes

Hsp70 and Hsp40 are essential for translocation into the Endoplasmic Reticulum (ER) and mitochondria. In yeast, translocation can occur either co-translationally or post-translationally. When proteins are post-translationally translocated across the ER membrane, cytoplasmic chaperones such as Ssa1p (Hsp70) and Ydj1p (Hsp40) are required to maintain the solubility of proteins before translocation. In fact, reduction of Ssa1p in the *SSA1*, *SSA2*, *SSA4* triple knockout strain or shifting the *ydj1-151* temperature sensitive strain to a nonpermissive temperature leads to an accumulation of ER and mitochondrial pre-proteins in the cytosol (CAPLAN *et al.* 1992; DESHAIES *et al.* 1988). In addition, both co- and post- translational translocation require ER lumen chaperones such a Kar2p (Hsp70) and Sec63p (Hsp40) (BRODSKY *et al.* 1995). Accumulation of preproteins has also been seen in yeast containing thermosensitive alleles in *kar2* and *sec63* (ROTHBLATT *et al.* 1989; VOGEL *et al.* 1990). In fact, Sec63p is a dedicated translocation-specific J-protein. Other ER luminal J-proteins, Scj1p and Jem1p, do not appear to play a role in translocation as yeast containing mutations in these genes do not have translocation defects (NISHIKAWA *et al.* 2001).

1.3.3 Activation of receptors/kinases

Hsp90 is an essential protein in yeast and is responsible for folding numerous clients. In fact, the Protein Kinase C (PKC) signaling pathway appears to be regulated by Hsp90. A yeast two hybrid screen was performed to identify Hsp90 clients using the yeast Hsp90 isoform, Hsp82, which contained the E33A mutation as bait. This mutation inhibits ATPase activity and prevents client protein release. This screen identified many known Hsp90 cochaperones, including

Ydj1p, Sba1p (HOP), and Sti1p (HIP) (MILLSON *et al.* 2005). The authors also identified Mpk1, a downstream kinase in the PKC pathway, as a novel Hsp90 client protein. Interestingly, interaction of Mpk1p and Hsp82p increased after heat shock and mutation of Hsp82p led to decreased Mpk1p transcription (MILLSON *et al.* 2005). These results suggest that Hsp90 is required for Mpk1p activation and links transcription of PKC pathway targets to the heat shock response.

S. cerevisiae can also be used as a model system to analyze hormone receptor folding in *vivo*. The folding requirements of androgen receptor (AR) (CAPLAN *et al.* 1995), estrogen receptor (ER) (PICARD *et al.* 1990), and glucocortocoid receptor (GR) (PICARD *et al.* 1990) have been determined using yeast genetics. For example, the Yamamoto lab showed that Hsp82p was required to hold GR and ER in a folding competent state *in vivo* (PICARD *et al.* 1990). Ydj1p and Sse1p are also required for maximal receptor activation *in vivo* (CAPLAN *et al.* 1995; GOECKELER *et al.* 2002).

1.3.4 Multiprotein complex rearrangement

One of the best characterized roles of Hsp70/Hsp40 in multiprotein complex rearrangement is the removal of clathrin from coated vesicles (CCV). Clathrin is a vesicle coat protein used during receptor mediated endocytosis and during Golgi-sorting events (BRODSKY *et al.* 2001). Vesicle uncoating utilizes Hsp70 and a specialized J-protein, auxilin. Yeast auxilin, Swa2p, has an N-terminal clathrin binding domain, a TPR domain for Hsp70 interaction and a C-terminal J domain (GALL *et al.* 2000; PISHVAEE *et al.* 2000). Swa2p binds clathrin through the N-terminal region and recruits Ssa1p (Hsp70) via the TPR and J domains (XIAO *et al.* 2006). Indeed, the J domain of Swa2p stimulates Ssa1p ATPase activity by 20 fold (GALL *et al.* 2000). *In vitro*

studies with mammalian auxilin show that the J domain stimulates Hsp70, which then binds tightly to clathrin and leads to distortion of the clathrin structure to induce vesicle uncoating (JIANG *et al.* 2000; UNGEWICKELL *et al.* 1995).

1.4 CHAPERONES AND DISEASE

As mentioned previously, chaperones play a role in a plethora of human diseases. This section will focus on the roles of Hsp70/Hsp40 in a few select diseases.

1.4.1 Aggregation diseases

A large number of diseases are caused by the aggregation of proteins such as β Amyloid (Aβ) in Alzheimer's disease, α synuclein in Parkinson's disease, and prion protein (PrP^{Sc}) in Creutzfeldt-Jakob's disease (SELKOE 2003). Alzheimer's disease is characterized by the formation of 8-10 nm amyloid fibrils of Aβ protein with a characteristic β sheet structure (SELKOE 2004). For many years, it was debated whether the fibrils were responsible for, or a consequence of, Alzheimer's disease. It is currently hypothesized that the pre-fibril intermediates are the toxic stage of aggregate formation and that the fibrils are a protective way of sequestering the aggregation prone protein.

The currently proposed mechanism for fibril formation is that Aβ is an inherently aggregation prone protein (BOOTH *et al.* 1997). Properly folded Aβ can transition into a partially folded molten globule with exposed hydrophobic domains. These domains can interact to form organized oligomers, which then act as seeds to convert other native proteins into the

aggregation prone state. Many labs have shown that chaperones, including Hsp70 and Hsp40, are involved in preventing formation of the toxic intermediates, by binding hydrophobic patches in the molten globules and preventing their aggregation (EVANS *et al.* 2006; MUCHOWSKI *et al.* 2000; RAMAN *et al.* 2005). Thus, increased Hsp70 levels or activity may tip the equilibrium of Aβ folding/ aggregation towards folding. A recent study by the Gestwicki lab showed that Hsp70/Hsp40 and Hsp90 inhibit Aβ aggregation *in vitro* (EVANS *et al.* 2006). In fact, an Hsp70 agonist also inhibited Aβ aggregation, further suggesting that chaperone modulation could be used to treat amyloid diseases.

1.4.2 Cancer

One defining characteristic of cancer cells is a misregulation of many essential proteins, including alterations of Hsp70 and Hsp90 levels. Chaperones, including Hsp70 and Hsp90, are upregulated in various cancers including breast, lung, and cervical cancer (BONAY *et al.* 1994; CIOCCA *et al.* 1993; KIM *et al.* 1998a; MYUNG *et al.* 2004; RALHAN and KAUR 1995; VOLM *et al.* 1995; YANO *et al.* 1996). However, it is unclear if changes in expression lead to the cancerous phenotype or if these changes are in response to the cancerous phenotype. Some studies have suggested that over-expression of chaperones is sufficient for transformation. For example, Hsp70 over-expression in some primary cell lines is sufficient for transformation, and transgenic mice constitutively over-expressing Hsp70 develop T-cell lymphomas (SEO *et al.* 1996; VOLLOCH and SHERMAN 1999). Other studies suggest that the reduction of Hsp70 levels by antisense RNA is sufficient to induce apoptosis (NYLANDSTED *et al.* 2000). This phenomena appears to be breast cancer cell-specific because cell lines derived from breast tissue and lung fibroblasts do not undergo apoptosis when Hsp70 levels are decreased (NYLANDSTED *et al.*

2000). Also, human hsc70 with missense mutations in the ATPase domain may be associated with sporadic breast cancer development, but the importance of this finding is unknown (BAKKENIST *et al.* 1999).

Other studies have indicated that chaperones play a protective role as increased chaperone levels may help off-set stresses such as hypoxia and chemotherapeutic treatment. In fact, Hsp70 over-expression in breast cancer tissues is correlated with increased resistance to chemotherapy and consequently poor overall prognosis (BARNES *et al.* 2001; CIOCCA *et al.* 1993; MELENDEZ *et al.* 2006). The action of Hsp70 may also be direct since Hsp70 is known to inhibit apoptosis through several mechanisms. For example, Hsp70 inactivates the activity of pro-apoptotic signaling kinases such as c-Jun N-terminal kinase (JNK1), prevents mitochondrial permeabilization and cytochrome c release, and inhibits the maturation of procaspases including procaspase-3 and procaspase-7 (GABAI *et al.* 2002; KOMAROVA *et al.* 2004; RASHMI *et al.* 2004). Prevention of apoptosis is especially problematic since many chemotherapeutic approaches are aimed at initiating apoptosis in cancer cells. Together, these facts emphasize the importance of identifying chaperone modulators as anti-cancer drugs.

1.4.3 Small molecule modulators of molecular chaperones

Despite the numerous roles of chaperones in disease, currently very few drugs are available that target molecular chaperones. Geldanamycin (GA) and GA derivatives bind Hsp90 with a much higher affinity than ADP or ATP and act as a competitive inhibitor of ATP binding (GRENERT *et al.* 1997; PRODROMOU *et al.* 1997; STEBBINS *et al.* 1997). GA is proposed to mimic the ADP bound state of Hsp90, which favors client ubiquitination and subsequent degradation (ISAACS *et al.* 2003; NECKERS 2002). For several decades, laboratory use of GA has altered a range of

tumorigenesis phenotypes, including cell growth inhibition and malignant to benign phenotypic conversion in such cells as breast cancer cells, prostate carcinoma cells, and Rous-sarcoma-infected rat kidney cells (OCHEL *et al.* 2001). While the precise mechanism of GA action is often unknown, its various effects are perhaps unsurprising considering the multitude of Hsp90 activities in the cell. For example, treatment of breast cancer, prostate cancer, and leukemia cell lines reduced the levels of mutant p53 by preventing Hsp90 from holding it in a stable complex (BLAGOSKLONNY *et al.* 1996; BLAGOSKLONNY *et al.* 1995). The Hsp90 clients $p210^{Bcr\text{-}Abl}$, HER-2, and HIF-1α are implicated in several types of cancer development. GA treatment of these cancers destabilizes the proteins and leads to their degradation, which in turn triggers apoptosis (ISAACS *et al.* 2003). However, inhibition of Hsp90 is often insufficient to treat cancer cells as the cells often compensate by over-expressing Hsp70 (BRODSKY and CHIOSIS 2006).

Until recently, 15-deoxysperagulin (DSG) was one of the few Hsp70 modulators available. DSG has been used as an immunosuppressive to inhibit kidney rejection after transplantation (TANABE *et al.* 2000). In fact, ~70% of kidney transplant patients who were treated with DSG showed an excellent or good response. However, recent studies show that other immunosuppressive regimens have a lower rate of kidney rejection (ISHIDA *et al.* 2007). DSG is probably an immunosuppressive because it interferes with the action of macrophages, cytolytic T cells, and B cells (HUGHES and GRUBER 1996). The molecular target of DSG was identified as Hsp70 using a DSG-Sepharose column. When cell lysates were applied to the column, only Hsp70 was bound to DSG in high quantities (NADLER *et al.* 1992). DSG interacts with Hsp70 with a relatively low affinity of K_D = 4 μM, but also interacts with Hsp90 at a similar affinity K_D = 5 μM (NADEAU *et al.* 1994). DSG stimulates yeast and bovine cytosolic Hsp70 steady state ATPase activity between 38 and 47%, but has no affect on the yeast ER

Hsp70, Kar2p (BRODSKY 1999). The low specificity and affinity prompted the Brodsky lab to identify a structural analog of DSG, NSC 630668-R/1 (R/1), which inhibits yeast Hsp70 ATP hydrolysis and J domain stimulation of Hsp70 in steady state ATPase assays (FEWELL *et al.* 2001). Interestingly, R/1 actually stimulates Hsp70 in single turnover assays. However R/1 has poor solubility and low affinity for Hsp70, suggesting that more potent Hsp70 modulators need to be created.

1.5 VIRUSES AND CHAPERONES

It is quite common for chaperone expression to be upregulated during the course of viral infection, as has been documented for Simian Virus 40 (SV40), Human Immunodeficiency Virus (HIV), Herpes Simplex Virus (HPV), and other viruses (SULLIVAN and PIPAS 2001). Once again, since chaperones are upregulated in response to cellular stress, it is often difficult to determine if this upregulation is in response to the stress upon viral infection or is required for the viral infection. Indeed, chaperones are involved in many aspects of the viral infection, including capsid uncoating, DNA replication, and virion assembly (SULLIVAN and PIPAS 2002). Many viruses utilize host cell chaperones for these processes, as has been discussed for λ phage, however some viruses code for their own chaperones. For example, beet yellows closterovirus (BYV) codes for an Hsp70-like protein with N-terminal ATPase activity (AGRANOVSKY *et al.* 1997), which is required for assembly of BYV virion tails (AGRANOVSKY *et al.* 1991; ALZHANOVA *et al.* 2007). Other viruses encode J-proteins which are used to corrupt host Hsp70 function. Perhaps the most studied instance of this can be found in the polyomavirus family.

These viruses code for a J domain containing protein which is essential for viral DNA replication and virion assembly.

1.5.1 General characteristics of polyomaviruses

Polyomaviruses infect a large number of organisms including humans, monkeys, rodents and birds. To date, 18 polyomaviruses have been discovered (ALLANDER *et al.* 2007; GAYNOR *et al.* 2007; JOHNE *et al.* 2005; JOHNE *et al.* 2006; PIPAS 1992). Polyomaviruses are non-enveloped DNA viruses with doubled stranded DNA genomes which code for only a few proteins (AHUJA *et al.* 2005). During polyomavirus infection, the virus enters the cells, uncoats, and releases its DNA. Polyomavirus host cells tend to be terminally differentiated, quiescent cells, which do not express the genes required for viral replication such as DNA polymerase. The early region of the polyomavirus genome is transcribed immediately after infection and includes the differentially spliced tumor antigens (TAgs) (Figure 9). In order to replicate viral DNA, TAg interferes with cell cycle regulators such as p53 and Rb to initiate the cell cycle. The late region of the viral genome includes the viral coat proteins, VP1, VP2, and VP3 and is transcribed late in infection after the viral DNA has been replicated. Finally, the DNA is assembled into the capsid, host cells are lysed, and the viral progeny infect surrounding cells.

Four human polyomaviruses have been identified. BK virus (BKV) and JC virus (JCV) were named for the original patients from whom the viruses were isolated (GARDNER *et al.* 1971; PADGETT *et al.* 1971). The newly identified KI polyomavirus (KIPyV) and WU virus (WUV) were named for the Karolinska Institutet and Washington University School of Medicine, respectively, where the viruses were identified (ALLANDER *et al.* 2007; GAYNOR *et al.* 2007). In addition, SV40 was a contaminant of the original polio vaccine and has been studied extensively

Figure 9: Genome map for the SV40 polyomavirus.

The genome is separated into early gene products, Large TAg (LT), small tAg (sT), and 17kD TAg (17kT) and late gene products, VP1, VP2, and VP3. Figure from AHUJA *et al*. 2005.

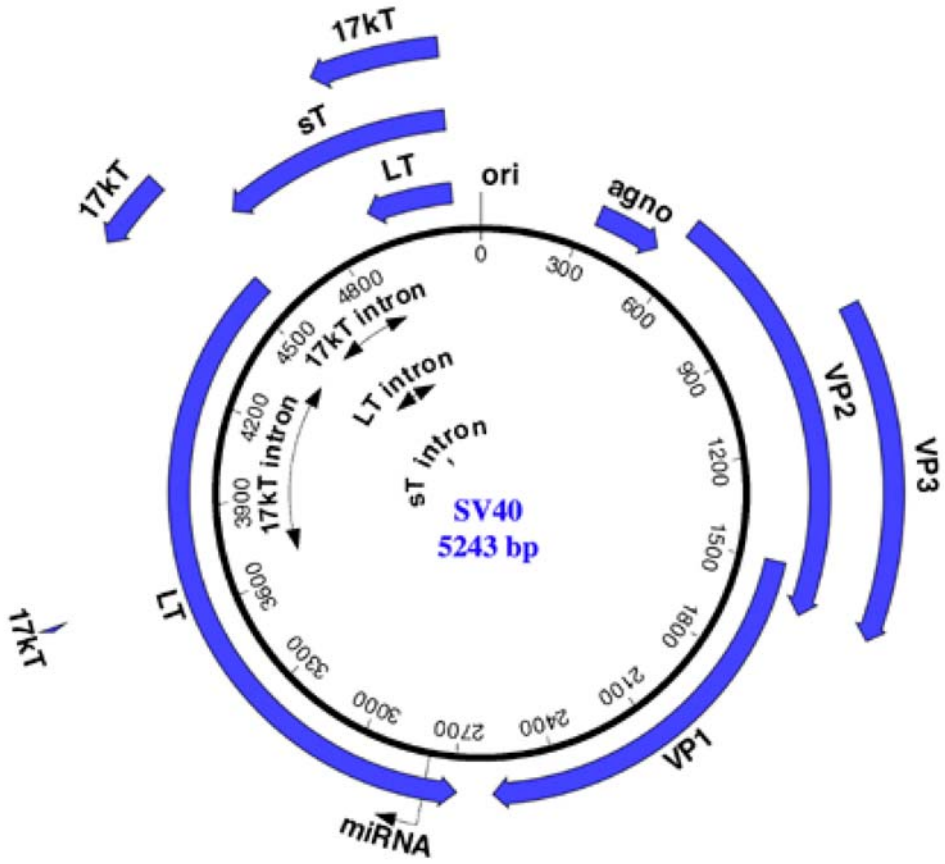
17kT
sT
LT
ori
agno
17kT
VP2
VP3
17kT intron
LT intron
sT intron
17kT intron
SV40
5243 bp
LT
17kT
VP1
miRNA
0
300
600
900
1200
1500
1800
2100
2400
2700
3000
3300
3600
3900
4200
4500
4800

since its known introduction into humans (HILLEMAN 1998). BKV and JCV have been definitively linked to kidney nephropathy and progressive multifocal leukoencephalopathy (PML), respectively and BKV, JCV, and SV40 have controversial links to human cancer (EASH *et al.* 2006; WHITE and KHALILI 2004).

1.5.1.1 BK Virus (BKV)

BKV was initially discovered in the urine of a renal transplant patient (GARDNER *et al.* 1971), but most humans have a latent infection. Nearly half of all children under the age of three express BKV antibodies, and by age ten the number approaches 100% (BARBANTI-BRODANO *et al.* 1998). These infections are usually subclinical, or cause upper respiratory or urinary tract infections. The virus sets up a persistent infection in the kidneys, but seldom produces clinical symptoms in healthy individuals. However, in immunocompromised individuals the virus can reactivate and cause kidney nephropathy (COMOLI *et al.* 2006). This is especially well-documented in kidney transplant patients taking immunosuppressive drugs, where BKV associated nephropathy (BKVAN) is a major cause of kidney failure and subsequent rejection. BKV infection has also been connected to cellular transformation in cell culture, but the relevance of these data is debated (FIORITI *et al.* 2005).

1.5.1.2 JC Virus (JCV)

JCV is also an endemic virus with ~80% of adults possessing JCV antibodies (BARBANTI-BRODANO *et al.* 1998) though JCV infections generally occur slightly later in life than BKV infections. JCV infections are also usually subclinical, though occasionally JCV infections have been correlated with chronic meningoencephalitis. After the initial infection, JCV causes a latent infection of the kidney and central nervous system (EASH *et al.* 2006). In immunosuppressed

patients, JCV can reactive and cause progressive multifocal leukoencephalopathy (PML). This disease is caused by the viral-induced destruction of myelin-producing glial cells, which leads to demyelination of the central nervous system and a variety of brain disorders and death (KHALILI *et al.* 2003). Almost all PML cases are found in HIV positive individuals and 5% of all HIV positive patients have PML (BERGER 2003). While JCV appears to transform cells in culture and cause tumors in animal models at a much higher rate than BKV infection, its role in human cancers is unclear (EASH *et al.* 2006).

1.5.1.3 KI Virus (KIPyV) and WU virus (WUV)

Little is known about the newly identified KI and WU polyomaviruses. KIPyV was discovered in donated nasopharyngeal samples that were screened for novel human viruses by random PCR amplification (ALLANDER *et al.* 2007). Further studies uncovered KIPyV in additional nasopharyngeal samples and feces, but not in urine or blood, suggesting it may not infect the kidney like other human polyomaviruses. The KIPyV genome encodes the same proteins found in the human polyomaviruses, including large and small TAg and the viral coat proteins. Currently, this virus has not been linked to any human diseases.

WUV was PCR amplified from the nasopharyngeal aspirate from a pneumonia patient and was subsequently found in other respiratory, but not urine, samples (GAYNOR *et al.* 2007). Sequence analysis indicated that WUV is most similar to KIPyV (64-71% identity between putative TAg and viral coat coding regions). Also, preliminary studies suggest WUV is most prevalent in children under three or in immunocompromised adults, though its role in human disease is unclear.

1.5.1.4 Simian Virus 40 (SV40)

The natural host of SV40 is the kidney of the *Rhesus macaque* monkey. However, the original polio virus vaccine was produced on monkey kidney cells that contained SV40 as a contaminant and as a result millions of Americans were exposed to the virus. Shortly after its discovery as a contaminant of the vaccine, SV40 was found to induce tumor formation in newborn baby hamsters that are immunocompromised and is actually among the most oncogenic polyomaviruses in mouse model systems. However, to date, no definitive link between human cancers and SV40 has been established (POULIN and DECAPRIO 2006b). Because SV40 TAg is sufficient to cause tumorigenesis in some cell lines (CHEN *et al.* 1992; IBARAKI *et al.* 1998), SV40 has become a model system for human cancer research. The study of SV40 TAg has led to the elucidation of basic aspects of cell biology, including identification of the tumor suppressor p53, RNA splicing, and nuclear localization signals (CARBONE 2001).

SV40 is also a model system for the study of BKV and JCV. These viruses grow poorly in the laboratory, which makes them difficult to study or screen for potential treatments (FARASATI *et al.* 2005; KNOWLES and SASNAUSKAS 2003). Luckily, since SV40 has been studied in the laboratory for years and many *in vivo* and *in vitro* assays have been developed to characterize its pathogenesis, it can serve as a model system for BKV and JCV infections.

1.5.2 Functional domains of SV40 Large Tumor Antigen (TAg)

Three alternately spliced TAg proteins are transcribed immediately after SV40 infection, large TAg, small tag, and tiny tag. Large TAg is the 708 amino acid protein that contains many independently folding domains that allow this single protein to initiate the cell cycle and viral

DNA replication upon infection (Figure 10). Unless otherwise stated, all references to TAg in this document refer to SV40 large TAg. A description of the various domains of TAg follows.

1.5.2.1 The TAg J domain

The N-terminal 102 amino acids of TAg contain a J domain, which has been shown to interact with Hsp70 (SAWAI and BUTEL 1989; SULLIVAN *et al.* 2001). This domain is also essential for DNA replication, virion assembly, and tumorigenesis (PEDEN and PIPAS 1992; PIPAS *et al.* 1983; SPENCE and PIPAS 1994b; SRINIVASAN *et al.* 1989) and mutations in the HPD motif disrupt these abilities (SRINIVASAN *et al.* 1997). Amino acids 7-117 of TAg have been cocrystallized with the pocket region (amino acids 380-772) of the retinoblastoma (Rb) tumor suppressor (KIM *et al.* 2001). The pocket domain is conserved between Rb family members and is an essential region for tumor suppressor activity. This structure shows that the J domain extends between residues 7 and 102, which is followed by a flexible linker region that binds Rb (see below). Several features unique to the TAg J domain were discovered. First, α helix I of the J domain is extended and is about twice as long as seen in other J domains. Second, the J domain contains an extended loop between helix III and IV that faces the Rb binding pocket (KIM *et al.* 2001). It is unclear why TAg has this loop in the J domain, but it may in part be responsible for binding to other proteins.

Consistent with this hypothesis, prior coimmunoprecipitation studies showed that large proteins of 185 kDa and 193 kDa interact with the TAg N terminus (KOHRMAN and IMPERIALE 1992; TSAI *et al.* 2000). The DeCaprio lab showed that p185 and p193 were identical and had homology to the E3 ubiquitin ligase Cul7 from the cullin family of proteins (ALI *et al.* 2004) which binds TAg through residues 69-83 in the extended loop domain (KASPER *et al.* 2005).

Figure 10: Structural representation of the TAg monomer.

The J domain (DnaJ), origin binding domain (obd), zinc binding domain (Zn-D), and ATPase domain (AAA+) are combined from previous NMR and crystal structures. Dotted lines represent linker regions between the domains with unknown structure. No structural information is available for the Host Range Domain, which is represented in yellow. Figure from GAI *et al*. 2004.

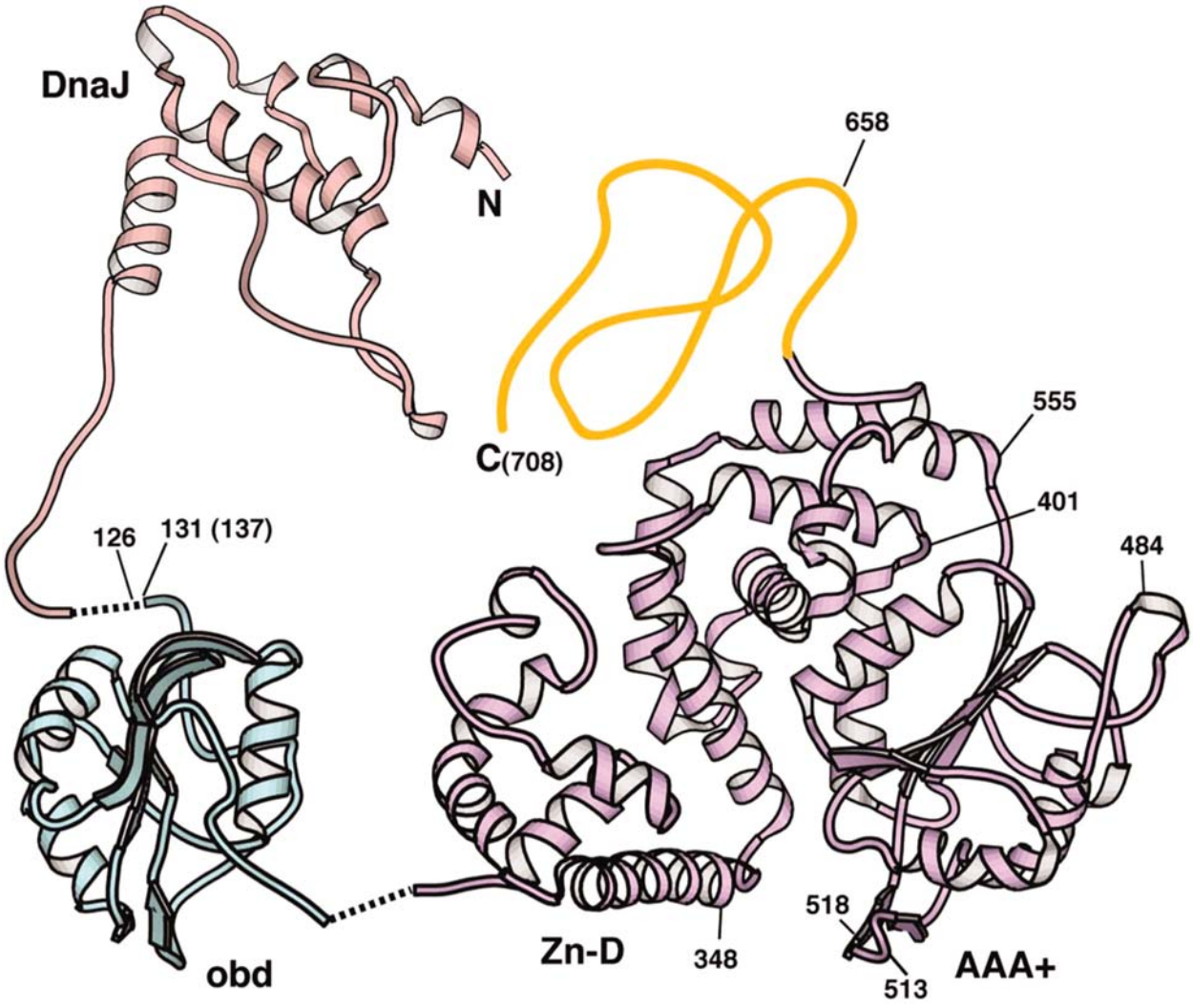
DnaJ
N
658
C(708)
555
401
484
126
131 (137)
obd
Zn-D
348
518
513
AAA+

Cullins are scaffolds for the SCF multi-component complex that functions as an E3 ubiquitin ligase with Skp1 and F-box proteins. Like other cullins, Cul7 binds the ring domain containing protein Roc1, the F-box protein Fbx29, and Skp1 to form an SCF-like complex (DIAS *et al.* 2002). TAg's interaction with Cul7 is important for transformation, and is independent of other known interactions in the TAg N terminus (ALI *et al.* 2004; KASPER *et al.* 2005; KOHRMAN and IMPERIALE 1992).

Like other J domains, the TAg J domain has specificity in its interactions with Hsp70 chaperones as shown by *in vivo* domain swap experiments and biochemical analysis. The TAg J domain can functionally replace the J domains of *E. coli* DnaJ and *S. cerevisiae* Ydj1p (FEWELL *et al.* 2002; KELLEY and GEORGOPOULOS 1997). In addition, the TAg J domain stimulates the ATPase activity of mammalian and yeast Hsp70 *in vitro* (SRINIVASAN *et al.* 1997). Also, if the TAg J domain is replaced by the J domain of JCV TAg, which is 75% identical (PIPAS 1992) or the J domains of human J-proteins DNAJ2 and HSJ1, these chimeric proteins can substitute for TAg in *in vivo* assays (CAMPBELL *et al.* 1997; SULLIVAN *et al.* 2000b) However, not all J domains can substitute for the TAg J domain as the J domain of DnaJ and Ydj1p are unable to support SV40 viral replication or cellular transformation (SULLIVAN *et al.* 2000b).

1.5.2.2 The N-terminal flexible linker domain

The N-terminal linker of TAg consists of residues 103-134. Despite its small size, several protein interaction sites and the nuclear localization sequence are found in this region. One of the best characterized TAg targets is the protein associated with Retinoblastoma (Rb), and Rb family members, p130 and p107. TAg binds Rb via a consensus Rb binding motif, LxCxE, at residues 103-107 (DECAPRIO *et al.* 1988). Rb binds to the transcription factor E2F, and acts as a repressor, preventing cell cycle progression. TAg binds to Rb and releases E2F from Rb to allow

E2F dependent transcription of S phase genes. It was initially proposed that TAg sequestered Rb and prevented it from inhibiting E2F activity. However, since both the LxCxE motif and a functional J domain are required to inhibit Rb, the chaperone model for E2F release was proposed (Figure 11) (BRODSKY and PIPAS 1998). In this model, TAg forms a complex with Rb/E2F and Hsp70 through the LxCxE motif and the J domain. The J domain stimulates Hsp70 ATP hydrolysis, and the resulting energy is used to release E2F from Rb. Much experimental evidence supports this theory. First, TAg does not compete for E2F binding with Rb since the LxCxE and E2F binding sites are unique (KIM *et al.* 2001). Second, TAg, Rb, and E2F can form a stable complex (SULLIVAN *et al.* 2000a). Third, addition of Hsp70 and an ATP regenerating system releases E2F from Rb in an ATP dependent mechanism (SULLIVAN *et al.* 2000a). Fourth, a D44N in the TAg J domain or mutation of the LxCxE motif inhibits E2F release from Rb (SULLIVAN *et al.* 2000a).

Another TAg target is Bub1, a protein kinase involved in chromatid segregation during mitosis and that functions as a checkpoint for mitosis. Bub1 was discovered via yeast two hybrid and co-immunoprecipitation experiments to interact with TAg (COTSIKI *et al.* 2004). Bub1 interacts with TAg residues 89-97, probably through a conserved WEXWW sequence, found in almost all large TAgs. The Bub1 interaction with TAg is potentially important for transformation, since TAg mutants that do not bind to Bub1 are defective for inhibiting cellular transformation (COTSIKI *et al.* 2004). This interaction may allow TAg to bypass a spindle checkpoint and proceed into mitosis.

An unknown phosphatase is also predicted to bind to the N terminus of TAg. During G_0 and G_1 phase of the cell cycle, the Rb family member p130 exists in a hypophosphorylated form and is hyperphosphorylated during the G_1 to S transition. p130 is also degraded during late S

Figure 11: The chaperone model for E2F release from Rb.

In a quiescent cell, E2F dependent transcription is repressed by the tumor suppressor, Rb. Rb, E2F, Hsp70 (70), and TAg form a complex and the TAg J domain stimulates the ATPase activity of Hsp70. This energy is used to release Rb from E2F and allow synthesis of E2F-dependent genes.

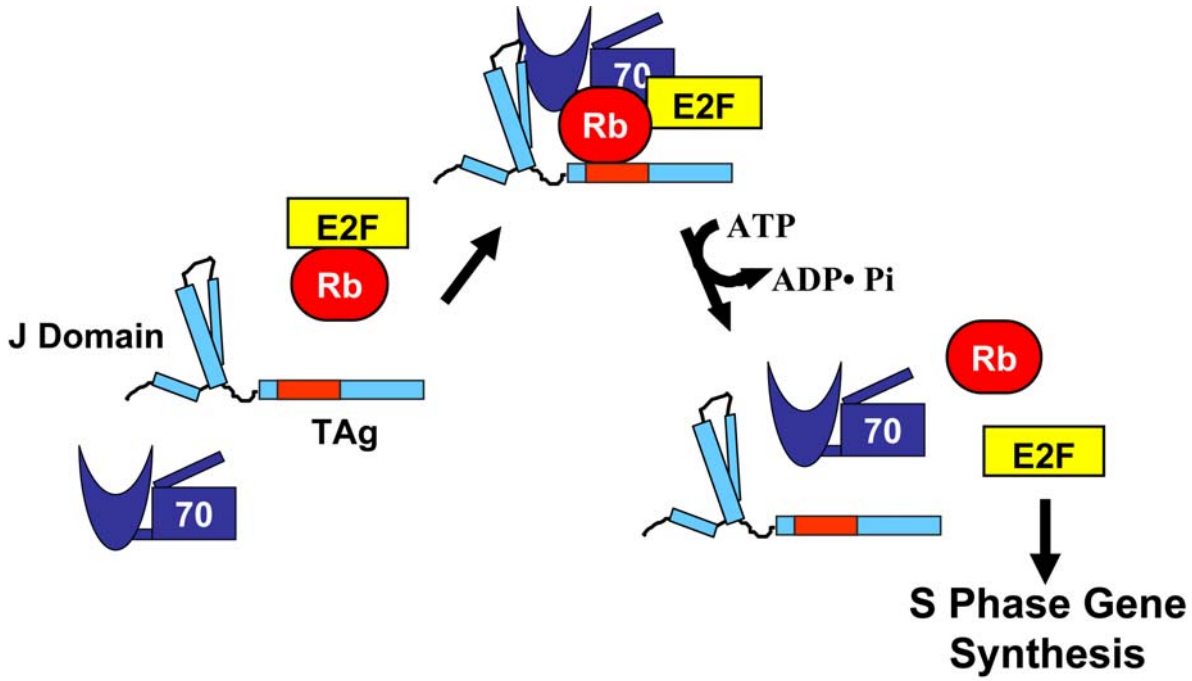
70
Rb
E2F
ATP
ADP• Pi
E2F
Rb
J Domain
TAg
70
Rb
70
E2F
S Phase Gene
Synthesis

and G_2 phase in an SCF dependent manner (TEDESCO *et al.* 2002). Expression of the TAg N-terminal region with a functional J domain and LxCxE motif is sufficient to maintain p130 in a hypophosphorylated state (STUBDAL *et al.* 1997; STUBDAL *et al.* 1996). *In vitro* experiments from the DeCaprio lab showed that this was due to the recruitment of a unknown phosphatase (LIN and DECAPRIO 2003).

Finally, the TAg nuclear localization signal (NLS) is found from amino acids 126-132 and has an extremely basic sequence, KKKRKV (KALDERON *et al.* 1984). The TAg NLS was the first NLS identified and is considered a canonical NLS. The TAg NLS binds importin α, which is responsible for transporting proteins with a canonical NLS into the nucleus (ADAM and ADAM 1994). The NLS sequence is the minimal TAg sequence that can be inserted onto a cytoplasmic protein to redirect it to the nucleus and has become a model system to study nuclear import (LANFORD *et al.* 1986).

1.5.2.3 Origin binding domain

The origin binding domain is found from amino acids 135-249 and is required for TAg to bind to the SV40 DNA origin of replication. The SV40 genome contains a 64 basepair origin of replication consisting of a central palindrome of four GAGGC basepairs flanked by an AT rich region and imperfect inverted repeats called the early palindrome. Two TAg monomers bind to pentanucleotide repeats 1 and 3 and nucleate binding of double hexamers (JOO *et al.* 1998; JOO *et al.* 1997). Assembly of the first hexamer aids in the assembly of a second hexamer to create a dodecamer through a cooperative mechanism (PARSONS *et al.* 1991). The two halves of the dodecamer are arranged in a "head to head" manner.

1.5.2.4 Zinc binding domain

The zinc binding domain is found from amino acids 250-370. This was initially identified as a zinc finger domain since it contained the conserved zinc finger motif ($Cx_2Cx_{15}Hx_3H$) in residues C302, C305, H317, and H320. Mutations in these residues, and H313, of the zinc binding domain abolish viral replication, whereas mutations in all other residues in the sequence have no phenotype (LOEBER *et al.* 1989). Recent crystallographic studies have suggested that this domain does not have the typical zinc finger structure, but instead appears more globular (LI *et al.* 2003a). In addition, the structure confirms that C302, C305, H313, and H317 coordinate zinc. The zinc binding domain is required for hexamerization, since an N-terminal truncation that removed all amino acids through C302 abolished hexamerization but an N-terminal truncation mutant through amino acid 256 that contained an intact zinc binding motif did not (LI *et al.* 2003a). The zinc binding domain, due to its role in hexamerization, is also part of the minimal helicase domain.

1.5.2.5 ATPase and p53 binding domain

The ATPase/p53 binding domain is located between residues 371-624 and is essential for both viral replication and transformation. The ATPase domain is a canonical AAA+ ATPase domain, which binds and hydrolyzes ATP (BRADLEY *et al.* 1987; ERZBERGER and BERGER 2006). ATP binding, but not hydrolysis, is required for hexamerization (MASTRANGELO *et al.* 1989). Structural studies indicate that the TAg hexamer exists in an "all or none binding mode" in which all subunits exist in the same state: ATP bound, ADP bound, or nucleotide free (GAI *et al.* 2004). This suggests a concerted mechanism for ATP hydrolysis and ADP release. In contrast to hexamerization, ATP hydrolysis is required for TAg helicase activity (MASTRANGELO *et al.* 1989).

The ATPase domain overlaps with the p53 binding domain. Early mapping studies suggested that the interaction of p53 with TAg was bipartite, and requires residues 350-450 and 550-650 (KIERSTEAD and TEVETHIA 1993). However, recent structural studies suggest this assignment is artificial, and the residues required for p53 binding cluster together (LI *et al.* 2003a). Also, the p53 residues important for TAg interaction cluster on the same side of the structure as the p53 DNA binding domain. This suggests a simple model for how TAg prevents p53 from binding to promoters: TAg binds and prevents p53 from interacting with the promoters directly (LI *et al.* 2003a). However, it is unlikely to be this simple because several studies suggest that the J domain is also involved in p53 disruption, though the mechanism is not well understood (QUARTIN *et al.* 1994; RUSHTON *et al.* 1997).

1.5.2.6 Linker domain and host range domain

Following the ATPase domain is a C-terminal linker domain (625-669) found in only a few polyomavirus TAgs. This domain has no known biological role (PIPAS 1992). At the extreme C-terminus is the host range domain (670-708), which is required for SV40 growth in some cell lines. Wild type SV40 can replicate in BSC40 and CV-1 monkey kidney cell lines. However, mutations in the host range domain prevent viral replication in CV-1 cells but have no effect on SV40 growth in BSC40 cells (PIPAS 1985). In addition, viruses with host range mutations are cold sensitive and cannot grow in either of the cell lines at 32°C (PIPAS 1985). It is believed that host range mutations prevent proper virion assembly (SPENCE and PIPAS 1994a). Recent studies have defined an acetylation site in the host range domain at K697 which is not required for host range function (POULIN and DECAPRIO 2006a).

1.5.3 SV40 replication

SV40 DNA replication is a complicated task that requires most TAg domains. TAg associates with the SV40 origin of replication via the origin binding domain. ATP binding to the ATPase domain aids in high affinity binding to the *ori* and allows hexamerization and dodecamer assembly at the origin (MASTRANGELO *et al.* 1989). The central cavity of TAg hexamers is positively charged, possibly aiding in the interaction with DNA (LI *et al.* 2003a). The TAg hexamer partially melts the DNA and associates with proteins required for replication including topoisomerase, replication protein A (RPA), and DNA polymerase α primase (pol-prim). After replication is initiated, a "polymerase switch" occurs and pol-prim is replaced by RF-C, PCNA, and DNA polymerase δ (YUZHAKOV *et al.* 1999). The TAg dodecamer then acts as a helicase, hydrolyzing ATP, and unwinding the DNA. To explain how TAg acts as a helicase, the Chen lab has proposed an "iris hypothesis" in which ATP hydrolysis is coupled to DNA melting (LI *et al.* 2003a). Indeed, structural studies show several distinct structures of TAg that have different central channel widths and a slight twist of the zinc binding domain relative to the ATPase domain. Conversion between these structures would expand and contract the central pore and twist the zinc binding domain relative the ATPase domain and TAg uses this twisting motion to melt the DNA.

The TAg J domain is also essential for viral DNA replication *in vivo*, but its role is currently unclear. Most mutations in the J domain lead to reduced DNA synthesis by the virus and little virus production (COLLINS and PIPAS 1995; PEDEN and PIPAS 1992). However, in an *in vitro* replication assay, J domain mutants still replicate DNA (COLLINS and PIPAS 1995; WEISSHART *et al.* 1996). Hsp70 is not required for a replication assay with minimal, purified,

components and addition of Hsp70 does not improve reaction efficiency (SULLIVAN and PIPAS 2002). Further study is needed to understand this discrepancy.

1.5.4 Screen for novel TAg J domain mutants

In order to better understand the role of the TAg J domain in viral replication and transformation, Sheara Fewell in the Brodsky lab screened for novel TAg J domain mutants using a TAg J domain-Ydj1p chimeric protein (T-Ydj1p) (FEWELL *et al.* 2002). Random PCR mutagenesis of the TAg J domain and yeast recombination into a *YDJ1* C-terminal gapped vector was used to identify 14 temperature sensitive point mutations in helix II and III of the TAg J domain. Many of the residues were in conserved residues that were known to contact Hsp70 through NMR perturbation and other mutational studies (Figure 12).

To better understand the molecular impact of the mutations, two solvent exposed mutations in the J domain were chosen for further study. H42R is in the HPD motif and is predicted to interact with Hsp70. K53R is on helix III and is not perturbed by Hsp70 binding. A buried mutation in helix II predicted to disrupt the structure was also chosen, but the mutant was unstable. When the H42R and K53R mutation were introduced into the SV40 genome, the virus was unable to replicate in BSC40 cells or transform a rodent cell line. In addition, purified TAg containing either the H42R or K53R mutation was defective for stimulating Hsp70 ATP hydrolysis or dissociating Rb/E2F complexes. Together, this analysis showed that chaperone function of TAg is directly related to virus function. Since K53R is on helix III of the J domain, which is not predicted to interact with Hsp70 but is essential for J domain activity, it could potentially interact with an unknown protein that affects TAg chaperone activity. It is

Figure 12: A yeast screen uncovers novel TAg J domain mutations.

The mutants identified in the yeast screen (FEWELL *et al*. 2002) were mapped onto the structure of DnaJ. The N-terminus is represented in red and the HPD is represented in purple. The residues shown in yellow and green are perturbed by Hsp70 binding by NMR studies (GREENE *et al*. 1998), and a subset of these residues were mutated in the screen (green). The blue residues were additional residues that were mutated in the screen. The DnaJ residues Y25, H33, and K48 correlate with Y34, H42, and K53 in the TAg sequence. The DnaJ ribbon diagram was adapted from CHEETHAM and CAPLAN 1998.

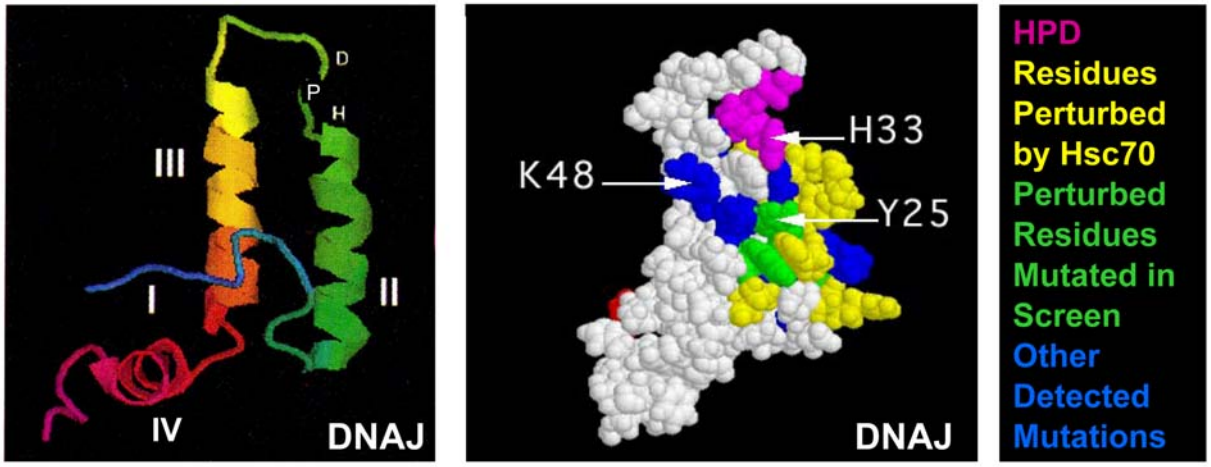
D
P
H
III
I
II
IV
DNAJ
H33
K48
Y25
DNAJ
HPD
Residues
Perturbed
by Hsc70
Perturbed
Residues
Mutated in
Screen
Other
Detected
Mutations

hypothesized that other proteins interact with the TAg J domain and aid in the release of E2F from Rb. *In vitro* release of Rb from E2F by TAg is greatly enhanced by cell lysate, suggesting that a component of the lysate aids in this reaction. Candidates for this component include cochaperones that stimulate the Hsp70 ATPase cycle, but further study is needed to discover which proteins are involved.

1.6 DISSERTATION OVERVIEW

Despite the fact that SV40 TAg has been studied for over 40 years many questions remain about how it replicates and transforms cells. One particularly important region required for both of these functions is the N-terminal J domain. Some aspects of the role of the TAg J domain in transformation have been well defined, such as the release of Rb from E2F. However, even this story is incomplete as *in vitro* reconstituted Rb/E2F release assays require cell lysate. In addition, the role of the J domain in other processes, such as viral DNA replication and virion assembly, is unclear. This dissertation sought to answer questions that still surround the roles of the TAg J domain in replication and transformation. In Chapter 2.0, I present a yeast multi-copy screen that sought to identify novel TAg J domain interacting proteins, such as the unidentified proteins in the cell lysate that aid in E2F release. Although novel TAg J domain interacting proteins were not identified from this screen, a connection between yeast chaperones and cell wall assembly was revealed. In Chapter 3.0, I discuss the identification of several classes of small molecule chaperone modulators that inhibit TAg J domain stimulation of Hsp70. Some of these compounds inhibited breast cancer cell proliferation in the low micromolar range. Finally in Chapter 4.0, I discuss the characterization of a small molecule that dramatically inhibits TAg J

domain stimulation of Hsp70 and endogenous TAg ATPase activity. This compound inhibited both SV40 replication *in vivo* and SV40 DNA synthesis *in vitro*.

2.0 THE HSP40 MOLECULAR CHAPERONE YDJ1P, ALONG WITH THE PROTEIN KINASE C PATHWAY, AFFECTS CELL-WALL INTEGRITY IN THE YEAST SACCHAROMYCES CEREVISIAE

2.1 INTRODUCTION

Despite the many decades since the discovery of SV40 TAg, much is still not known about how it transforms cells. In fact, novel TAg interacting proteins are still being identified. As described in Section 1.5.4, there is evidence that novel TAg J domain interacting proteins exist and interact through helix III of the J domain. In order to identify novel TAg J domain interacting proteins and/or to better understand the functional relationship of this domain to cellular physiology, I performed a multi-copy yeast suppressor screen to identify suppressors of the temperature sensitive phenotype of *T(K53R)-YDJ1* in *ydj1Δ* yeast. Indeed, I uncovered a link between cytosolic chaperones and the yeast cell wall.

Cell wall biogenesis is an intricate cellular process, which has been best characterized in *Saccharomyces cerevisiae* (LESAGE and BUSSEY 2006; LEVIN 2005), but surprisingly few chaperones have been directly implicated in this process. The yeast cell wall is composed of 85% polysaccharides and 15% proteins (NGUYEN *et al.* 1998), which are found in two distinct layers. The electron-transparent inner layer is composed of 80-90% β1,3-glucan chains and 1-2% chitin, which are covalently "glued" together by β1,6-glucans (NGUYEN *et al.* 1998; OSUMI

1998). In contrast, the electron dense outer layer is composed of glycosylphosphatidylinositol (GPI) and Pir glycoproteins (OSUMI 1998), which protect the cell wall and aid in cellular recognition. GPI proteins are attached to the β1,3-glucan chains via β1,6-glucan, whereas Pir glycoproteins are linked directly to β1,3-glucans. Synthesis of β1,3-glucan chains and chitin takes place at the yeast cell wall by known synthases (DOUGLAS *et al.* 1994; MAZUR *et al.* 1995; QADOTA *et al.* 1996; SANTOS and SNYDER 1997; VALDIVIA and SCHEKMAN 2003), but the location of β1,6-glucan synthesis is unknown, in part because the synthase has not yet been identified (SHAHINIAN and BUSSEY 2000).

The primary component of the cell wall is β1,3-glucan. Numerous genetic and biochemical assays suggest that Fks1p and Fks2p/Gsc2p are the catalytic subunits of the β1,3-glucan synthase. These multipass transmembrane proteins are localized to sites of polarized growth, yeast with mutations in these genes have decreased β1,3-glucan, and the *fks1Δfks2Δ* double knockout yeast strain is inviable (DOUGLAS *et al.* 1994; MAZUR *et al.* 1995). Unfortunately, *in vitro* recapitulation of β1,3-glucan synthesis has not been performed because purification of enzymatically active Fks1p and Fks2p/Gsc2p has been difficult. Fks1p is expressed during mitotic growth and may require the PKC pathway (Figure 13) for expression since Fks1p expression is dependent on Swi4p and upregulated by hyperactivated Mpk1p (IGUAL *et al.* 1996; JUNG and LEVIN 1999), both downstream components of the PKC pathway. Fks2p is expressed in the presence of limited glucose or on alterative carbon sources (MAZUR *et al.* 1995), and upon heat shock but may require the PKC pathway for continued expression (ZHAO *et al.* 1998).

The covalent linkages between the β1,3-glucan polymers is provided by β1,6-glucan. At this time, the location of β1,6-glucan synthesis is unknown. β1,6-glucan is entirely localized to

Figure 13: The canonical PKC signaling pathway.

See text for details.

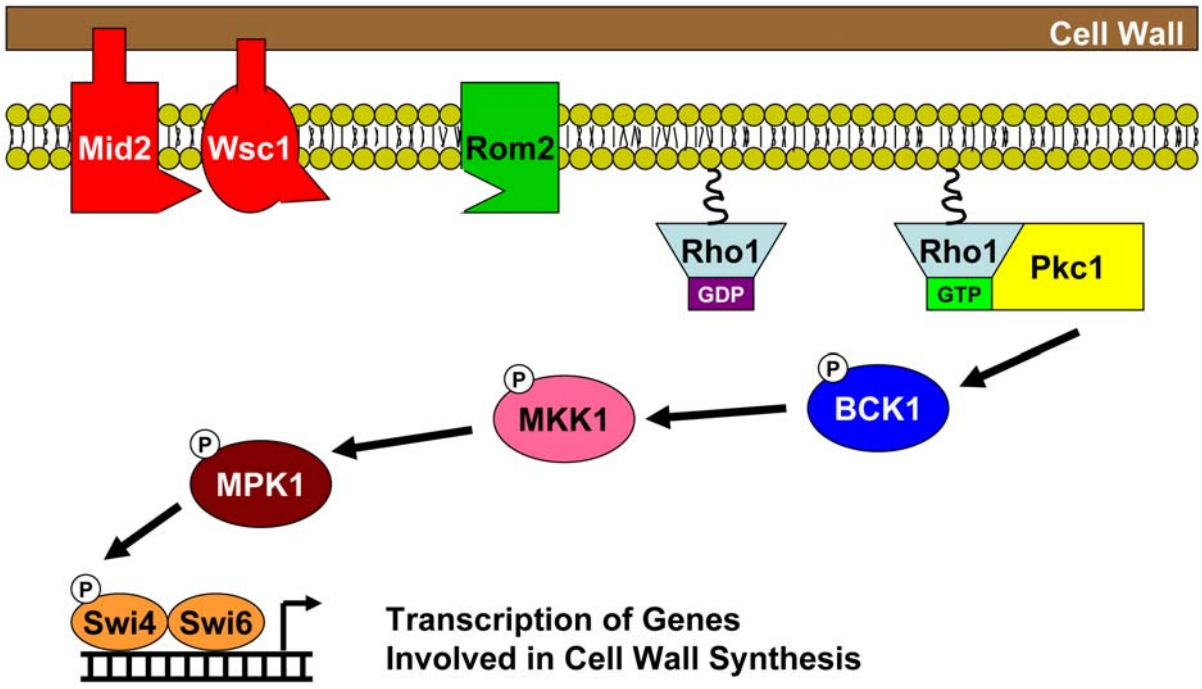
Cell Wall
Mid2
Wsc1
Rom2
Rho1
GDP
Rho1
GTP
Pkc1
P
BCK1
P
MKK1
P
MPK1
P
Swi4
Swi6
Transcription of Genes
Involved in Cell Wall Synthesis

the cell wall, suggesting it is synthesized at this site (MONTIJN *et al.* 1999). However, β1,6-glucan synthesis clearly requires the secretory pathway because a mutant allele in the gene encoding an ER luminal Hsp70, BiP, reduces the amount of β1,6-glucan at the cell wall when either of the two ER glucosidases are also disabled (SIMONS *et al.* 1998). Mutations in numerous other genes in the secretory pathway also result in reduced β1,6-glucan at the cell wall (SHAHINIAN and BUSSEY 2000). Finally, over-expression of several Golgi-resident proteins proposed to aid in β-glucan synthesis suppresses the growth defect in strains mutated for the gene encoding Pkc1p (NEIMAN *et al.* 1997; ROEMER *et al.* 1994). Thus, the current model of β1,6-glucan synthesis suggests that it is synthesized at the cell wall, but requires a protein or precursor molecule that must transit the secretory pathway.

Yeast cell wall composition is altered throughout the yeast cell cycle and in response to cell wall stress conditions. Yeast have developed three MAP kinase pathways to regulate cell wall composition and integrity, the PKC and HOG pathways and the poorly characterized SVG pathway (GUSTIN *et al.* 1998; HEINISCH *et al.* 1999; MAGER and SIDERIUS 2002). Cell wall integrity is highly regulated and it is not known how these pathways interact to maintain the cell wall. Each pathway is activated in response to complex intracellular and extracellular cues, which alters cellular gene expression. For example, the PKC pathway is induced by heat shock or hypotonic conditions whereas the HOG pathway is initiated by hypertonic conditions. It is unknown how the SVG pathway is first induced, but it has been hypothesized that it is triggered in response to mannoprotein loss (LEE and ELION 1999). Interestingly, cross-talk between the signaling pathways is common. For example, many of the signaling proteins are shared between the HOG and SVG pathway, but separate responses can be detected. Also, the PKC pathway is inhibited during conditions in which the HOG pathway is activated, and it has been hypothesized

that the SVG pathway takes over for the PKC pathway once the HOG pathway is activated (MAGER and SIDERIUS 2002). In addition, genetic data suggest that the PKC and SVG pathway have overlapping functions. For example, inactivation of the SVG and PKC pathways leads to synthetic growth defects (LEE and ELION 1999). However, inactivation of the HOG and PKC pathways does not cause a growth defect.

The PKC pathway is the primary signaling pathway responsible for maintenance of cell wall integrity (Figure 13) (GUSTIN *et al.* 1998). In *Saccharomyces cerevisiae*, there is only one gene encoding protein kinase C (*PKC1*). During the normal cell cycle, Pkc1p plays a role in cell wall synthesis of the growing bud. The PKC pathway also maintains cell wall integrity during heat shock, hypotonic stress, and after exposure to cell wall-damaging drugs, and is activated during polarized cell growth, such as during shmoo formation, bud growth, and upon actin perturbation (LEVIN 2005). It is proposed that detection of cell wall stress occurs through transmembrane proteins such as Mid2p and Wsc1p, which perform redundant functions, but do not share any sequence identity. Mid2p and Wsc1p extend an extracellular domain, which is extensively modified by O-mannosylation, into the cell wall (PHILIP and LEVIN 2001; RAJAVEL *et al.* 1999). It is hypothesized that this domain interacts with carbohydrates in the cell wall and senses cell wall stress. This is relayed to the cytoplamic region of the proteins which interact with the nucleotide exchange factor Rom2p (and possibly Rom1p). Rom2p is responsible for the removal of GDP from Rho1p which allows subsequent GTP rebinding. This activated form of Rho1p then activates Pkc1p and initiates a kinase cascade through Bck1p (MAPKKK), Mkk1p and Mkk2p (MAPKK), and Mpk1p/Slt2p (MAPK), which then phosphorylates two transcription factors, Rlm1p and Swi4p (MADDEN *et al.* 1997; WATANABE *et al.* 1995). Rlm1 activates genes that encode for components of the cell wall and factors responsible for cell wall synthesis and the

SBF complex (Swi4p and Swi6p) activates G1/S specific cell wall genes (JUNG and LEVIN 1999; SPELLMAN *et al.* 1998).

In this chapter, I describe the results of the yeast multi-copy suppressor screen in *ydj1Δ* yeast expressing a *T-YDJ1* construct with the K53R mutation [*T(K53R)-YDJ1*]. I identified the yeast Hsp70, Ssa1p, as a suppressor of the K53R allele. This indicates that the screen can identify proteins that interact with the TAg J domain (SRINIVASAN *et al.* 1997). I also uncovered a previously unknown connection between Ydj1p and yeast cell wall biogenesis. Specifically, I observed cell wall defects in *ydj1Δ* and Hsp90 temperature sensitive mutants, and discovered that up-regulation of the Protein Kinase C (PKC) pathway can rescue these defects. These studies are the first to implicate cytosolic Hsp40 chaperones in maintenance of the yeast cell wall. This chapter also includes a description of several mammalian proteins tested for their genetic interaction with the TAg J domain and the identification of a novel bacterial J-protein, HopI1.

2.2 MATERIALS AND METHODS

2.2.1 Yeast strains and methods

S. cerevisiae yeast strains used in this chapter are listed in Table 2. Unless otherwise indicated all yeast cultures were grown in yeast extract-peptone-dextrose (YPD) or selective synthetic complete medium (SC) with 2% glucose at room temperature or at 26° (ADAMS *et al.* 1997). Cell wall phenotypes were tested on YP or SC-ura medium with the addition of 0.4 M NaCl, 1 M sorbitol, or 20 μg/mL calcofluor white (CW), and 2% glucose. Yeast transformation was performed by the lithium acetate procedure (ITO *et al.* 1983). For all serial dilutions, overnight

Table 2: Yeast strains utilized during this study

Yeast Strain	Genotype	Source
W303	*MATα ade2-1 leu2-3,112 his3-11,15 trp1-1ura3-1 can1-100*	This lab
ydj1-151	*MATα ade2-1 leu2-3,112 his3-11,15 trp1-1 ura3-1 can1-100 ydj1-2::HIS3 LEU2::ydj1-151*	CAPLAN *et al*. 1992
ACY95b	*MATα ade2-1 leu2-3,112 his3-11,15 trp1-1 ura3-1 can1-100 ydj1-2::HIS3 pAV4*	CAPLAN *et al*. 1992
JN516	*MATα leu2-3,112 his3-11,15 ura3-52 trp1-Δ1 lys2 SSA1 ssa2::LEU2 ssa3::TRP1 ssa4::LYS2*	BECKER *et al*. 1996
JB67	*MATα leu2-3,112 his3-11,15 ura3-52 trp1-Δ1 lys2 ssa1-45::URA3 ssa2::LEU2 ssa3::TRP1 ssa4::LYS2*	BECKER *et al*. 1996
p82a	*MAT**a** ade2-1 leu2-3,112 his3-11,15 trp1-1 ura3-1 can1-100 hsc82::LEU2 hsp82::LEU2 pTGPD-HSP82*	NATHAN and LINDQUIST 1995
G313N	*MAT**a** ade2-1 leu2-3,112 his3-11,15 trp1-1 ura3-1 can1-100 hsc82::LEU2 hsp82::LEU2 pTGPD-HSP82-G313N*	FLISS *et al*. 2000
G170D	*MAT**a** ade2-1 leu2-3,112 his3-11,15 trp1-1 ura3-1 can1-100 hsc82::LEU2 hsp82::LEU2 pTGPD-HSP82-G170D*	NATHAN and LINDQUIST 1995
STI1/SSE1	*MAT**a** GAL2 his2-11,15 leu2-3,112 lys1 lys2 trp1Δ1 ura3-52*	NICOLET and CRAIG 1989
sti1Δsse1Δ	*MAT**a** GAL2 his2-11,15 leu2-3,112 lys1 lys2 trp1Δ1 ura3-52 sti1::HIS3 sse1::KANR*	LIU *et al.* 1999

cultures were diluted back to early log phase (0.3-0.4 OD) and allowed to grow 2-5 hrs. Cell densities were normalized to the lowest OD and cells were serially diluted ten-fold. Unless specifically indicated, all growth assays were performed at 26°, 30°, 35°, and 37° for 3-7 days.

2.2.2 Molecular techniques

All plasmids used in this chapter are listed on Table 3. *T-YDJ1* and *T(K53R)-YDJ1* constructs were derived from the pOW4 *T-YDJ1* plasmid, which is derived from plasmid YCplac33 (GIETZ and SUGINO 1988) and contains the *T-YDJ1* chimeric gene (FEWELL *et al.* 2002) expressed from the alcohol dehydrogenase 1 (*ADH*) promoter. This chimera consists of amino acids 1-82 of T antigen, which encompasses most of the J-domain, and amino acids 71-409 of Ydj1p, which contains the Glycine/Phenylalanine-rich and zinc finger-like regions and thus the putative substrate binding domain (FAN *et al.* 2005; JOHNSON and CRAIG 2001; KIM *et al.* 2001). pOW4 *T(K53R)-YDJ1* was created with the Quikchange Site-directed Mutagenesis Kit (Stratagene) using pOW4 *T-YDJ1* as a template. *GPD*314 was created by removing the strong glycerol 3-phosphate dehydrogenase (*GPD*) promoter, Multiple Cloning Site, and *CYC1* terminator from *GPD*425 with *Sac*I and *Kpn*I and inserting it into similarly digested pRS314. The pOW4 *T-YDJ1* and pOW4 *T(K53R)-YDJ1* vectors were digested with *Eco*RI and *Xho*I and the ~1.2 kb inserts were ligated into p*GPD*314 and p*TEF414* (MUMBERG *et al.* 1995) to create *GPD*314 *T-YDJ1*, *GPD*314 *T(K53R)-YDJ1*, *TEF*414 *T-YDJ1* and *TEF*414 *T(K53R)-YDJ1*. *TEF*414 contains the moderate Translational Elongation Factor (*TEF*) promoter. *TEF*414 *T(H42R)-YDJ1* was created with the Quikchange Mutagenesis Kit using *TEF*414 *T-YDJ1* as a template. The inserts in all constructs were subjected to DNA sequence analysis. An additional mutation, D127G, was detected in all constructs at nucleotide 380 in a non-conserved residue between the

Table 3: Plasmids used in this study

Plasmid	Gene	Vector	Reference/Source
pCMS02-T-YDJ1	*T-YDJ1*	*pOW4*	WRIGHT *et al.* 2007
pCMS08-T(K53R)-YDJ1	*T(K53R)-YDJ1*	*pOW4*	WRIGHT *et al.* 2007
pCMS23-T-YDJ1	*T-YDJ1*	*pGPD314*	WRIGHT *et al.* 2007
pCMS24-T(K53R)-YDJ1	*T(K53R)-YDJ1*	*pGPD314*	WRIGHT *et al.* 2007
pCMS39-T-YDJ1	*T-YDJ1*	*pTEF414*	WRIGHT *et al.* 2007
pCMS41-T(K53R)-YDJ1	*T(K53R)-YDJ1*	*pTEF414*	WRIGHT *et al.* 2007
pCMS123-T(H42R)-YDJ1	*T(H42R)-YDJ1*	*pTEF414*	WRIGHT *et al.* 2007
pAV4	*YDJ1*	*pRS316*	CAPLAN *et al*. 1992
pCMS125-REC102	*REC102*	*pRS426*	WRIGHT *et al.* 2007
pSR6	*CHS5*	*pRS316*	SANTOS *et al*. 1997
pSR23	*CHS5*	*pRS426*	SANTOS *et al.* 1997
p1245	*MID2-HA*	*YEp352*	RAJAVEL *et al*. 1999
p1300	*MID2-GFP*	*pRS314*	RAJAVEL *et al*. 1999
YEp/STM1	*STM1*	*YEp213*	HATA *et al.* 1998
pCMS119-YLR149c	*YLR149c*	*pRS426*	WRIGHT *et al.* 2007
SYP1pRS316	*SYP1*	*pRS316*	MARCOUX *et al*. 2000
SYP1pRS426	*SYP1*	*pRS416*	MARCOUX *et al*. 2000
YEp351-SSA1	*SSA1*	*YEp351*	E. Craig
pRS426-GPD-(His)$_6$-SSA1	*SSA1*	*pGPD426*	MCCLELLAN and BRODSKY 2000
p1657	*SLG-HA*	*YEp352*	RAJAVEL *et al*. 1999
pSUS1	*SUS1*	*pRS316*	RODRIGUEZ-NAVARRO *et al.* 2004
pFW46	*CYC8*	*pRS316*	WILLIAMS and TRUMBLY 1990
pRT81	*CYC8*	*YEp24*	TRUMBLY 1988
pCMS118-CIS1	*CIS1*	*pRS426*	WRIGHT *et al.* 2007
pSKN1-IV	*SKN1*	*YCp50*	ROEMER *et al*. 1993
pThi4ura3	*THI4*	*pRS416*	SINGLETON 1997
pFR22 (YEpU-PKC1)	*PKC1*	*YEp352*	ROELANTS *et al*. 2004
pDLB759	*BCK1*	*YEp352*	D. Lew/D. Levin
pRS314 BCK1-20	*BCK1-20*	*pRS314*	LEE and LEVIN 1992
pCMS147-BCK1-20	*BCK1-20*	*pRS426*	WRIGHT *et al.* 2007
pDLB823	*MKK1*	*pRS314*	HARRISON *et al*. 2004
pDLB824	*MKK1^{DD}*	*pRS314*	HARRISON *et al*. 2004
pCMS148-MKK1^{DD}	*MKK1^{DD}*	*pRS426*	WRIGHT *et al.* 2007
pDLB758	*MPK1*	*YEp352*	D. Lew/D. Levin
pNC267	*STE7-myc*	*2μ, CYC1*	ZHOU *et al*. 1993
YEp352-Kss1	*KSS1*	*YEp352*	MA *et al*. 1995
p181HOG1ha3	*HOG1-HA*	*YEplac181*	WINKLER *et al*. 2002
pCMS155-HOG1-HA	*HOG1-HA*	*pRS426*	WRIGHT *et al.* 2007
p111PBS2	*PBS2*	*YEplac111*	WINKLER *et al*. 2002
p112PBS2	*PBS2*	*YEplac112*	I. Ota
pCMS154-Hsp82	*Hsp82*	*pRS426*	WRIGHT *et al.* 2007
pcDNA3.1-BAG-1S	BAG-1S	*pcDNA3.1*	J. Hohfeld
pCMS160-BAG-1S	BAG-1S	*pGPD426*	WRIGHT *et al.* 2007

pET-28a-HspBP1	HspBP1	*pET28a*	RAYNES *et al*. 1998
pCMS158-HspBP1	HspBP1	*pGPD426*	WRIGHT *et al.* 2007
pP28-FlagPKCη	PKCη	*pP28*	LACHMANN *et al*. 2003
pCMS159-PKCη	PKCη	*pGPD426*	WRIGHT *et al.* 2007
pRC/CMV-193	Cul7	*pRC/CMV*	TSAI *et al*. 2000
pCMS157-Cul7	Cul7	*pGPD426*	WRIGHT *et al.* 2007
JJ203	*I-YDJ1*	*pTEF414*	JELENSKA *et al*., 2007
JJ204	*I-YDJ1*	*pTEF414*	JELENSKA *et al*., 2007
JJ205	*I(HPD/QAA)-YDJ1*	*pTEF414*	JELENSKA *et al*., 2007
JJ206	*I(HPD/QAA)-YDJ1*	*pTEF414*	JELENSKA *et al*., 2007
pCMS166-I-YDJ1(03)	*I-YDJ1*	*pGPD426*	JELENSKA *et al*., 2007
pCMS167-I-YDJ1(04)	*I-YDJ1*	*pGPD426*	JELENSKA *et al*., 2007
pCMS168-I(HPD/QAA)-YDJ1(05)	*I(HPD/QAA)-YDJ1*	*pGPD426*	JELENSKA *et al*., 2007
pCMS169-I(HPD/QAA)-YDJ1(06)	*I(HPD/QAA)-YDJ1*	*pGPD426*	JELENSKA *et al*., 2007

Glycine/Phenylalanine-rich and zinc finger-like regions of *YDJ1* (CAPLAN and DOUGLAS 1991); however, the presence of this mutation did not affect the growth of yeast expressing T-Ydj1p relative to T(K53R)-Ydj1p.

The yeast genes, *REC102*, *YLR149c*, *CIS1* and *HSP82*, were amplified by PCR from genomic wild type yeast (W303) DNA with primers created against regions 50-200 bp upstream of the TATA box and 15-250 bp downstream of the stop codon. The PCR products were digested with the appropriate restriction enzymes and ligated into pRS426 (CHRISTIANSON *et al.* 1992). The sequence of each insert was confirmed by sequence analysis. pRS426 *HSP82* had an A493T mutation at a non-conserved residue in the middle region of Hsp82p. This mutation did not alter Hsp82p function since expression of the corresponding protein restored growth in the *hsp82* G170D and *hsp82* G313N temperature sensitive strains, and the protein was able to support cell growth as the only copy of Hsp82p in the cell (Figure 14). To create a high-copy *BCK1-20* expression vector, an ~6.5 kb fragment containing *BCK1-20* under the control of the endogenous promoter was removed from *pRS314BCK1-20* (LEE and LEVIN 1992) using *Xho*I and *Not*I and ligated into pRS426. A high-copy version of $MKK1^{DD}$ was created by removing an ~1.6 kb fragment containing $MKK1^{DD}$ under the control of the endogenous promoter from *pDLB824* (HARRISON *et al.* 2004) using *Eco*RI and *Sac*I and ligating this fragment into pRS426. To obtain the pRS426 *HOG1-HA* expression plasmid, an ~2.5 kb fragment containing *HOG1-HA* under the control of the endogenous promoter was PCR amplified from *p181HOG1ha3* (WINKLER *et al.* 2002) and ligated into pRS426. The *HOG1* PCR primers encompassed DNA ~125 bp upstream of the TATA box and introduced two stop codons immediately downstream of the 3' HA tag.

Figure 14: *HSP82* A493T can support cell growth as the only Hsp90 in the yeast cell.

p82a yeast were transformed with *HSP82* A493T or pRS426 and transformants were selected on SC-ura-trp. Three colonies from each transformation were then restreaked onto 5-FAA to remove the plasmid encoding *HSP82*, or onto YPD, SC-trp, or SC-ura. Wild type yeast (W303) and ACY95b were also restreaked as controls and plates were incubated at 26° for 6 days. As expected all colonies grew on YPD, but the W303 strain was unable to grow on SC-trp or SC-ura and the ACY95b strain was unable to grow on SC-trp. Hsp82p A493T was able to function as the sole Hsp90 on 5-FAA compared to vector controls.

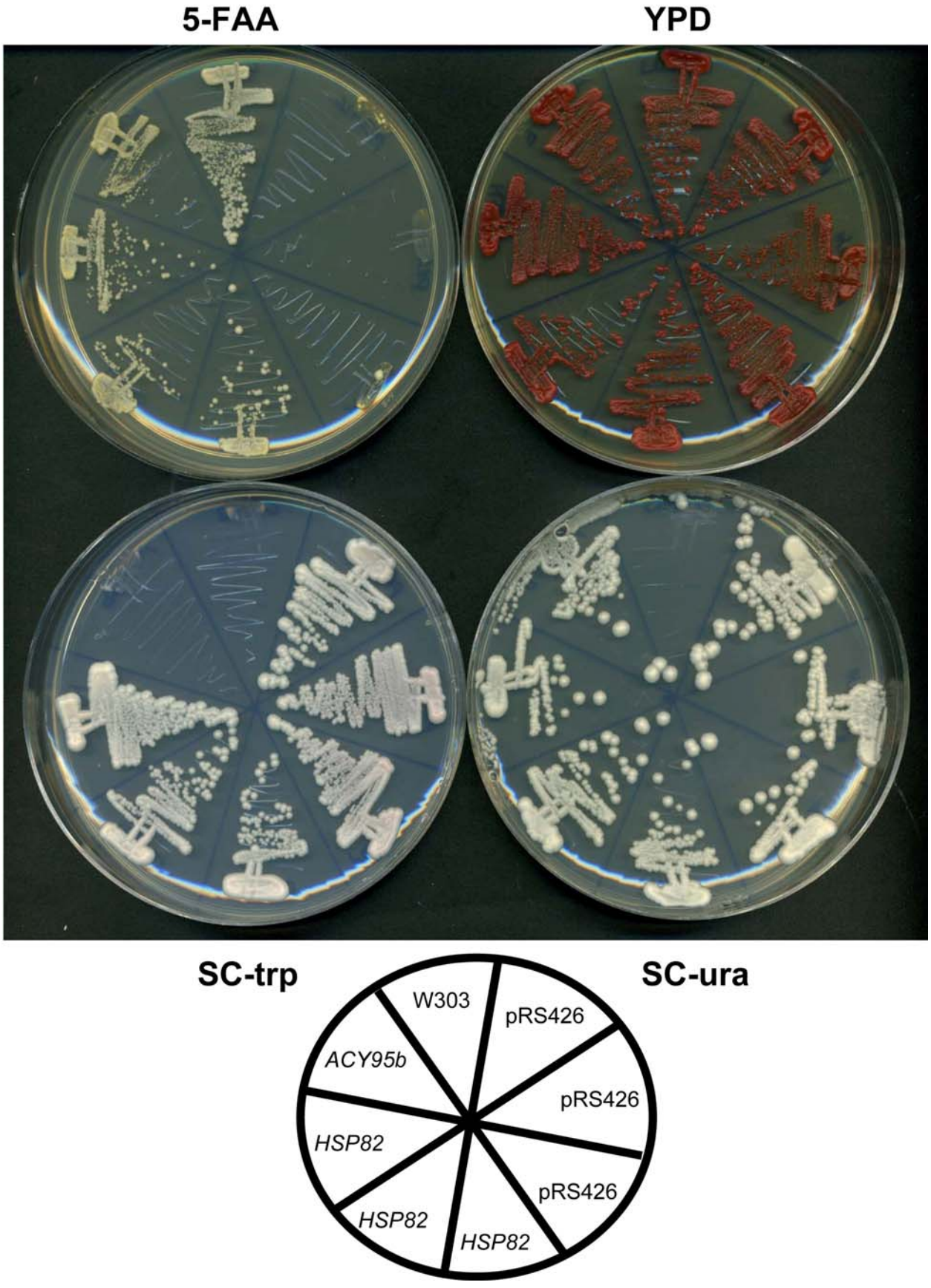
5-FAA
YPD
SC-trp
SC-ura
W303
pRS426
ACY95b
pRS426
HSP82
pRS426
HSP82
HSP82

Several mammalian genes were PCR amplified from mammalian expression vectors and inserted into the yeast expression vector, p*GPD*426. BAG-1S was PCR amplified from the *pcDNA3.1*-BAG-1S vector using primers beginning at the ATG start site and ending 10 basepairs downstream of the stop codon. The PCR product was digested with *Hind*III and *Xho*I and an ~700 basepair insert was ligated into p*GPD*426. HspBP1 was PCR amplified from *pET-28a-HspBP1* (RAYNES and GUERRIERO 1998) using primers that began at the start codon and ended 18 basepairs downstream of the stop codon. I digested with *BamH*I and *Xho*I and inserted an ~1 kb section of DNA into p*GPD*426. PKCη was PCR amplified from *pP28-FlagPKC*η (LACHMANN *et al.* 2003) using primers that began at the start codon and ended at the stop codon. The PCR product was digested with *EcoR*I and *Sal*I and an ~2 kb fragment was inserted into *GPD*426. Cul7 was PCR amplified from *pRC/CMV-193* (TSAI *et al.* 2000) using primers to the region 16 basepairs before the ATG and 24 basepairs downstream of the stop codon. This was digested with *Spe*I and *Hind*III and an ~5.5 kb insert was ligated into *GPD*426.

Two constructs that contained the HopI1 J domain were created. The TAg J domain was removed from *TEF*414 *T-YDJ1* by Joanna Jelenska in the Greenberg lab at the University of Chicago and replaced by the putative HopI1 J domain as described (JELENSKA *et al.* 2007) to create the *I-YDJ1* plasmids. pJJ203 codes for amino acids 355-424 of HopI1 and pJJ204 codes for amino acids 352-424 of HopI1. The pJJ205 and pJJ206 constructs contain an HPD to QAA mutation in the HPD motif from pJJ203 and pJJ204, respectively. The *I-YDJ1* genes were removed from the appropriate vectors using *EcoR*I and *Xho*I and the ~1.2 kb fragments were inserted into *GPD*426. All primer sequences used in this chapter are found in Table 4.

Table 4: Primers used in this study

Gene	Oligonucleotide	Restriction Site	Sequence (5' to 3')
TAg-H42R	SWF11	N/A	AAATGCAAGGAGTTTCGTCCTGATAAAGGAGGAG
TAg-H42R	SWF12	N/A	CTCCTCCTTTATCAGGACGAAACTCCTTGCATTT
TAg-K53R	SWF9	N/A	GAGATGAAGAAAAAATGAGGAAAATGAATACTCTG
TAg-K53R	SWF10	N/A	CAGAGTATTCATTTTCCTCATTTTTTCTTCATCTC
BAG1 -	CMS92	*Xho*I	CTACTCGAGCTGCTACACCTCACTCG
BAG1 +	CMS91	*Hind*III	CTAAAGCTTATGAATCGGAGCCAGGC
CIS1 -	CMS07	*Eco*RI	GATGAATTCGAGAGTCTCATCCATGCGGC
CIS1 +	CMS03	*Bam*HI	AGCGGATCCGACAGAAGCACCACTCTTGTGG
Cul7 -	CMS88	*Hin*dIII	CTTAAGCTTCTACCCCCAACCCCATATCC
Cul7 +	CMS87	*Spe*I	CTTACTAGTCTTCTGAGGTGCCACGATG
HOG1 -	CMS50	*Hin*dIII	CAAAAGCTTCTCTGGTTACCCTACATGG
HOG1 +	CMS49	*Sac*I	CAAGAGCTCTCACTAAGCAGCGTAATCTGGACC
HSP82 -	CMS52	*Bam*HI	GACGGATCCCCTATTCAAGGCCATGATGTTC
HSP82 +	CMS51	*Sal*I	GTTGTCGACGCTACTAAGAGGATAAGAGATGG
HspBP1 -	CMS56	*Xho*I	GACCTCGAGGCAAGAAGCCACCTGG
HspBP1 +	CMS55	*Bam*HI	CTCGGATCCATGTCAGACGAAGGCTCAAGG
PKCη -	CMS94	*Sal*I	CTAGTCGACCTAGGGTTGCAATTCTGGAG
PKCη +	CMS93	*Eco*RI	CTGGAATTCATGTCGTCTGGCACCATG
REC102 -	CMS02	*Eco*RI	GATGAATTCGGAGAACTTGAAGGGCCGACC
REC102 +	CMS01	*Bam*HI	AGCGGATCCGCGCAACAGCACGTTAGTTCACC
YLR149c -	CMS08	*Xho*I	GCTCTCGAGGGCTGAAGTTCAACATAAGTC
YLR149c +	CMS05	*Bam*HI	AGCGGATCCCAGTTAGGGCTTCCTCTACGC

Underlined characters represent the restriction site.

2.2.3 Low-copy suppressor screen in *ydj1-151*

A pilot screen for suppressors of the *T(K53R)-YDJ1* thermosensitive phenotype in the *ydj1-151* yeast was performed. pOW4 *T(K53R)-YDJ1* was transformed into the *ydj1-151* strain and expression was verified by immunoblot using the anti-TAg J domain antibody 419 (HARLOW *et al.* 1981) (Figure 15). A *CEN-TRP1* yeast genomic library in a pRS200 vector (ATCC #77164) was transformed into these cells and transformants were selected on SC–ura-trp for 3-4 days at 37°. Approximately 6,000 colonies were screened and the fastest growing 20 colonies were restreaked on SC-ura-trp. Of these, 8 colonies had improved growth compared to the vector control. The plasmid DNA was rescued from these strains and retransformed into the *ydj1-151* strain to determine if the phenotype was plasmid dependent. One plasmid partially restored growth after transformation and the plasmid DNA was sequenced at the University of Pittsburgh DNA Sequencing Facility using the T3 and T7 primers.

2.2.4 High-copy suppressor screen in *ydj1Δ*

To search for high-copy suppressors of the *T(K53R)-YDJ1* thermosensitive phenotype in *ydj1Δ* yeast, a *ydj1Δ* strain (ACY95b) containing a pRS316 derived *CEN-YDJ1* expression vector [pAV4, (CAPLAN *et al.* 1992)], was plated on 5-fluoroorotic acid (5-FOA) to select for yeast that had lost *pAV4*. The surviving *ydj1Δ* cells were then transformed with *TEF*414 *T(K53R)-YDJ1* and grown on SC-trp medium and expression of T(K53R)-Ydj1p was verified by immunoblot analysis using both the anti-TAg J domain antibody 419 (HARLOW *et al.* 1981) and an antibody

Figure 15: T-Ydj1p and T(K53R)-Ydj1p are expressed in the both the *ydj1-151* and *ydj1Δ* strains.

Cell lysates from the indicated strains were resolved by SDS-PAGE and immunoblots were performed with either an αTAg or αYdj1p antibody. Sec61p served as a loading control.

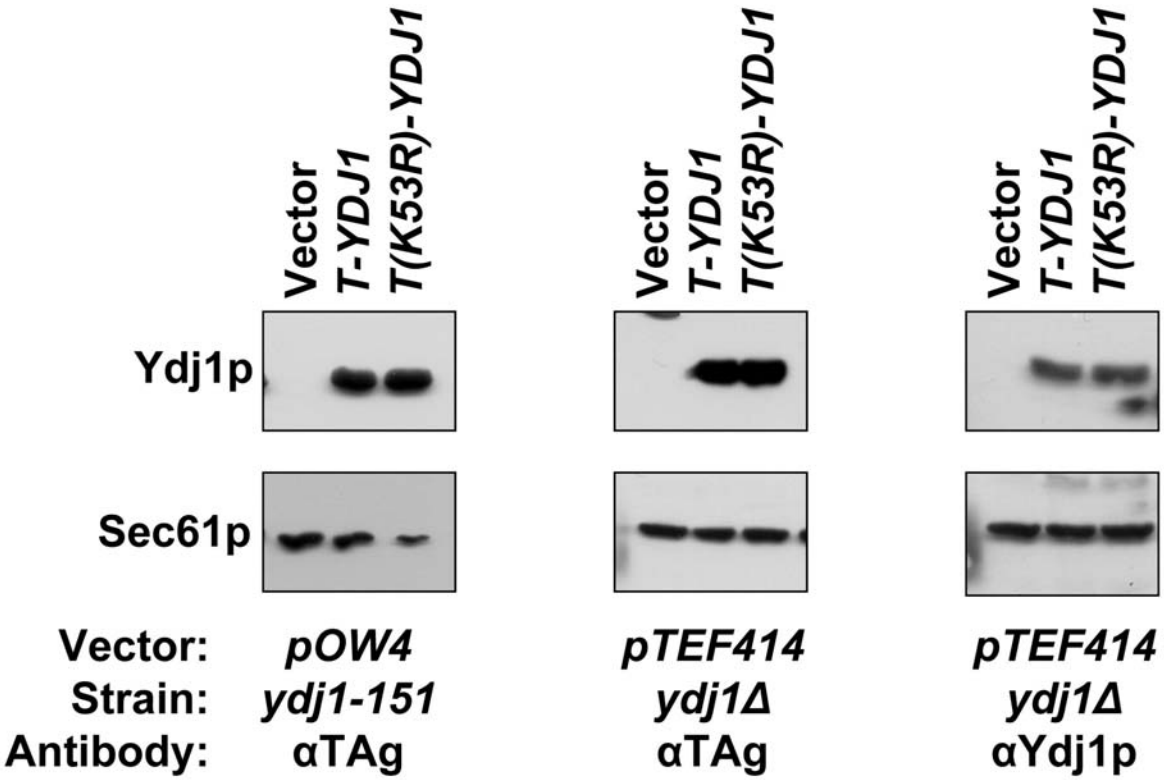
Vector
T-YDJ1
T(K53R)-YDJ1
Vector
T-YDJ1
T(K53R)-YDJ1
Vector
T-YDJ1
T(K53R)-YDJ1
Ydj1p
Sec61p
Vector: pOW4 pTEF414 pTEF414
Strain: ydj1-151 ydj1Δ ydj1Δ
Antibody: αTAg αTAg αYdj1p

against Ydj1p (CAPLAN and DOUGLAS 1991) (Figure 15). Next, a 2μ-*URA3* yeast genomic library in the YEp24 vector (CARLSON and BOTSTEIN 1982) was introduced into these cells and transformants were selected on SC-ura-trp at 35° for 4 days. Approximately 80,000 colonies were screened, and 61 colonies appeared to contain plasmids that suppressed the *T(K53R)-YDJ1* growth defect when restreaked onto SC-ura-trp at 35°. The plasmid DNA from these cells was isolated and retransformed into *ydj1Δ* yeast expressing T(K53R)-Ydj1p. Upon retransformation, 21 plasmids improved growth to varying extents. Of these, eight unique plasmids were obtained as assessed by restriction digest analysis and DNA sequence analysis from the University of Pittsburgh DNA Sequencing Facility using the primers KA109 and KA110 (kind gift from the Arndt lab, University of Pittsburgh).

2.2.5 Biochemical and immunological methods

To prepare cellular proteins for immunoblot analysis, 10 mL of yeast were grown to an OD of 0.3-0.9 in the appropriate selective medium at room temperature and the cells were pelleted and resuspended in 0.8 mL of 100 mM Tris, pH 8.0, 20% glycerol, 1 mM dithiothreitol (DTT), 1 mM phenylmethylsulfonyl fluoride (PMSF), 1 μg/mL leupeptin, and 0.5 μg/mL pepstatin A. The cells were lysed by agitation with glass beads and crude protein concentrations were determined by measuring the A_{280}. Protein concentrations in each sample were normalized and total protein was resolved by SDS-PAGE, transferred to nitrocellulose, and immunoblotted with the indicated antiserum. Antiserum against ribosomal protein L3 (a kind gift of J. Warner, Albert Einstein College of Medicine), Sec61p (STIRLING *et al.* 1992) or Gas1p (DOERING and SCHEKMAN 1996) was used to establish loading controls. Antisera against Sse1p (GOECKELER *et al.* 2002) and Ydj1p (CAPLAN and DOUGLAS 1991) were described previously. Antiserum against Hsp82p was

provided by A. Caplan, Mount Sinai School of Medicine. J. Pipas, University of Pittsburgh, provided antiserum against Cul7 originally from L. Field, Indiana University School of Medicine. Anti-Bag-1 C-16 antiserum (Santa Cruz Biotechnology) was provided by D. DeFranco, University of Pittsburgh. Antiserum against HspBP1 was provided by V. Guerriero, University of Arizona. Anti-Ssa1p antiserum was prepared by J. Brodsky, University of Pittsburgh, in rabbits using a GST-fusion protein that contained amino acids 586-831 of Ssa1p (provided by E. Craig, University of Wisconsin). Antibodies against the HA epitope were obtained from Roche and antibodies against Pkc1p were obtained from Santa Cruz Biotechnology. Bound antibodies were visualized using anti-mouse, anti-rabbit, or anti-sheep antibodies coupled to horseradish peroxidase and the Supersignal West Pico Chemiluminescent Substrate Kit (Pierce). Chemiluminescent signal was detected using a Kodak 440CF Image Station and quantified using Kodak 1D (V. 3.6) software.

2.2.6 Lyticase digestion assays

Two sets of lyticase assays were performed to compare cell wall digestion rates. The first set compared *ydj1Δ* yeast containing *pAV4* (*YDJ1*) or vector control at room temperature and the second set compared wild type (W303) to *ydj1Δ* yeast at 30°. The indicated strains were grown to exponential phase (0.4-1.0 OD). Cells were washed in water and resuspended in 100 mM Tris pH 9.4, 10 mM DTT for 10-20 min. Cells were then harvested and resuspended in lyticase buffer (0.7 M Sorbitol, 0.5% Dextrose, 10 mM Tris pH 7.4, 0.75% Yeast Extract, 1.5% Bacto Peptone) to 3 OD/mL. A total of 6 OD of each strain were incubated with or without 3µL of lyticase (SHEN *et al.* 1991). Samples were incubated at room temperature or 30° and aliquots

were removed every 5 min during a 30 min timecourse and A_{600} was determined using a spectrophotometer.

2.2.7 Immunoprecipitations

Immunoprecipitations were performed as previously described (YAM *et al.* 2005) with minor alterations. Briefly, 200 OD of cells were collected and resuspended in Buffer A (50 mM Tris pH 7.5, 10 mM HEPES pH 7.5, 100 mM KCl, 5 mM $MgCl_2$, 10% Glycerol, 0.1% Triton, 1 mM PMSF, 1 µg/mL Leupeptin, 0.5 µg/mL Pepstatin A) and lysed by glass bead lysis. The supernatant was incubated with the indicated antibody for 1 hr, followed by incubation with Protein A Sepharose (GE Healthcare) for 30 min. The beads were washed twice with Tris-buffered saline (TBS) plus 0.05% Tween and twice with TBS plus 1% Tween. Immunoblots were performed as described in Section 2.2.5.

2.2.8 Subcellular fractionation

Sub-cellular fractionation of Mid2p was performed by differential centrifugation as previously described (KABANI *et al.* 2002a) with minor changes. A total of 100 ODs of either wild type (W303) or *ydj1Δ* yeast expressing Mid2p-HA were resuspended in 2 mL PLB (20 mM HEPES, pH 7.4, 100 mM NaCl, 20 mM $MgCl_2$, 1 mM PMSF, 1 µg/mL leupeptin, 0.5 µg/mL pepstatin A) and cells were broken by glass bead lysis. Unbroken cells were removed by centrifugation at 1400 x *g* for 5 min and 1 mL of the supernatant (L) was subjected to a medium-speed spin (16,000 x *g*) for 15 min at 4°. The pellet (P1) was resuspended in 250 µL PLB and half of the supernatant (S1) was saved. The remaining supernatant was subjected to a high-speed spin

(150,000 x *g*) for 15 min at 4°. The resulting pellet (P2) was resuspended in 100 µL PLB and the remaining supernatant (S2) was saved. Total protein concentration in L, S1, P1, S2, and P2 was normalized by Coomassie Brilliant blue staining of polyacrylamide gels. The samples were resolved by SDS-PAGE, and immunoblots were performed as described above.

2.2.9 Immunofluorescence

Indirect immunofluorescence microscopy was performed as described previously (COUGHLAN *et al.* 2004). Briefly, wild type (W303) or *ydj1Δ* yeast strains over-expressing Mid2p-HA were grown to mid-log phase, fixed in 3.7% formaldehyde, and treated with 20 µg/mL zymolyase for 45 min at 37°. Cells were incubated with primary antibodies [HA 1:250 and Kar2p (BRODSKY and SCHEKMAN 1993) 1:250] overnight at 4° and in secondary antibodies (Alexa Fluor 488 goat anti-mouse 1:250, Alexa Fluor 568 goat anti-rabbit 1:250; Molecular Probes) for 2 hr at room temperature. To visualize DNA, the cells were finally incubated in 2 µg/mL 4,6-Diamidino-2-phenylindole dihydrochloride (DAPI) for 5 min at room temperature.

2.2.10 Electron microscopy

Electron microscopy was performed as previously described (KAISER and SCHEKMAN 1990). In brief, the indicated stains containing either the *MID2-HA* expression vector or YEp352 (HILL *et al.* 1986) were fixed in 2.5% glutaraldehyde, processed, sectioned, and affixed to 0.125% formvar-coated grids. Sections counterstained with uranyl acetate and Reynold's lead citrate were examined on JEM-1011 or JEM-1210 (JEOL) transmission electron microscopes. Cell wall thickness was measured using AMTv542 image capture software (Advanced Microscopy

Techniques). A total of 12-16 similarly sized, budding cells from each culture were chosen, and the cell wall thicknesses at ten points around the mother cell were measured. The average for each cell was calculated and these numbers were averaged for each culture to determine the mean cell wall thickness.

2.3 RESULTS

2.3.1 Identification of the known *ydj1-151* multi-copy suppressor, *SSE1*

The Brodsky lab previously reported on a yeast TAg expression system in which the TAg J domain replaced the homologous domain in a yeast Hsp40, Ydj1p. By PCR mutagenesis of the inserted J domain, new mutations in this domain were isolated, some of which conferred strong phenotypes when inserted into full-length TAg and into SV40 (FEWELL *et al.* 2002). One mutant allele that conferred profound phenotypes was *T(K53R)-YDJ1*. In order to understand better how specific Hsp40 mutations impact yeast cell growth, the *T-YDJ1* chimera with the K53R mutation [*T(K53R)-YDJ1*] was cloned behind two constitutive promoters, the weak alcohol dehydrogenase 1 (*ADH*) promoter and the strong glyceraldehyde-3-phosphate dehydrogenase (*GPD*) promoter, and introduced into *ydj1-151* yeast.

To determine the ideal screening protocol, several growth conditions were tested (Table 5) to identify conditions in which *ydj1-151* yeast containing *T(K53R)-YDJ1* were temperature sensitive relative to *T-YDJ1*. Coexpression of T(K53R)-Ydj1p and Sse1p was used as a positive control for suppressor identification as *SSE1* is a known suppressor of the *ydj1-151* strain (GOECKELER *et al.* 2002). In the strains containing *T(K53R)-YDJ1* behind the *GPD* promoter, no

Table 5: Initial screening conditions tested

Yeast Strain	Vector	Conditions Tested	Vectors Lacking Insert	*T-YDJ1+* vector	*T(K53R)-YDJ1+* vector	*T(K53R)-YDJ1+ SSE1*
ydj1-151	*pOW4*	26°, 3 d	+++	+++	+++	+++
ydj1-151	*pOW4*	26°, 1 d; 35° 2 d	+	+++	+++	+++
ydj1-151	*pOW4*	26°, 1 d; 37° 2 d	-	+++	++	++
ydj1-151	*pOW4*	26°, 2 d; RP, 35° 2 d	+	+++	+++	+++
ydj1-151	*pOW4*	26°, 2 d; RP, 37° 2 d	+	+++	+++	+++
ydj1-151	*pOW4*	37°, 3 d	-	+++	-	++
ydj1-151	*pGPD*	26°, 3 d	+++	+++	+++	+++
ydj1-151	*pGPD*	26°, 1 d; 35° 2 d	++	+++	+++	+++
ydj1-151	*pGPD*	26°, 1 d; 37° 2 d	-	+++	+	+
ydj1-151	*pGPD*	26°, 2 d; RP, 35° 2 d	+++	+++	+++	+++
ydj1-151	*pGPD*	26°, 2 d; RP, 37° 2 d	+++	+++	+++	+++
ydj1-151	*pGPD*	37°, 3 d	-	+++	-	-
Yeast Strain	Vector	Conditions Tested	Vectors Lacking Insert	*T-YDJ1+* vector	*T(K53R)-YDJ1+* vector	*T(K53R)-YDJ1+ YDJ1*
ydj1Δ	*pGPD*	26°, 3 d	-	++	++	+++
ydj1Δ	*pGPD*	26°, 1 d; 35° 2 d	-	++	++	+++
ydj1Δ	*pGPD*	26°, 1 d; 37° 2 d	-	++	++	+++
ydj1Δ	*pGPD*	35°, 3 d	-	++	++	+++
ydj1Δ	*pGPD*	37°, 3 d	-	+	+	+++
ydj1Δ	*pTEF*	26°, 3 d	-	+	+	+++
ydj1Δ	*pTEF*	26°, 1 d; 35° 2 d	-	+	-	+++
ydj1Δ	*pTEF*	26°, 1 d; 37° 2 d	-	-	-	+++
ydj1Δ	*pTEF*	35°, 3 d	-	+	-	+++
ydj1Δ	*pTEF*	37°, 3 d	-	-	-	+++

RP=Replica plate

conditions were identified in which *SSE1* was able to rescue growth relative to the vector control. However, using strains containing *T(K53R)-YDJ1* behind the *ADH* promoter, one condition (37° for 3 days) was identified in which *ydj1-151* yeast containing *T(K53R)-YDJ1* were temperature, but *SSE1* over-expression rescued this defect. These results suggest that *T(K53R)-YDJ1* copy number is an important determinant of cell growth.

Next, a low-copy suppressor screen was performed as described in Section 2.2.3 using a *TRP* marked library. Upon transformation with the library, suppressors were screened at 37°. Unfortunately, slow-growing background yeast colonies were detected on all plates, including those not transformed with library DNA fragments. I hypothesized this was due to reversion of the *ydj1-151* allele during the transformation. In small scale transformations *ydj1-151* revertants were seldom produced, but it is possible that in a large scale transformation reversion was more prevalent. Despite this, the fastest growing 20 colonies were restreaked and 8 colonies had improved growth relative to the vector control. The plasmid DNA was rescued and one plasmid restored growth upon retransformation. Sequence analysis revealed that this plasmid contained *SSE1* and two novel genes, *YPL107w* and *YPL105c*. Little is known about either protein, though *YPL107w* interacts with Vid22p, a protein involved in fructose-1,6-bisphosphatase degradation, by yeast two hybrid analysis (ITO *et al.* 2001). *YPL105c* may function in protein synthesis since it associates with many translation and splicing factors (ITO *et al.* 2001). Regardless, I concluded several things from this pilot screen. First, I uncovered a known *ydj1-151* suppressor, *SSE1*, indicating the potential validity of the screen. Second, *T(K53R)-YDJ1* expression level is important for identifying suppressors. Third, screening in the *ydj1-151* strain was difficult, probably due to reversion of the *ydj1-151* allele.

2.3.2 Identification of suppressors of *T(K53R)-YDJ1* and *ydj1Δ* yeast

A second screen was performed that remedied the problems identified in Section 2.3.1. First, I used the *ydj1Δ* strain to obviate reversion of the *ydj1-151* phenotype. Second, I cloned the *T(K53R)-YDJ1* gene behind the moderate *TEF* promoter on a *TRP* plasmid (*TEF*414) as described in Section 2.2.2. I chose this plasmid because a high-copy *URA* marked yeast genomic library was available, which could increase the sensitivity of the screen. Expression of wild type *T-YDJ1*, but not *T(K53R)-YDJ1* restored growth in the *ydj1Δ* strain at 35° (Figure 16). Several screening conditions were tested and the ideal condition was determined to be continuous incubation at 35° (Table 5). Next, a high-copy suppressor screen was performed to uncover suppressors of the temperature sensitive *T(K53R)-YDJ1* phenotype, as described in Section 2.2.4. Upon retransformation, eight unique plasmids were obtained that partially suppressed the *T(K53R)-YDJ1* thermosensitive phenotype at 35° (Table 6). Of note, none of the plasmids rescued the temperature sensitive phenotype to the levels seen when T-Ydj1p was expressed (Figure 16). However, plasmid *pCMS154* moderately rescued the *T(K53R)-YDJ1* phenotype and was the strongest suppressing plasmid uncovered in the screen.

To determine which of the genes in the eight isolated inserts conferred improved growth, 13 individual genes were chosen for further analysis. These included genes encoding chaperones, transcription factors, and proteins of unknown function, and several that had a common link to cell wall synthesis or integrity (see below). Each gene was amplified by PCR and cloned into a pRS426 vector or was obtained from colleagues (Tables 3,6). Next, the vectors were transformed into the *ydj1Δ* strain either containing or lacking the *T(K53R)-YDJ1* expression vector and tested for their ability to rescue the temperature sensitive growth defect. It should be noted that *ydj1Δ* yeast lacking the T(K53R)-Ydj1p expression vector grew poorly at

Table 6: Summary of the results obtained from the screen.

Times Recovered	Gene	Plasmid Name	Vector	Improves *T(K53R)-YDJ1* growth at 35°?	Improves *ydj1Δ* growth at 30°?
6	*REC102*	*pCMS125-REC102*	*pRS426*	-	-
	CHS5	*pSR6*	*pRS316*	-	-
	CHS5	*pSR23*	*pRS426*	-	-
	MID2-HA	*p1245*	*YEp352*	+++	+++
	MID2-GFP	*p1300*	*pRS314*	ND	+++
5	*STM1*	*Yep/STM1*	*YEp213*	-[a]	-
	YLR149c	*pCMS119-YLR149c*	*pRS426*	-	-
3	*RIM1*	ND	ND	ND	ND
	SYP1	*SYP1pRS316*	*pRS316*	-	-
	SYP1	*SYP1pRS426*	*pRS426*	+	+
	RPS14a	ND	ND	ND	ND
2	*SSA1*	*Yep351-SSA1*	*YEp351*	++	-[b]
	SSA1	*pRS426-GPD-(His)$_6$-SSA1*	*pGPD426*	+	-[b]
	EFB1	ND	ND	ND	ND
	ERP2	ND	ND	ND	ND
2	*SLG1-HA*	*p1657*	*YEp352*	++	+++
2	*SUS1*	*pSUS1*	*pRS316*	-	-
	CYC8	*pFW46*	*pRS316*	-	+
	CYC8	*pRT81*	*YEp24*	++	++
	YBR113w	ND	ND	ND	ND
1	*YDR020c*	ND	ND	ND	ND
	FAL1	ND	ND	ND	ND
	CIS1	*pCMS118-CIS1*	*pRS426*	++	-
	SES1	ND	ND	ND	ND
1	*SKN1*	*pSKN1-IV*	*YCp50*	+	-
	THI4	*pThi4ura3*	*pRS416*	-	-
	ENP2	ND	ND	ND	ND

Eight unique plasmids were isolated in the screen that allowed growth of the *ydj1Δ* yeast expressing T(K53R)-Ydj1p at 35° upon retransformation, and the number of times each plasmid was identified is indicated. Select individual genes found on each plasmid isolated in the screen were tested for improved growth of *T(K53R)-YDJ1* at 35° and *ydj1Δ* at 30°. Seven genes improved growth at 35° of *ydj1Δ* yeast expressing T(K53R)-Ydj1p and four genes improved the slow growth phenotype of *ydj1Δ* yeast at 30°. +++ = Moderate rescue, ++ = Weak rescue, + = Poor rescue ND = Not determined, *a* = Papillae colonies detected, *b* = *ydj1Δ* yeast with high copy *SSA1* expression vectors grew worse than empty vector controls.

Figure 16: *pCMS154* in multiple copies moderately rescues the *T(K53R)-YDJ1* growth defect at 35°.

Ten-fold serial dilutions of *ydj1Δ* yeast expressing wild type T-Ydj1p or T(K53R)-Ydj1p, and containing a vector control, a Ydj1p expression vector (*pAV4*), or three plasmids recovered in the screen, *pCMS153*, *pCMS154*, and *pCMS156,* were plated on SC-ura-trp and grown for 5 days at the indicated temperatures. The plasmid *pCMS154* contains a yeast genome fragment that includes the genes *REC102*, *CHS5*, and *MID2* and moderately improves the growth of yeast containing the *T(K53R)-YDJ1* expression vector at 35°. The plasmid *pCMS156* contained the genes *STM1* and *YLR149c* and led to papillae colony growth at 35° whereas the plasmid *pCMS153* did not improve growth of the *ydj1Δ* strain containing the *T(K53R)-YDJ1* expression vector at 35°.

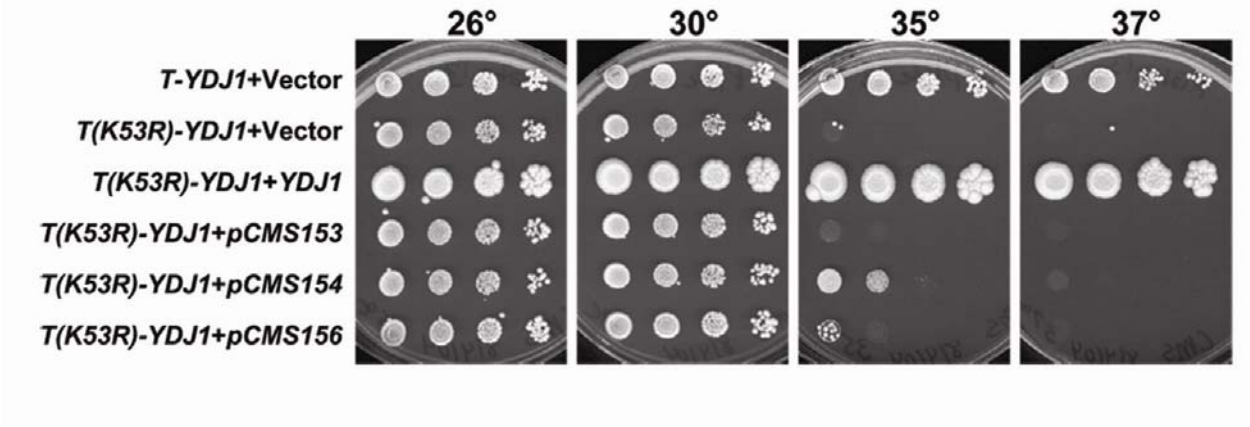
26°
30°
35°
37°
T-YDJ1+Vector
T(K53R)-YDJ1+Vector
T(K53R)-YDJ1+YDJ1
T(K53R)-YDJ1+pCMS153
T(K53R)-YDJ1+pCMS154
T(K53R)-YDJ1+pCMS156

temperatures above 26°, and those containing the vector grew poorly above 30°, consistent with T(K53R)-Ydj1p exhibiting partial activity (FEWELL *et al.* 2002). However, over-expression of seven genes suppressed the slow growth phenotype of *T(K53R)-YDJ1* at 35° to varying degrees, and four of these (*MID2*, *SLG1/WSC1*, *CYC8*, *SYP1*) also improved the growth of the *ydj1Δ* strain lacking the expression vector variably at 30° (Table 6). Notably, *ydj1Δ* yeast containing *pCMS154* (which harbors *MID2*) or containing a vector engineered specifically for *MID2* over-expression conferred the same degree of rescue (Table 6, and Figure 18A, below). Over-expression of an eighth gene, *STM1*, did not alter the temperature sensitive phenotype but led to papillae colony formation [see Figure 16 for data on the abilities of *MID2 (pCMS154*) and *STM1* (*pCMS156*) containing plasmids isolated from the screen to suppress the temperature sensitive growth phenotype].

Among the genes tested only one improved the growth of T(K53R)-Ydj1p-expressing yeast but had a negative effect on *ydj1Δ* yeast lacking the expression vector. The gene is *SSA1*, which encodes a yeast Hsp70 that is known to interact with Ydj1p (Figure 17A-B) (BECKER *et al.* 1996; CYR *et al.* 1992; MCCLELLAN and BRODSKY 2000). *SSA1* over-expression in yeast containing YEp351 *SSA1* was verified by immunoblot analysis (Figure 17C-D). One interpretation of this result is that Ssa1p may directly bind the J domain in T(K53R)-Ydj1p and partially repair the lesion conferred by mutating lysine 53 (since only moderate rescue was observed).

In contrast, four suppressors (*MID2*, *SLG1*/*WSC1*, *CYC8*, *SYP1*) were identified that suppressed to varying extents the phenotypes associated with both the deletion of the *YDJ1* locus and the phenotype associated with the *T(K53R)-YDJ1* expression vector (Table 6; see Figure 18A-B for an example of studies with the rescue conferred by *MID2*). To verify the expression

Figure 17: *SSA1* improves the growth of strains possessing the *T(K53R)-YDJ1* thermosensitive phenotype.

Cultures of *ydj1Δ* yeast expressing T(K53R)-Ydj1p were transformed with a high-copy *SSA1*-containing or an empty vector and were serially diluted onto either SC-ura-trp or SC-ura. Plates were incubated for 4 days. High-copy *SSA1* (A) allows some growth of *ydj1Δ* yeast containing the *T(K53R)-YDJ1* expression vector at 35°, (B) but slows the growth of *ydj1Δ* yeast. Immunoblot analysis indicates that Ssa1p is over-expressed (C) 2.1 fold in the *ydj1Δ* strain expressing T(K53R)-Ydj1p and (D) 2.6 fold in the *ydj1Δ* yeast strain.

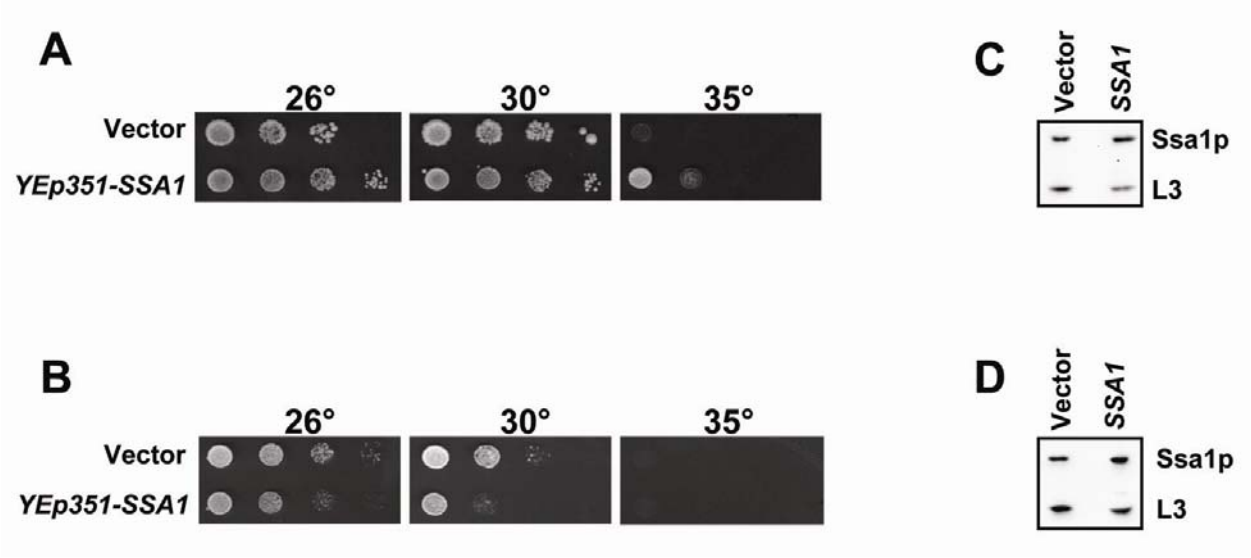
A
26°
30°
35°
Vector
YEp351-SSA1
B
26°
30°
35°
Vector
YEp351-SSA1
C
Vector
SSA1
Ssa1p
L3
D
Vector
SSA1
Ssa1p
L3

Figure 18: *MID2* suppresses the thermosensitive growth defect of *ydj1Δ* yeast.

(A) *ydj1Δ* yeast expressing T(K53R)-Ydj1p were transformed with the *MID2*-containing multicopy plasmid isolated in the screen (*pCMS154*), an empty vector, or a multicopy *MID2-HA* containing vector, and were serially diluted onto SC-ura-trp. Plates were incubated for 4 days. (B) High-copy *MID2-HA* also suppresses the growth defect in the *ydj1Δ* strain lacking the T(K53R)-Ydj1p expression vector, as assessed in part (A). Mid2p is expressed in the *T(K53R)-YDJ1*-containing *ydj1Δ* strain (C) as well as in the *ydj1Δ* strain (D) as indicated by immunoblot analysis.

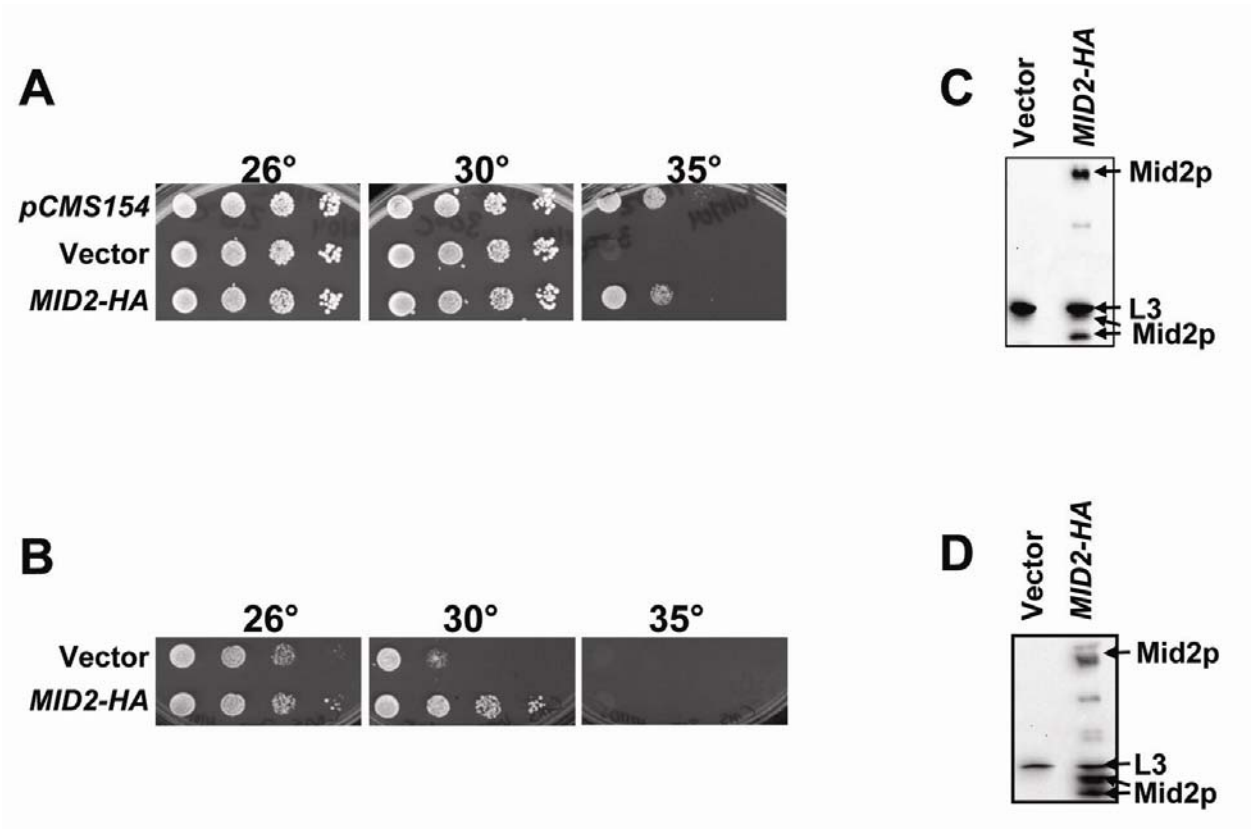
A
26°
30°
35°
pCMS154
Vector
MID2-HA
B
26°
30°
35°
Vector
MID2-HA
C
Vector
MID2-HA
Mid2p
L3
Mid2p
D
Vector
MID2-HA
Mid2p
L3
Mid2p

of the strongest suppressor, Mid2p, an immunoblot analysis against the HA epitope tag (Figure 18C-D) was performed and Mid2p resolved as three distinct bands of 40kD, 47kD, and 200kD. This is consistent with the presence of both immature and highly *O*-glycosylated forms of Mid2p (LOMMEL *et al.* 2004). To determine if the observed improvement of growth was allele-specific, *MID2-HA* was over-expressed in the *ydj1Δ* strain containing the *T(H42R)-YDJ1* expression vector, which contains an H42R mutation in the conserved HPD motif in the TAg J domain (FEWELL *et al.* 2002). I found that *MID2-HA* over-expression also suppressed the slow growth phenotype of *ydj1Δ* yeast containing the *T(H42R)-YDJ1* expression vector at 30° (Figure 19A). Taken together, these results suggest that *MID2* suppression is independent of TAg J domain mutant alleles, but is instead the consequence of improved growth of the *ydj1Δ* strain.

2.3.3 *PKC1* and constitutively activated components of the PKC pathway improve the *ydj1Δ* slow-growth phenotype

Mid2p and Slg1p/Wsc1p are plasma membrane proteins that sense yeast cell wall stress and activate the PKC pathway (PHILIP and LEVIN 2001), which leads to the transcription of genes involved in cell wall synthesis (JUNG and LEVIN 1999). Since Mid2p and Slg1p/Wsc1p are components of the PKC pathway and several other of our identified suppressors (Table 6) — Syp1p (MARCOUX *et al.* 2000), Skn1p (ROEMER *et al.* 1994) and Cis1p (MANNING *et al.* 1997) — are genetically linked to *PKC1* or *MID2*, the ability of *PKC1* to suppress the *ydj1Δ* growth phenotype was investigated. A 2μ *PKC1* over-expression plasmid was transformed into *ydj1Δ* cells and *ydj1Δ* cells expressing T(K53R)-Ydj1p, and moderate rescues of *T(K53R)-YDJ1* growth at 35° (Figure 20A) and *ydj1Δ* growth at 30° (Figure 20B) were observed. The over-expression of Pkc1p in these strains was verified by immunoblot analysis as shown in Figure

Figure 19: *MID2* and *PKC1* improve the growth of the *ydj1Δ* yeast expressing T(H42R)-Ydj1p.

ydj1Δ yeast containing *T(K53R)-YDJ1* or *T(H42R)-YDJ1* were transformed with (A) *MID2* or (B) *PKC1* or an empty vector and serially diluted onto SC-ura-trp and incubated for 4 days at the indicated temperatures.

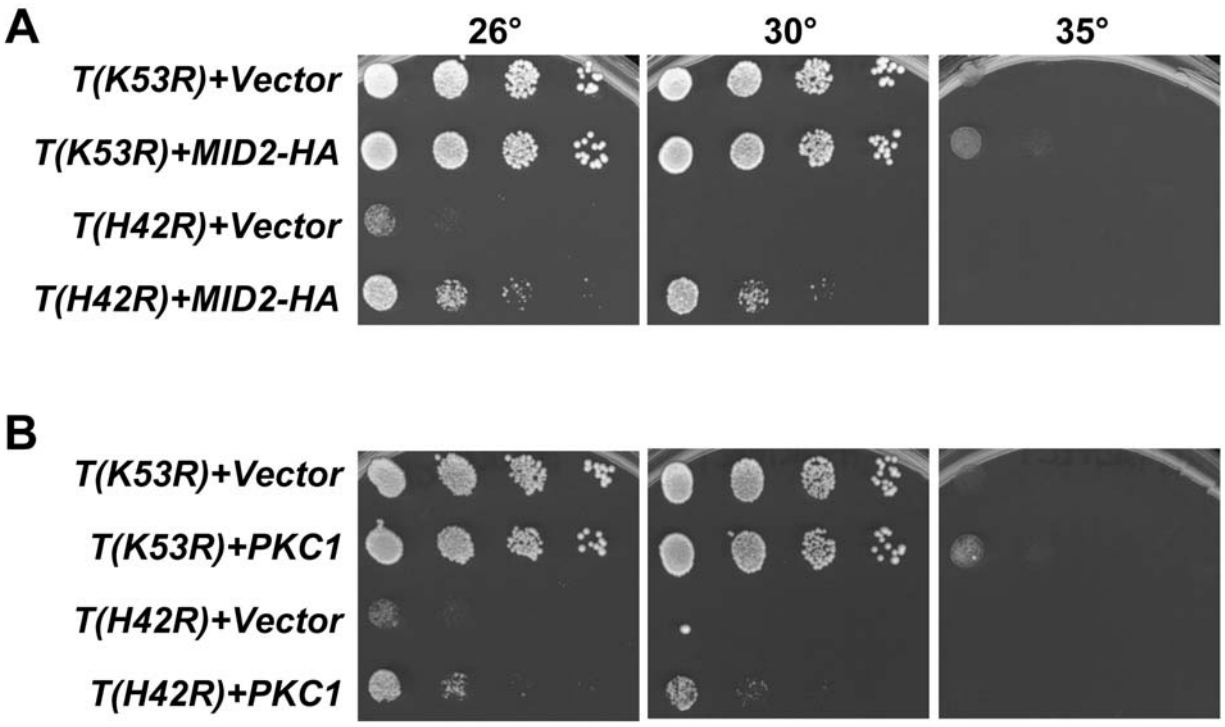
A
26°
30°
35°
T(K53R)+Vector
T(K53R)+MID2-HA
T(H42R)+Vector
T(H42R)+MID2-HA
B
T(K53R)+Vector
T(K53R)+PKC1
T(H42R)+Vector
T(H42R)+PKC1

Figure 20: Introduction of a high-copy *PKC1* containing vector and over-expression of constitutively active components in the PKC pathway improve the slow growth phenotype of the *ydj1Δ* strain.

A multi-copy *PKC1*-containing vector and a vector control were transformed into (A) *ydj1Δ* yeast expressing T(K53R)-Ydj1p and (B) *ydj1Δ* yeast, and the transformants were serially diluted ten-fold and incubated for 4 days at the indicated temperatures. Immunoblot analysis indicates (C) 1.8 fold overexpression of Pkc1p in the *ydj1Δ* strain expressing T(K53R)-Ydj1p and (D) 3.1 fold overexpression of Pkc1p in the *ydj1Δ* strain. (E) Plasmids containing constitutively active, multi-copy *BCK1-20* and $MKK1^{DD}$ alleles transformed into the *ydj1Δ* strain also improve the *ydj1Δ* temperature sensitive defect, though to a lesser extent than *MID2* or *PKC1*.

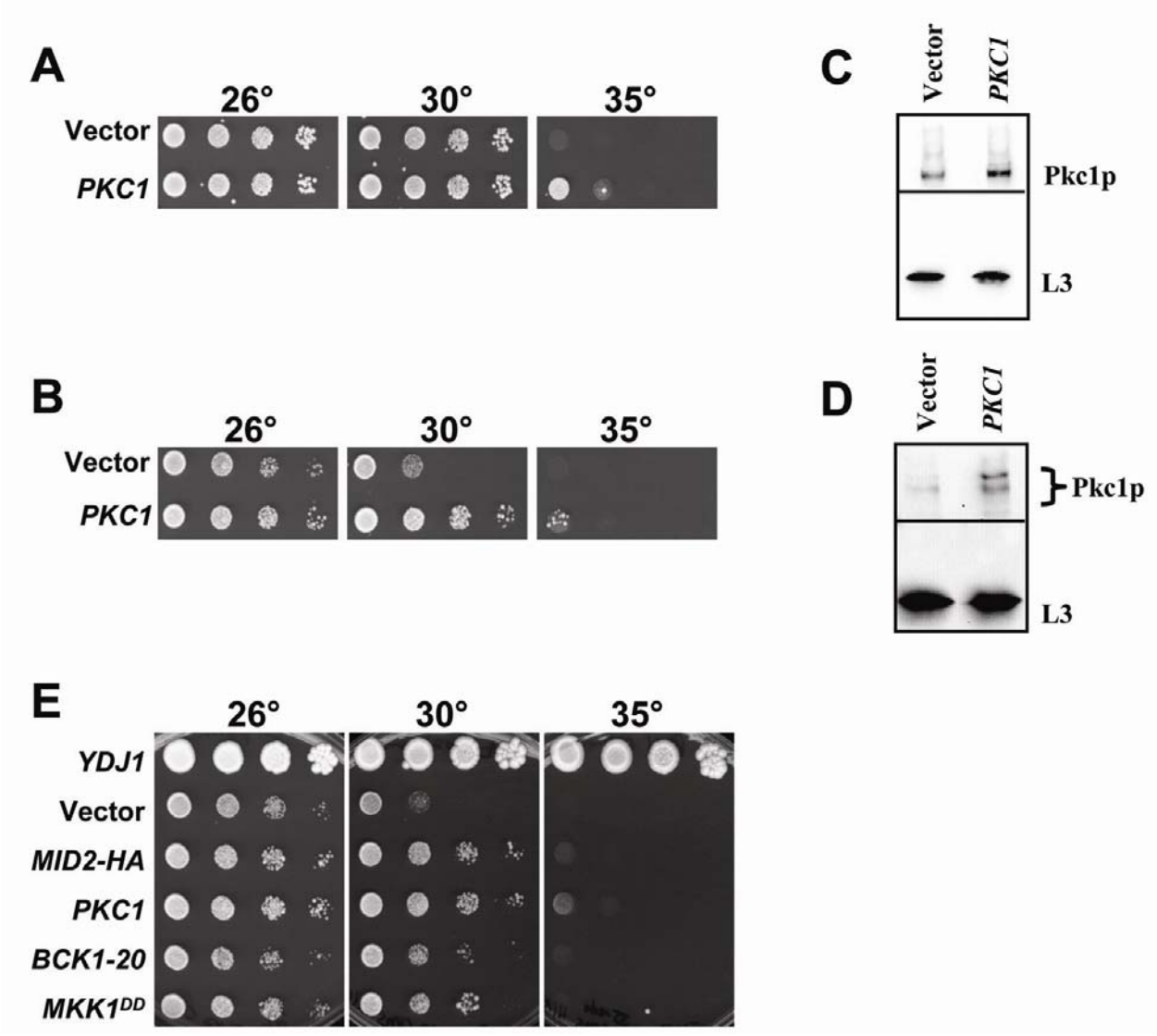
A
26°
30°
35°
Vector
PKC1
B
26°
30°
35°
Vector
PKC1
C
Vector
PKC1
Pkc1p
L3
D
Vector
PKC1
Pkc1p
L3
E
26°
30°
35°
YDJ1
Vector
MID2-HA
PKC1
BCK1-20
MKK1DD

20C-D. Interestingly, over-expression of *PKC1* also improved the growth of *ydj1Δ* yeast expressing T(H42R)-Ydj1p at 30° (Figure 19B).

The PKC signaling pathway is initiated by the phosphorylation of Pkc1p and terminates with transcription factor activation via the Bck1p, Mkk1p/Mkk2p, and Mpk1 kinases (LEVIN 2005). To determine if over-expression of downstream members of the PKC pathway also rescued the *ydj1Δ* slow growth phenotype, plasmids engineered for the expression of constitutively active *BCK1* and *MKK1* alleles were introduced into the mutant strain. *BCK1-20* has an alanine to proline mutation at position 1174, immediately upstream of the kinase domain, which is believed to mimic Bck1p phosphorylation by Pkc1p (LEE and LEVIN 1992). $MKK1^{DD}$ contains two serine to aspartic acid mutations in the kinase domain, which mimics Mkk1p phosphorylation (HARRISON *et al.* 2004). As shown in Figure 20E, over-expression of *BCK1-20* or $MKK1^{DD}$ slightly improved the *ydj1Δ* growth defect. In contrast, over-expression of wild type Mkk1p or Bck1p failed to confer improved growth (Figure 21), consistent with the previously reported necessity of using constitutively active forms of these kinases (HARRISON *et al.* 2004; LEE and LEVIN 1992). In any event, these results indicate that activation of the PKC pathway can ameliorate the *ydj1Δ* temperature sensitive growth phenotype.

In addition to the PKC pathway, yeast have two other cell wall integrity pathways, the HOG and SVG pathways (MAGER and SIDERIUS 2002). Each pathway is activated under different conditions, but cross-talk between the HOG and SVG pathways is common. The HOG and SVG pathways even contain some common signaling proteins (GUSTIN *et al.* 1998; LEE and ELION 1999; O'ROURKE and HERSKOWITZ 1998). To examine if over-expression of HOG and SVG pathway components impact the growth of *ydj1Δ* yeast, two genes in the HOG pathway (*HOG1* and *PBS2*) and SVG pathway (*KSS1* and *STE7*) were over-expressed in the *ydj1Δ* strain.

Figure 21: Over-expression of *BCK1* and *MPK1* do not restore growth of the *ydj1Δ* strain.

ydj1Δ yeast were transformed with a 2μ *BCK1* and *MPK1* plasmid or a vector lacking insert. The strains were serially diluted onto SC-ura and incubated at the indicated temperatures for 4 days. *ydj1Δ* yeast with the *pAV4-YDJ1* expression vector were used as controls. *BCK1* and *MPK1* did not improve the growth of the *ydj1Δ* strain relative to the vector control.

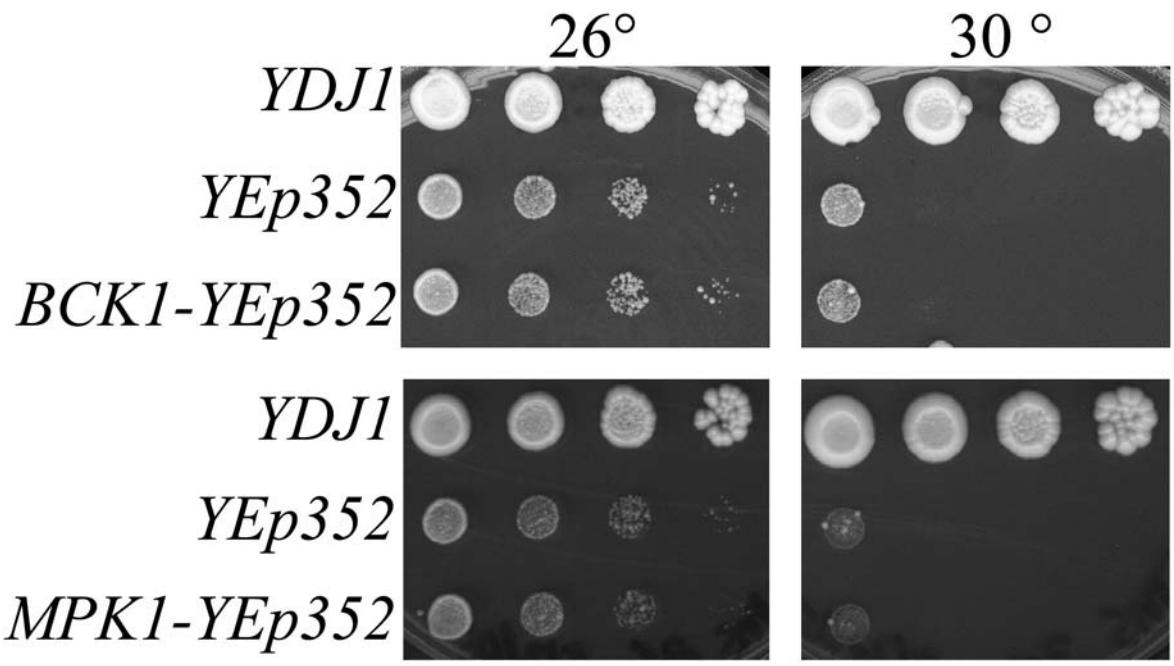
26°
30 °
YDJ1
YEp352
BCK1-YEp352
YDJ1
YEp352
MPK1-YEp352

Hog1p and Kss1p are MAP kinases that initiate the expression of specific genes and Pbs2p and Ste7p are the MAPK kinases that phosphorylate Hog1p and Kss1p, respectively (BREWSTER *et al.* 1993; LEE and ELION 1999). Previously, connections between the signaling pathways were examined by over-expressing *STE7* in the *mkk1Δmkk2Δ* strain (YASHAR *et al.* 1995). However, the over-expression of these proteins had no effect on the *ydj1Δ* slow growth phenotype (Figure 22). These results suggest that rescue of the *ydj1Δ* slow growth phenotype is limited to the PKC pathway and cannot be remedied by upregulation of alternative pathways that may sense cell wall integrity

2.3.4 *MID2* and *PKC1* partially suppress the temperature sensitive phenotype of *hsp82* mutant strains

Because Ydj1p functions in multiprotein chaperone complexes with Ssa1p, a cytoplasmic Hsp70, and the yeast Hsp90 homologue, Hsp82p (BECKER *et al.* 1996; CAPLAN *et al.* 1995; CYR *et al.* 1992; KIMURA *et al.* 1995; MCCLELLAN and BRODSKY 2000), each of the seven suppressors was also over-expressed in the temperature sensitive *SSA1* strain, *ssa1-45*, and Mid2p and Pkc1p were over-expressed in the temperature sensitive *hsp82* G313N and *hsp82* G170D strains (BOHEN and YAMAMOTO 1993; FLISS *et al.* 2000; NATHAN and LINDQUIST 1995). None of the suppressors, including *MID2* or *PKC1* (data not shown; see Figure 23A for data on *MID2* and *PKC1*), rescued the temperature sensitive phenotype of *ssa1-45* yeast, even though immunoblots verified that Mid2p and Pkc1p were over-expressed (Figure 23B). In contrast, over-expression plasmids encoding *MID2-HA* and *PKC1* partially suppressed the growth defect of both *hsp82* G313N and *hsp82* G170D (Figure 24A). Since the Hsp90 complex contains several other cochaperones including Sti1p (HOP), Sba1p (p23), and Sse1p (Hsp110)

Figure 22: Over-expression of SVG and HOG pathway members do not improve the growth of *ydj1Δ* yeast.

(A) *KSS1* and *STE7* or (B) *PBS2* and *HOG1* overexpression plasmids were transformed into *ydj1Δ* yeast and selected on the appropriate medium. The yeast were serially diluted and incubated at the indicated temperatures for 4 days. Yeast containing *MID2* and *YDJ1* expression vectors or plasmids lacking insert were used as controls. (C) Hog1p expression was verified using an antibody against the HA epitope tag.

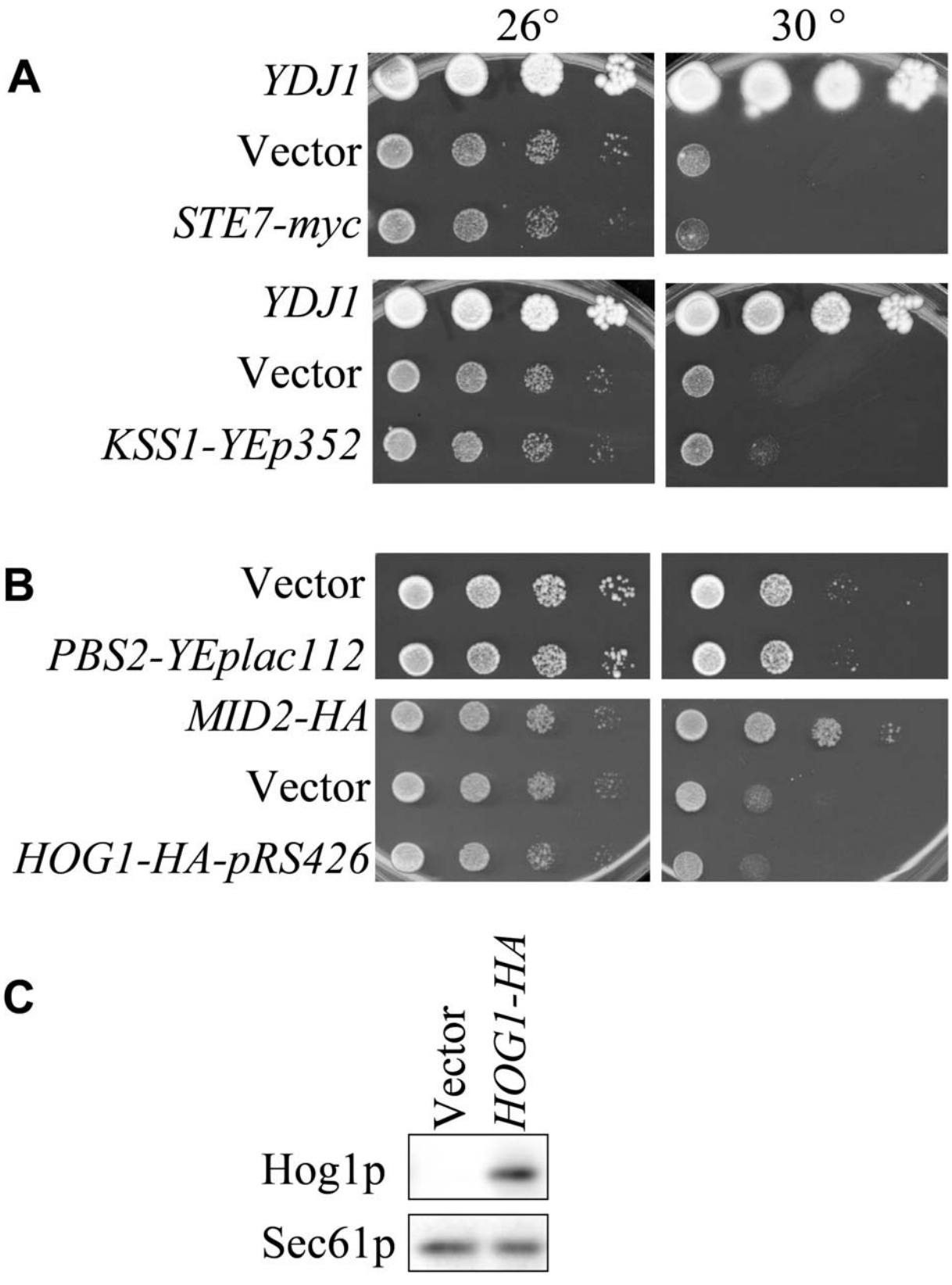
26°
30 °
A
YDJ1
Vector
STE7-myc
YDJ1
Vector
KSS1-YEp352
B
Vector
PBS2-YEplac112
MID2-HA
Vector
HOG1-HA-pRS426
C
Vector
HOG1-HA
Hog1p
Sec61p

Figure 23: Multi-copy *MID2* and *PKC1*-containing plasmids do not improve the temperature-sensitive growth defects of *ssa1-45* temperature sensitive mutants.

The *ssa1-45* yeast strain was transformed with multi-copy *MID2-HA* or *PKC1* containing vectors or with an empty vector. This strain and an isogenic strain containing a wild type version of the mutated genes were serially diluted ten-fold on SC-ura for 3-4 days at the indicated temperatures. (A) *MID2-HA* and *PKC1* do not rescue the temperature sensitive growth phenotype of *ssa1-45* yeast. (B) Over-expression of Mid2p-HA (left) and Pkc1p (right) in the *ssa1-45* strain were verified by immunoblot analysis.

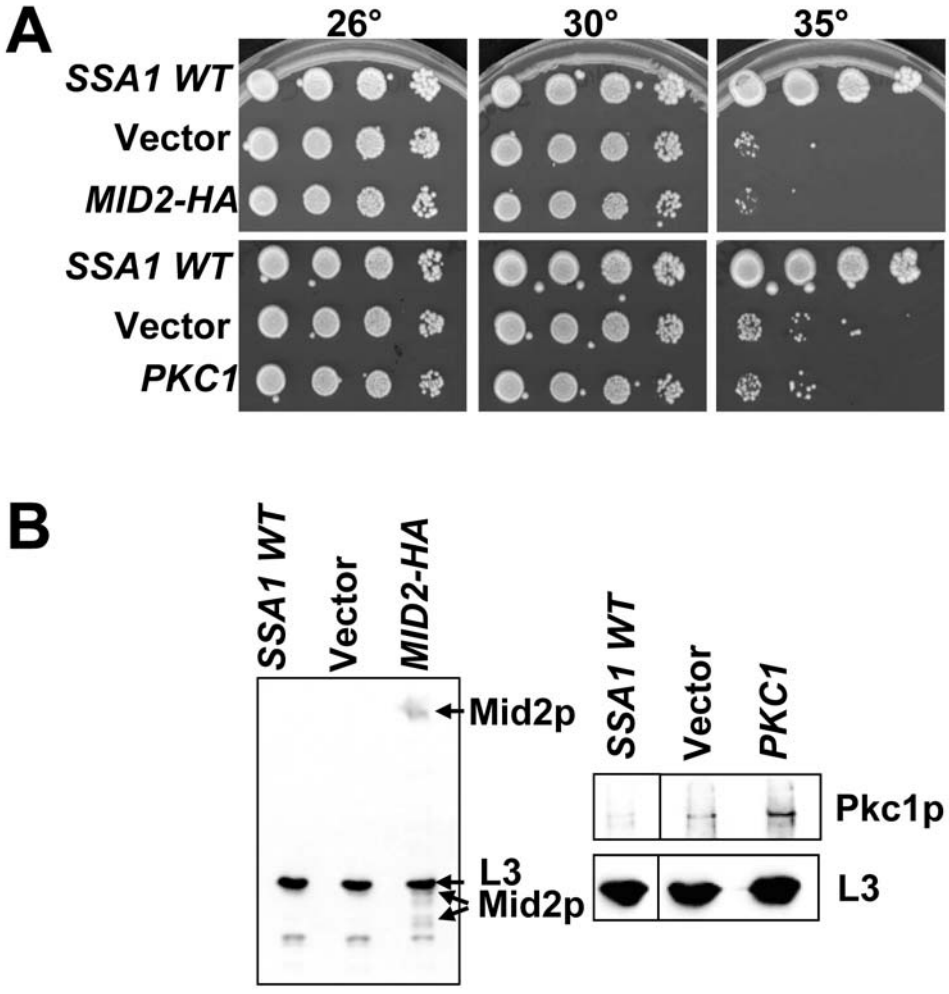
A
26°
30°
35°
SSA1 WT
Vector
MID2-HA
SSA1 WT
Vector
PKC1
B
SSA1 WT
Vector
MID2-HA
Mid2p
L3
Mid2p
SSA1 WT
Vector
PKC1
Pkc1p
L3

Figure 24: Over-expression of *MID2* and *PKC1* suppress the growth defect of the *hsp82* G170D and *hsp82* G313N strains.

(A) *hsp82* G170D or (B) *hsp82* G313N yeast strains were transformed with a *MID2* or *PKC1* overexpression vectors or a vector lacking insert and transformants were selected on SC-ura-trp. These strains and an isogenic wild type were serially diluted ten-fold and incubated at the indicated temperatures for 3 days. Expression of Mid2p-HA and Pkc1p in the (C) *hsp82* G170D or (D) *hsp82* G313N yeast strains was verified by immunoblot.

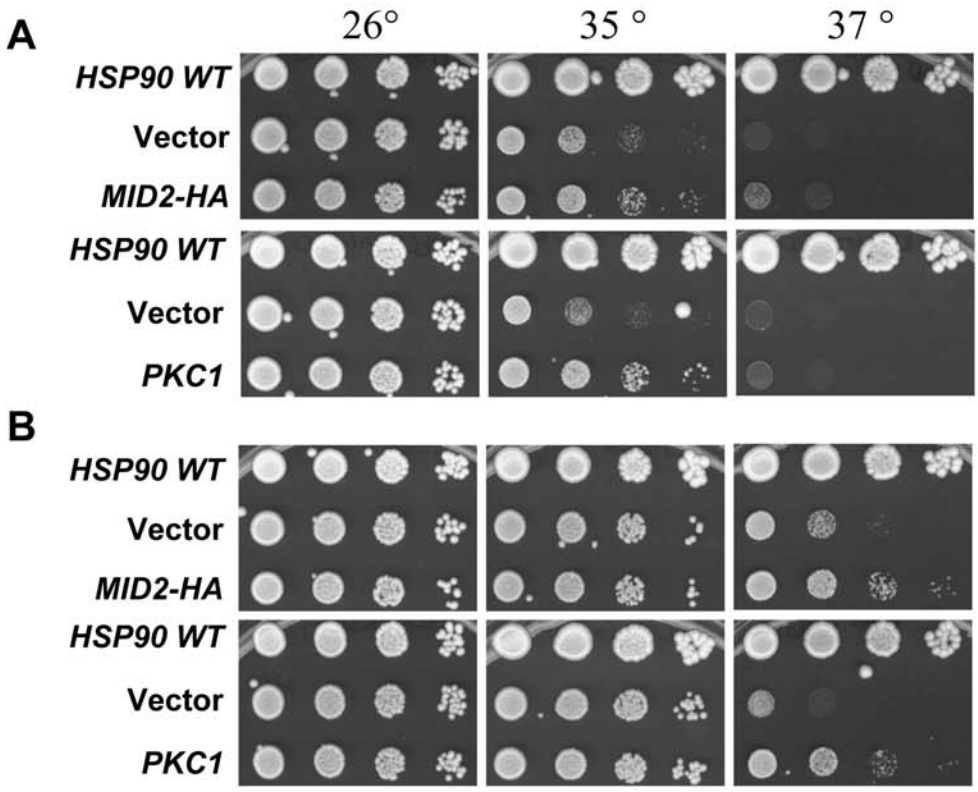
A
26°
35 °
37 °
HSP90 WT
Vector
MID2-HA
HSP90 WT
Vector
PKC1
B
HSP90 WT
Vector
MID2-HA
HSP90 WT
Vector
PKC1

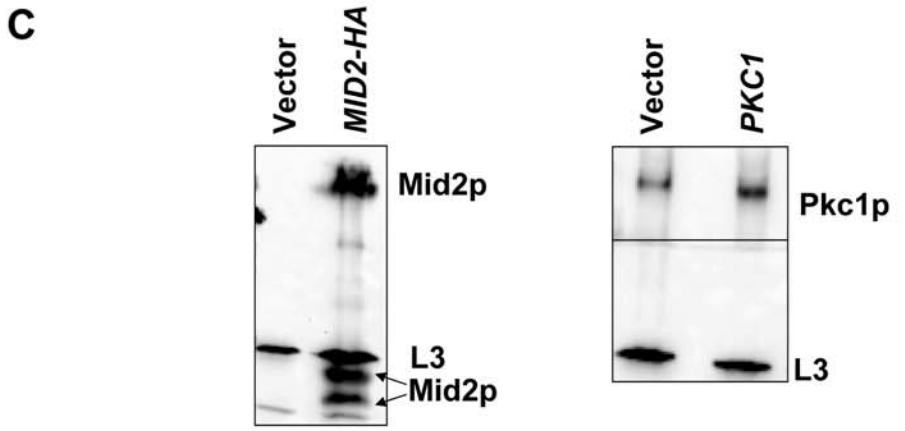
C
Vector
MID2-HA
Mid2p
L3
Mid2p
Vector
PKC1
Pkc1p
L3

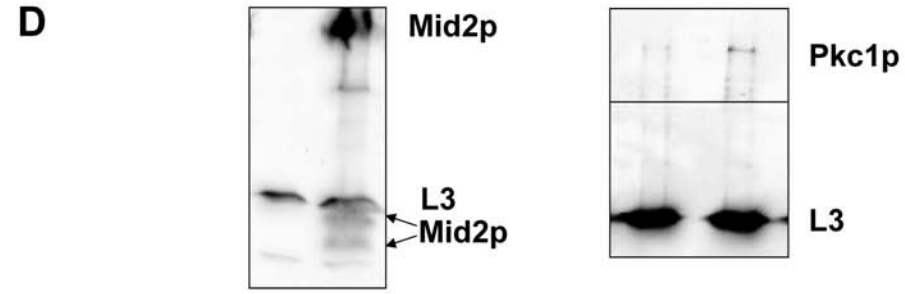
D
Mid2p
L3
Mid2p
Pkc1p
L3

(CHANG *et al.* 1997; FANG *et al.* 1998; LIU *et al.* 1999), we also examined whether the introduction of *MID2* and *PKC1* over-expression plasmids remedied the *sse1Δsti1Δ* temperature sensitive phenotype (LIU *et al.* 1999). Little effect on cell growth was observed (Figure 25) at 37°. These data suggest that Mid2p or Pkc1p over-expression primarily impacts the growth of the Hsp40 and Hsp90 mutant strains, and suggest that Hsp40 and Hsp90 play a role in yeast cell wall integrity. These combined data also suggest that the mode of Ssa1p-mediated suppression of the *ydj1Δ* strain when T(K53R)-Ydj1p is expressed (see Section 2.3.2) is distinct.

Because over-expression of Mid2p and Pkc1p improved the growth of *hsp82* mutant strains, we investigated whether over-expression of Hsp82p could rescue the *ydj1Δ* slow growth phenotype and if, like Ssa1p, Hsp82p also suppressed the *T(K53R)-YDJ1* growth defect. To this end, the *HSP82* locus was PCR amplified from the yeast genome and inserted in the high-copy pRS426 vector, and the plasmid was transformed into both the *ydj1Δ* strain and into the *ydj1Δ* strain expressing T(K53R)-Ydj1p. Despite two to three-fold over-expression, *HSP82* was unable to rescue either the *T(K53R)-YDJ1* or *ydj1Δ* temperature sensitive phenotypes (Figure 26).

Chaperone levels are tightly regulated (HJORTH-SORENSEN *et al.* 2001; STONE and CRAIG 1990) and basal chaperone expression levels might dictate whether a given chaperone can be over-expressed. Thus, endogenous concentrations of Ssa1p and Hsp82p were determined in the presence or absence of Mid2p or Pkc1p over-expression in both the wild type and *ydj1Δ* strains. Not surprisingly, in *ydj1Δ* cells containing a vector control, Ssa1p is upregulated 1.6 to 2.7 fold and Hsp82p is upregulated 1.4 to 3.2 fold when compared to the wild type strain (Figure 27, compare lanes 1 and 4). When Mid2p and Pkc1p are over-expressed, we observed a slight, additional, upregulation of Hsp82p in the *ydj1Δ* strain (Figure 27, lanes 2 and 3). These results suggest that Hsp82p and Ssa1p and likely other gene products are induced to compensate for the

Figure 25: Over-expression of *MID2* or *PKC1* does not restore growth in the *sti1Δsse1Δ* yeast strain.

(A) The *MID2-HA* and *PKC1* expression vector or a vector lacking the insert was transformed into the *sti1Δsse1Δ* yeast strain. The strains were serially diluted ten-fold and incubated at the indicated temperatures for 3 days. (B) Expression of Mid2p-HA was verified by immunblot using antibodies against the HA epitope tag.

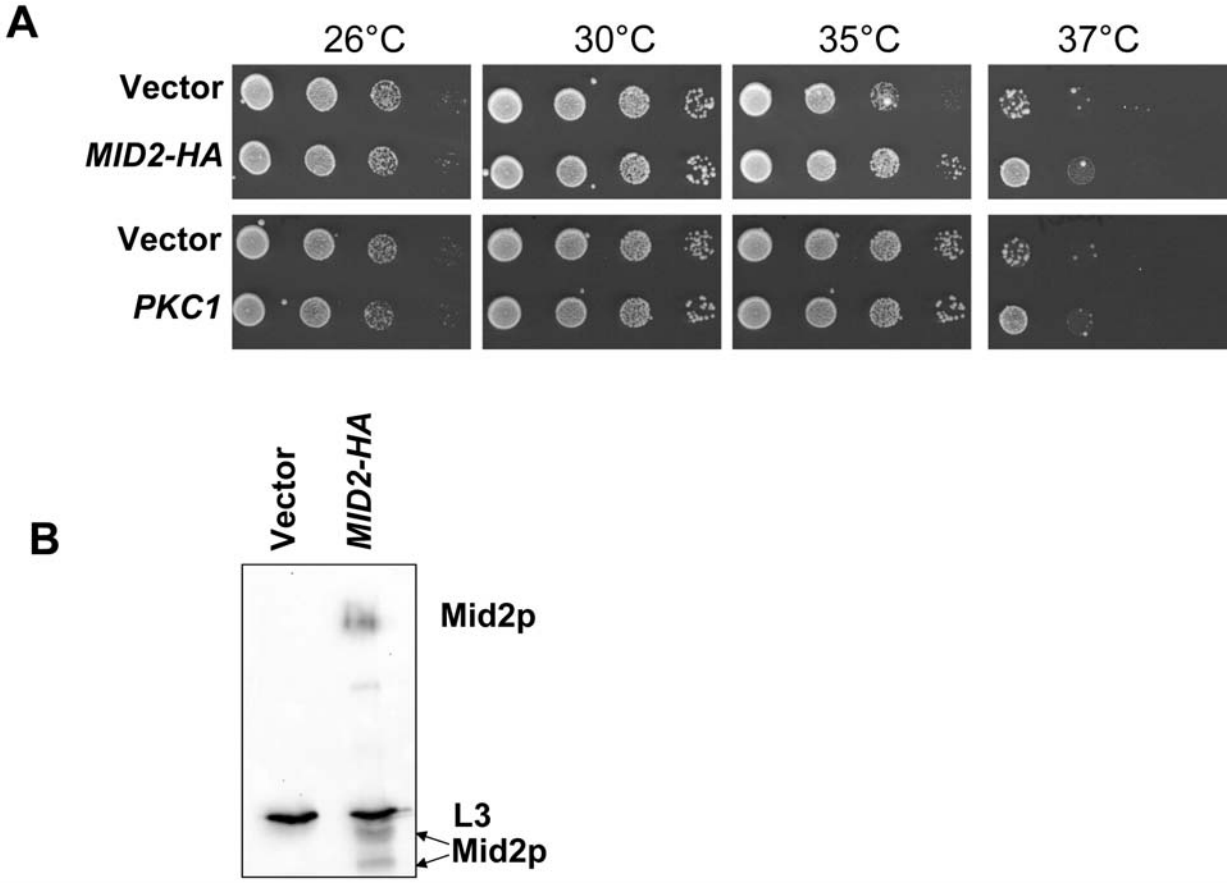
A
26°C
30°C
35°C
37°C
Vector
MID2-HA
Vector
PKC1
B
Vector
MID2-HA
Mid2p
L3
Mid2p

Figure 26: Introduction of a high-copy *HSP82* containing vector does not improve the temperature sensitive phenotype of *T(K53R)-YDJ1* or the slow growth phenotype of the *ydj1Δ* strain .

A multi-copy *HSP82*-containing vector and a vector control were transformed into (A) *ydj1Δ* yeast expressing T(K53R)-Ydj1p and (B) *ydj1Δ* yeast, and the transformants were serially diluted ten-fold and incubated for 4 days at the indicated temperatures. Hsp82p is overexpressed (A) 3.5 fold in *ydj1Δ* yeast expressing T(K53R)-Ydj1p and (B) 3.1 fold in *ydj1Δ* yeast.

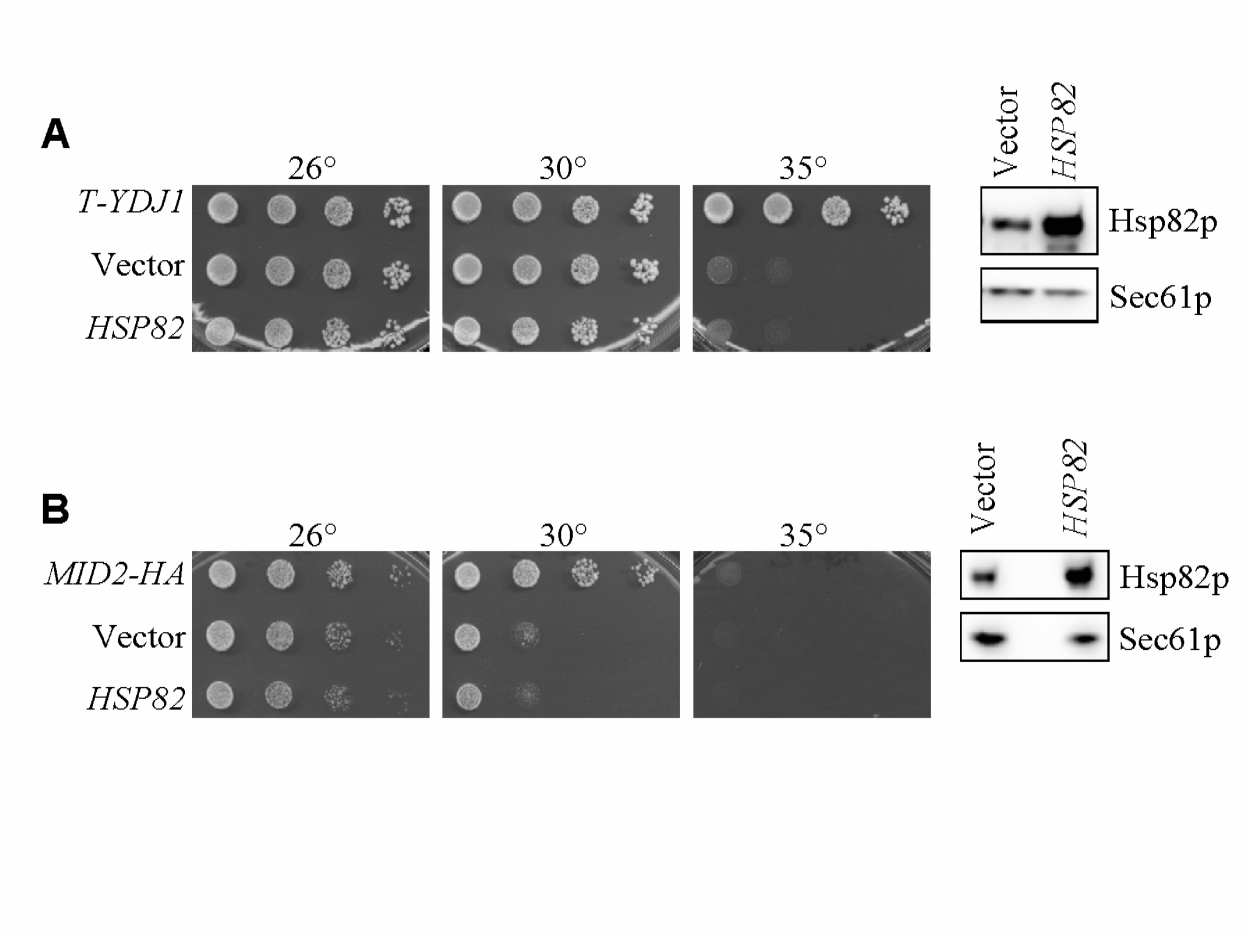
A
26°
30°
35°
T-YDJ1
Vector
HSP82
Vector
HSP82
Hsp82p
Sec61p
B
26°
30°
35°
MID2-HA
Vector
HSP82
Vector
HSP82
Hsp82p
Sec61p

Figure 27: Hsp82p and Ssa1p are upregulated in the *ydj1Δ* strain.

Mid-log phase cells from the indicated strains were lysed, protein levels were normalized, and total proteins were resolved by SDS-PAGE. Immunoblots with the indicated antibodies were performed.

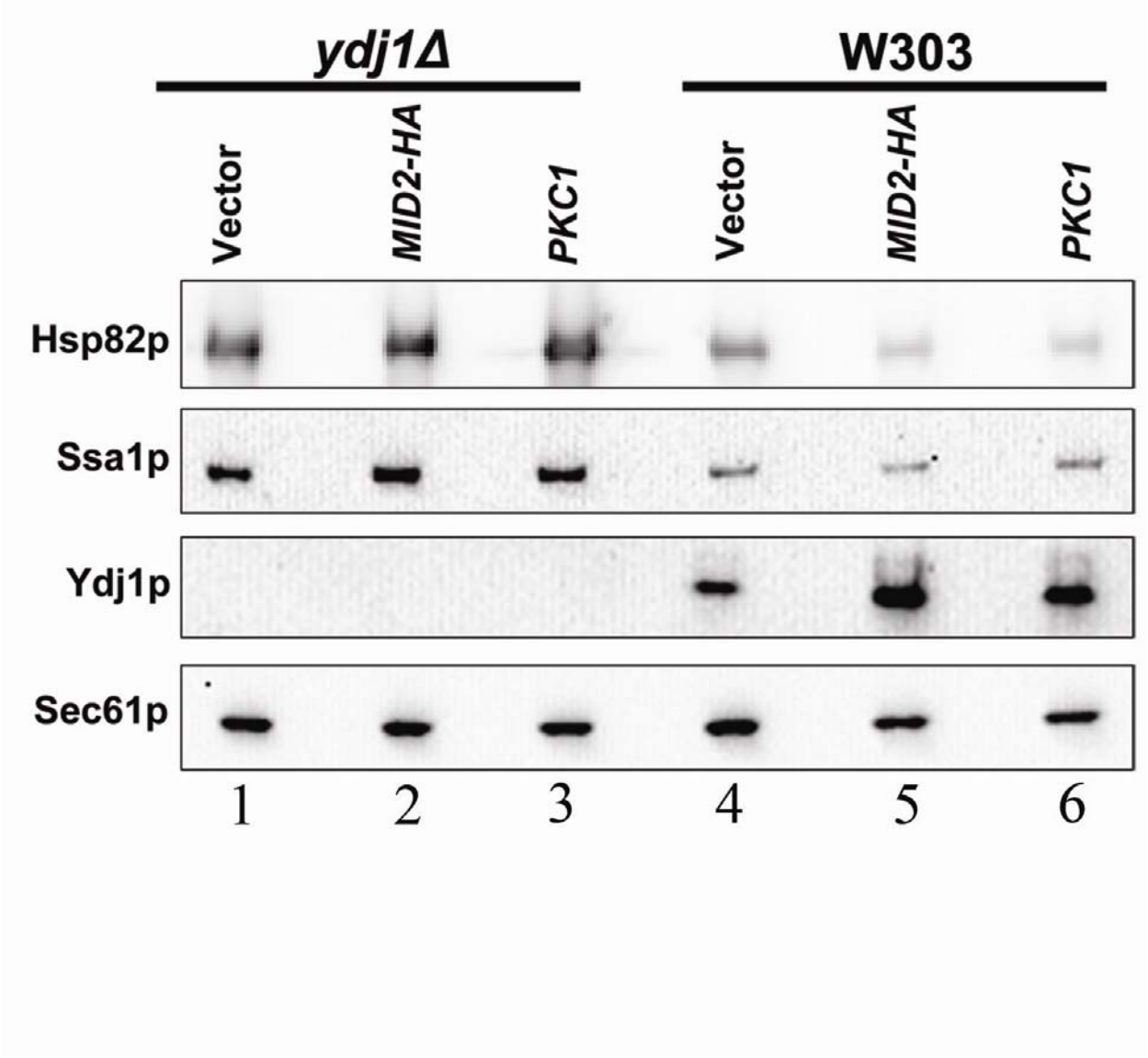
ydj1Δ
W303
Vector
MID2-HA
PKC1
Vector
MID2-HA
PKC1
Hsp82p
Ssa1p
Ydj1p
Sec61p
1
2
3
4
5
6

lack of Ydj1p, and may explain why Ssa1p or Hsp82p over-expression alone does not ameliorate the temperature sensitive phenotype of *ydj1Δ* yeast (Figure 17 and Figure 26).

2.3.5 The *ydj1Δ* and *hsp82* temperature sensitive strains show phenotypes consistent with cell wall defects

Since the PKC pathway is involved in yeast cell wall maintenance (LEVIN 2005), mutation of pathway members leads to cell wall defects and several detectable growth phenotypes. For example, the poor growth of *pkc1Δ* yeast is rescued by incubation in osmostabilizing reagents, such as 1 M sorbitol or 0.5 M NaCl (LEVIN and BARTLETT-HEUBUSCH 1992). In addition, *pkc1* mutant yeast are sensitive to the cell wall dye calcofluor white (CW) (SCHMITZ *et al.* 2001), which binds and perturbs the architectural integrity of this structure. Some studies have also shown that yeast with cell wall defects are more sensitive to lyticase treatment which digests the β1,3-glucan in the yeast cell wall. Since the introduction of additional copies of *MID2* and *PKC1* affect the growth of *ydj1Δ* and *hsp82* yeast, it was possible that these mutant strains also have cell wall defects, as hinted at by previous studies (LUSSIER *et al.* 1997; YANG *et al.* 2006).

To begin to test this hypothesis, the lyticase digestion efficiencies of wild type or *ydj1Δ* yeast cell walls were compared. Wild type and *ydj1Δ* yeast were treated with lyticase and culture density was compared to an untreated control. However, *ydj1Δ* yeast were not preferentially digested by lyticase (Figure 28). This suggests that the levels of β1,3-glucan are unaltered in *ydj1Δ* yeast. Next, *ydj1Δ* cells with or without a *YDJ1* single-copy expression vector (*pAV4*) were examined on medium supplemented with 0.4 M NaCl. Growth of *ydj1Δ* yeast was partially restored in the presence of salt (Figure 29A). In addition, the growth of wild type and *ydj1Δ* yeast was tested in the presence of sorbitol or CW. As expected for strains having cell wall

Figure 28: The cell wall in the *ydj1Δ* yeast strain is not preferentially sensitive to lyticase.

Wild type (red triangle) and *ydj1Δ* (green circle) yeast were treated with lyticase and cell wall digestion was monitored over 30 min. The starting density of each strain was normalized to 100%. The results were compared to samples of untreated wild type (blue diamond) and *ydj1Δ* (purple square) yeast.

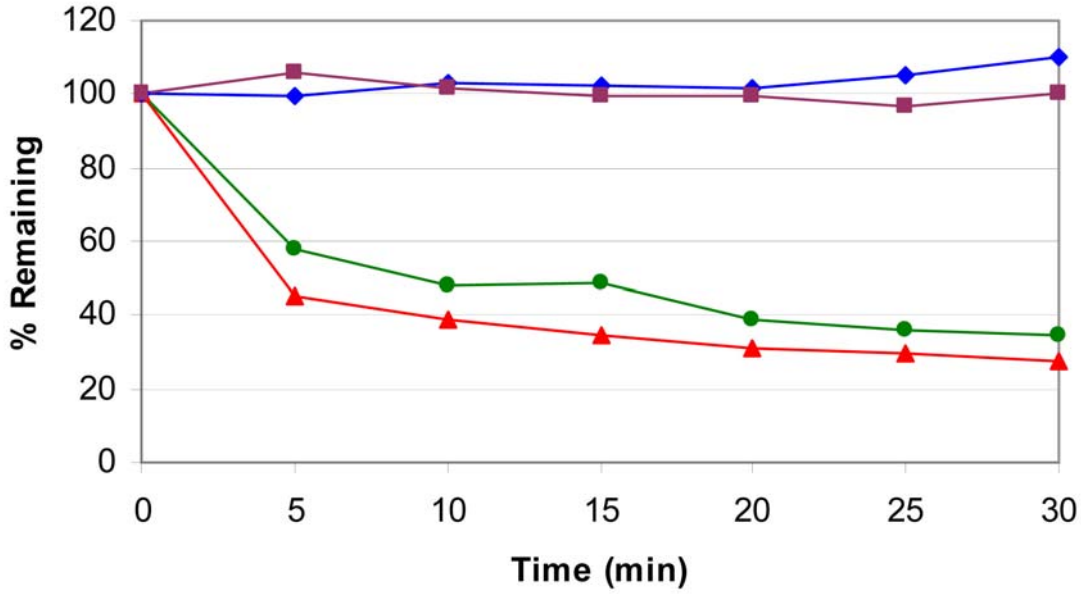
120
100
80
60
40
20
0
% Remaining
0
5
10
15
20
25
30
Time (min)

Figure 29: The *ydj1Δ* and *hsp82* temperature sensitive mutant strains have phenotypes consistent with defects in cell wall synthesis.

(A) Top, tenfold serial dilutions of *ydj1Δ* yeast either expressing Ydj1p ("*YDJ1*") or lacking the expression vector were plated on YPD either lacking or containing 0.4 M NaCl, 1 M sorbitol, or 20 μg/mL calcofluor white at the indicated temperatures for 3 days. Middle and bottom, wild type or *ydj1Δ* yeast were incubated on control or sorbitol or calcofluor white (CW)-containing media as above. (B) *HSP82* and *hsp82* yeast were grown on either YPD or YPD with either 1 M sorbitol or 20 μg/mL CW at the indicated temperatures for 3 days. All the yeast strains are *ade-* and have a pink coloration. *ydj1Δ* yeast also obtained the pink coloration after longer incubations (not shown).

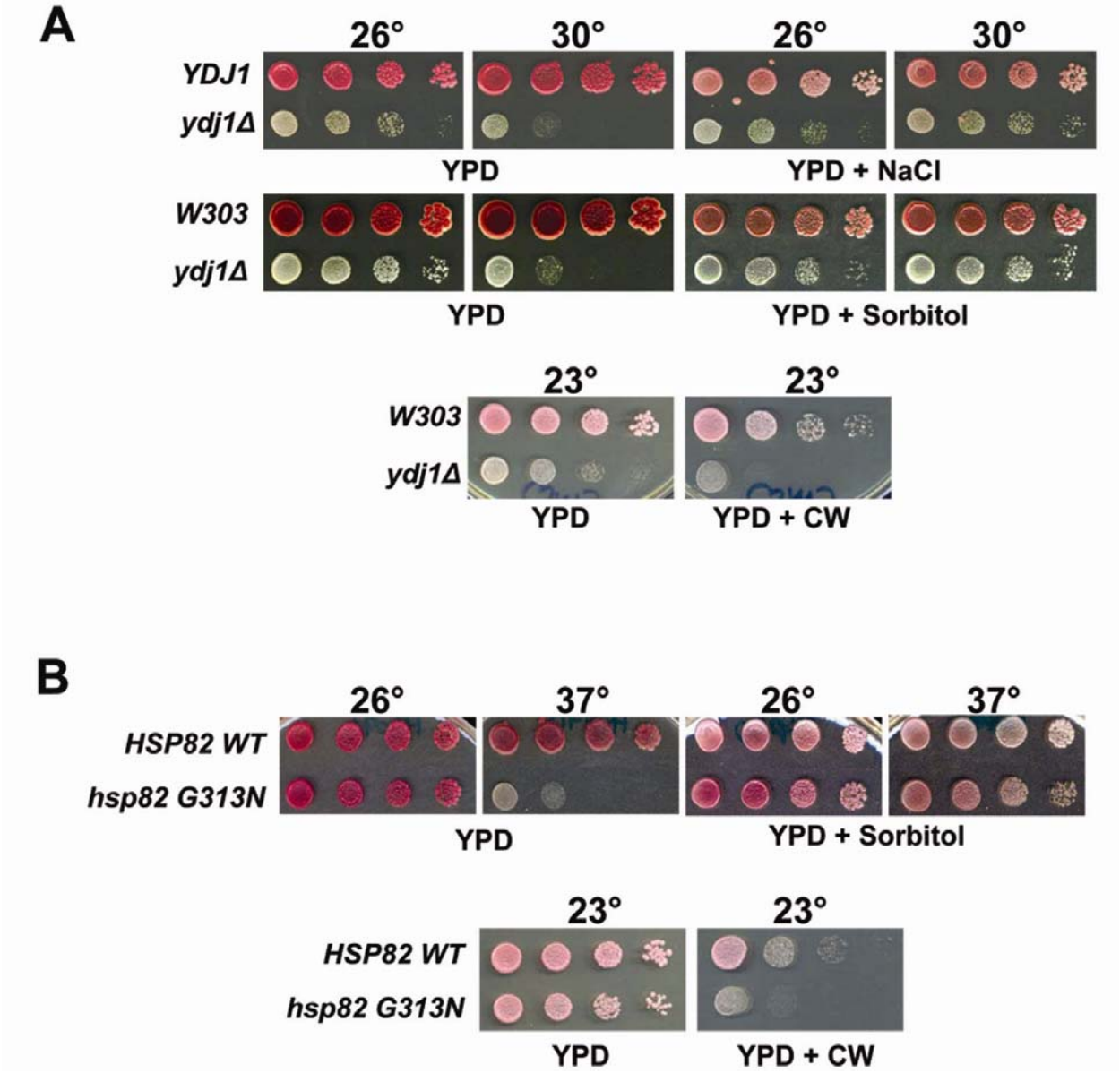
A
26°
30°
26°
30°
YDJ1
ydj1Δ
YPD
YPD + NaCl
W303
ydj1Δ
YPD
YPD + Sorbitol
23°
23°
W303
ydj1Δ
YPD
YPD + CW
B
26°
37°
26°
37°
HSP82 WT
hsp82 G313N
YPD
YPD + Sorbitol
23°
23°
HSP82 WT
hsp82 G313N
YPD
YPD + CW

defects, the growth of *ydj1Δ* yeast was enhanced on 1 M sorbitol at 30° and was sensitive to CW at 23°. The growth of *hsp82* G313N strains was also restored on high sorbitol at 37° and showed sensitivity to CW at 23° (Figure 29B). Notably, the growth of *ydj1Δ* on sorbitol resembled the growth seen upon over-expression of Mid2p or Pkc1p (Figure 18B and 20B). When Mid2p or Pkc1p was over-expressed on high sorbitol containing medium, *ydj1Δ* cells grew at temperatures as high as 37° (Figure 30). Mid2p or Pkc1p over-expression also rescued the CW sensitivity of the *ydj1Δ* strain at 30° (Figure 31). These results indicate that *ydj1Δ* and Hsp82 mutant strains have a cell wall defect, and that Mid2p and Pkc1p may repair this defect.

2.3.6 Mid2p is not dramatically mislocalized or aggregated in *ydj1Δ* yeast

Ydj1p is involved in the translocation of nascent polypeptides into the ER (CAPLAN *et al.* 1992) and is able to retain aggregation-prone proteins in solution (CYR 1995). I therefore hypothesized that Mid2p might be mislocalized or aggregated in *ydj1Δ* yeast, which would prevent accurate sensing of cell wall integrity and cause cell wall defects. But, at least some of the over-expressed Mid2p might escape to the plasma membrane and partially restore cell wall integrity. To test this hypothesis, the solubility of Mid2p was determined by differential centrifugation in wild type and *ydj1Δ* yeast strains over-expressing Mid2p-HA. In both wild type and *ydj1Δ* yeast, the majority of the Mid2p-HA localized to the first pellet (P1; 76% and 80% of the total protein assayed, i.e., the "load", respectively) (Figure 32A), consistent with Mid2p membrane residence. Sec61p, a component of the ER membrane translocon (DESHAIES *et al.* 1991), fractionated similarly. In wild type yeast, 14% of the total Mid2p localized to the second pellet (P2), which is nearly identical to the amount of Mid2p found in the P2 from *ydj1Δ* yeast (15%). Intriguingly, only 1.6% of Mid2p fractionated in the second supernatant (S2), which represents clarified

Figure 30: Mid2p or Pkc1p over-expression, coupled with growth on 1 M sorbitol, restores growth of the *ydj1Δ* strain to 37°.

Ten-fold serial dilutions of *ydj1Δ* yeast over-expressing Mid2p, Pkc1p, or containing a vector control were plated on SC-ura or SC-ura+sorbitol and incubated for 4 days at the indicated temperatures.

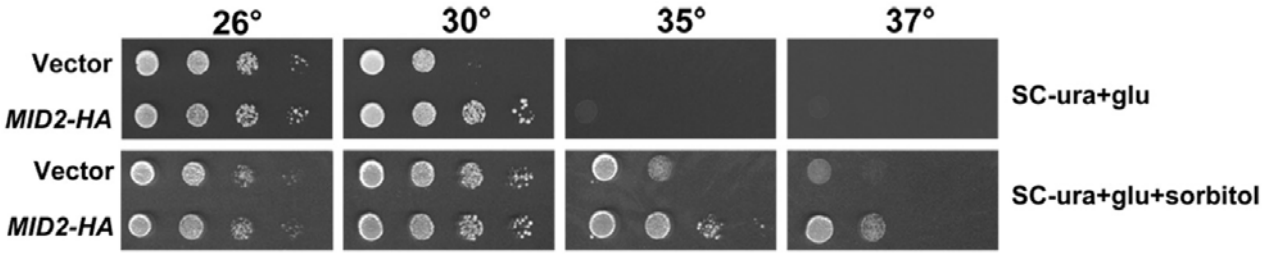
26°
30°
35°
37°
Vector
MID2-HA
Vector
MID2-HA
SC-ura+glu
SC-ura+glu+sorbitol

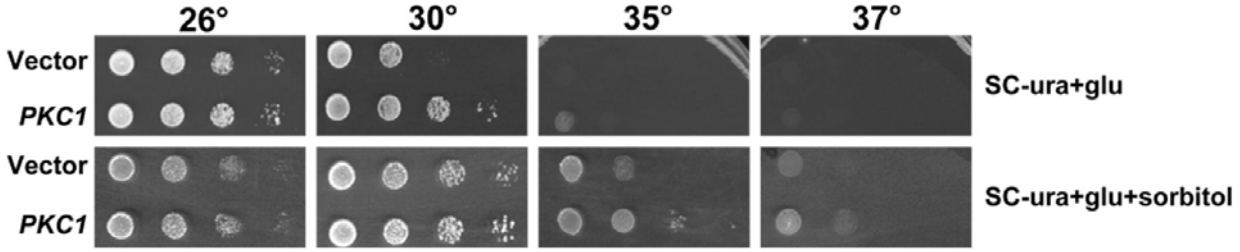
26°
30°
35°
37°
Vector
PKC1
Vector
PKC1
SC-ura+glu
SC-ura+glu+sorbitol

Figure 31: Over-expression of *MID2* and *PKC1* can partially restore growth of the *ydj1Δ* strain in the presence of calcofluor white (CW).

PKC1 and *MID2-HA* overexpression vectors were transformed into the *ydj1Δ* strain. These strains were serially diluted ten-fold onto (A) SC-ura or (B) SC-ura+CW and incubated at the indicated temperatures for 4 days. Yeast containing an *YDJ1* expression vector or a vector control were used as controls.

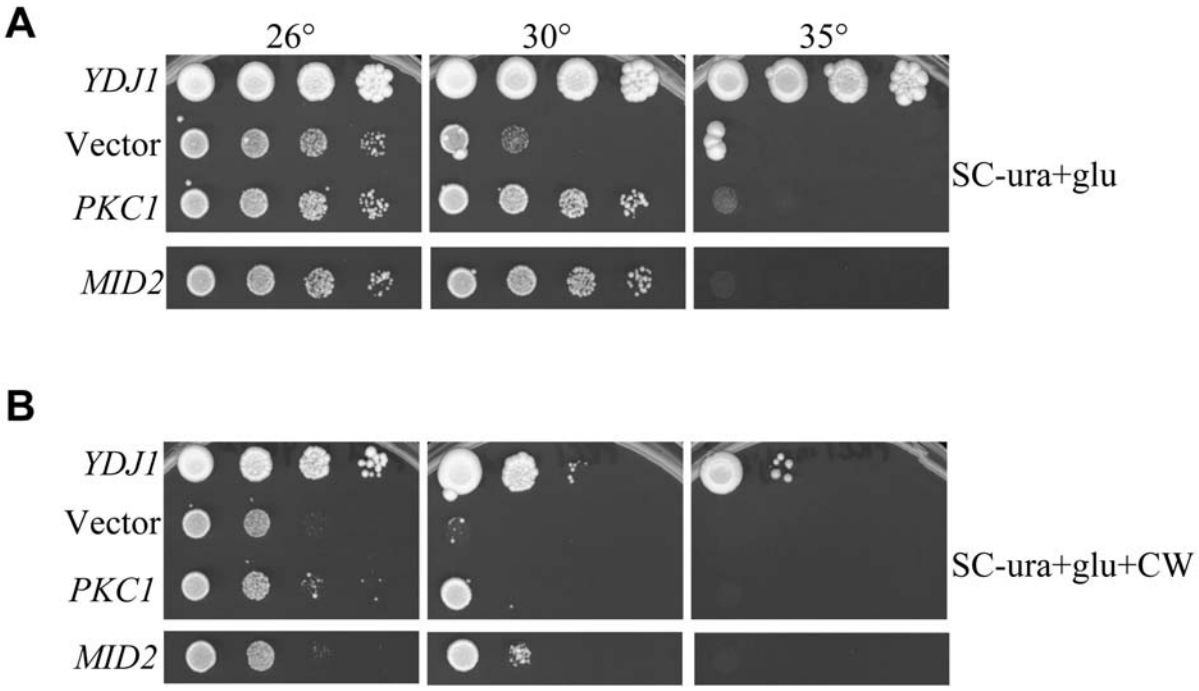
A
26°
30°
35°
YDJ1
Vector
PKC1
MID2
SC-ura+glu
B
YDJ1
Vector
PKC1
MID2
SC-ura+glu+CW

Figure 32: Only a modest increase in Mid2p aggregation is evident in *ydj1Δ* yeast.

(A) Wild type or *ydj1Δ* yeast over-expressing Mid2p were lysed and the sub-cellular fractionation of Mid2p was determined by differential centrifugation. Sec61p, a component of the translocon, is an integral membrane protein, whereas Sse1p, a cytoplasmic chaperone, is primarily in soluble fractions. L = Load; S1 = First, medium-speed supernatant; P1= First, medium-speed pellet; S2 = Second, high-speed supernatant; P2 = Second, high-speed pellet. (B) Mid2p localization was determined by indirect immunofluorescence using an antibody against the HA epitope in wild type or *ydj1Δ* yeast over-expressing Mid2p. For comparison, the ER was visualized using an antibody against the ER resident chaperone, Kar2p, and the nucleus was visualized with DAPI staining. The distended ER and enlarged cell volume of *ydj1Δ* yeast is commonly observed.

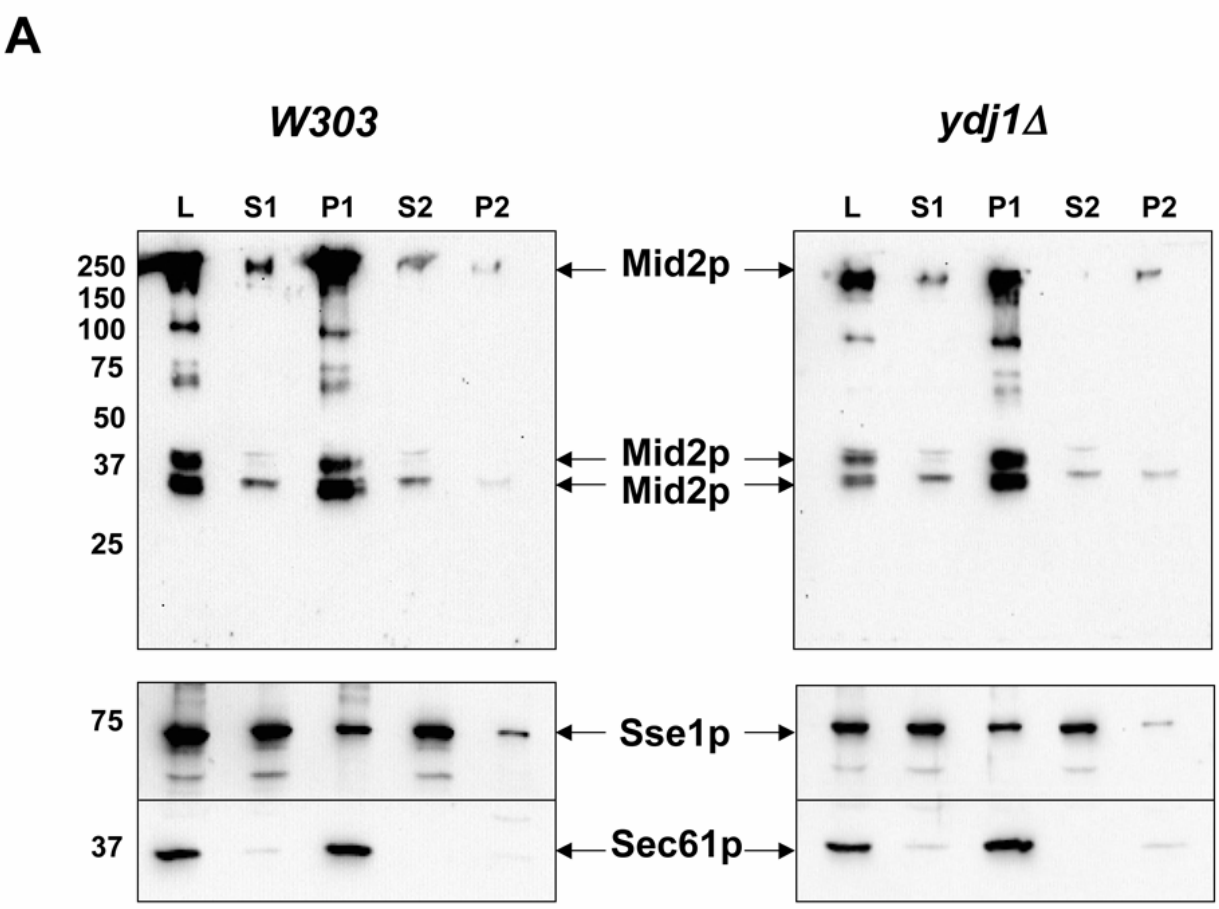
A
W303
ydj1Δ
L
S1
P1
S2
P2
250
150
100
75
50
37
25
Mid2p
Mid2p
Mid2p
75
37
Sse1p
Sec61p

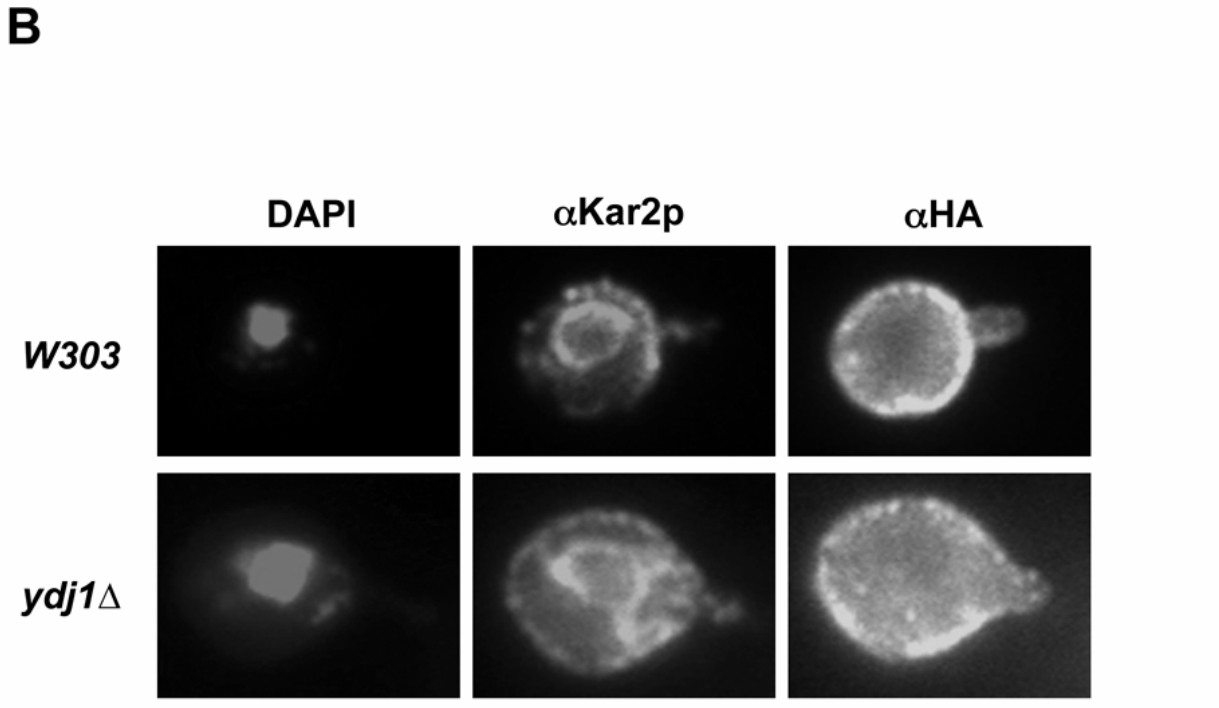
B
DAPI
αKar2p
αHA
W303
ydj1Δ

cytosol (the cytosolic Sse1p chaperone was used as a marker) in *ydj1Δ* cells compared to 6.3% in wild type yeast. The small decrease in the levels of soluble, cytosolic, Mid2p in fractionated lysates prepared from *ydj1Δ* yeast may be due to an increase in protein aggregation, although only a minor percentage of the total cellular Mid2p is affected.

To investigate whether the sub-cellular localization of Mid2p was grossly altered when *YDJ1* was deleted, indirect immunofluorescence microscopy was performed. Mid2p-HA was over-expressed in wild type and *ydj1Δ* yeast and its location was determined using an antibody against the HA epitope tag. As shown in Figure 32B, Mid2p clearly localized to the plasma membrane in wild type yeast, which is in agreement with previously published data (KETELA *et al.* 1999; RAJAVEL *et al.* 1999). Some protein also resided in large intracellular bodies, which may be late secretory vesicles. In *ydj1Δ* yeast, Mid2p localization was unchanged. Together, these results suggest that Mid2p is not significantly mislocalized or aggregated in the *ydj1Δ* yeast strain.

If Mid2p requires Ydj1p for localization or folding, a direct interaction might be detectable. Co-immunoprecipitation experiments were performed to determine if Mid2p and Ydj1p are found in the same complex. *MID2-HA* or an empty vector control was transformed into wild type and *ydj1Δ* yeast. Mid2p-HA was then immunoprecipitated using an antibody against the HA epitope tag and co-precipitated chaperones were detected by Western blot. Despite the presence of Ydj1p, Ssa1p, and Hsp82 in the cell lysate, none of the chaperones were detected in a complex with Mid2p (Figure 33A). Reverse reactions in which Ydj1p was immunoprecipitated with an anti-Ydj1p antibody did not detect any co-precipitated Mid2p, despite the presence of Mid2p in the cellular lysate (Figure 33B). These results suggest that

Figure 33: Mid2p does not co-immunoprecipitate with molecular chaperones.

(A) Mid2p-HA was precipitated from cellular lysate from the indicated strains using the antibody against the HA epitope tag. The presence of co-precipitating molecular chaperones and the translocon was probed using antibodies against Hsp82p, Ssa1p, Ydj1p, and Sec61p. (B) Ydj1p was precipitated from cellular lysate using an αYdj1p antibody. Mid2p does not coimmunoprecipitate. *=heavy chain IgG, PAS= protein A sepharose bead control.

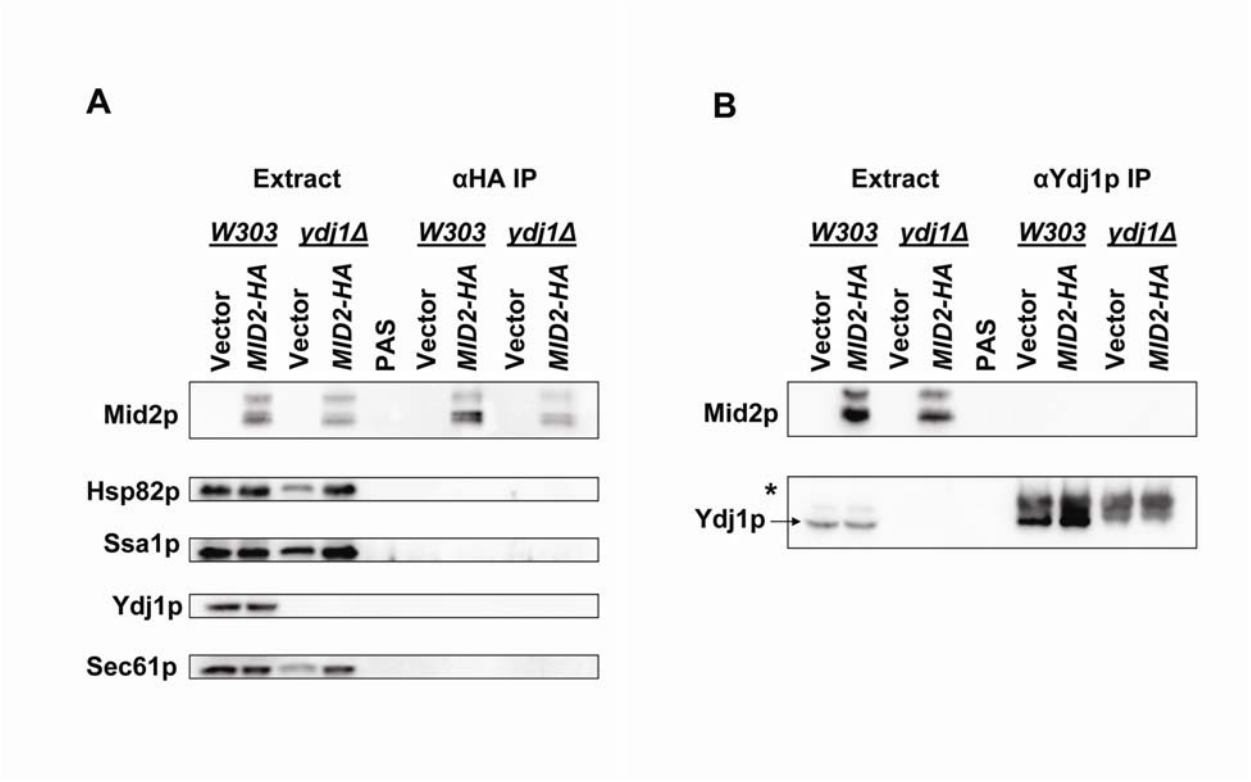
A
Extract
αHA IP
W303
ydj1Δ
W303
ydj1Δ
Vector
MID2-HA
Vector
MID2-HA
PAS
Vector
MID2-HA
Vector
MID2-HA
Mid2p
Hsp82p
Ssa1p
Ydj1p
Sec61p
B
Extract
αYdj1p IP
W303
ydj1Δ
W303
ydj1Δ
Vector
MID2-HA
Vector
MID2-HA
PAS
Vector
MID2-HA
Vector
MID2-HA
Mid2p
*
Ydj1p

Mid2p and Ydj1p do not directly interact and further eliminates the importance of Ydj1p in the folding and localization of Mid2p.

In addition to its role in cell wall integrity, Mid2p has been implicated in actin cytoskeleton rearrangement (MARCOUX *et al.* 2000). Therefore, it was formally possible that Mid2p over-expression rescues actin cytoskeletal defects in the *ydj1Δ* strain and thus improves growth. To determine if the actin cytoskeleton was perturbed in the *ydj1Δ* strain, we used fluorescence microscopy to visualize cortical actin patches in wild type and *ydj1Δ* yeast. In both strains, phalloidin staining showed several punctate "dots" around the yeast cell periphery (Figure 34), characteristic of cortical actin staining (ADAMS and PRINGLE 1984). This result suggests that the actin cytoskeleton is not grossly affected in the *ydj1Δ* strain, and that Mid2p over-expression improves the growth of *ydj1Δ* cells through a different mechanism.

2.3.7 *MID2-HA* over-expression thickens the cell wall of *ydj1Δ* yeast

Another reason that Mid2p might improve the growth of *ydj1Δ* yeast is that Mid2p over-expression may thicken the yeast cell wall (MARCOUX *et al.* 2000), possibly due to an increase in chitin (KETELA *et al.* 1999). Thus, we hypothesized that extra copies of Mid2p would rescue *ydj1Δ* growth and the cell wall defect by strengthening and/or enlarging this structure. To test this hypothesis, wild type or *ydj1Δ* cells lacking the *T(K53R)-YDJ1* expression vector but containing the *MID2-HA* over-expression vector or an empty vector control were analyzed by electron microscopy. We first noted that *ydj1Δ* cells were generally larger than wild type cells and contained an enlarged vacuole (Figure 35A), which is consistent with previously published data (CAPLAN and DOUGLAS 1991). Next, the distance between the outside of the cell wall and the plasma membrane was measured in similarly sized budding wild type or *ydj1Δ* cells and the

Figure 34: The actin cytoskeleton is not perturbed in the *ydj1Δ* yeast strain.

Actin patches were visualized using phalloidin in wild type and *ydj1Δ* yeast. Actin was detected in cortical patches around the cellular periphery. DAPI was used to visualize the nucleus.

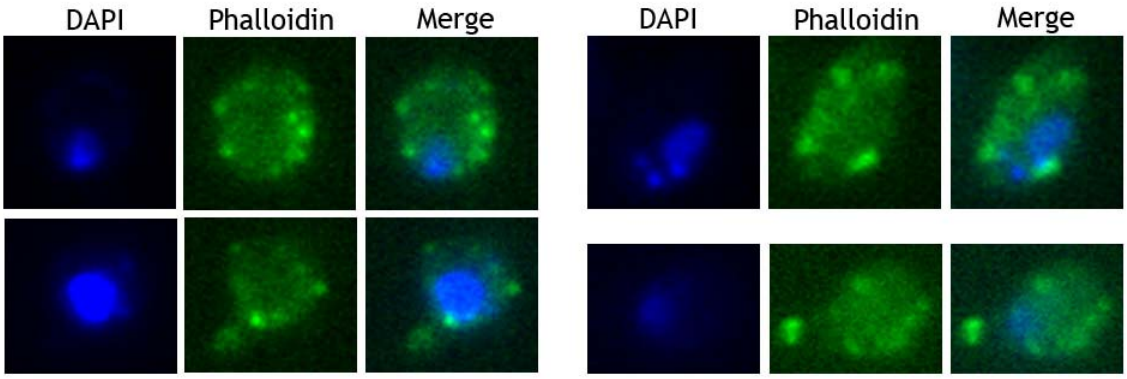

Strain: *W303*

Strain: *ydj1Δ*

Figure 35: Over-expression of Mid2p thickens the cell wall of *ydj1Δ* yeast.

Wild type or *ydj1Δ* strains containing a *MID2-HA* expression vector or vector control were analyzed by electron microscopy. (A) Two examples of single, budding yeast from each strain are shown. Mid2p over-expression in the *ydj1Δ* strain thickens the entire cell wall (top) or at select locations (bottom-arrow) compared to the vector control. Wild type yeast are shown at ~25,000x magnification and *ydj1Δ* yeast are shown at ~15,000x magnification. (B) A higher magnification of *ydj1Δ* containing a *MID2-HA* expression vector or vector control is shown. (C) The average cell wall thickness for each strain was calculated; cell wall thickness of *ydj1Δ* cells over-expressing Mid2p versus those containing the vector control, $p<0.0001$.

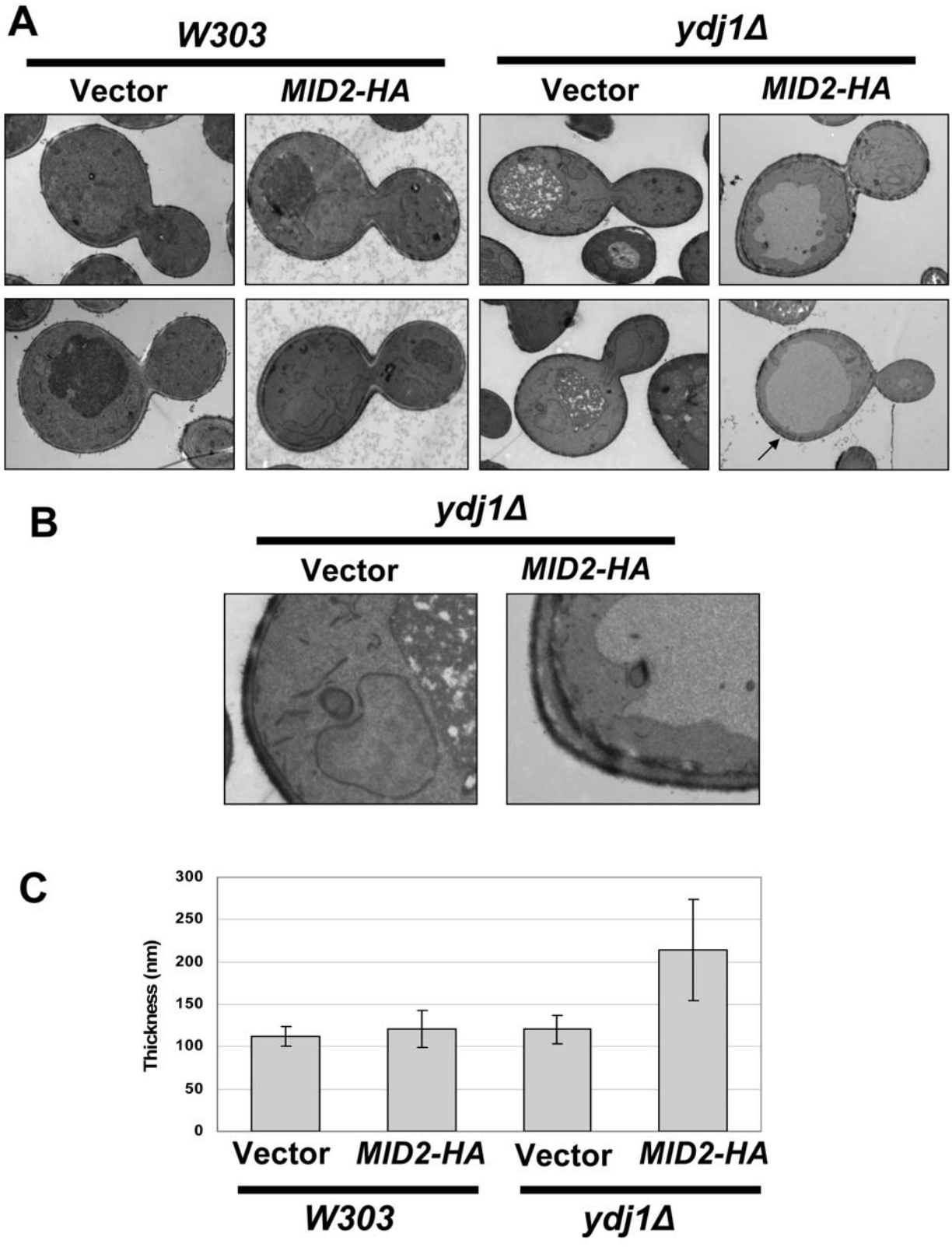
A
W303
ydj1Δ
Vector
MID2-HA
Vector
MID2-HA
B
ydj1Δ
Vector
MID2-HA
C
Thickness (nm)
300
250
200
150
100
50
0
Vector
MID2-HA
Vector
MID2-HA
W303
ydj1Δ

results were quantified as described in the Section 2.2.10. Despite the difference in cell size, the cell wall thickness of the two strains was similar (Figure 35A). This suggests that the cell wall defect in *ydj1Δ* yeast arises due to an aberrant cell wall composition. Strikingly, over-expression of Mid2p in the *ydj1Δ* cells almost doubled the average thickness of the cell wall from 120 nm to 214 nm (Figure 35B-C). The increased thickness was seen in the inner electron transparent layer of the cell wall, which consists of β1,3-glucan, β1,6-glucan and chitin (OSUMI 1998). Occasionally the increased cell wall thickness was localized to a single region of the yeast cell wall (see the region identified by the arrow in Figure 35A), but in most cells the increased thickness was present throughout the cell periphery. Interestingly, over-expression of Mid2p did not uniformly increase the thickness of the cell wall in the wild type yeast strain, though yeast with a thicker cell wall in limited regions around the cell were observed in some cases. Overall, I conclude that Mid2p over-expression rescues the *ydj1Δ* cell wall defect by increasing its thickness.

2.3.8 Directed screening does not identify "factor X"

As hoped, the yeast suppressor screen identified several genes that rescued to some degree the slow growth phenotype of *ydj1Δ* yeast expressing T(K53R)-Ydj1p. However, it is unlikely that these proteins encode Factor X (SULLIVAN and PIPAS 2002), a putative TAg-interacting protein (See Discussion). Thus, I examined the effects on T(K53R)-Ydj1p-expressing *ydj1Δ* yeast when known or suggested TAg interactors were simultaneously produced. I first investigated whether BAG-1 or HspBP1 expression alter the *T(K53R)-YDJ1* thermosensitive phenotype because these mammalian NEFs are known to interact with Hsp70 and promote ADP dissociation (ALBERTI *et al.* 2003; KABANI *et al.* 2002b; RAYNES and GUERRIERO 1998). Thus, the defect in J domain-

Hsp70 function evident in T(K53R)-Ydj1p-expressing *ydj1Δ* yeast might be repaired by producing a factor that enhances the Hsp70 ATPase cycle. Over-expression of BAG-1S or HspBP1 did not restore growth to the *ydj1Δ* strain expressing T(K53R)-Ydj1p at 35° (Figure 36A-B). Interestingly, BAG-1S, but not HspBP1, partially restored growth of the *ydj1Δ* strain (Figure 37A-B) at 30°. This indicates that BAG-1S may stimulate the Ssa1p ATP hydrolysis cycle in the absence of Ydj1p.

I also tested the effect of expressing Cul7 and PKCη in the *ydj1Δ* strain expressing T(K53R)-Ydj1p. Cul7 is a member of an SCF ubiquitin ligase complex that helps direct specific proteins for proteasomal degradation (ALI *et al.* 2004; DIAS *et al.* 2002). Cul7 binds to the TAg J domain in the extended loop between helices III and IV (KASPER *et al.* 2005), a region that is encoded in the chimeric *T-YDJ1* construct used in our studies. PKCη is a human PKC isoform from a novel class of PKC proteins. PKCη functionally substitutes for Pkc1p in yeast cells since it rescues *pkc1Δ* yeast (NOMOTO *et al.* 1997). However, Cul7 over-expression had no effect on *ydj1Δ* cells expressing T(K53R)-Ydj1p, and even made *ydj1Δ* cells grow poorer than vector controls (Figures 36C and 37C). Expression of PKCη in *ydj1Δ* cells with or without T(K53R)-Ydj1p was toxic (data not shown). Thus, unlike *SSA1* or *MID2*, Cul7 and PKCη cannot suppress defects in the Ydj1p chaperone defects.

2.3.9 HopI1 contains a *bona fide* J domain

Pseudomonas syringae is a gram negative bacterium that is the causal agent of leaf spot, leaf blight, and canker disease (SETUBAL *et al.* 2005). *P. syringae* infection interferes with host cell processes through the secretion of effector proteins into the cell by a type III secretion system (NOMURA *et al.* 2005; TANG *et al.* 2006). These effectors are often required for infection by

Figure 36: HspBP1, BAG-1S and Cul7 do not improve growth in the *ydj1Δ* strain expressing T(K53R)-Ydj1p. HspBP1, BAG-1S, and Cul7 expression vectors or vector controls were transformed into the *ydj1Δ* strain expressing T(K53R)-Ydj1p and selected for on SC-ura-trp. The strains were serially diluted ten-fold and incubated for 4 days at the indicated temperatures. Yeast containing a *T-YDJ1* expression vector were used as a control. Expression was verified by immunoblot and Sse1p, Sec61p, and Gas1p were used as loading controls.

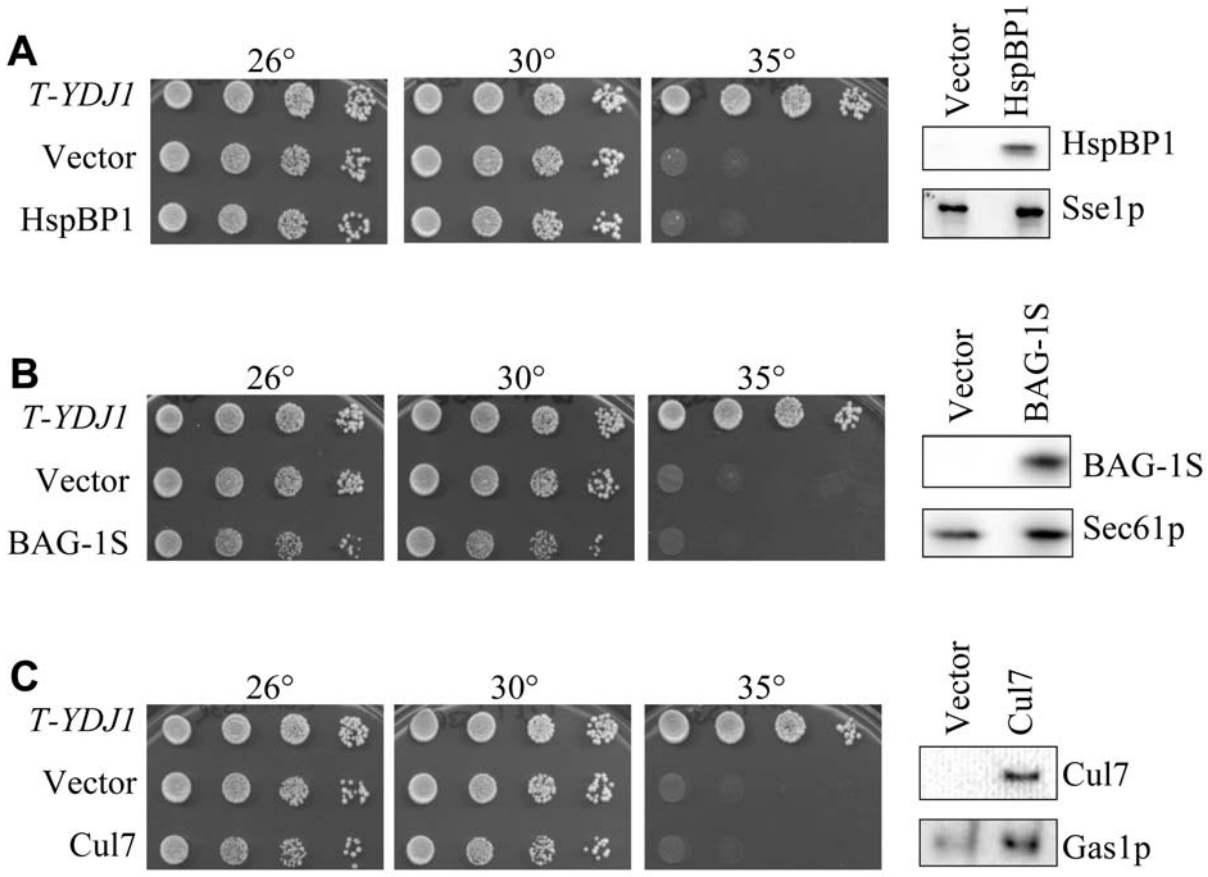
A
26°
30°
35°
T-YDJ1
Vector
HspBP1
Vector
HspBP1
HspBP1
Sse1p
B
26°
30°
35°
T-YDJ1
Vector
BAG-1S
Vector
BAG-1S
BAG-1S
Sec61p
C
26°
30°
35°
T-YDJ1
Vector
Cul7
Vector
Cul7
Cul7
Gas1p

Figure 37: HspBP1, BAG-1S and Cul7 do not improve growth in the *ydj1Δ* strain.

MID2-HA, HspBP1, BAG-1S, and Cul7 expression vectors or vector controls were transformed into the *ydj1Δ* strain and selected for on SC-ura. The strains were serially diluted ten-fold and incubated for 4 days at the indicated temperatures. HspBP1, BAG-1S and Cul7 were expressed as verified by immunoblot, using Sse1p, Sec61p, and Gas1p were as loading controls.

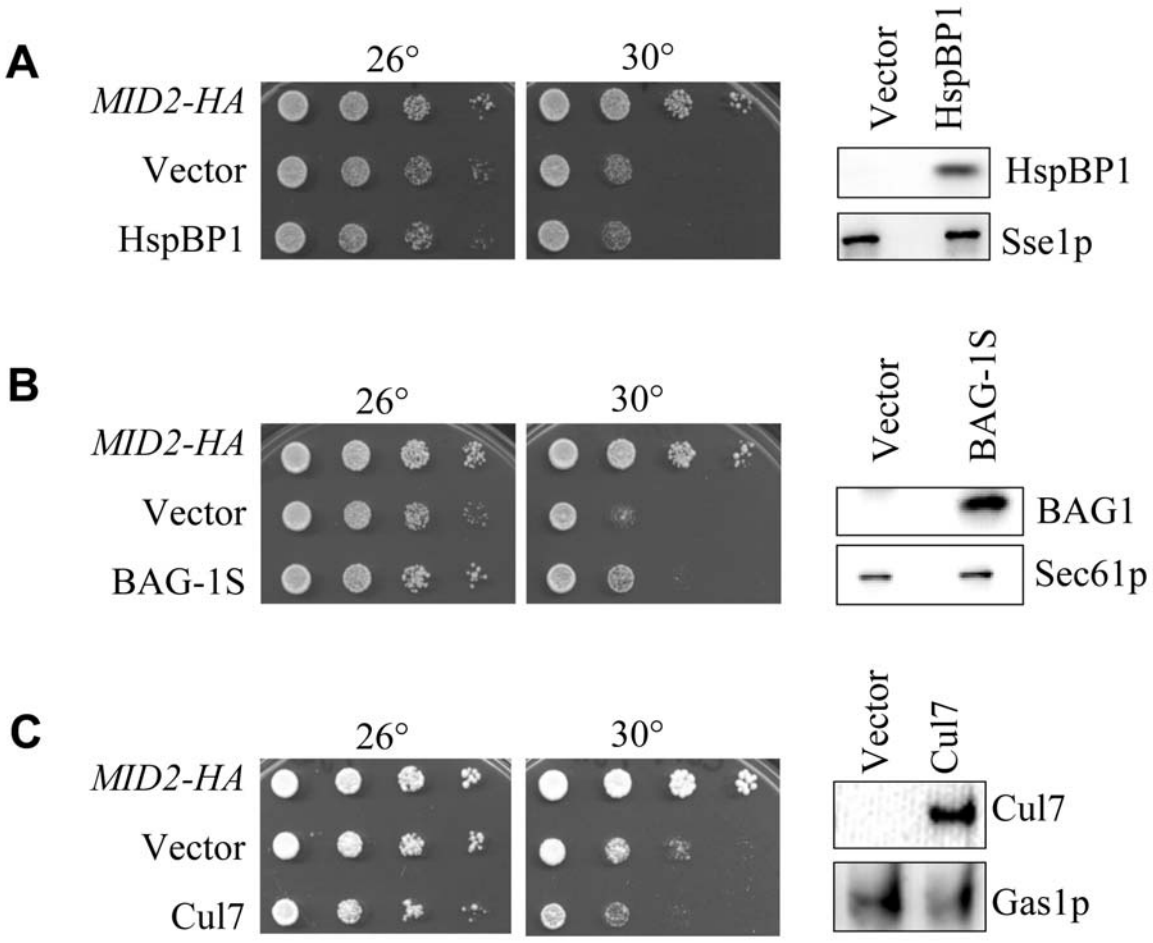
A
26°
30°
MID2-HA
Vector
HspBP1
Vector
HspBP1
HspBP1
Sse1p
B
26°
30°
MID2-HA
Vector
BAG-1S
Vector
BAG-1S
BAG1
Sec61p
C
26°
30°
MID2-HA
Vector
Cul7
Vector
Cul7
Cul7
Gas1p

suppressing the plant defenses and facilitating bacterial growth. The effector protein, HopI1 plays a role in bacterial virulence, since the disruption of the gene with a transposon led to reduced bacteria titer and decreased chlorosis, or yellowing of the leaves (GUTTMAN *et al.* 2002). HopI1 has a C-terminal region that has homology to the J domain (GUTTMAN *et al.* 2002).

To determine if the putative J domain of HopI1 is a functional J domain, the corresponding domain in *YDJ1* was replaced with the HopI1 J domain (*I-YDJ1*). The chimeric gene was then inserted behind the moderate *TEF* and strong *GPD* promoters as described in Section 2.2.2. I found that the introduction of these vectors, but not a vector control, into the *ydj1Δ* yeast strain significantly improved growth at 30° (Figure 38A). Because the HPD motif in J domain-containing proteins is essential for interaction with Hsp70s, the HPD motif was mutated to QAA (*I(HPD/QAA)-YDJ1*). The introduction of these constructs failed to complement the *ydj1Δ* slow growth phenotype (Figure 38A) and in fact inhibited growth when the protein was driven by the *GPD* promoter. Expression of the chimeric proteins was verified by immunoblot (Figure 38B). These data suggest that the mutated version of I-Ydj1p fails to interact with Hsp70 and may act as a dominant negative, one that binds client proteins but lacks the ability to bind to Hsp70. Mutation of H42R in the *T-YDJ1* HPD motif also leads to this dominant negative phenotype (Figure 19). Taken together, these results indicate that HopI1 contains a functional J domain.

Figure 38: The introduction of an *I-YDJ1*-containing vector improves the growth of *ydj1Δ* yeast at 30°.

Ten-fold serial dilutions of *ydj1Δ* yeast containing the indicated plasmids were plated on SC-trp or SC-ura and grown for 5 days at the indicated temperatures. A Ydj1p expression plasmid (*pAV4*) and the SV40 TAg/YDJ1 chimera (*T-YDJ1*) were used as positive controls. (B) Expression was confirmed by immunoblot analysis.

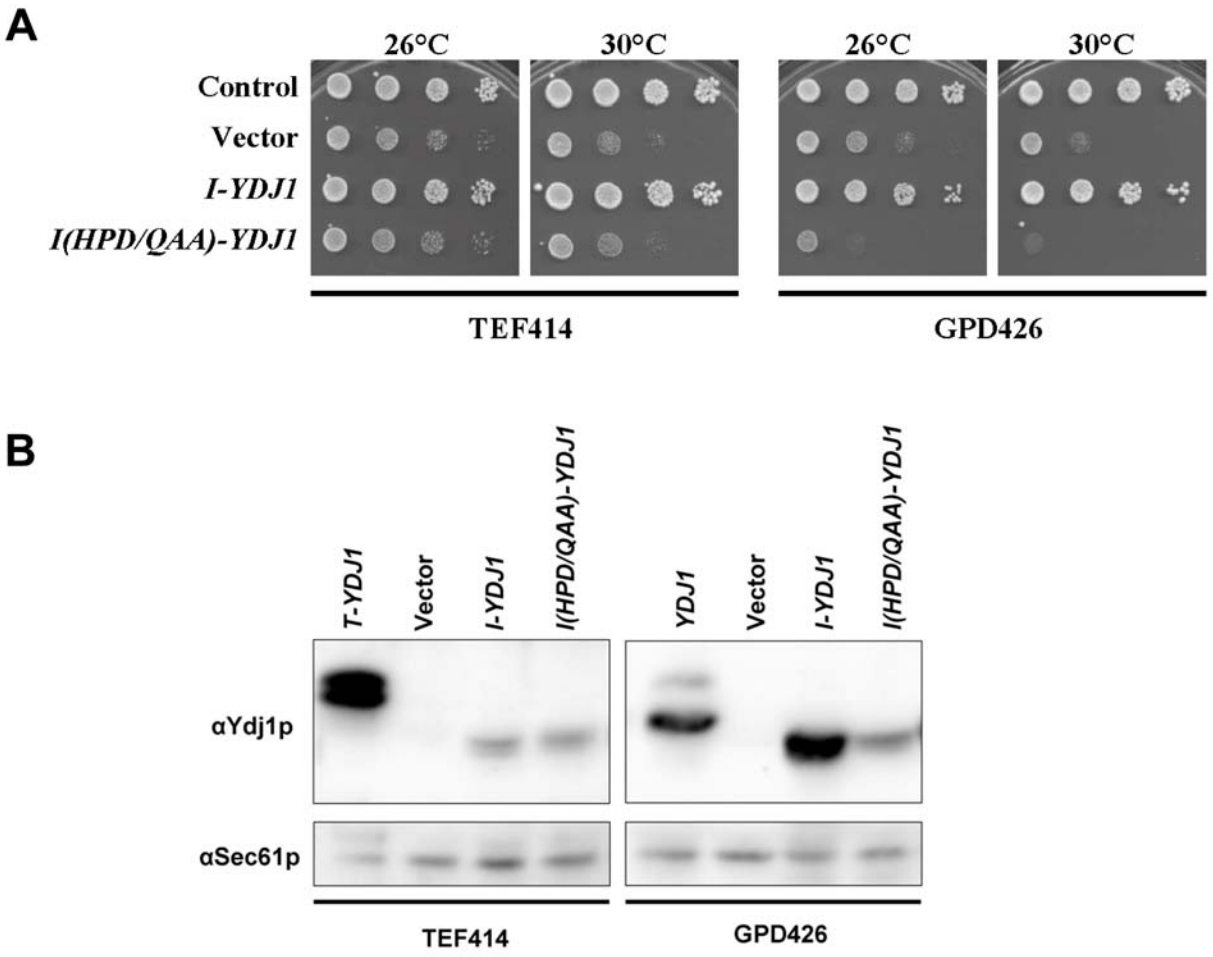
A
26°C
30°C
26°C
30°C
Control
Vector
I-YDJ1
I(HPD/QAA)-YDJ1
TEF414
GPD426
B
T-YDJ1
Vector
I-YDJ1
I(HPD/QAA)-YDJ1
YDJ1
Vector
I-YDJ1
I(HPD/QAA)-YDJ1
αYdj1p
αSec61p
TEF414
GPD426

3.0 IDENTIFICATION OF HSP70 MODULATORS THAT INHIBIT BREAST CANCER CELL PROLIFERATION

3.1 INTRODUCTION

The Hsp70 class of molecular chaperones is essential for normal cell function and misregulation of these proteins can cause or worsen diseases, including breast cancer (BARNES *et al.* 2001; CIOCCA *et al.* 1993). In addition, simply decreasing Hsp70 levels can be sufficient to cause apoptosis in breast cancer cells (NYLANDSTED *et al.* 2000). To this end, we sought to identify Hsp70 modulators that could inhibit Hsp70 ATPase activity and induce apoptosis. Two Hsp70 modulators, DSG and R/1 (discussed in Section 1.4.3) served as starting compounds for these studies. However, both DSG and R/1 have relatively low affinities for Hsp70, and also may not be specific for inhibition of Hsp70. In fact, DSG binds to both Hsp70 and Hsp90 with relatively similar affinities (NADEAU *et al.* 1994). Finally, R/1 is fairly insoluble which makes *in vivo* use difficult. Thus, I hoped to identify more potent, specific, and soluble structural analogs of DSG and R/1 which could induce apoptosis in breast cancer cells.

In this chapter, I discuss the identification of small molecule modulators that inhibit breast cancer cell proliferation. I screened structural analogs of DSG and R/1 for modulation of Hsp70 ATPase activity or the Hsp70/J domain interaction and identified several new classes of chaperone modulators. I discuss in detail the compound MAL3-101, which selectively inhibited

TAg stimulation of Hsp70 and also inhibited breast cancer cell proliferation in two cell lines. To identify more potent analogs of MAL3-101, chemical derivatives were synthesized and tested in the breast cancer proliferation assays. Distinct chemical classes of MAL3-101 derivatives also inhibited breast cancer cell proliferation, some at lower concentrations than MAL3-101. Like MAL3-101, many of these compounds also inhibit TAg stimulation of Hsp70. These compounds may be precursors for more specific and potent compounds that can be used to treat breast cancer.

3.2 MATERIALS AND METHODS

3.2.1 Materials

Ssa1p and TAg were purified as described previously (CANTALUPO *et al.* 1999; MCCLELLAN and BRODSKY 2000). The Hlj1p J domain containing the first 89 amino acids of the yeast Hsp40, Hlj1p, fused to GST at the N- terminus and containing a hexahistidine tag at the C-terminus was purified as described previously with minor modifications (YOUKER *et al.* 2004). A saturated overnight culture of *E. coli* containing the GST-Hlj1p-6His expression vector was diluted to 0.05 OD/mL in 1 L and incubated at 30° for 2 hrs until the culture density was 0.14 OD/mL. Protein expression was induced with 0.2 mM IPTG for 7 hrs until the culture reached a density of 0.7 OD/mL. The cells were harvested, resuspended in 25 mL Buffer 88 (20 mM HEPES, pH 6.8, 150 mM KOAc, 5 mM MgOAc, 250 mM sorbitol) and frozen in liquid nitrogen. The initial batch purification was performed as described previously (YOUKER *et al.* 2004) and dialyzed overnight into Hsp70 dialysis buffer (50 mM Tris-HCl, pH 7.4, 50 mM NaCl, 2 mM $MgCl_2$, 0.8

mM DTT, 5% glyercol). The protein was then added to 2 mL of Q Sepharose beads re-equilibrated in dialysis buffer and rotated for 2 hrs at 4°. Bound protein was eluted with dialysis buffer that had increasing amounts of NaCl up to 1M. The flowthrough and 50 mM NaCl elutions, which had the majority of the Hlj1p chimera as assessed by Coomassie stained SDS-polyacrylamide gels were pooled, concentrated, and frozen in liquid nitrogen.

The purified Ydj1p was provided by Sheara Fewell and purified as described in (CYR *et al.* 1992). Two purified DnaK proteins, a near full length version containing amino acids 2-638 and a truncated version containing amino acids 2-605 were provided by Erik Zuiderweg from the University of Michigan These proteins were purified over an ATP agarose column and excess ATP was removed by PD10 buffer exchange. Human Hsp70 (corresponding to the gene, HSPA1A) was provided by Doug Placais and purified from bacteria or was purchased from Stressgen (NSP-555).

3.2.2 Single turnover ATPase assay

Single turnover ATPase assays were performed as described (FEWELL *et al.* 2004). In short, 25 µg of Hsp70 (Ssa1p or human Hsp70) was combined with 25 µM ATP and 100 µCi α^{32}P-ATP in Single Turnover Complex Buffer (STCB) (100 mM KCl, 25 mM HEPES pH 7.5, 11 mM MgOAc) and incubated for 30 min on ice to allow the Hsp70-ATP complex to form. Purification over a NICK column (GE Healthcare) removed the unbound ATP from the Hsp70-ATP complex. Peak fractions were combined and glycerol was added to a final concentration of 10%. The samples were frozen in single-use aliquots in liquid nitrogen. For each reaction in which endogenous Hsp70 ATPase activity was measured, tubes were rapidly thawed at 30° and combined with DMSO or an equal volume of the test compound. Aliquots of 6 µL were

removed during a 10 min timecourse and combined with 2 µL 4x Stop Solution (2 M LiCl, 4 M Formic Acid, 36 mM ATP). Reactions were spotted in duplicate on thin layer chromatography plates (Selecto Scientific, #11078) and developed in 0.5 M LiCl, 1M Formic Acid. Percent ATP hydrolyzed was determined by phosphorimager analysis. In reactions where TAg or Ydj1p was added, the initial reaction included the co-chaperone and the thawed Hsp70-ATP complex was added immediately to the reaction, already at 30°. After 60 sec, the compound or DMSO were added and the reaction was continued for 9 min. For all reactions in which the endogenous Hsp70 ATPase activity was assessed, the values at the zero sec timepoint were set to 0, and for all cochaperone stimulated reactions the values at the 60 sec timepoint were set to 0. Results from multiple experiments were averaged and kinetic data were obtained using KaleidaGraph. The results were fit to a single exponential using the equations: m1*(exp(-m2*m0))+m3; m1=60, m2=0.08, m3=100 or m1*(1-exp(-m2*m0)); m1=100, m2=0.005, where m1=reaction amplitude, m2=rate of hydrolysis and m3=total ATP hydrolyzed. The first equation was used for the experiments described in 3.3.1 and the second equation was used to quantify all other reactions. The second equation was used to ensure a more representative fit for the data. Similar kinetics was obtained using either equation. All error bars represent standard deviations of the data.

3.2.3 ATPase assay

Purified protein and test compounds were preincubated on ice in 50 mM HEPES pH 7.4, 50 mM NaCl, 2 mM $MgCl_2$, 10 mM DTT for 15 minutes. The reaction was started by adding 1 nmol ATP and 0.2 µCi α^{32}P-ATP and moving the reaction to 30°. A 30 min timecourse was performed and aliquots were removed and added to Stop Solution. Duplicate reactions were

plated on TLC plates and developed in 0.5 M LiCl, 1M Formic Acid. Total pmol ATP hydrolyzed was determined by phosphorimager analysis. The percent hydrolysis at the zero timepoint was subtracted from the percent hydrolyzed at each timepoint, and the data were averaged. The data were then fit to a linear regression that originated at the origin. All error bars represent standard deviations of the data.

3.2.4 Assays for interactions between Hlj1p and Ssa1p

A total of 5 μg GST-Hlj1p-6His was prebound to 12.5 μL glutathione agarose beads in GST binding buffer (20 mM Tris pH, 8.0, 100 mM KCl, 5 mM $MgCl_2$, 0.1% NP40, 2% Glycerol, 1 mM DTT, 1 mM EDTA, 1 mM PMSF) and rotated for 1 hr at 4°. The unbound GST-Hlj1p-6His was removed with 2 washes of GST binding buffer. A total of 3 μg Ssa1p was preincubated with nucleotide and MAL3-101 or DMSO for 12 min before it was added to the bead suspension and rotated for 2 hrs at 4°. The final concentration of MAL3-101 was 30 μM. After 2 hrs, the beads were washed with 50 μL GST binding buffer two times, resuspended in TCA Sample Buffer, and the bound proteins were resolved via SDS-PAGE. The gel was stained with Coomassie Brilliant Blue and quantified using the Kodak 440CF Image Station and quantified using Kodak 1D (V. 3.6) software. Three reactions were performed in the presence of either ATP or ADP. The experimental data were averaged and the reactions performed in the presence of ATP were normalized to 100%.

3.2.5 Cell proliferation assays

The cell proliferation assays were performed as previously described (CORY *et al.* 1991; MINGUEZ *et al.* 2003) using the breast cancer cell lines SK-BR-3 and MDA-MB-468 and the "normal" fibroblast cell line WI-38. Briefly, the indicated cells were plated in 96 well plates and allowed to attach and grow for 48 hrs. The test compounds or DMSO were titrated (0.08-50 μM) into the wells and incubated with the cells for 3-6 days. The cells were treated with 3-(4,5-dimethylthiazol-2-yl)-5-(3-carboxymethoxyphenyl)-2-(4-sulfophenyl)-2H-tetrazolium (MTS), which is converted by succinate dehydrogenase to a formazan in living cells. The absorbance of the formazan was measured at A_{490}. The concentration of compound where proliferation is 50% of the DMSO control was then calculated and is stated below as GI_{50}.

3.3 RESULTS

3.3.1 The identification of Hsp70/J-domain modulators

I sought to identify compounds with structural similarity to DSG and R/1 which could modulate the endogenous Hsp70 ATPase activity or the J domain-stimulated Hsp70 ATPase activity. The isolation of such compounds could lead to the identification of a Structure Activity Relationship (SAR) for these effects. A total of 30 compounds from either the National Cancer Institute (www.dtp.nci.nih.gov) or the University of Pittsburgh Center for Chemical Methodologies and Library Development (UPCMLD) were identified in substructure analogy searches by Dr. Billy Day, Department of Pharmaceutical Science, with structural similarity to R/1. The structures of

select compounds are shown in Figure 39. To determine the effects of these compounds on endogenous Hsp70 ATPase activity, Dr. Sheara Fewell, a previous post-doc in the lab, tested the compounds in a single turnover assay at three concentrations. In these assays, Ssa1p was prebound to ATP and ATP hydrolysis was measured independent of ATP binding or release (FEWELL *et al.* 2004). Ssa1p was chosen since it can be purified with high yield and with few contaminants. In contrast, mammalian Hsp70 tends to have a higher starting percentage of hydrolysis in single turnover assays, which makes quantification more difficult, and contains more impurities. Seven compounds stimulated the rate of ATP hydrolysis by ≥ 2.5 fold at 300 μM (Table 7). The strongest stimulator, MAL3-90 stimulated the rate of Ssa1p ATPase activity 5.2 fold, which was nearly comparable to R/1 (Figure 40A).

Next, the effect of the compounds on J-protein stimulation of Ssa1p was tested. First, I showed that in equimolar amounts to the concentration of ATP-bound Ssa1p, SV40 TAg and Ydj1p stimulate Ssa1p ATP hydrolysis 6-8 fold in a single turnover assay (Figure 40B-C). I then tested the effects of the 12 compounds from the UPCMLD on TAg and Ydj1p stimulation of Ssa1p in the single turnover assays. Five compounds (MAL3-38, MAL3-39, MAL3-54, MAL3-90, and MAL3-101) altered TAg stimulation of Hsp70 ≥ 2 fold (Table 8), and most compounds had similar effects in the presence of Ydj1p [e.g. MAL3-38 and MAL3-90 (Figures 40B-C)]. Interestingly, these compounds had several different effects on cochaperone-stimulated Hsp70 ATP hydrolysis. One class of compounds, which included MAL3-55, stimulated the rate of Ssa1p ATP hydrolysis but inhibited TAg stimulation of Hsp70. This was generally seen as a decrease in the rate of ATP hydrolysis and subsequently a decrease in the amplitude of the reaction. A second set of compounds, exemplified by MAL3-90, strongly increased the rate of TAg stimulation of Hsp70, but had an overall inhibitory effect due to a decrease in reaction

Figure 39: Structure of select chaperone modulators, including parental compounds 15-Deoxyspergualin (DSG) and NSC 630668-R/1 (R/1).

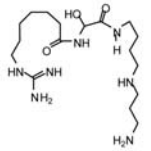

15-Deoxyspergualin
MW=470

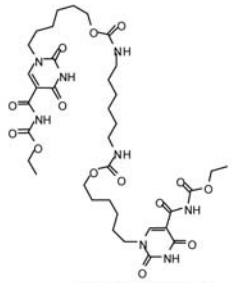

NSC 630668-R/1
MW=823

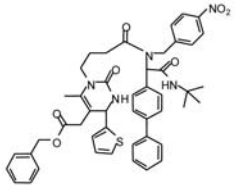

MAL3-38
MW=812

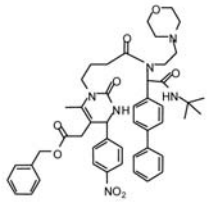

MAL3-39
MW=830

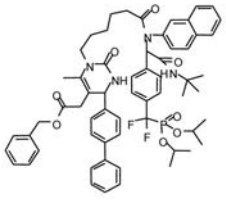

MAL3-55
MW=1040

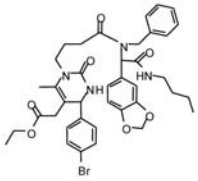

MAL3-90
MW=747

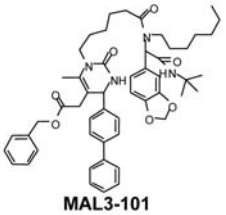

MAL3-101
MW=918

Table 7: The effect of the DSG and R/1 analogs on Ssa1p ATPase activity

	100 µM		300 µM		600 µM	
Drug	**Rate ATP Hydrolysis***	**Fold Change**	**Rate ATP Hydrolysis***	**Fold Change**	**Rate ATP Hydrolysis***	**Fold Change**
DMSO	2.0 ± 0.1					
R/1			11.6 ± 1.0	5.8		
624392	ND	ND	1.6 ± 0.1	-1.3	1.4 ± 0.2	-1.4
642393	ND	ND	1.2 ± 0.3	-1.7	ND	ND
624903	ND	ND	0.9 ± 0.3	-2.2	ND	ND
624904	ND	ND	1.4 ± 0.1	-1.4	ND	ND
624905	ND	ND	1.7 ± 0.2	1.2	ND	ND
624906	ND	ND	1.1 ± 0.2	-1.8	1.8 ± 0.7	-1.1
624907	ND	ND	2.4 ± 0.5	1.2	ND	ND
624908	ND	ND	1.8 ± 0.1	-1.1	ND	ND
625194	2.0 ± 0.2	1	3.6 ± 0.2	1.8	2.7 ± 0.4	1.4
625195	6.1 ± 0.5	3	3.4 ± 0.3	1.7	2.5 ± 0.3	1.3
625512	2.3 ± 0.2	1.2	6.2 ± 0.7	3.1	6.0 ± 0.5	3
625513	2.2 ± 0.2	1.1	3.9 ± 0.3	2	4.9 ± 0.8	2.5
632006	ND	ND	2.8 ± 0.3	1.4	1.0 ± 0.2	2
655302	ND	ND	3.8 ± 0.5	1.9	1.5 ± 0.3	-1.3
ααδ9	ND	ND	1.2 ± 0.2	-1.7	ND	ND
ML2-193	3.2 ± 0.4	1.6	6.2 ± 0.5	3.1	4.5 ± 0.5	2.3
ML2-194	2.5 ± 0.3	1.3	4.1 ± 0.7	2.1	2.7 ± 0.1	1.4
ML2-214	1.8 ± 0.2	-1.1	3.4 ± 0.5	1.7	1.6 ± 0.3	1.3
ML2-215	2.3 ± 0.1	1.2	4.3 ± 0.4	2.2	4.2 ± 1.4	2.1
MAL3-38	3.5 ± 0.2	1.8	6.1 ± 0.8	3.1	4.1 ± 0.6	2
MAL3-39	ND	ND	2.1 ± 0.4	1	1.4 ± 0.7	-1.4
MAL3-40	3.5 ± 0.3	1.8	5.4 ± 0.5	2.7	6.0 ± 0.7	3
MAL3-51	ND	ND	1.7 ± 0.3	-1.2	1.6 ± 0.2	-1.3
MAL3-53	3.7 ± 0.2	1.9	4.9 ± 0.6	2.5	9.1 ± 1.0	4.6
MAL3-54	ND	ND	2.2 ± 0.3	1.1	2.5 ± 0.2	1.3
MAL3-55	1.3 ± 0.1	-1.5	2.8 ± 0.2	1.4	5.6 ± 0.9	2.8
MAL3-87	3.8 ± 0.3	1.9	4.5 ± 0.6	2.3	5.2 ± 0.7	2.6
MAL3-88	2.9 ± 0.3	1.5	3.1 ± 0.4	1.3	4.7 ± 0.7	2.4
MAL3-90	4.1 ± 0.6	2	10.3 ± 1.7	5.2	13.3 ± 1.6	6.7
MAL3-91	3.6 ± 0.3	1.8	5.8 ± 1.2	2.9	9.9 ± 1.3	5
MAL3-101	ND	ND	2.1 ± 0.3	1	2.4 ± 0.2	1.2

*=Rates of ATP hydrolysis are multiplied by 1000; ND=Not determined.

Table 8: The effect of the DSG and R/1 analogs on TAg stimulation of Ssa1p ATP hydrolysis

Drug	Rate ATP Hydrolysis*	Fold Change
DMSO	12.6 ± 0.3	—
R/1	8.3 ± 0.8	-1.5
MAL3-38	25.5 ± 8.7	2
MAL3-39	4.5 ± 1.2	-2.8
MAL3-40	18.9 ± 9.4	1.5
MAL3-51	11.1 ± 0.2	-1.1
MAL3-53	15.5 ± 3.1	1.2
MAL3-54	2.5 ± 1.7	-5.1
MAL3-55	6.8 ± 1.6	-1.8
MAL3-87	22.8 ± 9.4	1.8
MAL3-88	19.0 ± 5.6	1.5
MAL3-90	52.7 ± 14.3	4.2
MAL3-91	18.0 ± 6.0	1.4
MAL3-101	3.1 ± 0.3	-4.0

*=Rates of ATP hydrolysis are multiplied by 1000.

Figure 40: MAL3-38 and MAL3-90 stimulate the ATPase activity of Ssa1p, but inhibit J-protein stimulation of Ssa1p ATP hydrolysis in single turnover assays.

(A) 300 μM MAL3-38 (open circles), and MAL3-90 (open squares) stimulate Ssa1p ATP hydrolysis relative to a DMSO control (filled circles). This stimulation is similar to that seen with R/1 (open triangles). (B) 300 μM MAL3-38 initially increases the rate of J-protein stimulation of Ssa1p ATP hydrolysis, but inhibits the overall reaction by decreasing the reaction amplitude. Equimolar amounts of wild type TAg (filled circles) and Ydj1p (filled squares) stimulate Ssa1p ATP hydrolysis to similar levels. MAL3-38 inhibits the stimulation by TAg (open circles) and Ydj1p (open squares). (C) Like MAL3-38, 300 μM MAL3-90 inhibits J-protein stimulation of Ssa1p ATP hydrolysis by decreasing the reaction amplitude. Equimolar amounts of wild type TAg (filled circles) and Ydj1p (filled squares) stimulate Ssa1p ATP hydrolysis to similar levels. MAL3-90 inhibits the stimulation by TAg (open circles) and Ydj1p (open squares). The arrow indicates that the compounds were added at 60 sec.

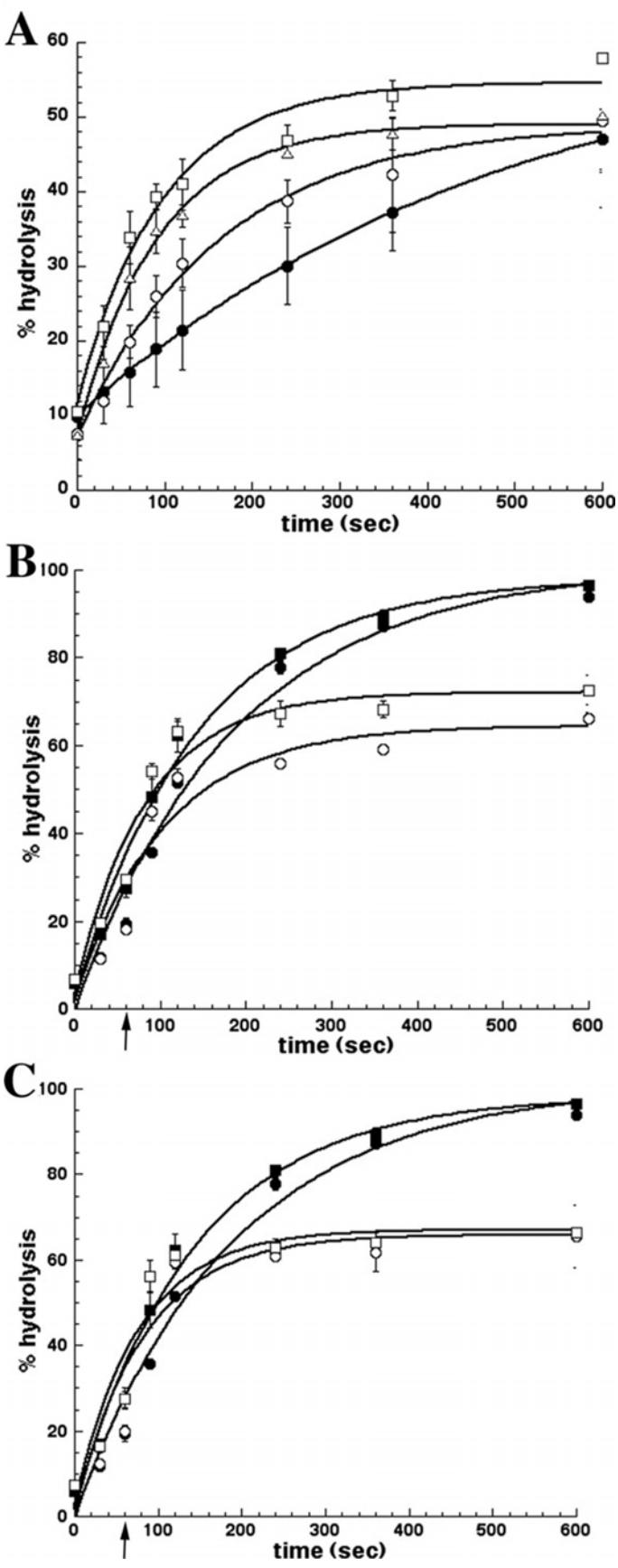
A
% hydrolysis
time (sec)
B
% hydrolysis
time (sec)
C
% hydrolysis
time (sec)

amplitude (Table 8, Figure 40C). In fact, compounds that strongly stimulated Ssa1p ATP hydrolysis were also more likely to stimulate the rate of TAg action on Hsp70 and lead to an overall inhibition of the reaction by decreasing the final amplitude.

Interestingly, three compounds, MAL3-39, MAL3-54 and MAL3-101, inhibited TAg stimulation of Hsp70 ATPase activity, but had no effect on endogenous Hsp70 ATPase activity (Figures 41A-B). This suggests that the compounds may prevent the interaction between Hsp70 and the J domain or prevent Hsp70 from changing conformation in response to the J domain. Intriguingly, the effect of MAL3-101 on TAg stimulation of Hsp70 ATP hydrolysis may be specific as MAL3-101 had no affect on Ydj1p stimulation of Ssa1p (Figure 41C). However, MAL3-101 is not a general inhibitor of TAg activity as Dr. Fewell showed it has no effect on TAg ATPase activity independent of Hsp70 and the J domain (FEWELL *et al.* 2004). In conclusion, I helped identify several classes of Hsp70 modulators, including a class that selectively inhibits cochaperone activity.

3.3.2 Characterization of MAL3-101

MAL3-101 represents a member of a unique class of Hsp70 modulator, which selectively inhibits stimulation of Hsp70 by TAg. To better understand the action of this compound on Hsp70 activity *in vitro*, I titrated MAL3-101 into the single turnover assay in the presence of TAg. At lower compound concentrations (30 μM and 100 μM), MAL3-101 had little effect on TAg stimulation of Hsp70 (Figure 42A), indicating a concentration dependent effect of the compound. However, increasing amounts of TAg overcame the inhibition seen with 300 μM MAL3-101 (Figure 42B).

Figure 41: MAL3-39 and MAL3-101 selectively inhibit J-protein stimulation of Ssa1p.

(A) 300 μM MAL3-39 or (B) 300 μM MAL3-101 were added to reactions that either contained 1 μg TAg (open squares) or lacked TAg (open circles). These reactions were compared with DMSO controls in the presence (filled squares) or absence (filled circles) of TAg. (C) MAL3-39 (open squares) and MAL3-101 (open diamonds) had no affect on Ydj1p stimulation of Ssa1p compared to a DMSO control (filled circles). Ssa1p treated with DMSO in the absence of cochaperone (filled circles) was used as a control.

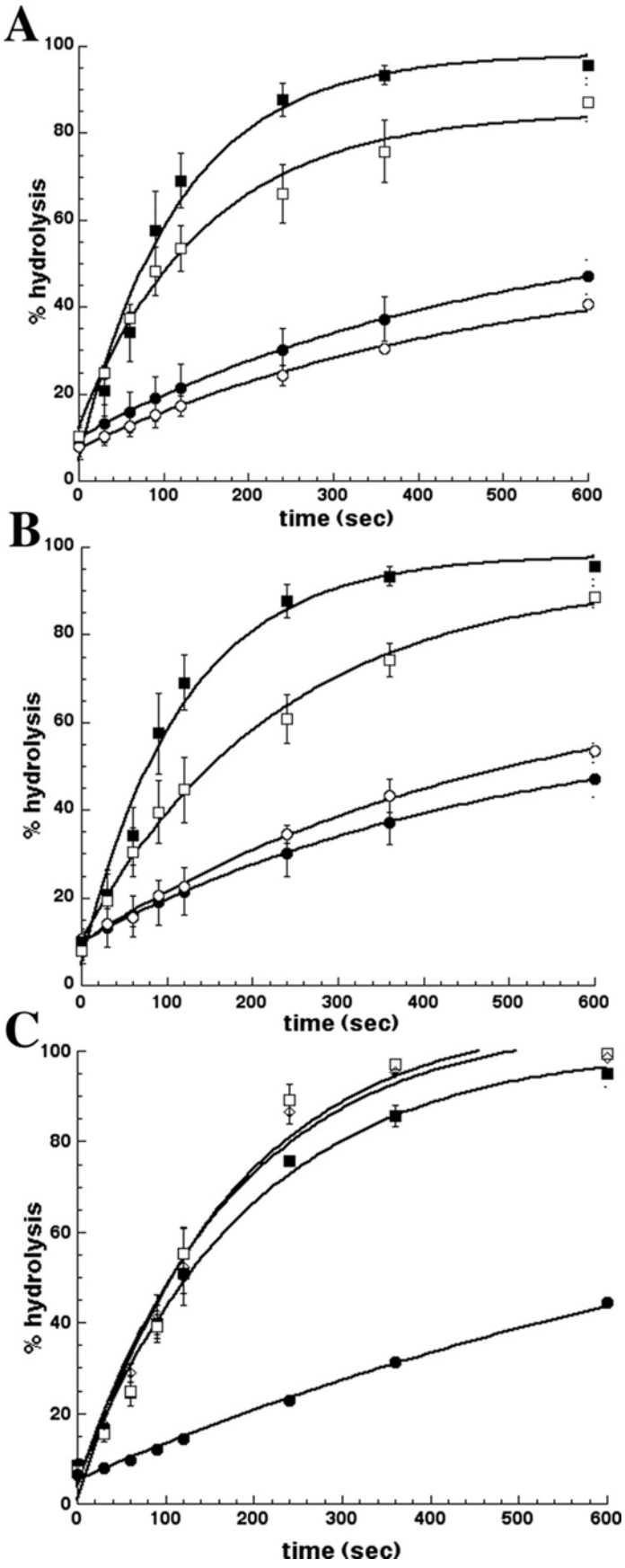
A
B
C
% hydrolysis
time (sec)
0
20
40
60
80
100
0
100
200
300
400
500
600

Figure 42: Concentration dependence of MAL3-101 and TAg in the single turnover assays.

(A) TAg stimulated Ssa1p ATP hydrolysis was determined in the presence of DMSO (filled squares), 30 μM MAL3-101 (open circles), 100 μM MAL3-101 (open squares), or 300 μM MAL3-101 (open triangles). An unstimulated Ssa1p reaction is shown (filled circles). (B) TAg stimulated Ssa1p ATP hydrolysis was determined in the presence of DMSO (filled circles) or 300 μM MAL3-101 and increasing amounts of TAg. TAg concentrations are 0.02 μM TAg (open circles), 0.05 μM TAg (open squares), 0.11 μM TAg (open triangles), 0.22 μM TAg (open, inverted triangles), 0.67 μM TAg (crosses).

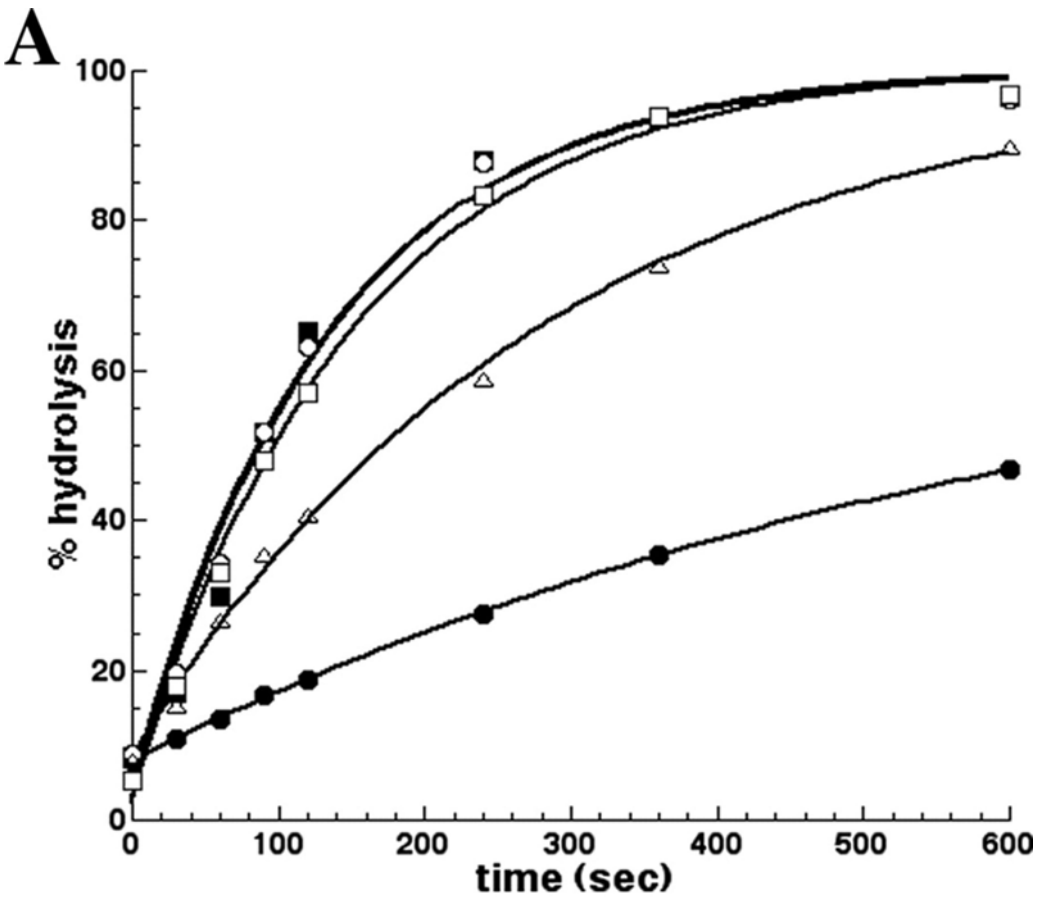
A
% hydrolysis
time (sec)
0
20
40
60
80
100
0
100
200
300
400
500
600

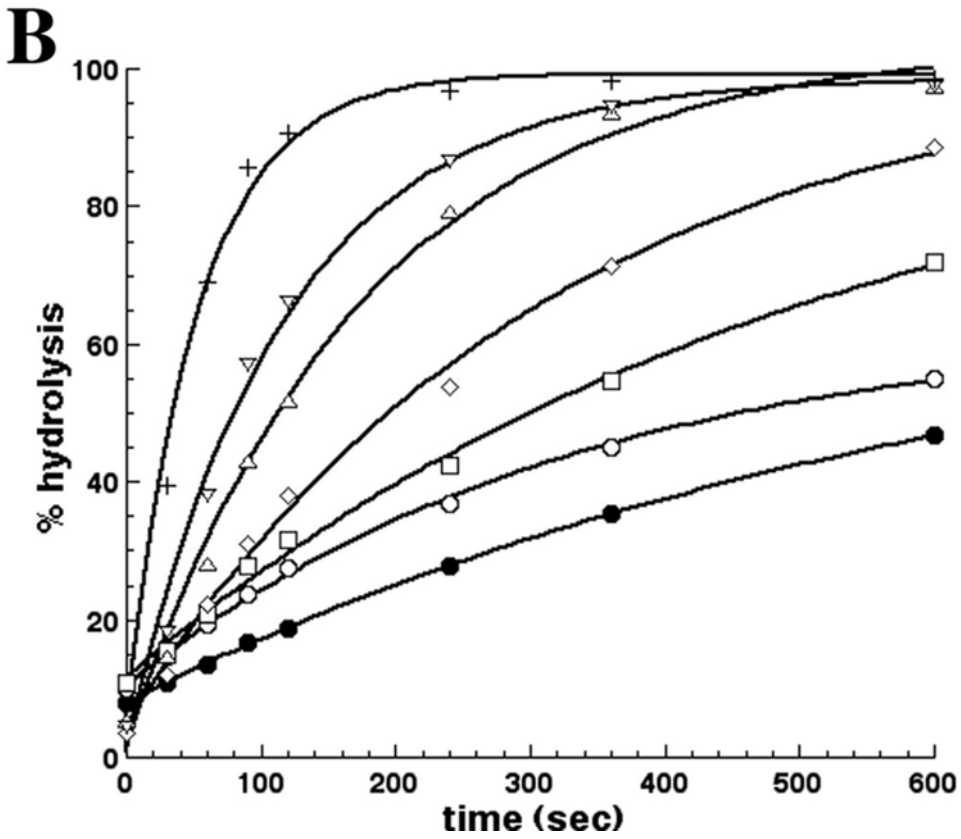
B
% hydrolysis
time (sec)
0
20
40
60
80
100
0
100
200
300
400
500
600

I hypothesized that if MAL3-101 interfered with the interaction between the J domain and Hsp70, this could be shown using coprecipitation studies. To test this hypothesis, I incubated GST-Hlj1p-His with glutathione beads and examined whether 30 μM MAL3-101 could interfere with Ssa1p binding to GST-Hlj1p-His. If the MAL3-101 inhibited the interaction between the J domain and Ssa1p, a decrease in the amount of co-chaperone bound to Ssa1p in the presence of ADP would be predicted. When the level of Hsp70 associated with GST-Hlj1p-His in the presence of ATP was normalized to 100%, little difference between the amount bound to Ssa1p in the presence of ADP was seen (70% Ssa1p bound with DMSO compared to 73% of Ssa1p bound with MAL3-101) (Figure 43). This result suggests that MAL3-101 has little effect on the binding between the two domains. However, this experiment has many caveats. First, the concentration of MAL3-101 used was quite low. At this concentration, little effect on TAg stimulation of Ssa1p was detected. Second, MAL3-101 shows some specificity for J domain inhibition as it inhibits TAg-stimulated Ssa1p ATP hydrolysis, but not Ydj1p-stimulated hydrolysis. It is possible that MAL3-101 has no effect on GST-Hlj1p-His stimulation of Ssa1p. Therefore, coprecipitation experiments should be repeated using TAg. Third, these experiments require a stable interaction between the J domain and Hsp70, which is not always seen *in vitro* (RUSSELL *et al.* 1999). It is possible that MAL3-101 can only inhibit the transient interaction between the J domain and Hsp70. However, these results suggest MAL3-101 may inhibit the conformational change induced by J domain interaction with Hsp70, not the actual interaction.

3.3.3 Identification of a putative, minimal pharmocophore

Due to the low number of Hsp70 modulators available and their relative complexity, determining a SAR has proven difficult. However, based on the analysis of the compounds described in

Figure 43: MAL3-101 does not interfere with Ssa1p binding to GST-Hlj1p-His.

Purified GST-Hlj1p-His was bound to glutathione beads and incubated with the indicated nucleotide and purified Ssa1p that had been preincubated with 30 μM MAL3-101 or DMSO. The amount of Ssa1p bound to GST-Hlj1p-His was visualized on a Coomassie blue stained SDS-polyacrylamide gel. The amount of Ssa1p bound to GST-Hlj1p-His was normalized to 100. A representative gel is shown.

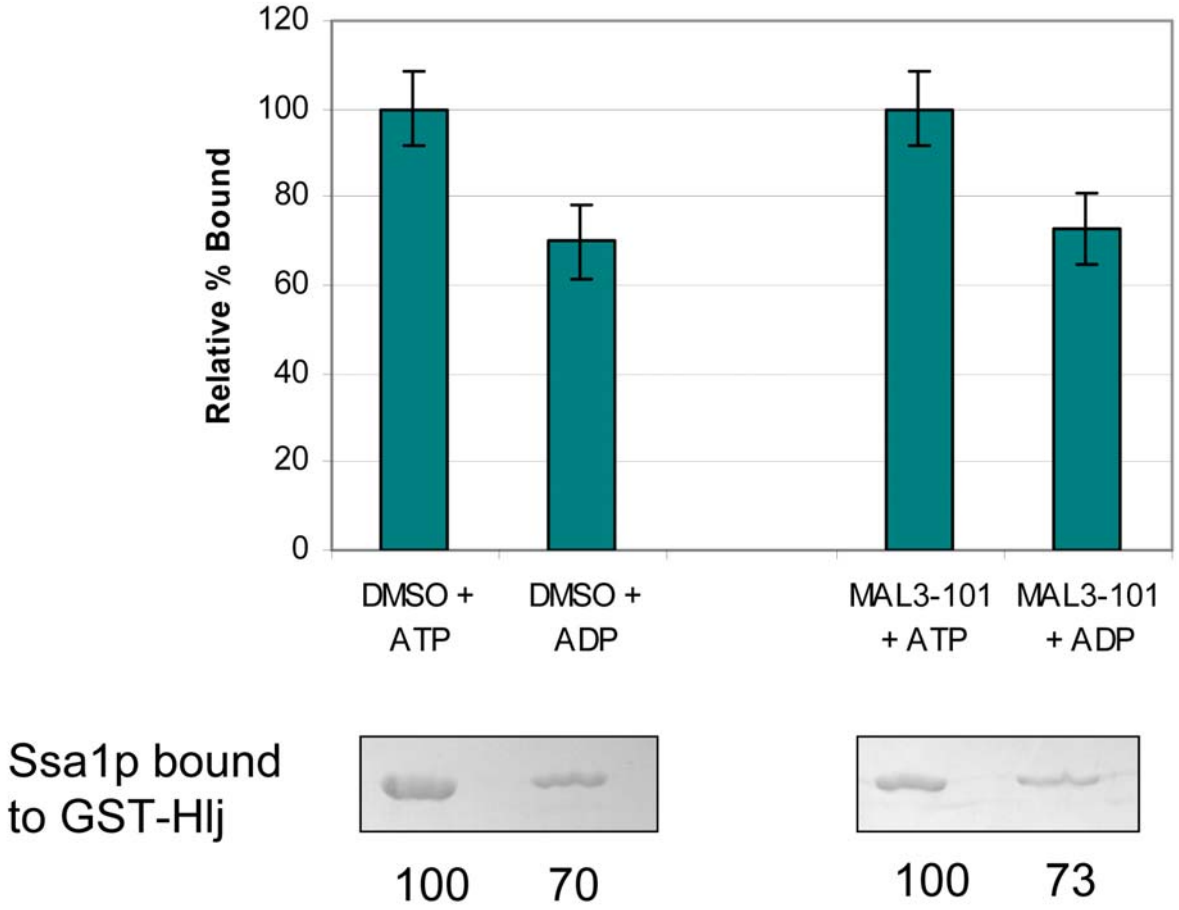
120
100
80
60
40
20
0
Relative % Bound
DMSO + ATP
DMSO + ADP
MAL3-101 + ATP
MAL3-101 + ADP
Ssa1p bound to GST-Hlj
100
70
100
73

Figure 44: Structures of compounds that were proposed to contain the putative minimal pharmocophore.

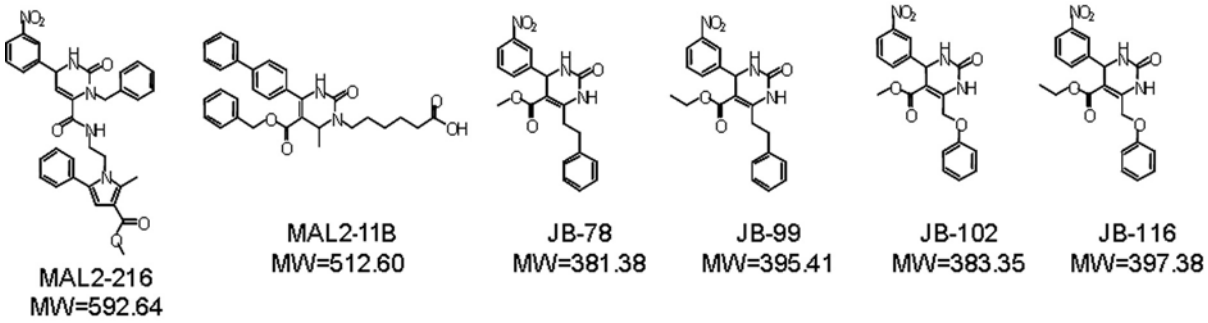

Section 3.3.1, compounds, JB-78, JB-99, JB-102, JB-116, MAL2-11B, and MAL2-216, were obtained from UPCMLD, and their structure is shown in Figure 44. These compounds contain many of the same structural characteristics as the DSG and R/1 analogs, but were much smaller in mass and were predicted to have higher solubility. These six compounds were also chosen to allow the identification of the minimal pharmocophore. They may also prove valuable *in vivo* due to their higher solubility.

I tested JB-78, JB-99, JB-102, JB-116, MAL2-11B, and MAL2-216 in single turnover assays to determine if they altered Ssa1p ATP hydrolysis or TAg stimulation of Ssa1p. Five compounds stimulated Ssa1p ATP hydrolysis $\geq$ 2.7 fold (Table 9, Figure 45A) at 300 μM. Interestingly, these 5 compounds mimicked MAL3-90 when TAg was added to the experiment and increased the rate of TAg stimulation of Ssa1p between 2-7 fold, but decreased the reaction amplitude by almost half (Figure 45A). These results are also consistent with the observation that compounds that dramatically stimulate Hsp70 ATPase activity also stimulate TAg activity. The effects of the compounds were also tested by Fengfeng Xu, a rotation student in the lab, for their impact on endogenous Hsp70 activity with both Ssa1p and mammalian Hsp70 (Stressgen), and similar results were obtained. Interestingly, the compounds seemed to have a greater effect on mammalian Hsp70 ATP hydrolysis than Ssa1p. Future experiments will determine if the compounds also have a greater effect on TAg stimulation of mammalian Hsp70 ATP hydrolysis.

Perhaps the most interesting compound in this set was MAL2-11B. This compound had no effect on endogenous Hsp70 hydrolysis when tested with the two Ssa1p preps or mammalian Hsp70 (Figure 45B, data not shown). However, the compound dramatically inhibited TAg stimulation of Ssa1p, much more dramatically than MAL3-101 at 300 μM (Figure 45B). As

Figure 45: Two classes of compounds identified with a minimal pharmocophore.

(A) MAL2-216 and (B) MAL2-11B were added at 300 μM to the single turnover assay in the presence (light blue) or absence (dark blue) of 1 μg TAg. DMSO treated Ssa1p ATP hydrolysis in the presence (red) or absence (black) of TAg was used as a control. (C) TAg stimulated ATP hydrolysis was determined in the presence of DMSO (red), 30 μM MAL2-11B (purple), 100 μM MAL2-11B (green), and 300 μM MAL2-11B (blue). A reaction without TAg is shown in black.

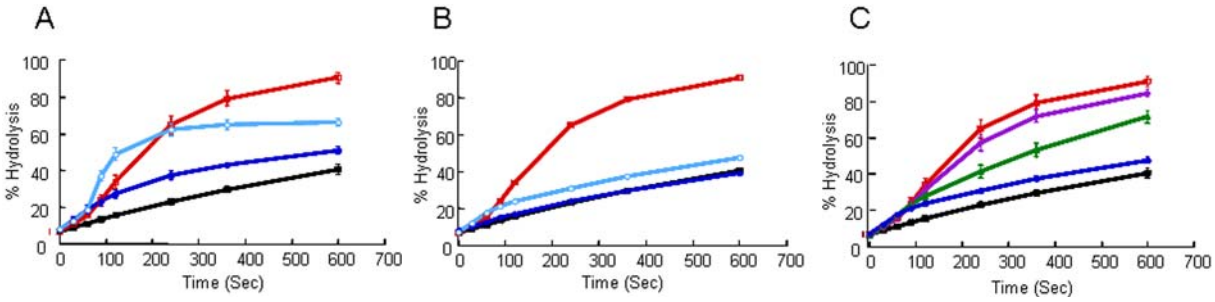

Table 9: The effects of the compounds with a "putative minimal pharmocophore" on Ssa1p stimulated ATP hydrolysis and TAg stimulation of Ssa1p ATP hydrolysis.

	Endogenous Ssa1p			TAg stimulated-Ssa1p		
	Rate ATP Hydrolysis*	**Fold Change**	**Amplitude**	**Rate ATP Hydrolysis***	**Fold Change**	**Amplitude**
DMSO	1.5±0.1		52.1	6.3		79.7
JB-78	3.1±0.3	2.1	50.0	20.3	3.2	42.3
JB-99	4.0±0.4	2.6	42.1	33.7	5.3	45.5
JB102	3.8±0.4	2.5	45.2	9.0	1.4	47.6
JB-116	4.4±0.7	2.9	36.4	18.5	2.9	49.4
MAL2-216	4.5±0.2	3.0	45.8	16.7	2.7	46.7
MAL2-11B	1.5±0	1.0	52.1	2.8	-2.3	43.9

*=Rates of ATP hydrolysis are multiplied by 1000.

shown previously (Figure 42A), MAL3-101 had little effect on TAg stimulated ATP hydrolysis at 30 μM or 100 μM. However, even at these concentrations, MAL2-11B significantly inhibited TAg stimulation of Ssa1p ATP hydrolysis (Figure 45C). This suggests that MAL2-11B may be a more potent Hsp70 co-chaperone modulator than MAL3-101.

3.3.4 MAL3-101 inhibits breast cancer cell proliferation

Since the six compounds identified in Section 3.3.3 may contain the minimal pharmocophore, have a lower mass, and likely are more soluble than previous compounds, they were tested for their effects on breast cancer cell proliferation. MAL3-101 was also tested since previous studies had suggested it was membrane permeable (FEWELL *et al.* 2004). These compounds were titrated onto SK-BR-3 breast cancer cells by Guangyu Zhu in the Billy Day lab, Department of Pharmaceutical Sciences, University of Pittsburgh, and after 3-4 days he determined the number of living cells using MTS, a colorimetric indicator of cell number. The concentration at which 50% of the treated cells are present relative to the DMSO control (GI_{50}) was determined. Based on his data, MAL3-101 inhibited SK-BR-3 cell proliferation at a GI_{50} of 9.3 μM and was the only compound tested to inhibit proliferation at a concentration lower than 15 μM (Table 10). A similar GI_{50} of 8.4 μM was observed when MAL3-101 was titrated onto a second breast cancer cell line, MDA-MB-468. However, in these assays, MAL3-101 may not be specific for breast cancer cell proliferation (Table 11). MAL3-101 also inhibited WI-38 fibroblast cells at a GI_{50} of 15 μM. Assuming all the compounds were able to enter the cell, two conclusions can be made. First, despite their shared kinetics, MAL3-101 and MAL2-11B act differently on breast cancer cells. Second, compounds that prevent a functional interaction between Hsp70 and J-proteins may be a viable treatment for breast cancer. However, additional

Table 10: The effect of the compounds on SK-BR-3 cell proliferation.

	SK-BR-3	SK-BR-3
Exposure time/d	3	4
MAL2-216 (μM)	>50	ND
MAL3-27 (μM)	>50	41±2
JB-78 (μM)	>50	41±2
JB-99 (μM)	38±4	38±8
JB-102 (μM)	>50	40±0
JB-116 (μM)	>50	37±2
MAL3-101 (μM)	9.3±2.2	11±2
Taxol (nM)	3.7±0.5	5.9±0.8

Table 11: MAL3-101 inhibits cell proliferation.

	SK-BR-3	SK-BR-3	MDA-MB-468	WI-38
Exposure time/d	3	4	6	5
MAL3-101 (μM)	9.3±2.2	11±2	8.4±1.0	15±12
Taxol (nM)	3.7±0.5	5.9±0.8	1.7±0.4	>50

compounds will need to be identified which are more specific for the chaperone isoforms that may be specifically induced in breast cancer cells.

3.3.5 Some MAL3-101 derivatives inhibit breast cancer cell proliferation

The study presented above suggests that the isolation of MAL3-101 analogs might identify additional inhibitors of breast cancer cell proliferation, perhaps with greater potency, and identify a functional group that is required for this activity. To this end, the Wipf lab at the UPCMLD synthesized 43 derivatives of MAL3-101 (WERNER *et al.* 2006). Like the previous UPCMLD compounds, the chemical derivatives of MAL3-101 were created through successive Biginelli and Ugi reactions. Fifteen compounds were synthesized using only the first Biginelli reaction, varying the aldehyde group present. These products were combined with *m*-butyl-isocyanide and various combinations of aldehydes and amines to create the final products via Ugi condensation reactions. In addition, the free diacid of MAL3-101 was created by hydrolysis of MAL3-101.

These 43 compounds were screened for inhibition of breast cancer cell proliferation by Guangyu Zhu in the Day lab, as described above. Seventeen compounds, including MAL3-101, inhibited breast cancer proliferation (Table 12). These compounds were from two chemical classes of MAL3-101 derivatives. These classes were compounds synthesized through the combined Biginelli and Ugi reactions with the aldehyde group varied in the Biginelli reaction or the amine group varied in the Ugi reaction. The GI_{50} for the active compounds ranged from 6 ± 0.4 μM to 42.6 ± 6 μM, with 9 compounds showing GI_{50} values < 10 μM. In this assay, the GI_{50} for MAL3-101 was 27 ± 2 μM, which was a slightly higher concentration than seen in previous assays and may suggest prep-to-prep variability. Since the GI_{50} values are lower than those

Table 12: Select MAL3-101 derivatives inhibit SK-BR-3 cell proliferation.

	Class	Chemical modification	SK-BR-3	Ssa1p ATPase		TAg Stimulated	
			GI_{50}	Fold Change	Amplitude	Fold Change	Amplitude
	DMSO CONTROL				61.212		83.993
MAL3-101	MAL3-101		27±2	1.7	48.045	-2.0	71.802
MAL3-51	MAL3-51		>50	1.1	93.148	-2.0	88
MAL2-11B	Biginelli acid	p-biphenylcarboxaldehyde	>50	1.1	54.09	-3.5	49.2
MAL2-10A	Biginelli acid	benzaldehyde	>50				
MAL2-06A	Biginelli acid	2-naphthaldehyde	>50				
MAL1-274	Biginelli acid	p-chlorobenzaldehyde	>50	1.3	64.585		
MAL2-13	Biginelli acid	p-nitrobenzaldehyde	>50				
DMT002272	Biginelli acid	o-biphenylcarboxaldehyde	>50	1.0	74.968	-5.0	84.299
MAL2-116-17	Biginelli acid	m-nitrobenzaldehyde	>50				
MAL2-116-20	Biginelli acid	p-trifluoromethylbenzaldehyde	>50				
DMT003034	Biginelli acid	cyclohexylcarboxaldehyde	>50	1.0	75.915	1.5	69.337
DMT003036	Biginelli acid	p-tert-butylbenzaldehyde	>50	1.0	74.042	-3.5	55.686
DMT003038	Biginelli acid	cyclopropylcarboxaldehyde	>50	1.1	48.254	1.0	68.45
DMT003116	Biginelli acid	p-cyclohexylbenzaldehyde	>50	-1.1	76.868		
DMT003042	Biginelli ester	p-biphenylcarboxaldehyde	>50	2.6	42.709	-1.2	68.72
DMT003044	Biginelli ester	benzaldehyde	>50	2.3	39.671	-1.3	54.295
DMT003046	Biginelli ester	cyclopropylcarboxaldehyde	>50	1.9	48.008	1.0	74.625
DMT003020	Free diacid		>50	1.1	60.406	-2.2	43.801
DMT003024	MAL3-39-like		>50	2.3	41.691	-5.0	95.147
DMT003082	Ugi-1	p-trifluoromethylbenzaldehyde	>50	1.0	65.746	-4.8	98.535
DMT003084	Ugi-1	p-tert-butylbenzaldehyde	29±0	1.2	56.496	-5.2	102.43
DMT003086	Ugi-1	m-nitrobenzaldehyde	6.0±0.4	1.1	74.295	-1.5	65.423
DMT003088	Ugi-1	benzaldehyde	6.5±0.7	1.1	76.802	-1.1	73.963
DMT003090	Ugi-1	p-chlorobenzaldehyde	16±6	1.5	49.917	-1.9	73.243
DMT003092	Ugi-1	p-nitrobenzaldehyde	6.9±0.4	1.0	52.617	-3.2	84.597
DMT003094	Ugi-1	naphthaldehyde	10±1	1.0	65.291	-2.9	86.443
DMT003096	Ugi-1	o-biphenylcarboxaldehyde	17±3	-1.1	56.078	-4.0	81.841
DMT003100	Ugi-1	cyclohexylcarboxaldehyde	6.3±1.0	1.2	65.173	-2.1	90.129
DMT003132	Ugi-1	cyclopropylcarboxaldehyde	6.2±0.4	1.2	74.185	-2.6	86.045
DMT003134	Ugi-1	p-cyclohexylbenzaldehyde	42±6	2.2	36.44		
DMT002218	Ugi-2	benzaldehyde	>50	3.2	34.654	1.1	68.669
DMT002220	Ugi-2	p-hydroxybenzaldehyde	>50	11.8	40.818	9.2	48.389
DMT002222	Ugi-2	p-biphenylcarboxaldehyde	>50	9.9	32.744	6.0	37.403
DMT002260	Ugi-2	m-ester-benzaldehyde	>50	3.7	29.923	1.1	50.224
DMT002262	Ugi-2	acetaldehyde	>50				
DMT002264	Ugi-2	cyclohexylcarboxaldehyde	>50				
DMT003058	Ugi-2	2-pyridinecarboxaldehyde	>50	4.2	32.815	5.5	29.619
DMT003112	Ugi-2	3-ester-4-hydroxybenzaldehyde	>50	19.1	31.362	2.1	61.348
DMT003114	Ugi-2	p-oxymethylester	48±5	1.1	55.201	1.2	67.145
DMT002286	Ugi-3	cyclohexenylethylamine	39±6	6.1	33.853	-1.2	64.808
DMT003052	Ugi-3	methoxyethylamine	8.8±0.3	1.5	54.419	-1.8	77.53
DMT003102	Ugi-3	benzylamine	14±2	1.5	57.099	-3.6	104.92
DMT003104	Ugi-3	phenethylamine	32±2	12.3	29.349	1.3	39.578
DMT003106	Ugi-3	2-pyridinemethylamine	7.1±0.4	1.0	63.43		
DMT003108	Ugi-3	2-pyridineethylamine	7.5±0.8	-1.1	81.21		
DMT003110	Ugi-3	tryptamine	>50	1.0	67.792		
PTX(nM)	CONTROL		6.1±1.2	N/A	N/A	N/A	N/A

obtained with MAL3-101, these results indicate that more potent inhibitors of breast cancer cell proliferation were identified.

The compounds were then examined via single turnover ATPase assay to determine if the effect on breast cancer cell proliferation was correlated to chaperone modulating activity. The compounds were tested for their effect on Ssa1p ATP hydrolysis and TAg stimulated ATP hydrolysis as described in Section 3.3.1. The chaperones modulators fell into distinct classes that were directly related to the chemical modifications made during synthesis (Table 12). The compounds that inhibited breast cancer cell proliferation had little effect on Ssa1p ATP hydrolysis, but all inhibited TAg stimulation of Ssa1p, to varying degrees similar to the action of MAL3-101. However, not all of these compounds inhibited breast cancer cell proliferation. For example, compounds that included just a Biginelli product with variations in the aldehyde group had virtually no effect on endogenous Ssa1p ATP hydrolysis, but inhibited TAg stimulation of Ssa1p ATP hydrolysis. Despite similar attributes, compounds in this class have no effect on breast cancer cell proliferation. This is exemplified by MAL2-11B (Figure 44B), which was described in Section 3.3.3 and was resynthesized and re-examined here. This indicates that a specific effect on cochaperone stimulation is not a predictor of effect on breast cancer cell proliferation.

In addition, other novel classes of chaperone modulators were identified. One class was the ester modification of select Biginelli aldehydes. These compounds (e.g. DMT003042, Figure 46) moderately stimulated Ssa1p ATP hydrolysis, but had no effect on TAg stimulated ATP hydrolysis in single turnover assays. Other compounds (e.g. DMT2220, Figure 46) dramatically stimulated both Ssa1p ATP hydrolysis and TAg stimulated Ssa1p ATP hydrolysis. These compounds had similar properties to MAL3-90, which was discussed in 3.3.1. Once again, this

Figure 46: Representative members from each of the classes of MAL3-101 derivatives.

These include Class B- Biginelli ester DMT003042, Class C- Ugi-1 DMT003096, Class D- Ugi-2 DMT002220, Class E- Ugi-3 DMT003102. The DMSO control reactions with 1 μg TAg (red squares) or without TAg (black squares) can be compared to compound treated reactions in the presence of TAg (green triangles) or absence of TAg (blue triangles). An example of Class A- Biginelli acid MAL2-11B can be seen in Figure 45B.

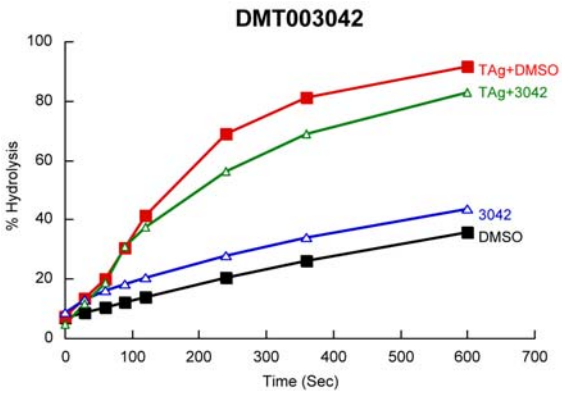
DMT003042
% Hydrolysis
Time (Sec)
TAg+DMSO
TAg+3042
3042
DMSO

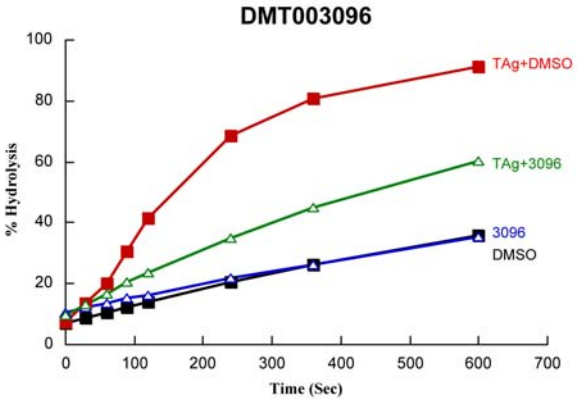
DMT003096
% Hydrolysis
Time (Sec)
TAg+DMSO
TAg+3096
3096
DMSO

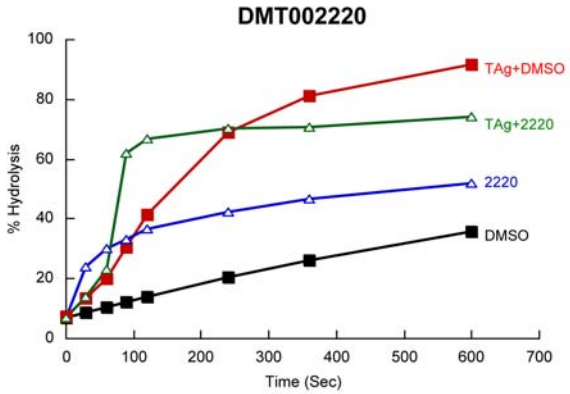
DMT002220
% Hydrolysis
Time (Sec)
TAg+DMSO
TAg+2220
2220
DMSO

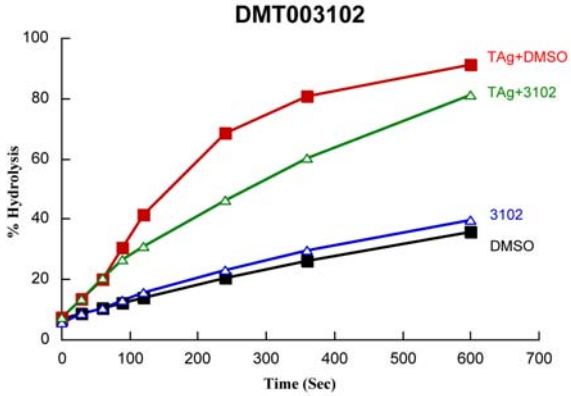
DMT003102
% Hydrolysis
Time (Sec)
TAg+DMSO
TAg+3102
3102
DMSO

correlates stimulation of Ssa1p ATP hydrolysis with increase in TAg stimulation of Ssa1p. However, not all inhibitors of TAg stimulated Hsp70 ATPase activity reduced breast cancer cell proliferation. This may arise if the compounds are not membrane permeable, inactivated, or target different intracellular co-chaperones. In conclusion, this approach identified several classes of Hsp70 modulators and correlated inhibition of cochaperone stimulation of Hsp70 ATPase activity to inhibition of breast cancer cell proliferation.

3.3.6 Novel Hsp70 modulators inhibit mammalian Hsp70 ATP hydrolysis

Based on our studies, the Gestwicki lab in the Life Sciences Institute at the University of Michigan created structurally similar compounds using a different synthetic protocol. These compounds were built from three hydrophobic amino acids upon which a Biginelli reaction was performed (see Figure 47A for representative structures). The Gestwicki lab had shown that some of these compounds (SW01, SW03, and SW07) are Hsp70 agonists and others (SW02, SW04, SW05, SW06, and SW08) are antagonists using a luciferase refolding assay (J. Gestwicki, unpublished data). In this assay, luciferase is denatured by guanidine HCl and diluted into rabbit reticulocyte lysate (RRL), which contains sufficient chaperones to allow luciferase refolding.

To determine if these compounds were Hsp70 modulators, I tested their effects on the ATPase activities of several Hsp70s. First, I tested the effects of the compounds on two different DnaK constructs. This Hsp70 was chosen because the Gestwicki lab hoped to map the compounds' binding sites on DnaK using NMR. The two constructs contained amino acids 2-638 (full length) or amino acids 2-605 (truncated), which is currently being used in the NMR studies (E. Zuiderweg, University of Michigan, personal communication). A total of 10 μg of

Figure 47: SW02 and SW03 inhibit Hsp70 ATP hydrolysis, but do not alter the total J-protein stimulated ATP hydrolysis.

(A) The structure of SW02 and SW03. (B) The ATPase activity of 10 μg Hsp70 was monitored in the presence of DMSO (diamonds), 500 μM SW02 (squares), or 500 μM SW03 (triangles). (C) GST-Hlj1p-His stimulated Hsp70 ATPase was determined in a similar ATPase assay. The amount of pmol hydrolyzed per min was calculated.

A

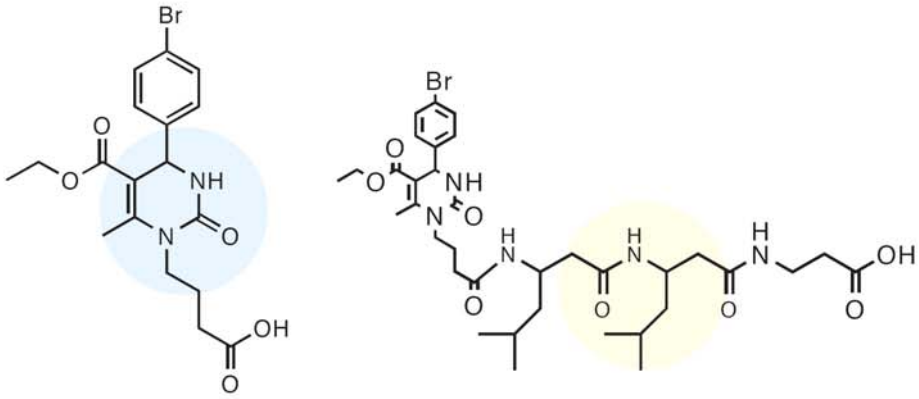

SW02 **SW03**

B

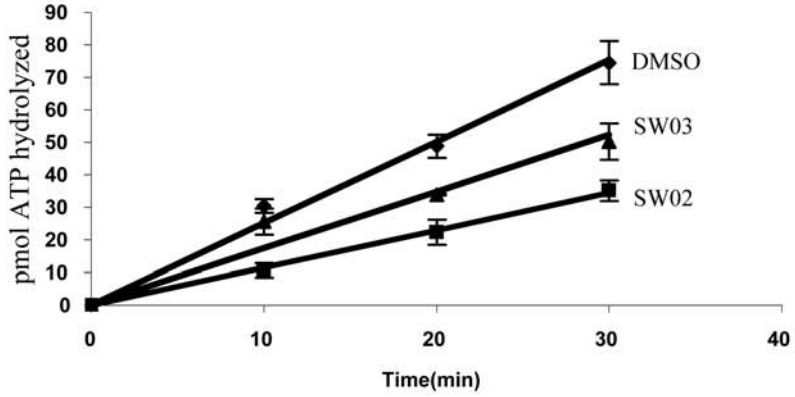

C

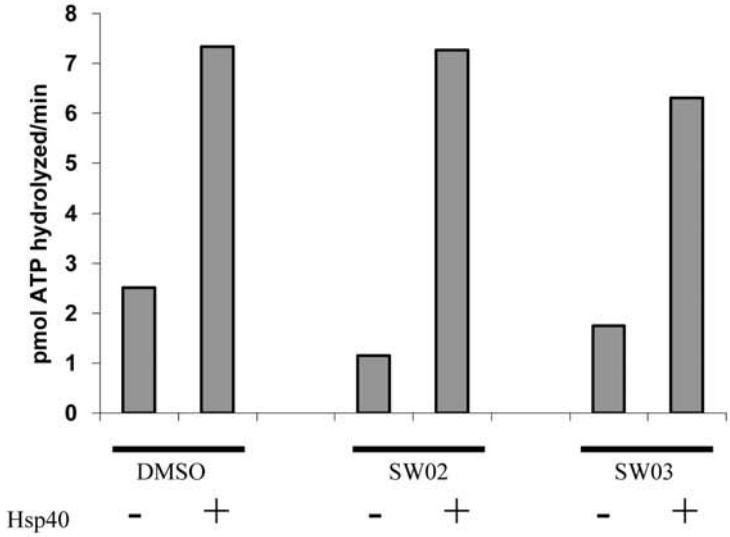

each DnaK protein was incubated with 10 μM SW01 or 100 μM SW02, SW03, SW04, SW06, and SW07, and tested in an ATPase assay. The concentrations were suggested by J. Gestwicki and were based off previous, unpublished, *in vivo* and *in vitro* results. This ATPase assay approximates steady state conditions as ATP binding, hydrolysis, and release are measured. The compounds showed little effect on the ATPase activity of either construct (Table 13), and the greatest effect observed was an ~24% decrease in full length DnaK ATPase activity in the presence of SW03.

I hypothesized that these compounds might have a more profound effect at a higher concentration or on human Hsp70 ATPase activity since they are active in the luciferase assay, which includes the mammalian Hsp70 found in RRL. I therefore tested the effects of 500 μM SW02 and SW03 on the ATPase activity of human Hsp70. These compounds were chosen since SW03 was an agonist and SW02 was an antagonist in the luciferase assay. Both SW02 and SW03 decreased Hsp70 ATPase activity by 31% and 54% respectively (Figure 47B). This result was unexpected since the compounds had differing effects on luciferase refolding, but could signify a difference between the two assays. For example, the ATPase assays utilize purified proteins in the absence of substrate, whereas the luciferase assay is performed in cell lysate and includes luciferase as a substrate. I also tested the compounds for inhibition of GST-Hlj1p-His stimulation of Hsp70 ATP hydrolysis in the ATPase assays. Like MAL3-101, neither SW02 nor SW03 had a significant effect on stimulation (Figure 47C, data not shown).

Since these compounds were structurally similar to MAL3-101, SW01 and SW02 were also tested for their effect on breast cancer proliferation as described above. SW01 was used instead of SW03 because it is believed to be cell permeable (J. Gestwicki, personal communication). The concentration of both drugs needed to inhibit 50% of the cell proliferation

Table 13: The SW compounds have little effect on DnaK ATP hydrolysis.

	DnaK (2-638)		DnaK (2-605)	
	pmol ATP hydrolyzed/min	**% DMSO**	**pmol ATP hydrolyzed/min**	**% DMSO**
DMSO	4.3456	---	3.5971	---
SW01	4.358	100.3	3.8983	108.4
SW02	3.7368	86.0	3.7974	105.6
SW03	3.2947	75.8	3.2436	90.2
SW04	3.5569	81.9	3.4544	96.0
SW06	3.7814	87.0	3.3286	92.5
SW07	4.4799	103.1	3.4948	97.2

was > 50 μM. Assuming the compounds enter the cells, this indicates that MAL3-101, SW01, and SW02, while Hsp70 modulators, have different *in vivo* activities. Alternatively, it is possible that the cells modify or destroy the compounds, thus rendering them inactive.

4.0 A NOVEL SMALL MOLECULE INHIBITS SV40 PRODUCTION BY PREVENTING VIRAL DNA SYNTHESIS

4.1 INTRODUCTION

Human polyomaviruses can cause several diseases, including BKVAN and PML (BARBANTI-BRODANO *et al.* 1998; BERGER 2003). The recent identification of the KI polyomavirus (ALLANDER *et al.* 2007) indicates that other human polyomaviruses probably exist that may also cause human disease. Unfortunately, few anti-viral compounds have been identified as potential treatments for these infections. Since BKV and JCV are difficult and time-consuming to grow in the laboratory, screening for novel drugs using these viruses has been problematic. However, since SV40 is highly similar to JCV and BKV and can be easily maintained in the lab, SV40 has become a model system for the study of human polyomaviruses. The SV40 TAg J domain is required for many aspects of viral replication, including cell cycle initiation, DNA replication, and virion assembly (SPENCE and PIPAS 1994b; SRINIVASAN *et al.* 1997; SULLIVAN *et al.* 2000a). As discussed in Section 1.5.2.2, the TAg J domain initiates S phase in non-proliferating kidney cells by releasing E2F from Rb. Also, most viruses that encode J domain mutations in TAg cannot replicate their DNA *in vivo*, and the few that can replicate DNA cannot form mature virions (SPENCE and PIPAS 1994b).

Many other proteins, including the Hsp70 and Hsp90 chaperones, play a role in viral replication. In addition to viral corruption of cellular Hsp70 via TAg J domain, Hsp70 is implicated in other aspects of the SV40 life cycle. For example, Hsp70 is probably involved in viral uncoating immediately after infection. Hsp70 co-precipitates with the viral coat protein, VP1, 3 hours after infection, and is required to disassemble virus particles *in vitro* (CHROMY *et al.* 2006). Hsp70 is also involved in viral coat assembly late in infection and binds the viral coat proteins VP1, VP2, and VP3 (CRIPE *et al.* 1995). The bacterial DnaK, DnaJ, and GrpE chaperones also assemble capsid-like particles *in vitro* (CHROMY *et al.* 2003), suggesting that the ability of chaperones to assemble capsids is conserved. Unlike the role of Hsp70 in virion assembly, Hsp90 is probably involved in TAg folding. Hsp90 and TAg co-precipitate from cells, and it is likely that Hsp90 only binds immature TAg proteins since Hsp90 bound denatured TAg but not wild type TAg *in vitro* (MIYATA and YAHARA 2000). Furthermore, addition of GA to TAg-expressing cells reduces the amount of intracellular TAg (MIYATA and YAHARA 2000). Taken together, these results suggest that Hsp90 binds immature TAg and that inhibition of Hsp90 leads to increased degradation of TAg. This is consistent with other reports indicating that premature dissociation of Hsp90 ligands effects their degradation (SCHNEIDER *et al.* 1996).

Since polyomavirus replication requires the viral-encoded TAg, specific TAg inhibitors could represent a novel class of replication inhibitors with potentially minimal side effects. Thus, I hypothesized that previously identified inhibitors of TAg J domain stimulation of Hsp70 might inhibit viral replication. To test this hypothesis, I decided to better characterize three compounds, MAL3-101, MAL2-11B, and MAL3-51 *in vitro* and determine if they inhibited SV40 replication *in vivo*. As presented in Chapter 3.0, MAL3-101 and MAL2-11B inhibit TAg stimulation of Ssa1p's ATPase activity, but have no effect on endogenous Ssa1p ATPase

activity. Also, MAL3-101 and some MAL3-101 derivatives inhibit breast cancer cell proliferation. This suggested that MAL3-101 is membrane permeable and targets at least one aspect that is vital for cell physiology. Further, as MAL3-101 inhibited TAg, but not Ydj1p stimulation of Hsp70, it might exhibit some selectivity for TAg and not target all Hsp70/J domain interactions in the cell. MAL2-11B was chosen because this compound fell into a different class of chaperone modulators than the MAL3-101 derivatives that inhibited breast cancer cell proliferation. Specifically, MAL2-11B had a much more dramatic effect on TAg stimulation of Ssa1p, and may be a more potent compound *in vivo*. Finally, I used MAL3-51 as a negative control since it is structurally similar to the previously identified chaperone modulators, but had no effect on Ssa1p ATP hydrolysis or on TAg stimulated Ssa1p ATP hydrolysis (FEWELL *et al.* 2004).

In chapter 4.0, I present evidence that MAL3-101 and MAL2-11B have strikingly different effects in *in vitro* ATPase assays, despite similar attributes in single turnover assays. MAL2-11B, and to a lesser extent, MAL3-101, slightly inhibited the ATPase activities of Hsp70 and Hsp90, suggesting that MAL2-11B might affect a broader range of proteins than MAL3-101. To further assess specificity, I investigated the effect of the compounds on TAg ATPase activity. In addition to dramatically inhibiting TAg stimulation of Hsp70, MAL2-11B also inhibited TAg ATPase activity independent of its effect on the TAg J domain. To determine whether the activity of other AAA+ ATPases are altered by MAL2-11B, I incubated the hexamer of Minichromosome Maintenance proteins 2-7 (MCM2-7) in the ATPase assays. Like TAg, the MCM hexamer plays an important role in eukaryotic DNA replication (MAIORANO *et al.* 2006). Indeed, MAL2-11B drastically reduced MCM ATPase activity. Using viral plaque assays, I then showed that MAL2-11B, but not MAL3-101 inhibited SV40 replication by approximately 4.5

fold. These results are consistent with the inhibition of both endogenous TAg ATPase activity and J domain-mediated stimulation of Hsp70 by MAL2-11B. Finally, MAL2-11B inhibited DNA replication *in vitro*, a process that requires a functional TAg ATPase domain but not a functional J domain. These data suggest that MAL2-11B and related compounds may serve as a novel class of AAA+ ATPase inhibitors that prevent SV40 viral replication.

4.2 MATERIALS AND METHODS

4.2.1 Reagents

Ssa1p and TAg was purified as described previously (CANTALUPO *et al.* 1999; MCCLELLAN and BRODSKY 2000). Purified MCM 2-7, kinesin, Hsp70, and wild type and the 5061 mutant form of TAg, were kind gifts from Matt Bochman, Troy Krzysiak, Doug Placais, and Paul Cantalupo, respectively. Cidofovir was provided by Dr. Abhay Vats, from the Children's Hospital of Pittsburgh. Mammalian Hsp90α was purchased from Stressgen (SPP-776).

4.2.2 Single turnover ATPase assay and ATPase assay

Single turnover ATPase assays and ATPase assays were performed as described in Section 3.2.2 and 3.2.3, respectively, and as published (CYR *et al.* 1992; FEWELL *et al.* 2004).

4.2.3 Viral plaque assay

Plaque assays (Figure 48) were modified from a previously published protocol (TREMBLAY *et al.* 2001). A total of $5x10^4$ BSC40 cells were plated in 200 µL MEM-10% FBS in each well of a 96-well plate and grown overnight. Then, $1x10^5$ pfu of the SV40 virus were added to an Multiplicity of Infection (MOI)=~2 and two wells were left uninfected as mock infection controls. After 2 hrs, the medium was changed and DMSO or a test compound was added to each well. All treatments were performed in duplicate. After two 2 days, the medium was changed again and the compounds or DMSO were re-added. After 2 additional days, the 96 well plates were frozen at -20° and the cells were lysed by three successive freeze/thaw cycles to obtain a viral stock. The viral stocks were diluted 1,000 and 10,000 fold in MEM-10% FBS. Then, 500 µL of the each dilution was added, in duplicate, to freshly confluent BSC40 cells in 6 cm dishes. After 2 hrs, the medium was removed and 4 mL of a 50/50 mixture of melted 1.8% Bacto-agar and 2x MEM lacking phenol red was added to the cells. The agar/media overlay was repeated on day 4 and day 7, but neutral red was added to a final concentration of 50µg/mL on day 7. Plaques were counted on day 8 and 9.

4.2.4 *In vitro* DNA replication assays

In vitro DNA replication assays were performed as previously described (CASTELLINO *et al.* 1997). Briefly, a timecourse was performed using 25 µL reactions that included 100 ng pUC.HSO, which contains the SV40 origin of replication, 90 µg HeLa cell extract, 500 ng TAg, 50 mM creatine phosphate, 2.5 µg creatine phosphokinase, and 2.5µCi α^{32}P-dCTP in 30 mM HEPES, pH 7.8, 7 mM $MgCl_2$, 100 mM EDTA, 1 mM DTT, 4 mM ATP, 0.2 mM CTP, 0.2 mM

Figure 48: Viral replication is monitored by a viral plaque assay.

See text for details.

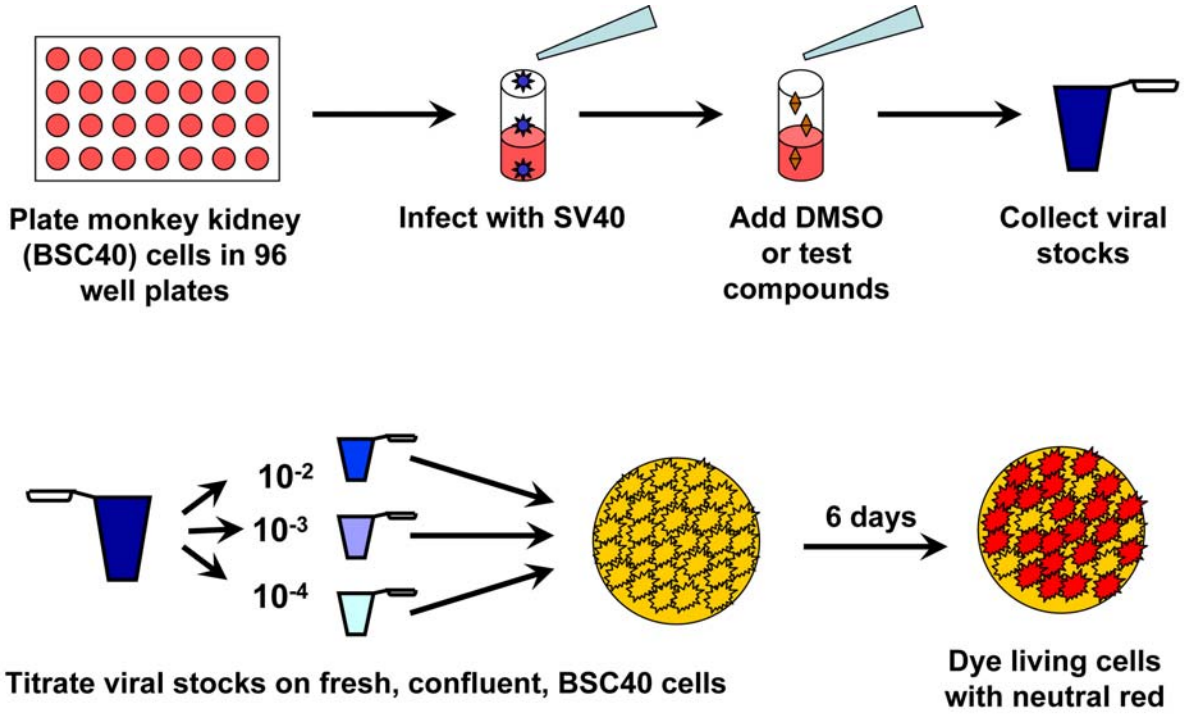
Plate monkey kidney (BSC40) cells in 96 well plates
Infect with SV40
Add DMSO or test compounds
Collect viral stocks
10^{-2}
10^{-3}
10^{-4}
Titrate viral stocks on fresh, confluent, BSC40 cells
6 days
Dye living cells with neutral red

UTP, 0.2 mM GTP, 25 μM dCTP, 100 μM dATP, 100 μM dTTP, 100 μM dGTP. Where indicated, equal volumes of DMSO or a test compound were added. Reactions were incubated for 2 hrs at 37° and 5 μL aliquots were removed every 30 min and added to 24 μL of Stop Solution (0.5% SDS, 10 mM Tris, pH 8.0, 5 mM EDTA, 0.3 mg/mL tRNA, and 1 mg/mL proteinase K) for 1 hr at 37°. Samples were placed on ice until the experiment was completed. The reactions were precipitated with ethanol, resolved on 1% agarose gel, and stained with ethidium bromide to verify equal DNA loading. The gel was dried and incorporated nucleotide was determined by phosphorimager analysis on a Fujifilm BAS-2500. When the effects of specific compounds were examined, half reactions were performed in triplicate, using similar conditions. Reactions were incubated at 37° for 1 hr at which time 50μL Stop Solution was added.

4.3 RESULTS

4.3.1 Modulators of TAg J domain stimulation of Hsp70 differentially affect the activities of other molecular chaperones

Since MAL3-101 inhibited breast cancer cell proliferation (Section 3.3.4), I wanted to determine if the compound could affect other processes that require the functional interactions between Hsp70s and J-proteins. As mentioned previously, the J domain of TAg is required, through its interaction with Hsp70, for various aspects of viral replication. In addition, MAL3-101 inhibits TAg, but not Ydj1p, stimulation of Ssa1p ATP hydrolysis, indicating that it may preferentially inhibit TAg J domain-dependent processes. I also examined MAL2-11B, which inhibits TAg

stimulation of Ssa1p more profoundly than MAL3-101 and therefore might be a more potent inhibitor of TAg- dependent SV40 replication.

I first wanted to better characterize MAL3-101 and MAL2-11B in ATPase assays using mammalian Hsp70 and Hsp90, which are the presumed intracellular targets of these compounds during polyomavirus infection. Since DSG binds to Hsp70 and Hsp90 with similar affinities (NADEAU *et al.* 1994), it was possible that our chaperone modulators might also affect the ATPase activities of both of these chaperones. I performed an ATPase assay using 10 µg of mammalian Hsp70 and 300 µM MAL3-101, MAL2-11B, and MAL3-51. In these ATPase assays, the compounds were preincubated with Hsp70 for 15 minutes on ice to allow the compound and protein to interact. ATP was added to initiate the reactions and the reactions were incubated at 30°. As predicted, MAL3-101, which had no effect on endogenous Hsp70 ATP hydrolysis, had little effect on mammalian Hsp70 ATP hydrolysis. In contrast, despite having no effect on Hsp70 ATP hydrolysis in a single turnover assay, MAL2-11B inhibited steady-state-like Hsp70 ATPase activity between 1.4 and 2-fold (Table 14 and Figure 49A). In spite of this modest affect, the response was concentration dependent as addition of 30 µM and 100 µM MAL2-11B reduced the inhibition of mammalian Hsp70 ATPase activity (Figure 49B). These results suggest that MAL2-11B does not inhibit Hsp70 ATPase activity, but slightly inhibits another step in the ATPase cycle, such as ATP binding or release. Control reactions performed with MAL3-51 showed that this compound also minimally altered Hsp70 ATPase activity between 1.1 and 1.4 fold (Table 14 and Figure 49A)

I next tested the effect of 300 µM of each compound on the ATPase activity of 10 µg mammalian Hsp90 (Stressgen). MAL2-11B slightly inhibited Hsp90 ATP hydrolysis by ~2.3 fold, whereas both MAL3-51 and MAL3-101 inhibited Hsp90 by less than 1.3 fold (Table 14,

Table 14: The effect of MAL2-11B, MAL3-51, and MAL3-101 on various ATPases.

	DMSO	MAL2-11B	MAL3-51	MAL3-101
Hsp70	100 (2) 100 (3)	57 (2) 67 (3)	107 (2) 70 (2)	114 (3) 93 (3)
Hsp90	100 (2)	43 (2)	92 (2)	79 (2)
TAg	100 (2) 100 (2)	23 (2) 9 (2)	85 (2) 103 (1)	92 (2) 100 (1)
MCM	100 (3)	5 (3)	98 (3)	102 (3)
Kinesin	100 (2)	-[a]	95 (2)	91 (2)

All reactions were normalized to the slope of the DMSO control, which was set to 100%. Each line represents a set of independent experiments. The number in parentheses represents independent reactions for each experiment. *a*=See discussion.

Figure 49: MAL2-11B slightly inhibits the ATPase activity of Hsp70 and Hsp90.

The ATPase activities of (A) 10 μg mammalian Hsp70 and (C) 10 μg mammalian Hsp90 were determined in the presence of DMSO (red diamond), or 300 μM MAL2-11B (blue circles), MAL3-51 (purple squares), and MAL3-101 (green triangles). (B) Mammalian Hsp70 ATPase activity was determined in the presence of DMSO (red diamonds) or 30 μM MAL2-11B (purple circles), 100 μM MAL2-11B (green circles), or 300 μM MAL2-11B (blue circles).

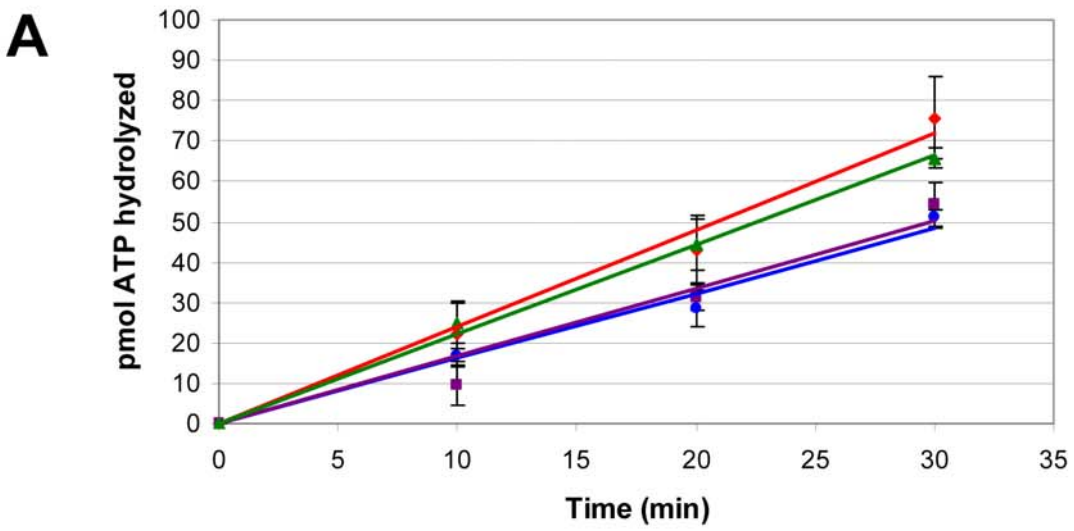
A
pmol ATP hydrolyzed
100
90
80
70
60
50
40
30
20
10
0
0
5
10
15
20
25
30
35
Time (min)

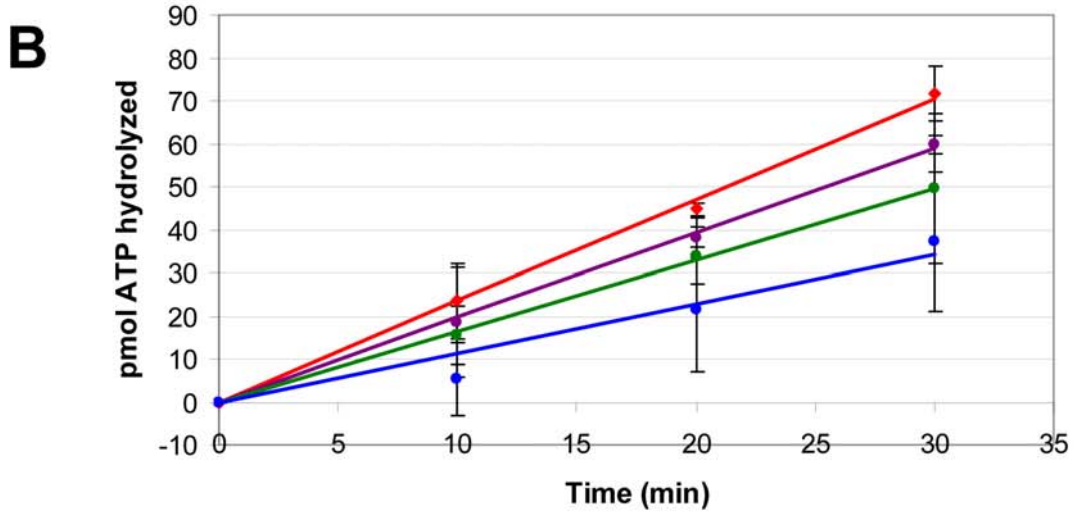
B
pmol ATP hydrolyzed
90
80
70
60
50
40
30
20
10
0
-10
0
5
10
15
20
25
30
35
Time (min)

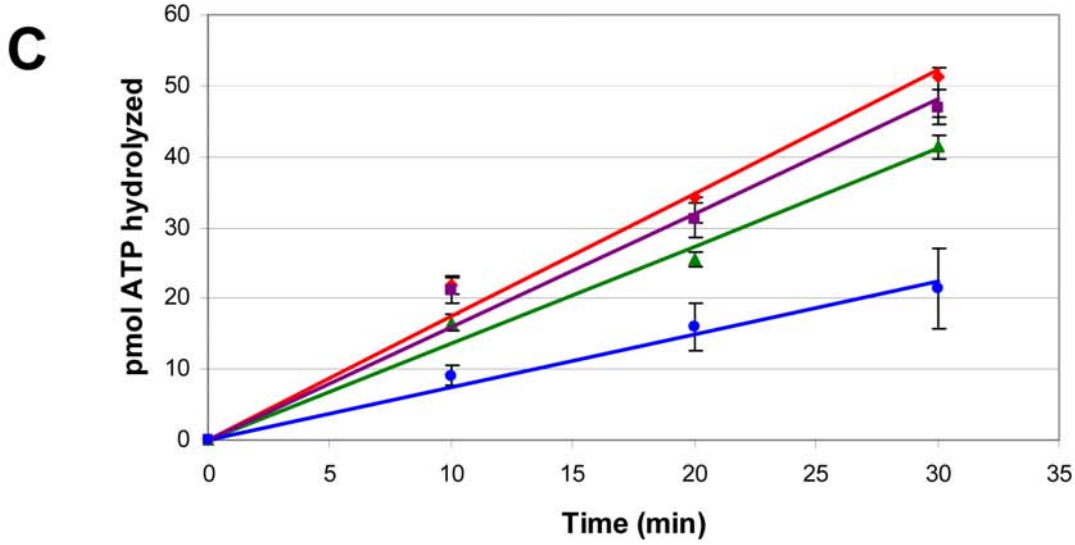
C
pmol ATP hydrolyzed
60
50
40
30
20
10
0
0
5
10
15
20
25
30
35
Time (min)

Figure 49C). Since the structure of DSG was used to develop structural algorithms that led to the identification of these compounds and binds to Hsp70 and Hsp90 (NADEAU *et al.* 1994), it is not surprising that some of our derivatives would also similarly affect both chaperones.

As mentioned previously, MAL3-101 inhibits TAg, but not Ydj1p, stimulation of Ssa1p ATP hydrolysis. However, the J-protein specificity of MAL2-11B had not previously been examined. I therefore tested the specificity of MAL2-11B on Ydj1p stimulation of Ssa1p in a single turnover assay. Even though equimolar Ydj1p stimulated Ssa1p to a similar extent as TAg, 300 μM MAL2-11B had very little effect on Ydj1p stimulated Ssa1p ATP hydrolysis (Figure 50). This indicates that like MAL3-101, MAL2-11B, may be specific for the TAg interaction with Hsp70.

4.3.2 MAL2-11B drastically inhibits the AAA+ ATPases SV40 TAg and MCM2-7

Since MAL2-11B slightly inhibited the ATPase activity of Hsp70 and Hsp90, I investigated whether MAL2-11B altered the activities of other ATPases. I first tested the effect of the compounds on TAg ATPase activity using 1 μg TAg. Surprisingly, 300 μM MAL2-11B inhibited TAg ATPase activity between 4.4 and 11 fold (Table 14, Figure 51A). This was in contrast to MAL3-51 and MAL3-101, which altered TAg ATP hydrolysis by only 1.0-1.2 fold (Table 14, Figure 51A). In fact, the levels of ATP hydrolysis after addition of MAL2-11B to TAg was similar to the level observed for the TAg ATPase mutant, 5061 (Figure 51A), which is replication defective (CASTELLINO *et al.* 1997). Preliminary data suggest that MAL2-11B inhibition of TAg is concentration dependent (data not shown). These results indicate that the effect of MAL2-11B on TAg is not limited to the J domain and extends to at least the ATPase domain.

Figure 50: MAL2-11B does not inhibit Ydj1p stimulation of Ssa1p.

A single turnover assay was used to monitor Ssa1p ATPase activity in the presence of Ydj1p. In the presence of DMSO, endogenous Ssa1p ATPase activity (black squares) was stimulated by Ydj1p (red squares). MAL2-11B had no effect on endogenous Ssa1p ATPase activity (blue triangles) or Ydj1p stimulated Ssa1p ATPase activity (green triangles).

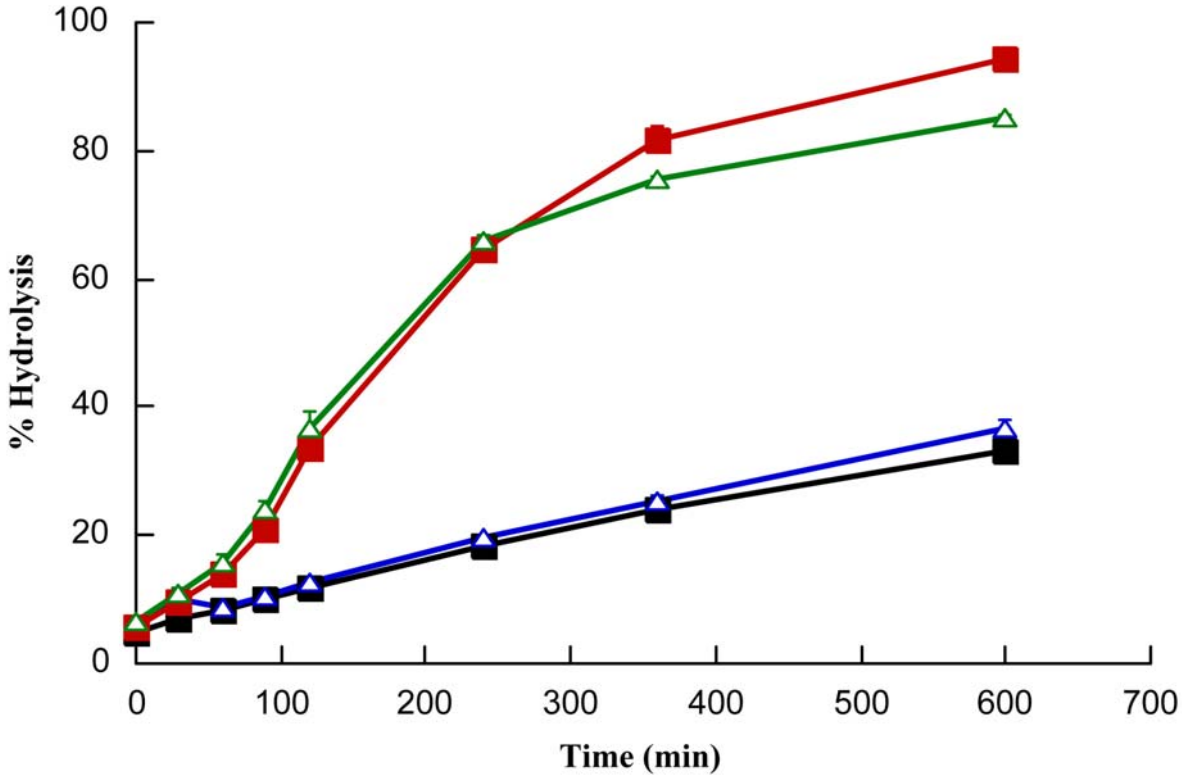
100
80
60
40
20
0
% Hydrolysis
0
100
200
300
400
500
600
700
Time (min)

Figure 51: MAL2-11B dramatically inhibits the ATPase activity of TAg and MCM.

The ATPase activity of (A) mammalian 10 μg TAg and (B) 5 μg yeast MCM was determined in the presence of DMSO (red diamond), or 300 μM MAL2-11B (blue circles), MAL3-51 (purple squares), and MAL3-101 (green triangles). In (A) the TAg ATPase mutant, 5061, is shown in light blue diamonds.

A

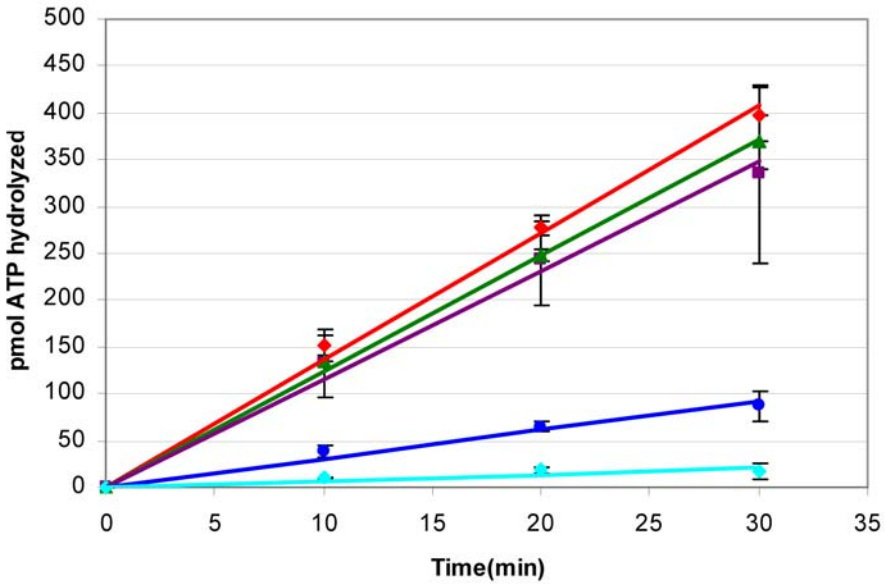
pmol ATP hydrolyzed
500
450
400
350
300
250
200
150
100
50
0
0
5
10
15
20
25
30
35
Time(min)

B

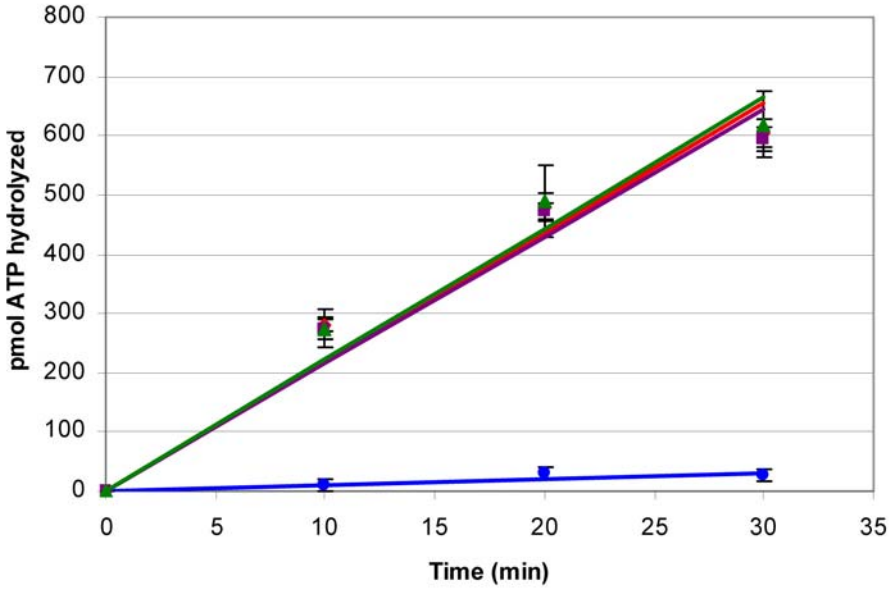
pmol ATP hydrolyzed
800
700
600
500
400
300
200
100
0
0
5
10
15
20
25
30
35
Time (min)

Since MAL2-11B inhibited TAg ATPase activity, I hypothesized that MAL2-11B might inhibit the ATPase activity of related AAA+ ATPases, such as the yeast AAA+ ATPase, MCM2-7. MCM is a heterohexamer composed of six MCM subunits named MCM2-7, which is proposed to be the replicative helicase in eukaryotic cells (MAIORANO *et al.* 2006). To test this hypothesis, 5 μg MCM2-7 was combined with 300 μM of each compound in an ATPase assay. MAL2-11B virtually abolished MCM ATPase activity by decreasing it to 9% of the DMSO control (Table 14, Figure 51B). However, MAL3-51 and MAL3-101 had virtually no affect on MCM ATPase activity. These results suggest that MAL2-11B may be a general inhibitor of AAA+ ATPases.

To determine if MAL2-11B inhibited all ATPases, I tested 300 μM of each compound on 10 μg kinesin in the ATPase assays. Kinesin binds microtubules and uses ATP hydrolysis to move along the microtubules (VALENTINE and GILBERT 2007). MAL3-51 and MAL3-101 did not affect kinesin ATPase activity at 300 μM (Table 14). However, MAL2-11B had an unexpected action on the ATPase activity of kinesin. As mentioned previously, the protein and compound are preincubated on ice in the absence of ATP, in the ATPase reactions. When 300 μM MAL2-11B was added to kinesin, it stimulated kinesin ATPase activity while on ice, since the zero timepoint was much higher than in the DMSO control. However, at later timepoints, no additional ATP hydrolysis was observed. To further explore this phenomenon, I titrated MAL2-11B into the kinesin ATPase assays. At 100 μM MAL2-11B, the initial ATP hydrolysis on ice was also observed, but to a much lower extent and additional ATP hydrolysis was still detected at the later timepoints. These results made interpretation difficult (See Discussion). Further experimentation is required to determine the effect of MAL2-11B on kinesin. Nonetheless, these results indicate that MAL2-11B inhibits AAA+ ATPases and represents the first-in-its-class compound with this activity.

4.3.3 MAL2-11B inhibits SV40 replication

SV40 replication requires nearly every domain in TAg, including the J domain and ATPase domain (COLLINS and PIPAS 1995; SIMMONS *et al.* 1993). Since MAL2-11B inhibited the function of both the TAg ATPase and the ability of the J domain to activate the ATPase activity of Hsp70, I decided to test if MAL2-11B also inhibited SV40 replication using viral plaque assays. The assay was set up so the entire SV40 replication process occurred in the presence of the compound. While this assay is quite time-consuming, it has distinct benefits over other techniques. First, it assays the entire cycle of viral replication. Other techniques, both *in vitro* and *in vivo*, focus on specific stages of infection such as E2F release, p53 stabilization, DNA replication, or virion assembly (COLLINS and PIPAS 1995; SPENCE and PIPAS 1994b; SULLIVAN *et al.* 2004). However, since TAg inhibitors could act at many stages in the viral life cycle, it was imperative to monitor all stages during SV40 infection. This assay also measures the yield of functional viruses. By comparison, Andrei and colleagues examined specific small molecule inhibitors of SV40 and murine polyomavirus replication by observing the cytopathic effect (CPE) on UC1-B or BS-C-1 cells after infection (ANDREI *et al.* 1997). This required microscopically observing the distinct phenotypes of infected cells and counting cells displaying the phenotype. To obtain an IC_{50} (concentration where the CPE of infected cells is half the DMSO control), many drug titrations were required. This approach required extensive microscopic analysis of infected cells and extensive drug titrations, and did not quantify functional viral output. Indeed, a secondary screen was required to determine if functional virus was produced. In addition, the Bocchetta lab created a highthroughput ELISA assay that identified a novel small molecule that inhibited the interaction between p53 and TAg (CARBONE *et al.* 2003). While this approach successfully monitored the p53 and TAg interaction, it did not

examine whether the identified molecules subsequently inhibited viral replication or tumorigenesis.

In viral replication assays, BSC40 cells, a monkey kidney cell line permissive for SV40 replication, were plated in 96 well plates at an MOI=~2. This MOI allowed all cells to be infected with virus. This ensured a consistent infection, but did not "force" the compounds to inhibit multiple SV40 viruses within one cell. The infection proceeded for 2-3 hours before the medium was changed. This allowed virus uptake independent of any effect of the compounds, and ensured any inhibition observed would be due to inhibition of viral replication, and not to inhibition of initial viral uptake. In addition, the compounds were added in duplicate to the SV40 infected cells twice over the four day incubation. The compound was added twice since the half-life of the compounds in the medium or cells at 37° is unknown. If the compounds prevent late stages in viral replication, adding fresh compound halfway through infection might inhibit replication that otherwise wouldn't occur.

To first establish the efficacy of using plaque assays to screen for anti-viral compounds, I titrated cidofovir into the assay. Cidofovir is a cytosine analog and has been shown to inhibit mouse polyomavirus and SV40 viral growth (ANDREI *et al.* 1997). This compound is currently being examined in clinical trials for its ability to treat BKVAN in children (GORCZYNSKA *et al.* 2005; HYMES and WARSHAW 2006). As shown in Figure 52, cidofovir showed a concentration dependent effect on SV40 replication, and inhibited viral replication at ~5 μg/mL, which is similar to the published concentrations of 3.8 μg/mL. At higher concentrations (1600 μg/mL), cidofovir killed the cells, which was visualized by loss of surface adhesion by the cells (data not shown).

Figure 52: Cidofovir inhibits SV40 replication in a concentration dependent manner.

Cidofovir was titrated onto SV40 infected BSC40 cells. The cells were lysed, viral stocks were collected, and titrated onto fresh BSC40 cells. After 7 days, the viable cells were dyed and total plaque forming units (PFU) were determined. Example plates from each dilution are shown.

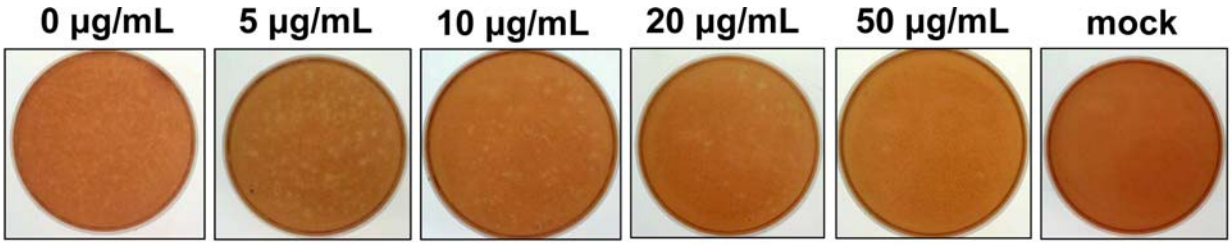
0 µg/mL
5 µg/mL
10 µg/mL
20 µg/mL
50 µg/mL
mock

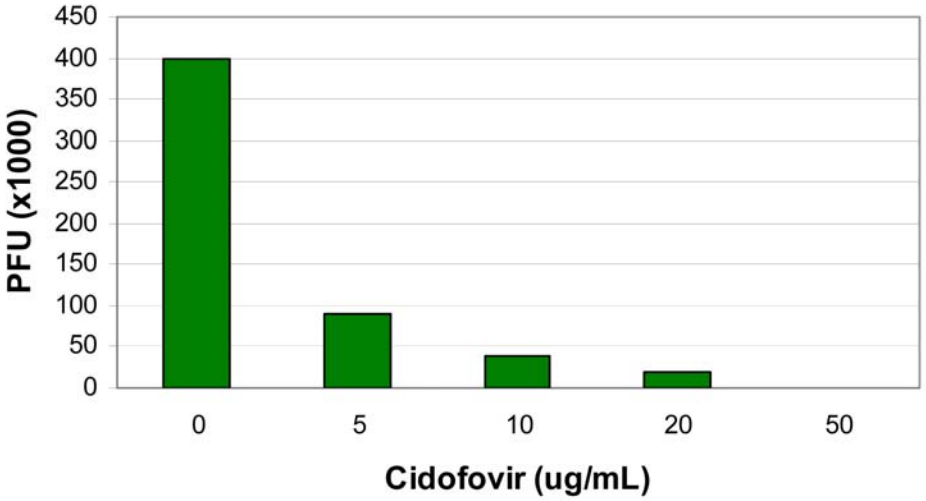
PFU (x1000)
450
400
350
300
250
200
150
100
50
0
0
5
10
20
50
Cidofovir (ug/mL)

Next, I added MAL2-11B, MAL3-51, and MAL3-101 to viral infected, BSC40 cells in the plaque assay. At 100 μM, MAL2-11B inhibited viral replication by ~4.5 fold, whereas MAL3-51 and MAL3-101 had little effect (Figure 53). A slight, but not statistically significant, decrease in viral replication was also observed using 30 μM MAL2-11B (data not shown). At this point, it is unknown if the reduction in viral replication is due to MAL2-11B inhibition of the TAg J domain, the ATPase domain, or an additional unknown phenomenon. However, as previously mentioned, 100 μM MAL2-11B was sufficient to reduce TAg stimulation of Hsp70 (Figure 45C), and preliminary data suggest that 100 μM MAL2-11B also inhibits TAg ATPase activity.

One way to determine the mechanism of inhibition of viral replication inhibition is to use compounds that are selective inhibitors of the TAg J domain or of the ATPase domain. For example, MAL3-101 inhibited the TAg J domain stimulation of Ssa1p and had no effect on TAg ATPase activity. Unfortunately at 100 μM, MAL3-101 was unable to affect the Hsp70/TAg interaction (Figure 42A), which may explain why 100 μM MAL3-101 does not inhibit viral replication. Unfortunately, I was unable to add higher concentrations of MAL3-101 since it precipitates out of solution (data not shown). Nonetheless, these results imply that MAL2-11B inhibits viral replication and may be a novel inhibitor of polyomavirus infection.

4.3.4 MAL-11B inhibits SV40 DNA replication *in vitro*

I hypothesized that inhibition of SV40 replication by MAL2-11B was due to the inhibition of viral DNA replication. DNA replication requires both the J domain and ATPase domain of TAg (CASTELLINO *et al.* 1997; SRINIVASAN *et al.* 1997). While the J domain is also required for virion assembly, most TAg J domain mutants cannot replicate DNA and never proceed to the

Figure 53: MAL2-11B inhibits SV40 replication.

Three independent experiments, each with two independent viral infections, were performed in the presence DMSO or 100 μM MAL2-11B, MAL5-51, or MAL3-101. The number of plaques per condition was averaged for each experiment and the DMSO control was normalized to one. Example plates from a single experiment are shown.

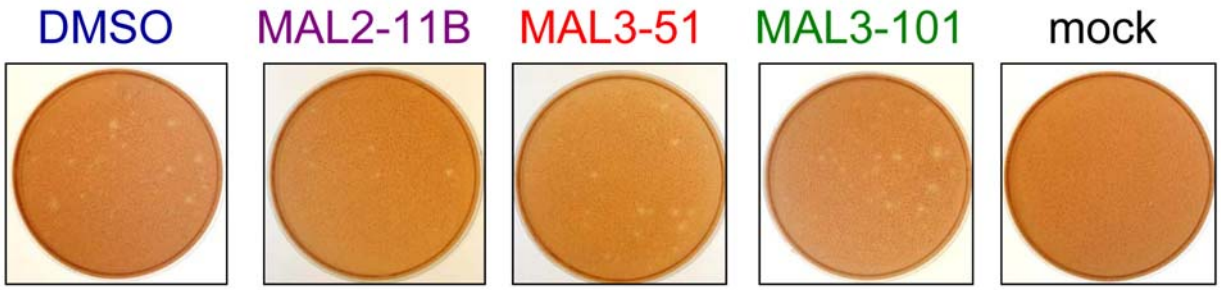
DMSO
MAL2-11B
MAL3-51
MAL3-101
mock

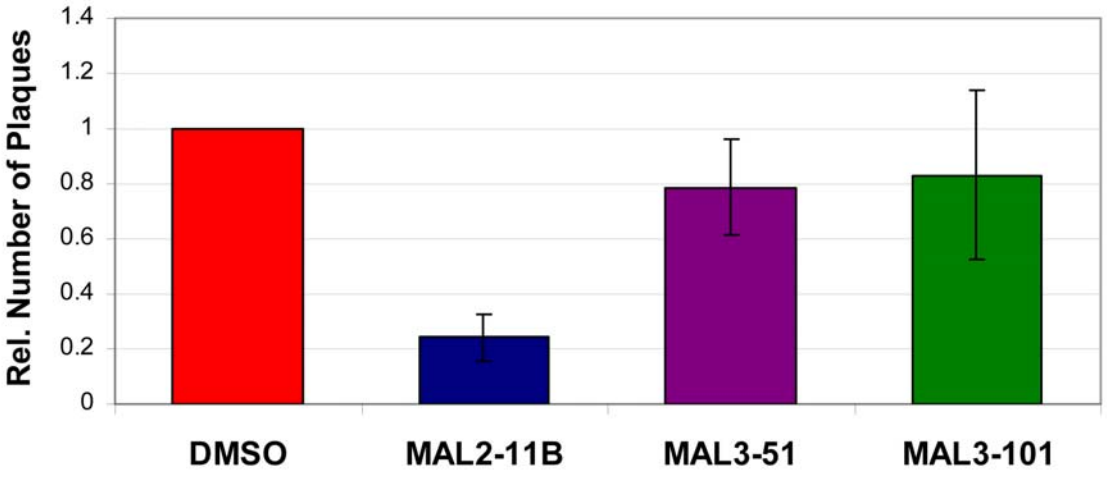
Rel. Number of Plaques
1.4
1.2
1
0.8
0.6
0.4
0.2
0
DMSO
MAL2-11B
MAL3-51
MAL3-101

virion assembly stage of infection. In addition, the *in vitro* replication assay is well established and has been used extensively to characterize specific defects in TAg mutants (CASTELLINO *et al.* 1997; OTT *et al.* 2002). Finally, the results from an *in vitro* replication assay can be correlated with data from *in vivo* DNA replication assays by isolation of viral DNA after infection.

To test my hypothesis, I added MAL2-11B, MAL3-51, and MAL3-101 to *in vitro* SV40 DNA replication assays. Since TAg is the only viral proteins required for replication, I combined TAg, HeLa cell extract, radioactive nucleotide, and DMSO or test compound with a plasmid containing the SV40 origin of replication (see Section 4.2.4). I removed aliquots every 30 min for 2 hrs, precipitated the products, and resolved the DNA by agarose gel electrophoresis. As shown in Figure 54A, TAg was required for DNA replication, and the appearance of high molecular weight DNA increased over time. However, the addition of MAL2-11B abolished DNA replication. MAL2-11B also inhibited background DNA repair as evidence by the disappearance of the low molecular weight DNA ladder. Next, the compounds were titrated into the DNA replication assay in triplicate and the reactions were stopped after 60 minutes. As shown in Figure 54B, MAL3-51 and MAL3-101 had no significant effect on DNA replication, whereas MAL2-11B inhibited replication in a concentration dependent manner.

I then hypothesized that MAL2-11B-like activity might be found in the other structurally related compounds discussed in Section 3.3.5. As shown in Figure 55, I titrated two structurally related compounds, DMT002272 and DMT003036, into the *in vitro* replication assay. These compounds were the product of Biginelli reactions and were identical to MAL2-11B except the aldehyde was varied. These compounds also inhibited DNA replication, though to a lesser extent than MAL2-11B. However, these effects correlate with the relative abilities of these molecules to decrease the TAg J domain stimulation of Ssa1p ATPase activity. Future studies will test if

Figure 54: MAL2-11B inhibits *in vitro* DNA replication.

In vitro DNA replication assays were performed in the presence of DMSO or 300 μM of the indicated compound. (A) A replication time-course was performed and the replicated DNA was resolved on an agarose gel. The TAg ATPase mutant 5061 was tested as a control. (B) Three replicates of each condition were performed and quantified. Compounds were tested at 30 μM, 100 μM, and 300 μM.

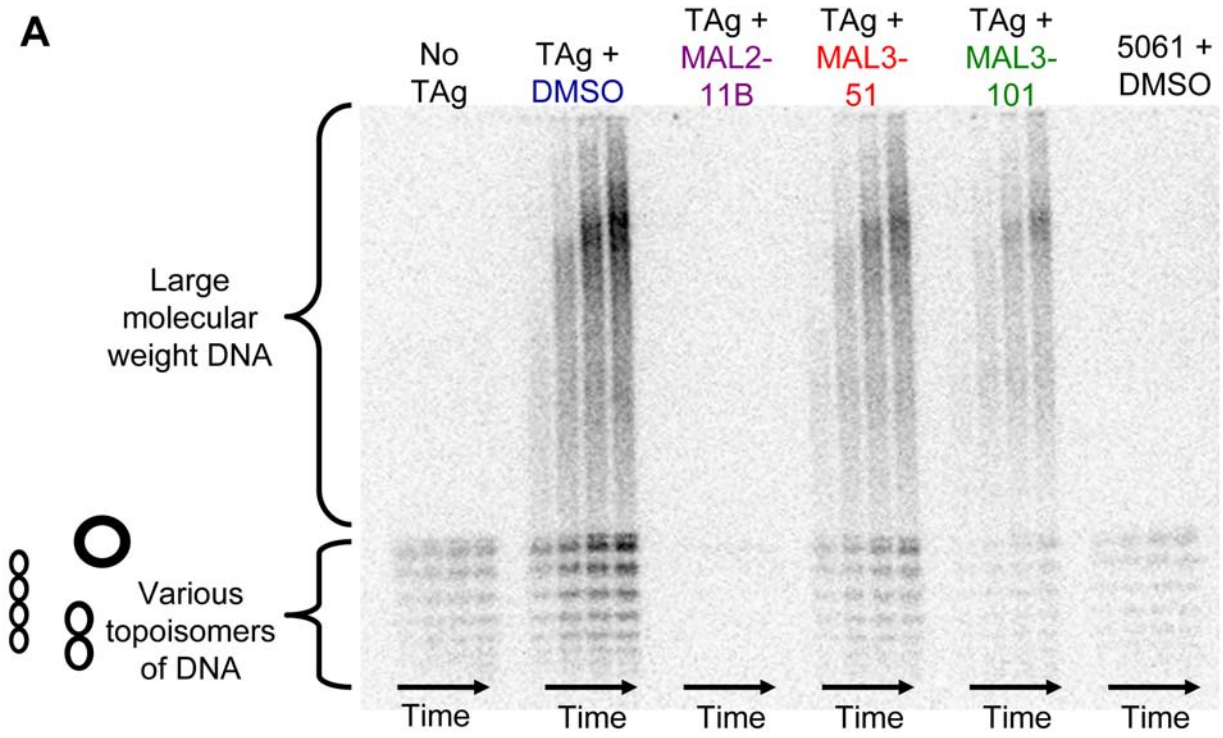
A
No TAg
TAg + DMSO
TAg + MAL2-11B
TAg + MAL3-51
TAg + MAL3-101
5061 + DMSO
Large molecular weight DNA
Various topoisomers of DNA
Time
Time
Time
Time
Time
Time

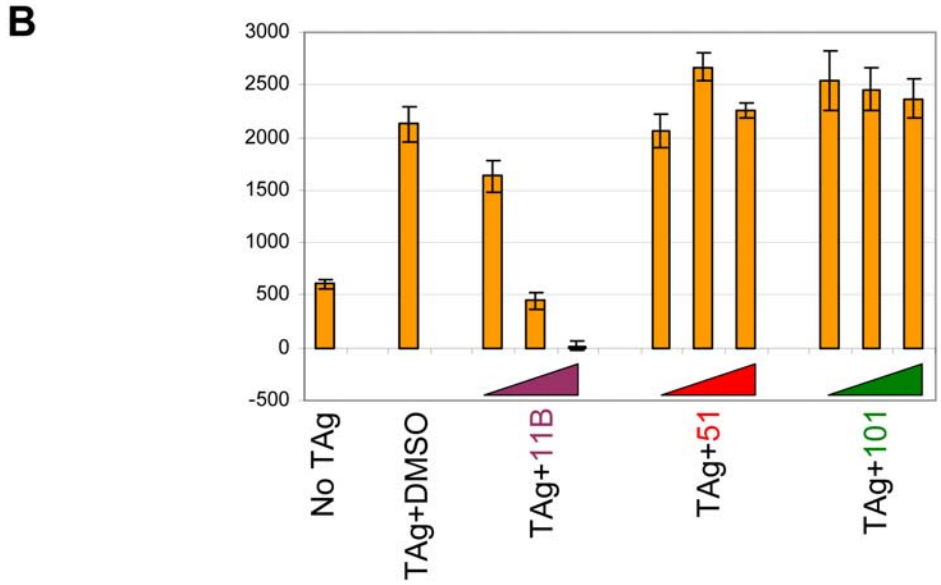
B
3000
2500
2000
1500
1000
500
0
-500
No TAg
TAg+DMSO
TAg+11B
TAg+51
TAg+101

Figure 55: MAL2-11B related compounds in the Biginelli acid class also inhibit *in vitro* DNA replication.

An *in vitro* DNA replication assay was performed in the presence of the indicated compounds. The effect of the compounds was examined at tested in triplicate at 30 μM, 100 μM, and 300 μM.

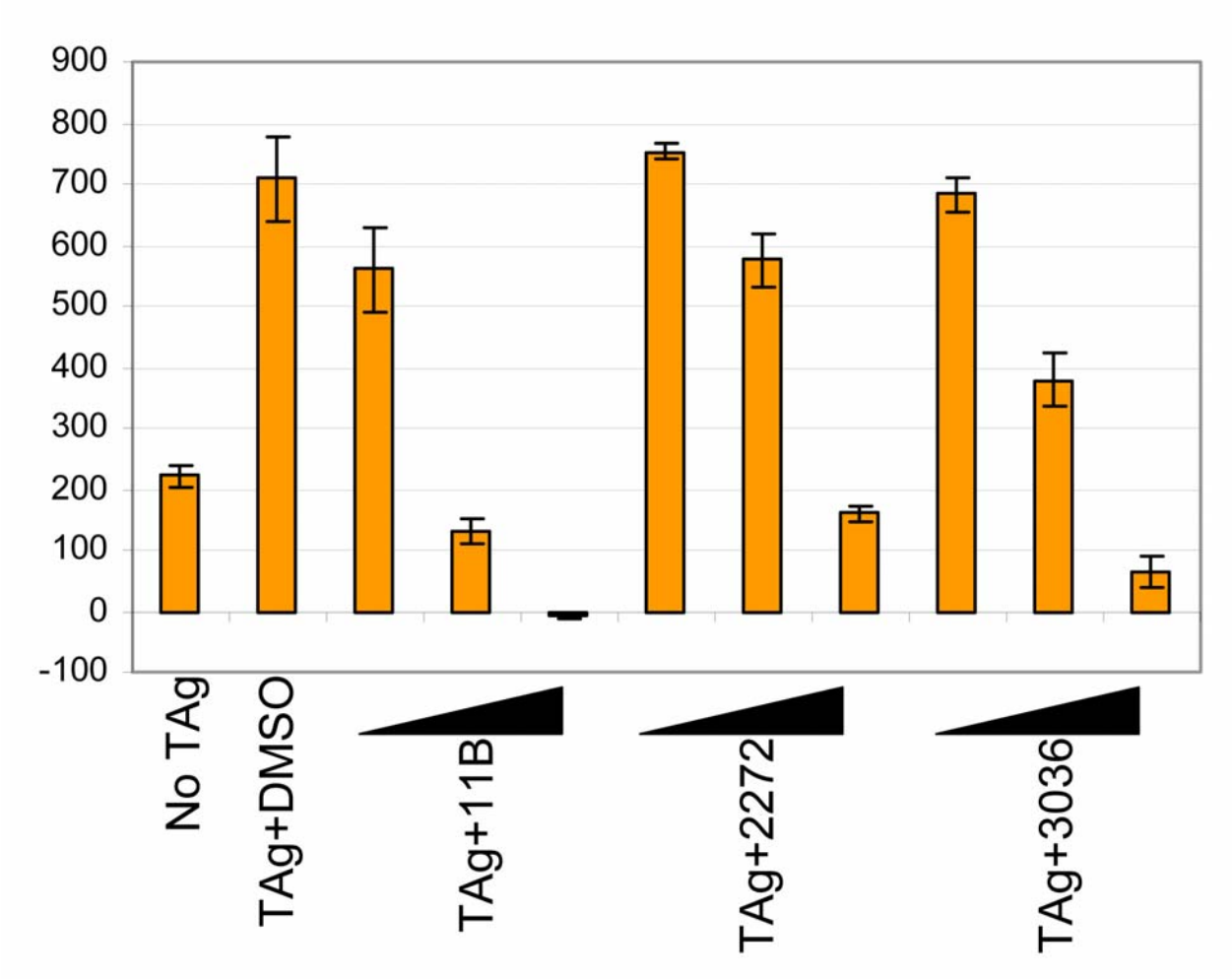
900
800
700
600
500
400
300
200
100
0
-100
No TAg
TAg+DMSO
TAg+11B
TAg+2272
TAg+3036

these compounds inhibit TAg ATPase activity or SV40 replication. Taken together, my results indicate that MAL2-11B, and related compounds, inhibit SV40 DNA synthesis *in vitro* and may explain how MAL2-11B inhibits SV40 replication *in vivo*.

5.0 DISCUSSION

Chaperones are essential for the maturation and localization of cellular proteins and are thus involved in nearly every aspect of cellular function. Given this, it is not surprising that many common diseases are directly related to chaperone level and function in the cell (AMARAL 2004; BARRAL *et al.* 2004; JOLLY and MORIMOTO 2000; SMITH *et al.* 2005). It is also not surprising that viruses have evolved the ability to corrupt chaperone function to allow viral replication. One example of this is seen with the SV40 protein, TAg, which is essential for viral replication and transformation (SRINIVASAN *et al.* 1997; SULLIVAN *et al.* 2000a). One major goal of this dissertation was to further characterize the role of SV40 TAg in replication and cellular transformation. To this end, I screened for novel TAg J domain interacting proteins using a yeast multi-copy suppressor screen. While I did not identify any unknown TAg J domain interacting proteins, I did identify a novel connection between the yeast cell wall and the cytosolic chaperones Hsp40 and Hsp90 (Chapter 2.0). A second goal of this dissertation was to identify small molecules that inhibited TAg J domain stimulation of Hsp70, which could then be used to inhibit SV40 replication and other Hsp70-associated diseases such as breast cancer. I identified several classes of chaperone modulators, including ones that selectively inhibit TAg stimulation of Hsp70. Select compounds in this class were shown to inhibit breast cancer cell proliferation (Chapter 3.0) or SV40 replication (Chapter 4.0). In the following pages, I summarize the results from each project and discuss the importance of the data and future efforts.

5.1 A MULTI-COPY YEAST SUPPRESSOR SCREEN IDENTIFIES A ROLE FOR MOLECULAR CHAPERONES IN THE YEAST CELL WALL

To identify novel TAg interacting proteins, I performed a yeast multi-copy suppressor screen. I screened for multi-copy suppressors of the K53R temperature sensitive mutation in the TAg-Ydj1p chimeric protein, T(K53R)-Ydj1p. I chose to use this mutation because it was in helix III of the J domain and NMR perturbation studies using DnaJ (GREENE *et al.* 1998) suggested that the solvent-exposed region in helix three that is occupied by the K53 residue would not be in contact with Hsp70. Since this mutation inhibited viral replication, transformation, and chaperone activity (FEWELL *et al.* 2002), I predicted that it interacted with a novel protein. Despite this, even if the K53R mutation unexpectedly disrupted the interaction with Hsp70, a yeast multi-copy suppressor screen might still identify proteins that act in concert with Hsp70, or in parallel pathways to this J-protein.

As hoped, the yeast suppressor screen identified several genes that rescued to some degree the thermosensitive phenotype of *ydj1Δ* yeast expressing T(K53R)-Ydj1p. Since we predicted that Hsp70 interacts with helix II of the TAg J domain, we were surprised that one of these genes was the Hsp70-encoding *SSA1* gene. There are two general explanations for this result. First, it is possible that additional copies of Hsp70 in the cell "fix" the aberrant conformation conferred by the K53R mutation; second, higher levels of Hsp70 might improve the function of a protein or process that lies downstream of the K53R-induced phenotype. In support of a direct interaction between Hsp70 with K53R, more recent NMR data suggests that Hsp70 interacts with additional residues in the polyomavirus J domain than in the DnaJ J domain, including residues on helix III (GARIMELLA *et al.* 2006). My results suggest that Hsp70

also interacts with helix III of SV40 TAg and that the screen can identify J domain-interacting proteins.

Another, weaker, suppressor of the *T(K53R)-YDJ1* phenotype that we identified was *CIS1*. In a previous study, *CIS1* was identified as a suppressor of a *cik1Δ* phenotype (MANNING *et al.* 1997). Cik1p cooperates with the Kar3p microtubule motor protein to catalyze karyogamy and chromosome segregation (PAGE and SNYDER 1992). Uncovering *CIS1* as a weak suppressor of the *T(K53R)-YDJ1* phenotype may be indicative of a link between Ydj1p function and microtubule homeostasis. In fact, Ssa1p and Ydj1p were previously suggested to be important for microtubule formation, and more specifically strains containing either an *ssa1* temperature sensitive allele (*ssa1-134*) or that were deleted for *YDJ1* showed irregular microtubule assembly at the non-permissive temperature after nocodazole treatment (OKA *et al.* 1998). Moreover, both the *ssa1-134* and *ydj1Δ* alleles exhibit synthetic interactions with *tub4-1*, which is a temperature sensitive allele in the gene encoding γ-tubulin. Therefore, improved growth of the *T(K53R)-YDJ1*-containing *ydj1Δ* strain by *CIS1* over-expression may be due to the rescue of a residual microtubule defect. Thus, it is unlikely that Cis1p is a novel TAg J domain interacting protein.

One rationale for why the multi-copy suppressor screen did not identify novel TAg J domain interacting proteins is that I used a yeast genomic library. I chose this library because the yeast genome is small and well annotated and I predicted that J domain interacting proteins would be conserved. However, it is possible that over-expression of select mammalian proteins could rescue the temperature sensitive defect of T(K53R)-Ydj1p. I therefore tested four mammalian proteins for the ability to restore growth of *ydj1Δ* yeast expressing T(K53R)-Ydj1p or *ydj1Δ*. I first tested human HspBP1 and BAG-1S because these are NEFs (HOHFELD and JENTSCH 1997; KABANI *et al.* 2002b) that might stimulate Hsp70 in the presence of a defective

Ydj1p cochaperone. Over-expression of these proteins did not improve growth in the *ydj1Δ* yeast expressing T(K53R)-Ydj1p. Unexpectedly, BAG-1S partially restored growth in the *ydj1Δ* strain, suggesting that it can aid Hsp70 function in the absence of cochaperone. I also tested the over-expression of Cul7, which may direct a TAg-interacting protein for ubiquitination and proteasomal degradation (ANDREWS *et al.* 2006; DIAS *et al.* 2002). Cul7 is of further interest since the TAg interaction with Cul7 is involved in cellular transformation and Cul7 binds to the TAg J domain in the extended loop between alpha helix three and four, which is present in the chimeric *T-YDJ1* construct used in my studies (KASPER *et al.* 2005). It is currently unclear if the chaperone function of the J domain is required for Cul7 dependent transformation. Unfortunately, over-expression of Cul7 did not improve the growth of the *ydj1Δ* strains expressing T(K53R)-Ydj1p. Interpretation of these results is difficult since there are many reasons why a mammalian protein could be non-functional in yeast. Finally, I attempted to examine if over-expression of PKCη could restore growth of *ydj1Δ* yeast. I predicted it would restore growth in *ydj1Δ* yeast since over-expression of *PKC1* in *ydj1Δ* yeast cells improves growth and PKCη can functionally replace *PKC1* in yeast (NOMOTO *et al.* 1997). Unfortunately, over-expression of PKCη was toxic to the *ydj1Δ* yeast cells. This could have been due to the high expression levels produced using the *GPD* promoter and these experiments should be repeated using a weaker promoter.

Despite the fact that "Factor X" was not identified using this screen, the screen still revealed a novel connection between the cell wall and cytosolic chaperones (WRIGHT *et al.* 2007). Specifically, I found that the growth of *ydj1Δ* and *hsp82* temperature sensitive yeast is improved by conditions that restore the viability of cells with mutations in cell wall components or regulators of cell wall biogenesis. I also found that the growth of these strains is hindered by a

compound that intercalates into the cell wall. In addition, I discovered that the viability of the *ydj1Δ* and *hsp82* temperature sensitive strains is improved by the over-expression of Mid2p—a cell wall component that is thought to sense the integrity of this structure and activates the PKC pathway when cell wall architecture is compromised (LEVIN 2005)—and by the over-expression of Pkc1p and activated components in the PKC pathway, which are known to trigger increased synthesis of cell wall components (IGUAL *et al.* 1996). Previous work indicated that the PKC pathway induces the synthesis of cell wall glycoproteins and proteins involved in cell wall biosynthesis, including Fks1p and Fks2p (β1,3-glucan synthase) and Chs3p (chitin synthase) (JUNG and LEVIN 1999), and that Mid2p over-expression increases the chitin concentration in the cell wall (KETELA *et al.* 1999). Indeed, we found that Mid2p over-expression is sufficient to thicken the cell wall in yeast lacking *YDJ1*, which provides a rationale for why we identified *MID2* as the strongest suppressor of the *ydj1Δ* slow-growth phenotype.

Besides identifying *MID2* and the PKC pathway as moderate suppressors of the slow-growth phenotype of *ydj1Δ* yeast, our screen uncovered several other genes with links to cell wall homeostasis and to the PKC pathway. For example, Syp1p, was discovered as a suppressor of yeast profilin deletion (*pfy1Δ*) (MARCOUX *et al.* 2000) and Cis1p was uncovered as a suppressor of a *cik1Δ* yeast strain (MANNING *et al.* 1997). Whereas Syp1p helps polarize actin patches, little else is known about Cis1p. Both of these previously published screens also uncovered Mid2p and Rom2p—another upstream component of the PKC pathway—as suppressors, which suggest potential links between Syp1p and Cis1p and the PKC pathway. In addition Cyc8p/Ssn6p, which is found in a co-repressor complex with Tup1p, regulates genes under a wide array of stress conditions, including growth in hypertonic media (PROFT *et al.* 2001; PROFT and STRUHL 2002). Finally, *SKN1* is a Golgi-resident protein with an ill-defined role in

β1,6-glucan synthesis and is homologous to *KRE6*, which exhibits synthetic interactions with *PKC1*, *MPK1*, and *MKK1/MKK2*; moreover, Kre6p over-expression can rescue a *pkc1Δ* lysis defect (ROEMER *et al.* 1994). In contrast, we were surprised to find that the over-expression of *CHS5,* which is involved in the transport of chitin synthase from the Golgi (SANCHATJATE and SCHEKMAN 2006), did not rescue the slow growth phenotype of *ydj1Δ* yeast.

Interestingly, suppression of the *ydj1Δ* slow growth phenotype was copy number dependent. For example, the over-expression of *T(K53R)-YDJ1* gene partially restored growth of *ydj1Δ* yeast. While the *ydj1Δ* strain has a slow growth phenotype at 30°, expression of *T(K53R)-YDJ1* behind the moderate *TEF* promoter rescued the slow growth phenotype at 30°, but was temperature sensitive at 35°. In addition, expression of *T(K53R)-YDJ1* behind the strong *GPD* promoter allowed the growth of *ydj1Δ* yeast at both 35° and 37°. These results suggest that *T(K53R)-YDJ1* is partially functional, which correlates with results on its *in vitro* activity (FEWELL *et al.* 2002). Since the only difference between these strains is *T(K53R)-YDJ1* copy number, these results also indicate that the amount of Ydj1p is important for growth.

Plasmid number was similarly essential for suppression of the *T(K53R)-YDJ1* temperature sensitive phenotype by many of the suppressors. For example, *SYP1* and *CYC8* did not restore growth of the *ydj1Δ* strain expressing T(K53R)-Ydj1p when expressed on a *CEN* plasmid, but improved growth when copy number was increased by expression on a 2μ plasmid. Finally, the partial function of T(K53R)-Ydj1p was responsible for the discovery of extremely weak suppressors. The *ydj1Δ* strain required expression of both T(K53R)-Ydj1p and the suppressors to even partially rescue growth at 35°. This effect was also seen in the *ydj1Δ* strain independent of *T(K53R)-YDJ1*. For example, when *BCK1-20* and $MKK1^{DD}$ were expressed on a *CEN* plasmid, they were unable to improve the growth of the *ydj1Δ* strain (data not shown).

However, when *BCK1-20* and *MKK1^{DD}* were expressed on a 2μ plasmid, they were able to improve the growth if the *ydj1Δ* strain (Figure 20). Knowing this, I predict that *SKN1* would also improve the growth of the *ydj1Δ* strain if expressed on a 2μ plasmid. Skn1p is involved in β,1-6 glucan synthesis and is functionally homologous to Kre6p (ROEMER *et al.* 1993), which has genetic links to the PKC pathway. I hypothesize that *SKN1* was obtained in the screen because it strengthened the cell wall like the other suppressors, and not because it directly interacted with T(K53R)-Ydj1p. Despite this, I still believe *SSA1* and *CIS1* are direct suppressors of the *T(K53R)-YDJ1* phenotype as discussed above since increased copy number of Ssa1p is toxic to the *ydj1Δ* cells and *CIS1* was expressed from a 2μ plasmid. Immunoblots are needed to verify Cis1p expression level. Cis1p expression could also be altered by expression behind several promoters to verify that increased expression does not rescue growth of the *ydj1Δ* strain.

These studies leave several questions unanswered. First, what is the role, if any, of Ssa1p in cell wall integrity? In most instances Hsp40 function is intricately linked to Hsp70 function and does not function independent of Hsp70 in the Hsp90 complex. Thus, we were surprised that over-expression of Mid2p or components in the PKC pathway failed to rescue the *ssa1-45* thermosensitive phenotype. One interpretation of this result is that Hsp40 and Hsp90, but not Hsp70, play a role in cell wall biosynthesis, and we note that *in vitro* experiments suggested that Ydj1p and Hsp82p may hold PR in a hormone binding competent state independent of Ssa1p (HERNANDEZ *et al.* 2002). However, another interpretation of this result is that allele-specific interactions underlie the ability of Mid2p and Pkc1p to improve the growth of *ydj1Δ* and *hsp82*, but not *ssa1-45* yeast. It is important to mention that the G170D and G313N mutations are in the Hsp82 ATPase domain and middle region, respectively (FLISS *et al.* 2000; NATHAN and LINDQUIST 1995), and have been shown to affect protein stability and Hsp82p client protein

activation (BOHEN 1995; LEE *et al.* 2002; YOUKER *et al.* 2004). In contrast, the *ssa1-45* allele encodes a P417L mutation in the peptide binding domain of Ssa1p (BECKER *et al.* 1996) and has been shown to compromise protein folding, translocation, and ER associated degradation (BECKER *et al.* 1996; KIM *et al.* 1998b; ZHANG *et al.* 2001). Moreover, the *hsp82* mutations reside in a strain that lacks chromosomal copies of *HSP82* and *HSC82*, whereas the *ssa1-45* mutation resides in a strain that lacks the *SSA2*, *SSA3*, and *SSA4* genes. Unfortunately, no other tight *ssa1* temperature sensitive strains exist in which we can further explore this phenomenon, and it is not clear how the necessary strain backgrounds for these studies impact the effects on cell wall integrity/signaling that we observed.

These results also lead to a second question: What is the nature of the cell wall defect in *ydj1Δ* yeast? As mentioned previously, *pkc1Δ* yeast have a thin cell wall, which is likely the cause of osmotic sensitivity. However, as shown in Figure 35, the cell wall in *ydj1Δ* yeast is not thinner than in wild type yeast. I propose that the cell wall of *ydj1Δ* yeast has reduced β1,6-glucan relative to wild type yeast. As described previously, 80-90% of the yeast cell wall is composed of β1,3-glucan and β1,6-glucan acts as the "glue" to hold it together. While β1,3-glucan and chitin are synthesized at the cell wall, it is unknown where β1,6-glucan is synthesized. One hypothesis is that β1,6-glucan is synthesized in the secretory pathway since defects in many secretory proteins lead to a cell wall defect. A second hypothesis is that a protein required for β1,6-glucan synthesis requires the secretory pathway for maturation. Since Ydj1p is involved in translocation of nascent polypeptide chains into the ER (CAPLAN *et al.* 1992), Ydj1p may also be involved in β1,6-glucan synthesis. This is particularly intriguing since I identified *SKN1* as a suppressor of *T(K53R)-YDJ1* (and potentially *ydj1Δ*, see above). I propose that the defect in the *ydj1Δ* strain is due to a decrease in the amount of β1,6-glucan,

which makes a weaker, but not thinner, cell wall. This would be consistent with the EM data. To test this hypothesis I would determine the amount of each cell wall component in *ydj1Δ* and wild type cells, by isolating the total alkali-insoluble glucan and using zymolyase to remove the β1,3-glucan. This process is relatively easy and the technique has been performed in many labs (MACHI *et al.* 2004; ROEMER *et al.* 1993). If this hypothesis is correct, these results would be the first to implicate cytosolic chaperones in β1,6-glucan synthesis.

There are still many unanswered questions about the connections between the cell wall integrity pathways. For example, it has been shown that activation of the HOG pathway leads to inactivation of the PKC pathway (MAGER and SIDERIUS 2002). Also, several connections between the two pathways and molecular chaperones exist. First, many kinases in all three pathways are probable Hsp90 substrates, such as Hog1p, Kss1p, and Mpk1p (MILLSON *et al.* 2005) as shown by yeast two hybrid. Second, the Hsp90 temperature sensitive strains have different phenotypes on medium with high sorbitol. Two Hsp90 temperature sensitive mutants (T22I and G81S) are sensitive to high sorbitol, which is a phenotype consistent with mutations in HOG pathway members (YANG *et al.* 2006) and these mutants and two other Hsp90 temperature sensitive mutants (G170D and G313N) are sensitive to calcofluor white, which is indicative of mutations in the PKC pathway (YANG *et al.* 2006). Third, I uncovered *CYC8* as a suppressor of the *ydj1Δ* strain. Cyc8p is a transcriptional repressor that is converted by Hog1p to an activator during osmotic stress.

To address the degree of cross-talk between the pathways and their role in mediating the *ydj1Δ* phenotype, I over-expressed two genes from the HOG pathway (*HOG1* and *PBS2*) and two genes from the SVG pathway (*KSS1* and *STE7*). None of these genes rescued the *ydj1Δ* slow growth phenotype. Trivially, this could be due to lack of expression, though Hog1p

expression was verified by western blot analysis (Figure 22C). Another hypothesis is that constitutively activated members of the pathways could restore growth in the *ydj1Δ* strain. Most studies of the downstream members of the signaling pathways use strains with deletions of the upstream kinases that must express constitutively activated downstream components. Without the upstream components, the wild type proteins are not properly phosphorylated in response to stress and are nonfunctional. However, studies on the cross-talk between the pathways do not require strains with mutations in the upstream components and therefore do not require constitutively active proteins. Nonetheless, it is possible that constitutively active forms of these kinases could rescue the *ydj1Δ* slow growth defect. To further investigate this proposal in my system, I would test constitutively expressed versions of *HOG1* and *STE7* genes (YAAKOV *et al.* 2003; YASHAR *et al.* 1995) to see if they rescue *ydj1Δ* yeast.

Even though activation of the PKC pathway suppressed the *ydj1Δ* strain slow growth defect independent of *T(K53R)-YDJ1*, the results presented here suggest a putative connection between TAg J domain function and the PKC pathway. Previous work demonstrated that TAg blocked the apoptotic response upon EGF withdrawal from mouse embryo cells (SLINSKEY *et al.* 1999), and chemical inhibition of the PKC pathway also inhibited apoptosis (A. SLINSKEY and J. M. PIPAS, unpublished data). In addition, the amount of an uncharacterized PKC phosphorylated substrate decreased in mouse intestines upon TAg expression (R. BEERMAN, M. T. SAENZ-ROBLES, J. M. PIPAS, unpublished data). While these results suggest a connection between TAg and PKC, much more work is clearly needed to define how the TAg J domain impacts the PKC pathway.

5.2 MAL3-101 AND RELATED COMPOUNDS INHIBIT BREAST CANCER CELL PROLIFERATION

Since Hsp70s and Hsp40s are involved in a plethora of human diseases and since there are very few chaperone modulators that have been identified, I screened for novel modulators of Hsp70 and Hsp40 activity. Prior to these studies, only a few Hsp70s modulators, including the structurally similar DSG and R/1 compounds had been described. DSG stimulated two different Hsp70s, Ssa1p and bovine Hsc70, in steady state assays, but had no effect on cochaperone stimulation by Ydj1p (BRODSKY 1999). However, DSG lacked specificity as it bound Hsp70 and Hsp90 with similar affinities (NADEAU *et al.* 1994). On the other hand, R/1 inhibited Ssa1p ATP hydrolysis in steady state assays and stimulated Ssa1p ATP hydrolysis in single turnover assays (FEWELL *et al.* 2001; FEWELL *et al.* 2004). I was particularly interested in R/1 because it also inhibited TAg stimulation of Hsp70. Unfortunately, R/1 is relatively large, insoluble, and difficult to obtain. I hypothesized that compounds that were structurally similar to R/1 might have similar *in vitro* effects on Hsp70 and TAg. The identification of structural analogs might allow for the identification of a structural motif responsible for chaperone modulating function and lead to the synthesis of more potent and soluble derivatives.

We therefore obtained 30 compounds that were structurally similar to DSG and R/1 from the Wipf lab at the University of Pittsburgh and from the NCI. Dr. Fewell tested the compounds for effects on endogenous Ssa1p ATPase activity using single turnover assays. Since ATP is prebound to Hsp70, this assay is specific for ATP hydrolysis and does not measure ATP binding or release. I then tested the effect of 12 of the compounds on TAg stimulation of Hsp70 ATPase activity. I chose TAg as my model J-protein for two main reasons. First, it is required for SV40 replication and transformation and any compounds that modified TAg activity could be potential

treatments for any virus-induced disease. Second, it is relatively easy to purify in high quantities and contains very few contaminants. Three distinct classes of chaperone modulators were identified during the screen:

Class 1. Compounds in this class stimulated endogenous Ssa1p ATP hydrolysis and had an overall inhibitory effect on TAg stimulation of Ssa1p. This class can be divided into two subclasses. Class 1A is characterized by MAL3-55 which slightly stimulated the rate of Ssa1p ATP hydrolysis by 1.4 fold and inhibited TAg stimulation by 1.8 fold by decreasing both the initial slope and the overall amplitude. It is likely that when the compound stimulates endogenous Ssa1p ATP hydrolysis this leads to a change in the protein that prevents complete stimulation by cochaperone (though the compounds could be directly interfering with the cochaperone as well). One possibility is that the hydrophobic characteristics of the compounds in this class mimic peptide binding. It would be interesting to perform single turnover assays in the presence of peptide and chaperone modulators. An example of Class 1B is MAL3-90. Compounds in this class dramatically stimulate Ssa1p ATPase activity. Addition of cochaperone leads to a "burst" which increases ATP hydrolysis to higher levels than with cochaperone alone. However, this is immediately followed by a decrease in amplitude and an overall inhibitory effect. It has been previously shown that rapid stimulation of Hsp70 ATPase activity can lead to polymerization of the Hsp70 molecules (KING *et al.* 1999). It is possible that the compounds stimulate Hsp70 polymerization and thus prevent the reaction from reaching completion.

Class 2. This class was exemplified by MAL3-101, which has no effect on Ssa1p ATP hydrolysis but inhibited TAg stimulated ATP hydrolysis. There are two models that I propose for the mechanism of action of this class of compounds. First, MAL3-101 may directly prevent interaction between the J domain and Hsp70. I have begun to address this hypothesis by

precipitating Ssa1p in the presence or absence of GST-Hlj1p-His and/or MAL3-101. Preliminary results suggest that MAL3-101 does not interfere with the interaction between the two chaperones. However, the low MAL3-101 concentration used and potential for MAL3-101 J domain specificity make interpretation of these results difficult. A second possibility is that MAL3-101 interferes with the stimulation of Hsp70 independent of chaperone-cochaperone interaction. The most-straightforward way to differentiate between these two models is to determine the binding site of the compound on Hsp70 or the J-protein. In collaboration with Dr. E. Zuiderweg at the University of Michigan, these experiments are in progress.

Class 3. Some compounds tested, such as MAL3-51, had little effect on either the Ssa1p ATPase activity or TAg stimulated ATPase activity. Despite the fact these compounds had little effect on chaperone activity, compounds in this class will help identify a minimal functional group required for chaperone modulation. Since there are only slight differences between each compound's structure, the changes that disrupt the chaperone modulating activity of these compounds may help us to identify which regions of the other compounds are necessary for function.

The complexity of the compounds and the distinct classes has made determination of an SAR difficult. As a next step toward this goal, I decided to examine a set of six compounds that were half the mass of previous compounds, but had many structural components in common. If these compounds affected chaperone activity, they could represent the minimal pharmocophore required for chaperone modulation. I tested these compounds in an Ssa1p single turnover assay in the presence or absence of TAg. Five of the compounds had similar kinetics as members of Class 1B described earlier. These compounds stimulated endogenous Ssa1p ATPase activity and initially increased TAg stimulation of Ssa1p, but decreased the overall amplitude of the reaction.

The sixth compound was a member of Class 2 and selectivity inhibited TAg stimulation of Ssa1p. These compounds may represent the minimal pharmocophore of their respective classes.

Since these compounds had a much lower mass, and thus were more likely to be soluble than previously identified compounds, I decided to test them in an *in vivo* assay to see if they could modulate Hsp70 activity *in vivo*. I also decided to test MAL3-101 since previous evidence using *in vitro* translocation assays suggested that it was membrane permeable (FEWELL *et al.* 2004). Yeast ER translocation requires two sets of Hsp70/Hsp40 chaperones, the cytosolic chaperones, Ssa1p and Ydj1p, and the ER luminal Kar2p and Sec63p (CAPLAN *et al.* 1992; DESHAIES *et al.* 1988; ROTHBLATT *et al.* 1989; VOGEL *et al.* 1990). In translocation assays, MAL3-101 inhibited pre-pro-α-factor (ppαF) translocation, suggesting that one, or both, of these chaperone pairs is inhibited by MAL3-101. However, translocation assays were performed with ppαF denatured with 8 M urea, which eliminates the need of Ssa1p or Ydj1p during translocation. Even with denatured ppαF, MAL3-101 inhibited translocation, which suggested that the compound is membrane permeable and interferes with the interaction between Kar2p and Sec63p.

I chose to test the compounds using a breast cancer cell proliferation assay. In this assay, the compounds are added to actively growing cells and after several days the total number of living cells is determined using the colorimetric indicator, MTS. The cell proliferation assay was chosen to test the compounds for several reasons. First it is high throughput which is important for studying large numbers of compounds. Since the single turnover assays are not high throughput, the cell proliferation assay could serve as a primary screen for compound activity and the single turnover could be a secondary assay to determine chaperone modulation. Second, the cell proliferation assay requires the compounds to be membrane permeable and also allows

testing a variety of cell lines. I chose to examine the effects of the compounds on breast cancer cell proliferation since these cells over-express Hsp70 and may be susceptible to modulation of Hsp70 activity. In fact, reduction of Hsp70 levels by antisense RNA is sufficient to induce breast cancer cell apoptosis (NYLANDSTED *et al.* 2000).

Guangyu Zhu from the Day lab at the University of Pittsburgh examined the 6 compounds with the putative minimal pharmocophores and MAL3-101 for their effects on the proliferation of SK-BR-3 breast cancer cells. The six Hsp70 modulators identified in the second round of screening had no effect on SK-BR-3 cells, but MAL3-101 inhibited proliferation of two different breast cancer cell lines, SK-BR-3 and MDA-MB-468, in the low micromolar range. These cell lines have been shown to be susceptible to Hsp70 antisense RNA treatment (NYLANDSTED *et al.* 2000). To test MAL3-101 specificity, G. Zhu used the WI-38 fibroblast cell line, which when treated with Hsp70 antisense RNA, did not undergo apoptosis (NYLANDSTED *et al.* 2000). Unexpectedly, MAL3-101 also inhibited WI-38 cell proliferation at similar concentrations. However, MAL3-101 is not universally toxic as it does not inhibit the proliferation of BSC40 cells (see below). This indicates that MAL3-101 is not specific for breast cancer cells, but this may be in part due to the relatively low compound affinity. Potentially, more soluble or potent MAL3-101 derivatives may increase specificity.

I propose several models for the mechanism of MAL3-101 inhibition of cellular proliferation. First, the compound might be inhibiting chaperone-dependent cell growth. As previously described chaperones play important roles in most cell processes and it would not be surprising if reduction in Hsp70 activity was sufficient to slow cellular growth or even stall growth at a particular stage in the cell cycle. This hypothesis could be tested by determining relative DNA content in the cells using flow cytometry. Second, it is possible that the MAL3-

101 initiates apoptosis. Unpublished results from the Chiosis lab suggest that MAL3-101 initiates apoptosis in the SK-BR-3 cell line as indicated by caspase-3 and PARP cleavage and caspase-3 activation. Regardless of which model is correct, it is also possible that MAL3-101 acts independently of Hsp70/J-proteins in the cell, and affects another, unknown, target. Some specificity studies have been performed and will be discussed in more detail below. However, it is clear that MAL3-101 does not affect all ATPases as it has minimal effect on mammalian Hsp70, mammalian Hsp90, TAg, MCM, or kinesin ATPase activity.

To obtain additional structural information on MAL3-101 and to attempt to find more soluble, potent compounds, 42 derivatives of MAL3-101 were synthesized (WERNER *et al.* 2006) and tested in the breast cancer proliferation assay using the SK-BR-3 cell line. These results were then correlated to *in vitro* affects on Hsp70 ATPase activity and TAg stimulation of Hsp70. The compounds that inhibited breast cancer proliferation fell into distinct chemical classes, and this was directly related to chaperone modulation. The classes are discussed in detail below.

Class A. Biginelli acids. These compounds are the product of a Biginelli reaction, and were not subsequently reacted in an Ugi reaction. The aldehyde group used in the Biginelli reaction was varied to obtain structural diversity. These compounds had no effect on breast cancer cell proliferation, though they had similar effects on MAL3-101 in the single turnover assays; i.e., they had no effect on Ssa1p ATP hydrolysis, but inhibited TAg stimulation of Ssa1p. It is unlikely that a lack of membrane permeability is responsible for the lack of effect on breast cancer cells because MAL2-11B is represented in this class, and as described below, this compound inhibited viral replication *in vivo*. Further characterization of this class will be discussed below.

Class B. Biginelli esters. These compounds are also the product of only a Biginelli reaction, except the Biginelli reactions utilized several esters instead of aldehydes to obtain structural diversity. These compounds had no effect on breast cancer cell proliferation and had novel effects in the single turnover assays. These compounds stimulated Ssa1p ATP hydrolysis, but had no effect J domain stimulation of Ssa1p. These compounds represent a unique class of chaperone modulators not discovered in previous screens.

Class C. Ugi 1. These compounds were the products of successive Biginelli and Ugi reactions. The Biginelli reactants were the compounds from Class A, which were then reacted in an Ugi condensation reaction. Most compounds in this class inhibited breast cancer proliferation with a GI_{50} lower than 10 μM. These compounds had very similar effects as MAL3-101 in relation to both endogenous Ssa1p ATP hydrolysis and TAg stimulated ATP hydrolysis. Thus, it is likely that the Ugi reaction is important for conferring the ability of the compounds to inhibit breast cancer cell proliferation.

Class D. Ugi 2. These compounds were also the products of successive Biginelli and Ugi reactions. However, these reactions had variations in the aldehyde group of the Ugi reaction, not in the Biginelli reaction. These compounds did not inhibit breast cancer proliferation. This indicates that for inhibition of breast cancer cell proliferation, the compounds are not tolerant to alterations in the aldehyde group of the Ugi reaction. These compounds had effects that were reminiscent of Class 1B of compounds. They generally stimulated Ssa1p ATP hydrolysis quite profoundly, and stimulated the initial TAg stimulation of Hsp70, before inhibiting the overall amplitude of the reaction. This suggests that the aldehyde group is important to stimulate Ssa1p ATP hydrolysis. At this point, their mechanism of action is unclear. The effects of these compounds were reminiscent of the five compounds previously tested in the breast cancer

proliferation assays, JB-78, JB-99, JB-102, JB-116, and MAL2-216. Consistent with this classification, none of these compounds inhibited breast cancer cell proliferation.

Class E. Ugi-3. Compounds in this class also were the products of successive Biginelli and Ugi reactions and utilized the same starting Biginelli product as the Ugi-2 class of compounds. However, in this class, the amine group was varied in the reaction instead of the aldehyde group. Compounds in this class had a variety of phenotypes, and some compounds inhibited breast cancer cell proliferation. Compounds that inhibited breast cancer cell proliferation had effects that were similar to compounds in the Ugi-1 class that also inhibited breast cancer cell proliferation.

Based on the data from the Chiosis lab on MAL3-101 (see above), I predict that the MAL3-101 derivatives that inhibit breast cancer cell proliferation will induce cellular apoptosis. Three assays could be utilized that easily detect apoptosis: Terminal Transferase-Mediated dUTP Nick End-Labeling Method (TUNEL), DNA laddering, and caspase activation. TUNEL assays monitor cleavage of DNA by labeling the 3' end of DNA fragments, whereas DNA laddering assays monitor DNA cleavage monitored on an ethidium bromide stained agarose gel. Finally, the activation of caspases can be determined by incubating cell lysates with a synthetic caspase substrate linked to a reporter protein. Substrate cleavage, and thus caspase activity, can be measured by colorimetric output or by fluorometry

For all *in vivo* studies three major caveats need to be mentioned. First, if compounds have no effect on cell proliferation, the most trivial explanation is that sufficient quantities of the compound are not membrane permeable. This is a distinct possibility with these compounds since many of the compounds are not very soluble and precipitate out of solution when added at high concentrations into the assays. This concern can be partially addressed by synthesizing

compounds with lower mass that are more soluble. Second, the compounds could be cleaved or modified upon entry into the cell, which could complicate any SAR analysis. Thus, the functional motif that we ultimately identify might not directly act on the target protein. Third, the *in vitro* system may examine a target for the compound that is irrelevant *in vivo*. Thus, it is possible that chaperone modulation is only a secondary effect. One way to identify the novel proteins that interact with the compounds would be to affix the compounds to beads, co-precipitate any interacting proteins and use mass spectrometry to determine the protein identity. A similar approach was used to show that DSG interacts with Hsp70 (NADLER *et al.* 1992). However this approach requires a large quantity of compound, assumes the protein target is abundant in the cell, and may not detect transient interactions.

5.3 MAL2-11B INHIBITS SV40 REPLICATION AND SV40 DNA SYNTHESIS

Through my efforts, I have also identified a novel inhibitor of SV40 replication. This compound, MAL2-11B, and a related compound, MAL3-101, inhibit TAg J domain stimulation of Hsp70 ATP hydrolysis. Despite these similarities, MAL3-101 had virtually no effect on viral replication. To better understand the difference between MAL2-11B and MAL3-101 and identify the mechanism by which MAL2-11B inhibited SV40 replication, I analyzed compound specificity on several ATPases. I determined that MAL2-11B, but not MAL3-101 slightly inhibited the endogenous ATPase activity of the mammalian chaperones, Hsp70 and Hsp90. Surprisingly, MAL2-11B (but not MAL3-101) drastically inhibited both TAg and MCM ATPase activity. Since the TAg ATPase domain, but not the TAg J domain is required for *in vitro* DNA replication, I tested the effects of the compounds on DNA replication and determined that

MAL2-11B abolished DNA replication. Based on these studies, I conclude that MAL2-11B inhibits SV40 replication by inhibiting TAg ATPase activity and subsequently DNA replication.

Since I screened for inhibitors of J domain stimulation of Hsp70, the discovery that one of these compounds (MAL2-11B) was also a TAg ATPase inhibitor was surprising. One possibly is that MAL2-11B binds at two locations in TAg and thus inhibition of the J domain and ATPase are distinctly different phenomena. Another possibility is that MAL2-11B completely unfolds the TAg monomer, thus preventing activity of all TAg domains. This is unsatisfying because the J and ATPase domains are independent and are connected by a flexible linker; it is also difficult to imagine how a small molecule interaction at one site allosterically disrupts a separate domain. Another, more satisfying explanation is that MAL2-11B inhibits hexamerization. In the absence of ATP, TAg exists at an equal level of dimer and hexamer in solution, which is converted to hexamer in the presence of ATP. Currently, we do not know the oligomerization state of TAg that functions in single turnover assays, though some data suggests it is a hexamer. First, as TAg is titrated into the single turnover assay, the initial rate of ATP hydrolysis increases. However, at very low concentrations of TAg, this effect is no longer apparent, suggesting a threshold for stimulation (data not shown). One possibility is that this represents the threshold for hexamerization. Second, single turnover experiments with several N-terminal TAg truncation mutants suggest there are two distinct classes of TAg mutations. An N-terminal truncation with the first 500 amino acids stimulates Ssa1p with near wild type efficiency. However, TAg mutants with only the first 136 or 260 amino acids have virtually no activity in the single turnover assay (data not shown). Fine mapping by Jacklynn Moskow, in the Pipas lab at the University of Pittsburgh, suggests that any TAg N-terminal construct that contains the J domain through the zinc binding region is sufficient for stimulating Ssa1p ATP

hydrolysis (J. Pipas, personal communication). This suggests hexamerization is required for activity, but hypotheses about protein length and buffer effects need to be addressed.

I was equally surprised by MAL2-11B inhibition of MCM ATPase activity. However, both MCM and TAg are AAA+ ATPases, and TAg has known helicase activity and MCM is a presumed helicase (MAIORANO *et al.* 2006). Matt Bochman, in the Schwacha lab at the University of Pittsburgh has shown that 300 μM MAL2-11B abolishes MCM binding to ssDNA, and MAL3-51 and MAL3-101 have no effect (personal communication). These reactions were performed in the presence of ATPγS, since ATP binding is sufficient for ssDNA binding. One possibility is that MAL2-11B competes with ATP at the nucleotide binding site. In support of this hypothesis, M. Bochman performed competition experiments and showed that decreasing ATPγS in the reactions made MAL2-11B more effective at preventing ssDNA binding. Another possibility is that MAL2-11B affects the structure of the hexamer. This could be addressed by performing immunoprecipitations in the presence or absence of MAL2-11B and determining if the interactions between the proteins are affected.

The final ATPase tested was kinesin. This ATPase was chosen because it was unrelated to the previous ATPases tested and fairly abundant in the cell. As mentioned earlier, MAL2-11B had a very different effect on kinesin than on the other ATPases. As opposed to inhibiting kinesin ATPase activity, MAL2-11B appeared to dramatically stimulate its ATPase activity while on ice, in a concentration dependent manner. More experiments are required before these data are completely understood. However, it is clear that MAL2-11B activity differs between ATPases, and does not globally inhibit the activities of all enzymes.

Since MAL2-11B inhibited both the TAg ATPase activity and TAg J domain stimulation of Hsp70, it was unsurprising that MAL2-11B inhibited viral replication. These results also

correlated with inhibition of DNA replication *in vitro*. Based on the biochemical data, several models can be proposed. It is most likely that the inhibition of SV40 replication is due to the inhibition of the TAg ATPase activity since MAL3-101 did not inhibit replication (though this could be due to the concentration tested). This is also supported by the results from the *in vitro* DNA replication assay, which does not require the TAg J domain for replication (COLLINS and PIPAS 1995; WEISSHART *et al.* 1996). Three other possibilities remain. First, inhibition of SV40 replication could be independent of TAg and dependent on another, unknown, protein. Second, SV40 replication could be inhibited at a stage in the SV40 life cycle that occurs before DNA replication, such as virion disassembly or cell cycle initiation. Finally, MAL2-11B could kill the cells. However, G. Zhu from the Day lab has shown that BSC40 cell proliferation is unaffected by MAL2-11B, MAL3-51, or MAL3-101.

There are several stages of the SV40 life cycle that are known to require Hsp70 or the TAg J domain which are potential targets of MAL2-11B. These included: disassembly of viral capsids, initiation of the cell cycle via E2F release, DNA replication, and virion assembly (CHROMY *et al.* 2006; CRIPE *et al.* 1995; SPENCE and PIPAS 1994b; SRINIVASAN *et al.* 1997; SULLIVAN *et al.* 2000a). I chose to test DNA replication first for three reasons. First, this process was one of the few that also required the TAg ATPase domain. Second, the *in vitro* replication assay is relatively quick and easy to perform. Third, the results of the *in vitro* replication assay could be verified by determining viral DNA yield *in vivo*. Addition of MAL2-11B virtually abolished DNA replication in a concentration dependent manner. Similar results were also seen with chemically related compounds. In fact, MAL2-11B inhibited the background repair synthesis that is normally seen in the *in vitro* replication assay, which suggests

that it may also interfere with additional cellular factors. This, however, is unsurprising based on the previously discussed *in vitro* data.

Unfortunately, the *in vitro* replication assay does not address the specificity of drug action. The *in vitro* replication assay uses HeLa cell lysate to provide the necessary cellular "machinery" for replication, and theoretically MAL2-11B could inhibit any protein required for replication. This may be especially relevant if MAL2-11B is not specific for TAg and interferes with other ATPases. Therefore, the Fanning lab at Vanderbilt University has included MAL2-11B in their *in vitro* replication assays and MAL2-11B also inhibits TAg-dependent replication (personal communication). These assays use purified components, instead of cell lysate, and the only protein components of the reaction are hRPA, topoisomerase I, pol-prim, and TAg. Future MAL2-11B titrations into the Fanning lab replication assay will determine if MAL2-11B inhibits replication at similar concentrations, which would suggest the inhibition of DNA synthesis in my DNA replication experiments is solely due to the inhibition of TAg ATPase activity. Formally, MAL2-11B may also inhibit the activities of hRPA, topoisomerase I, or pol-prim, but since these proteins are not ATPases, this is not expected.

Based on previous data several hypotheses exist for the mechanism of MAL2-11B inhibition of DNA replication. First, MAL2-11B could inhibit the J domain's role in DNA replication. However, the role of the J domain in replication is unclear and it is not required for *in vitro* DNA replication. Second, it is possible that MAL2-11B inhibits the TAg helicase activity. This requires ATP hydrolysis by the TAg ATPase domain and DNA binding to the DNA binding domain. As discussed previously, MAL2-11B inhibits TAg ATPase activity and MCM ssDNA binding activity, so either of these hypotheses is viable. Based on above studies, a third possibility is that TAg is unable to hexamerize in the presence of compound. As mentioned

previously, there is evidence that TAg hexamerization is required for TAg stimulation of Ssa1p in the single turnover assay. Also, ssDNA binding and helicase activity require TAg hexamerization. To see if this is the case, I will add MAL2-11B to *in vitro* TAg hexamerization assays that monitor hexamerization in the presence of ATP (CASTELLINO *et al.* 1997).

One major concern with these studies is the lack of MAL2-11B specificity. This complicates the interpretation of the *in vivo* data and may cause secondary effects during treatment. I am particularly interested in determining if the effect of MAL2-11B on chaperones, independent of TAg, is important for inhibition of viral replication. Chaperones are often upregulated in response to viral replication and MAL2-11B could inhibit these chaperones' activity. Thus, I plan to determine the levels of Hsp70 and Hsp90 before and after viral infection and determine if MAL2-11B alters these levels. In addition, I plan to determine if modulation of Hsp90 activity by GA can inhibit viral replication. Together, these experiments will examine the role that the chaperones play in viral replication independent of the TAg J domain.

Finally, perhaps the best way to address specificity is to screen for compounds that are specific TAg inhibitors and that do not interfere with the ATPase activities of other proteins. I can visualize several different assays that could be used to screen for novel SV40 inhibitors. Perhaps the easiest way is to screen for inhibitors of TAg ATPase activity, and counterscreen for compounds that do not affect a second ATPase, such as Hsp70. The *in vitro* replication assays could also be adapted to a high throughput system and could be used to screen for compounds that inhibit DNA replication. Unfortunately, compounds that inhibit aspects of replication independent of TAg would also be identified, and isolated compounds would need to be counterscreened using *in vitro* DNA replication assay with purified components.

Taken together, these results suggest that I have identified two strikingly different classes of J-protein modulators. The first class is represented by MAL3-101 and the Ugi-1 and Ugi-3 derivatives of MAL3-101. These compounds inhibit J-protein stimulation of Hsp70 and breast cancer cell proliferation. However, they do not inhibit SV40 propagation or SV40 DNA replication. The second class is represented by MAL2-11B and the Biginelli acid derivatives of MAL3-101. These compounds also inhibit J-protein stimulation but have no effect on breast cancer cell proliferation. In addition, MAL2-11B inhibits various ATPases, including the AAA+ ATPases, TAg and MCM. It is likely that the inhibition of viral replication is independent of J-protein stimulation of Hsp70, and may be due to inhibition of hexamerization. It is currently unclear how these compounds are handled intracellularly, but it is certainly possible that these compounds target different proteins. Much future research should be directed at further characterization of these different classes *in vivo* and *in vitro*. I predict that the future study of these and related compounds will yield viable treatment options for breast cancer and polyomavirus infection.

BIBLIOGRAPHY

ADAM, E. J., and S. A. ADAM, 1994 Identification of cytosolic factors required for nuclear location sequence-mediated binding to the nuclear envelope. J Cell Biol **125:** 547-555.

ADAMS, A., D. E. GOTTSCHLING, C. A. KAISER and T. STEARNS, 1997 *Methods in Yeast Genetics*. Cold Spring Harbor Laboratory Press, Cold Springs Harbor, New York.

ADAMS, A. E., and J. R. PRINGLE, 1984 Relationship of actin and tubulin distribution to bud growth in wild-type and morphogenetic-mutant Saccharomyces cerevisiae. J Cell Biol **98:** 934-945.

AGRANOVSKY, A. A., V. P. BOYKO, A. V. KARASEV, E. V. KOONIN and V. V. DOLJA, 1991 Putative 65 kDa protein of beet yellows closterovirus is a homologue of HSP70 heat shock proteins. J Mol Biol **217:** 603-610.

AGRANOVSKY, A. A., S. Y. FOLIMONOVA, A. S. FOLIMONOV, O. N. DENISENKO and R. A. ZINOVKIN, 1997 The beet yellows closterovirus p65 homologue of HSP70 chaperones has ATPase activity associated with its conserved N-terminal domain but does not interact with unfolded protein chains. J Gen Virol **78 (Pt 3):** 535-542.

AHNER, A., F. M. WHYTE and J. L. BRODSKY, 2005 Distinct but overlapping functions of Hsp70, Hsp90, and an Hsp70 nucleotide exchange factor during protein biogenesis in yeast. Arch Biochem Biophys **435:** 32-41.

AHUJA, D., M. T. SAENZ-ROBLES and J. M. PIPAS, 2005 SV40 large T antigen targets multiple cellular pathways to elicit cellular transformation. Oncogene **24:** 7729-7745.

ALBERTI, S., C. ESSER and J. HOHFELD, 2003 BAG-1--a nucleotide exchange factor of Hsc70 with multiple cellular functions. Cell Stress Chaperones **8:** 225-231.

ALI, S. H., J. S. KASPER, T. ARAI and J. A. DECAPRIO, 2004 Cul7/p185/p193 binding to simian virus 40 large T antigen has a role in cellular transformation. J Virol **78:** 2749-2757.

ALLANDER, T., K. ANDREASSON, S. GUPTA, A. BJERKNER, G. BOGDANOVIC *et al.*, 2007 Identification of a third human polyomavirus. J Virol.

ALZHANOVA, D. V., A. I. PROKHNEVSKY, V. V. PEREMYSLOV and V. V. DOLJA, 2007 Virion tails of Beet yellows virus: Coordinated assembly by three structural proteins. Virology **359:** 220-226.

AMARAL, M. D., 2004 CFTR and chaperones: processing and degradation. J Mol Neurosci **23:** 41-48.

ANDREI, G., R. SNOECK, M. VANDEPUTTE and E. DE CLERCQ, 1997 Activities of various compounds against murine and primate polyomaviruses. Antimicrob Agents Chemother **41:** 587-593.

ANDREWS, P., Y. J. HE and Y. XIONG, 2006 Cytoplasmic localized ubiquitin ligase cullin 7 binds to p53 and promotes cell growth by antagonizing p53 function. Oncogene **25:** 4534-4548.

ARLANDER, S. J., S. J. FELTS, J. M. WAGNER, B. STENSGARD, D. O. TOFT *et al.*, 2006 Chaperoning checkpoint kinase 1 (Chk1), an Hsp90 client, with purified chaperones. J Biol Chem **281:** 2989-2998.

BAKKENIST, C. J., J. KORETH, C. S. WILLIAMS, N. C. HUNT and J. O. MCGEE, 1999 Heat shock cognate 70 mutations in sporadic breast carcinoma. Cancer Res **59:** 4219-4221.

BARBANTI-BRODANO, G., F. MARTINI, M. DE MATTEI, L. LAZZARIN, A. CORALLINI *et al.*, 1998 BK and JC human polyomaviruses and simian virus 40: natural history of infection in humans, experimental oncogenicity, and association with human tumors. Adv Virus Res **50:** 69-99.

BARNES, J. A., D. J. DIX, B. W. COLLINS, C. LUFT and J. W. ALLEN, 2001 Expression of inducible Hsp70 enhances the proliferation of MCF-7 breast cancer cells and protects against the cytotoxic effects of hyperthermia. Cell Stress Chaperones **6:** 316-325.

BARRAL, J. M., S. A. BROADLEY, G. SCHAFFAR and F. U. HARTL, 2004 Roles of molecular chaperones in protein misfolding diseases. Semin Cell Dev Biol **15:** 17-29.

BECKER, J., W. WALTER, W. YAN and E. A. CRAIG, 1996 Functional interaction of cytosolic hsp70 and a DnaJ-related protein, Ydj1p, in protein translocation in vivo. Mol Cell Biol **16:** 4378-4386.

BERGER, J. R., 2003 Progressive multifocal leukoencephalopathy in acquired immunodeficiency syndrome: explaining the high incidence and disproportionate frequency of the illness relative to other immunosuppressive conditions. J Neurovirol **9 Suppl 1:** 38-41.

BLAGOSKLONNY, M. V., J. TORETSKY, S. BOHEN and L. NECKERS, 1996 Mutant conformation of p53 translated in vitro or in vivo requires functional HSP90. Proc Natl Acad Sci U S A **93:** 8379-8383.

BLAGOSKLONNY, M. V., J. TORETSKY and L. NECKERS, 1995 Geldanamycin selectively destabilizes and conformationally alters mutated p53. Oncogene **11:** 933-939.

BLOND-ELGUINDI, S., S. E. CWIRLA, W. J. DOWER, R. J. LIPSHUTZ, S. R. SPRANG *et al.*, 1993 Affinity panning of a library of peptides displayed on bacteriophages reveals the binding specificity of BiP. Cell **75:** 717-728.

BOHEN, S. P., 1995 Hsp90 mutants disrupt glucocorticoid receptor ligand binding and destabilize aporeceptor complexes. J Biol Chem **270:** 29433-29438.

BOHEN, S. P., and K. R. YAMAMOTO, 1993 Isolation of Hsp90 mutants by screening for decreased steroid receptor function. Proc Natl Acad Sci U S A **90:** 11424-11428.

BONAY, M., P. SOLER, M. RIQUET, J. P. BATTESTI, A. J. HANCE *et al.*, 1994 Expression of heat shock proteins in human lung and lung cancers. Am J Respir Cell Mol Biol **10:** 453-461.

BOOTH, D. R., M. SUNDE, V. BELLOTTI, C. V. ROBINSON, W. L. HUTCHINSON *et al.*, 1997 Instability, unfolding and aggregation of human lysozyme variants underlying amyloid fibrillogenesis. Nature **385:** 787-793.

BRADLEY, M. K., T. F. SMITH, R. H. LATHROP, D. M. LIVINGSTON and T. A. WEBSTER, 1987 Consensus topography in the ATP binding site of the simian virus 40 and polyomavirus large tumor antigens. Proc Natl Acad Sci U S A **84:** 4026-4030.

BREHMER, D., C. GASSLER, W. RIST, M. P. MAYER and B. BUKAU, 2004 Influence of GrpE on DnaK-substrate interactions. J Biol Chem **279:** 27957-27964.

BREHMER, D., S. RUDIGER, C. S. GASSLER, D. KLOSTERMEIER, L. PACKSCHIES *et al.*, 2001 Tuning of chaperone activity of Hsp70 proteins by modulation of nucleotide exchange. Nat Struct Biol **8:** 427-432.

BREWSTER, J. L., T. DE VALOIR, N. D. DWYER, E. WINTER and M. C. GUSTIN, 1993 An osmosensing signal transduction pathway in yeast. Science **259:** 1760-1763.

BRODSKY, F. M., C. Y. CHEN, C. KNUEHL, M. C. TOWLER and D. E. WAKEHAM, 2001 Biological basket weaving: formation and function of clathrin-coated vesicles. Annu Rev Cell Dev Biol **17:** 517-568.

BRODSKY, J. L., 1999 Selectivity of the molecular chaperone-specific immunosuppressive agent 15-deoxyspergualin: modulation of Hsc70 ATPase activity without compromising DnaJ chaperone interactions. Biochem Pharmacol **57:** 877-880.

BRODSKY, J. L., and G. CHIOSIS, 2006 Hsp70 molecular chaperones: emerging roles in human disease and identification of small molecule modulators. Curr Top Med Chem **6:** 1215-1225.

BRODSKY, J. L., J. GOECKELER and R. SCHEKMAN, 1995 BiP and Sec63p are required for both co- and posttranslational protein translocation into the yeast endoplasmic reticulum. Proc Natl Acad Sci U S A **92:** 9643-9646.

BRODSKY, J. L., and J. M. PIPAS, 1998 Polyomavirus T antigens: molecular chaperones for multiprotein complexes. J Virol **72:** 5329-5334.

BRODSKY, J. L., and R. SCHEKMAN, 1993 A Sec63p-BiP complex from yeast is required for protein translocation in a reconstituted proteoliposome. J Cell Biol **123:** 1355-1363.

BRODSKY, J. L., E. D. WERNER, M. E. DUBAS, J. L. GOECKELER, K. B. KRUSE *et al.*, 1999 The requirement for molecular chaperones during endoplasmic reticulum-associated protein degradation demonstrates that protein export and import are mechanistically distinct. J Biol Chem **274:** 3453-3460.

BUKAU, B., and A. L. HORWICH, 1998 The Hsp70 and Hsp60 chaperone machines. Cell **92:** 351-366.

BUSH, G. L., and D. I. MEYER, 1996 The refolding activity of the yeast heat shock proteins Ssa1 and Ssa2 defines their role in protein translocation. J Cell Biol **135:** 1229-1237.

CALDERWOOD, S. K., M. A. KHALEQUE, D. B. SAWYER and D. R. CIOCCA, 2006 Heat shock proteins in cancer: chaperones of tumorigenesis. Trends Biochem Sci **31:** 164-172.

CAMPBELL, K. S., K. P. MULLANE, I. A. AKSOY, H. STUBDAL, J. ZALVIDE *et al.*, 1997 DnaJ/hsp40 chaperone domain of SV40 large T antigen promotes efficient viral DNA replication. Genes Dev **11:** 1098-1110.

CANTALUPO, P., M. T. SAENZ-ROBLES and J. M. PIPAS, 1999 Expression of SV40 large T antigen in baculovirus systems and purification by immunoaffinity chromatography. Methods Enzymol **306:** 297-307.

CAPLAN, A. J., D. M. CYR and M. G. DOUGLAS, 1992 YDJ1p facilitates polypeptide translocation across different intracellular membranes by a conserved mechanism. Cell **71:** 1143-1155.

CAPLAN, A. J., and M. G. DOUGLAS, 1991 Characterization of YDJ1: a yeast homologue of the bacterial dnaJ protein. J Cell Biol **114:** 609-621.

CAPLAN, A. J., E. LANGLEY, E. M. WILSON and J. VIDAL, 1995 Hormone-dependent transactivation by the human androgen receptor is regulated by a dnaJ protein. J Biol Chem **270:** 5251-5257.

CARBONE, M., 2001 Introduction. Semin Cancer Biol **11:** 1-3.

CARBONE, M., J. RUDZINSKI and M. BOCCHETTA, 2003 High throughput testing of the SV40 Large T antigen binding to cellular p53 identifies putative drugs for the treatment of SV40-related cancers. Virology **315:** 409-414.

CARLSON, M., and D. BOTSTEIN, 1982 Two differentially regulated mRNAs with different 5' ends encode secreted with intracellular forms of yeast invertase. Cell **28:** 145-154.
CASTELLINO, A. M., P. CANTALUPO, I. M. MARKS, J. V. VARTIKAR, K. W. PEDEN *et al.*, 1997 trans-Dominant and non-trans-dominant mutant simian virus 40 large T antigens show distinct responses to ATP. J Virol **71:** 7549-7559.
CHANG, H. C., D. F. NATHAN and S. LINDQUIST, 1997 In vivo analysis of the Hsp90 cochaperone Sti1 (p60). Mol Cell Biol **17:** 318-325.
CHEETHAM, M. E., and A. J. CAPLAN, 1998 Structure, function and evolution of DnaJ: conservation and adaptation of chaperone function. Cell Stress Chaperones **3:** 28-36.
CHEN, J., G. J. TOBIN, J. M. PIPAS and T. VAN DYKE, 1992 T-antigen mutant activities in vivo: roles of p53 and pRB binding in tumorigenesis of the choroid plexus. Oncogene **7:** 1167-1175.
CHRISTIANSON, T. W., R. S. SIKORSKI, M. DANTE, J. H. SHERO and P. HIETER, 1992 Multifunctional yeast high-copy-number shuttle vectors. Gene **110:** 119-122.
CHROMY, L. R., A. OLTMAN, P. A. ESTES and R. L. GARCEA, 2006 Chaperone-mediated in vitro disassembly of polyoma- and papillomaviruses. J Virol **80:** 5086-5091.
CHROMY, L. R., J. M. PIPAS and R. L. GARCEA, 2003 Chaperone-mediated in vitro assembly of Polyomavirus capsids. Proc Natl Acad Sci U S A **100:** 10477-10482.
CHUNG, K. T., Y. SHEN and L. M. HENDERSHOT, 2002 BAP, a mammalian BiP-associated protein, is a nucleotide exchange factor that regulates the ATPase activity of BiP. J Biol Chem **277:** 47557-47563.
CINTRON, N. S., and D. TOFT, 2006 Defining the requirements for Hsp40 and Hsp70 in the Hsp90 chaperone pathway. J Biol Chem **281:** 26235-26244.
CIOCCA, D. R., G. M. CLARK, A. K. TANDON, S. A. FUQUA, W. J. WELCH *et al.*, 1993 Heat shock protein hsp70 in patients with axillary lymph node-negative breast cancer: prognostic implications. J Natl Cancer Inst **85:** 570-574.
COLLINS, B. S., and J. M. PIPAS, 1995 T antigens encoded by replication-defective simian virus 40 mutants dl1135 and 5080. J Biol Chem **270:** 15377-15384.
COMOLI, P., S. BINGGELI, F. GINEVRI and H. H. HIRSCH, 2006 Polyomavirus-associated nephropathy: update on BK virus-specific immunity. Transpl Infect Dis **8:** 86-94.
CONTI, E., M. UY, L. LEIGHTON, G. BLOBEL and J. KURIYAN, 1998 Crystallographic analysis of the recognition of a nuclear localization signal by the nuclear import factor karyopherin alpha. Cell **94:** 193-204.
CORY, A. H., T. C. OWEN, J. A. BARLTROP and J. G. CORY, 1991 Use of an aqueous soluble tetrazolium/formazan assay for cell growth assays in culture. Cancer Commun **3:** 207-212.
COTSIKI, M., R. L. LOCK, Y. CHENG, G. L. WILLIAMS, J. ZHAO *et al.*, 2004 Simian virus 40 large T antigen targets the spindle assembly checkpoint protein Bub1. Proc Natl Acad Sci U S A **101:** 947-952.
COUGHLAN, C. M., J. L. WALKER, J. C. COCHRAN, K. D. WITTRUP and J. L. BRODSKY, 2004 Degradation of mutated bovine pancreatic trypsin inhibitor in the yeast vacuole suggests post-endoplasmic reticulum protein quality control. J Biol Chem **279:** 15289-15297.
CRIPE, T. P., S. E. DELOS, P. A. ESTES and R. L. GARCEA, 1995 In vivo and in vitro association of hsc70 with polyomavirus capsid proteins. J Virol **69:** 7807-7813.
CYR, D. M., 1995 Cooperation of the molecular chaperone Ydj1 with specific Hsp70 homologs to suppress protein aggregation. FEBS Lett **359:** 129-132.

CYR, D. M., and M. G. DOUGLAS, 1994 Differential regulation of Hsp70 subfamilies by the eukaryotic DnaJ homologue YDJ1. J Biol Chem **269:** 9798-9804.
CYR, D. M., X. LU and M. G. DOUGLAS, 1992 Regulation of Hsp70 function by a eukaryotic DnaJ homolog. J Biol Chem **267:** 20927-20931.
DECAPRIO, J. A., J. W. LUDLOW, J. FIGGE, J. Y. SHEW, C. M. HUANG *et al.*, 1988 SV40 large tumor antigen forms a specific complex with the product of the retinoblastoma susceptibility gene. Cell **54:** 275-283.
DESHAIES, R. J., B. D. KOCH, M. WERNER-WASHBURNE, E. A. CRAIG and R. SCHEKMAN, 1988 A subfamily of stress proteins facilitates translocation of secretory and mitochondrial precursor polypeptides. Nature **332:** 800-805.
DESHAIES, R. J., S. L. SANDERS, D. A. FELDHEIM and R. SCHEKMAN, 1991 Assembly of yeast Sec proteins involved in translocation into the endoplasmic reticulum into a membrane-bound multisubunit complex. Nature **349:** 806-808.
DIAS, D. C., G. DOLIOS, R. WANG and Z. Q. PAN, 2002 CUL7: A DOC domain-containing cullin selectively binds Skp1.Fbx29 to form an SCF-like complex. Proc Natl Acad Sci U S A **99:** 16601-16606.
DITTMAR, K. D., D. R. DEMADY, L. F. STANCATO, P. KRISHNA and W. B. PRATT, 1997 Folding of the glucocorticoid receptor by the heat shock protein (hsp) 90-based chaperone machinery. The role of p23 is to stabilize receptor.hsp90 heterocomplexes formed by hsp90.p60.hsp70. J Biol Chem **272:** 21213-21220.
DITTMAR, K. D., and W. B. PRATT, 1997 Folding of the glucocorticoid receptor by the reconstituted Hsp90-based chaperone machinery. The initial hsp90.p60.hsp70-dependent step is sufficient for creating the steroid binding conformation. J Biol Chem **272:** 13047-13054.
DOERING, T. L., and R. SCHEKMAN, 1996 GPI anchor attachment is required for Gas1p transport from the endoplasmic reticulum in COP II vesicles. Embo J **15:** 182-191.
DOUGLAS, C. M., F. FOOR, J. A. MARRINAN, N. MORIN, J. B. NIELSEN *et al.*, 1994 The Saccharomyces cerevisiae FKS1 (ETG1) gene encodes an integral membrane protein which is a subunit of 1,3-beta-D-glucan synthase. Proc Natl Acad Sci U S A **91:** 12907-12911.
DRAGOVIC, Z., S. A. BROADLEY, Y. SHOMURA, A. BRACHER and F. U. HARTL, 2006a Molecular chaperones of the Hsp110 family act as nucleotide exchange factors of Hsp70s. Embo J **25:** 2519-2528.
DRAGOVIC, Z., Y. SHOMURA, N. TZVETKOV, F. U. HARTL and A. BRACHER, 2006b Fes1p acts as a nucleotide exchange factor for the ribosome-associated molecular chaperone Ssb1p. Biol Chem **387:** 1593-1600.
DUTTA, R., and M. INOUYE, 2000 GHKL, an emergent ATPase/kinase superfamily. Trends Biochem Sci **25:** 24-28.
EASH, S., K. MANLEY, M. GASPAROVIC, W. QUERBES and W. J. ATWOOD, 2006 The human polyomaviruses. Cell Mol Life Sci **63:** 865-876.
ERZBERGER, J. P., and J. M. BERGER, 2006 Evolutionary relationships and structural mechanisms of AAA+ proteins. Annu Rev Biophys Biomol Struct **35:** 93-114.
EVANS, C. G., S. WISEN and J. E. GESTWICKI, 2006 Heat shock proteins 70 and 90 inhibit early stages of amyloid beta-(1-42) aggregation in vitro. J Biol Chem **281:** 33182-33191.
FAN, C. Y., S. LEE, H. Y. REN and D. M. CYR, 2004 Exchangeable chaperone modules contribute to specification of type I and type II Hsp40 cellular function. Mol Biol Cell **15:** 761-773.

FAN, C. Y., H. Y. REN, P. LEE, A. J. CAPLAN and D. M. CYR, 2005 The type I Hsp40 zinc finger-like region is required for Hsp70 to capture non-native polypeptides from Ydj1. J Biol Chem **280:** 695-702.

FANG, Y., A. E. FLISS, J. RAO and A. J. CAPLAN, 1998 SBA1 encodes a yeast hsp90 cochaperone that is homologous to vertebrate p23 proteins. Mol Cell Biol **18:** 3727-3734.

FARASATI, N. A., R. SHAPIRO, A. VATS and P. RANDHAWA, 2005 Effect of leflunomide and cidofovir on replication of BK virus in an in vitro culture system. Transplantation **79:** 116-118.

FEWELL, S. W., B. W. DAY and J. L. BRODSKY, 2001 Identification of an inhibitor of hsc70-mediated protein translocation and ATP hydrolysis. J Biol Chem **276:** 910-914.

FEWELL, S. W., J. M. PIPAS and J. L. BRODSKY, 2002 Mutagenesis of a functional chimeric gene in yeast identifies mutations in the simian virus 40 large T antigen J domain. Proc Natl Acad Sci U S A **99:** 2002-2007.

FEWELL, S. W., C. M. SMITH, M. A. LYON, T. P. DUMITRESCU, P. WIPF *et al.*, 2004 Small molecule modulators of endogenous and co-chaperone-stimulated Hsp70 ATPase activity. J Biol Chem **279:** 51131-51140.

FIORITI, D., M. VIDETTA, M. MISCHITELLI, A. M. DEGENER, G. RUSSO *et al.*, 2005 The human polyomavirus BK: Potential role in cancer. J Cell Physiol **204:** 402-406.

FLAHERTY, K. M., C. DELUCA-FLAHERTY and D. B. MCKAY, 1990 Three-dimensional structure of the ATPase fragment of a 70K heat-shock cognate protein. Nature **346:** 623-628.

FLAHERTY, K. M., D. B. MCKAY, W. KABSCH and K. C. HOLMES, 1991 Similarity of the three-dimensional structures of actin and the ATPase fragment of a 70-kDa heat shock cognate protein. Proc Natl Acad Sci U S A **88:** 5041-5045.

FLAHERTY, K. M., S. M. WILBANKS, C. DELUCA-FLAHERTY and D. B. MCKAY, 1994 Structural basis of the 70-kilodalton heat shock cognate protein ATP hydrolytic activity. II. Structure of the active site with ADP or ATP bound to wild type and mutant ATPase fragment. J Biol Chem **269:** 12899-12907.

FLISS, A. E., S. BENZENO, J. RAO and A. J. CAPLAN, 2000 Control of estrogen receptor ligand binding by Hsp90. J Steroid Biochem Mol Biol **72:** 223-230.

FLYNN, G. C., T. G. CHAPPELL and J. E. ROTHMAN, 1989 Peptide binding and release by proteins implicated as catalysts of protein assembly. Science **245:** 385-390.

GABAI, V. L., K. MABUCHI, D. D. MOSSER and M. Y. SHERMAN, 2002 Hsp72 and stress kinase c-jun N-terminal kinase regulate the bid-dependent pathway in tumor necrosis factor-induced apoptosis. Mol Cell Biol **22:** 3415-3424.

GAI, D., R. ZHAO, D. LI, C. V. FINKIELSTEIN and X. S. CHEN, 2004 Mechanisms of conformational change for a replicative hexameric helicase of SV40 large tumor antigen. Cell **119:** 47-60.

GALL, W. E., M. A. HIGGINBOTHAM, C. CHEN, M. F. INGRAM, D. M. CYR *et al.*, 2000 The auxilin-like phosphoprotein Swa2p is required for clathrin function in yeast. Curr Biol **10:** 1349-1358.

GARDNER, S. D., A. M. FIELD, D. V. COLEMAN and B. HULME, 1971 New human papovavirus (B.K.) isolated from urine after renal transplantation. Lancet **1:** 1253-1257.

GARIMELLA, R., X. LIU, W. QIAO, X. LIANG, E. R. ZUIDERWEG *et al.*, 2006 Hsc70 contacts helix III of the J domain from polyomavirus T antigens: addressing a dilemma in the chaperone hypothesis of how they release E2F from pRb. Biochemistry **45:** 6917-6929.

GASSLER, C. S., A. BUCHBERGER, T. LAUFEN, M. P. MAYER, H. SCHRODER *et al.*, 1998 Mutations in the DnaK chaperone affecting interaction with the DnaJ cochaperone. Proc Natl Acad Sci U S A **95:** 15229-15234.

GASSLER, C. S., T. WIEDERKEHR, D. BREHMER, B. BUKAU and M. P. MAYER, 2001 Bag-1M accelerates nucleotide release for human Hsc70 and Hsp70 and can act concentration-dependent as positive and negative cofactor. J Biol Chem **276:** 32538-32544.

GAYNOR, A. M., M. D. NISSEN, D. M. WHILEY, I. M. MACKAY, S. B. LAMBERT *et al.*, 2007 Identification of a Novel Polyomavirus from Patients with Acute Respiratory Tract Infections. PLoS Pathog **3:** e64.

GENEVAUX, P., F. SCHWAGER, C. GEORGOPOULOS and W. L. KELLEY, 2002 Scanning mutagenesis identifies amino acid residues essential for the in vivo activity of the Escherichia coli DnaJ (Hsp40) J-domain. Genetics **162:** 1045-1053.

GEORGOPAPADAKOU, N. H., and T. J. WALSH, 1996 Antifungal agents: chemotherapeutic targets and immunologic strategies. Antimicrob Agents Chemother **40:** 279-291.

GIETZ, R. D., and A. SUGINO, 1988 New yeast-Escherichia coli shuttle vectors constructed with in vitro mutagenized yeast genes lacking six-base pair restriction sites. Gene **74:** 527-534.

GISLER, S. M., E. V. PIERPAOLI and P. CHRISTEN, 1998 Catapult mechanism renders the chaperone action of Hsp70 unidirectional. J Mol Biol **279:** 833-840.

GLOVER, J. R., and S. LINDQUIST, 1998 Hsp104, Hsp70, and Hsp40: a novel chaperone system that rescues previously aggregated proteins. Cell **94:** 73-82.

GOECKELER, J. L., A. STEPHENS, P. LEE, A. J. CAPLAN and J. L. BRODSKY, 2002 Overexpression of yeast Hsp110 homolog Sse1p suppresses ydj1-151 thermosensitivity and restores Hsp90-dependent activity. Mol Biol Cell **13:** 2760-2770.

GORCZYNSKA, E., D. TURKIEWICZ, K. RYBKA, J. TOPORSKI, K. KALWAK *et al.*, 2005 Incidence, clinical outcome, and management of virus-induced hemorrhagic cystitis in children and adolescents after allogeneic hematopoietic cell transplantation. Biol Blood Marrow Transplant **11:** 797-804.

GREENE, M. K., K. MASKOS and S. J. LANDRY, 1998 Role of the J-domain in the cooperation of Hsp40 with Hsp70. Proc Natl Acad Sci U S A **95:** 6108-6113.

GRENERT, J. P., B. D. JOHNSON and D. O. TOFT, 1999 The importance of ATP binding and hydrolysis by hsp90 in formation and function of protein heterocomplexes. J Biol Chem **274:** 17525-17533.

GRENERT, J. P., W. P. SULLIVAN, P. FADDEN, T. A. HAYSTEAD, J. CLARK *et al.*, 1997 The amino-terminal domain of heat shock protein 90 (hsp90) that binds geldanamycin is an ATP/ADP switch domain that regulates hsp90 conformation. J Biol Chem **272:** 23843-23850.

GUSTIN, M. C., J. ALBERTYN, M. ALEXANDER and K. DAVENPORT, 1998 MAP kinase pathways in the yeast Saccharomyces cerevisiae. Microbiol Mol Biol Rev **62:** 1264-1300.

GUTTMAN, D. S., B. A. VINATZER, S. F. SARKAR, M. V. RANALL, G. KETTLER *et al.*, 2002 A functional screen for the type III (Hrp) secretome of the plant pathogen Pseudomonas syringae. Science **295:** 1722-1726.

HA, J. H., and D. B. MCKAY, 1994 ATPase kinetics of recombinant bovine 70 kDa heat shock cognate protein and its amino-terminal ATPase domain. Biochemistry **33:** 14625-14635.

HAN, W., and P. CHRISTEN, 2003 Mechanism of the targeting action of DnaJ in the DnaK molecular chaperone system. J Biol Chem **278:** 19038-19043.

HANSEN, J. J., A. DURR, I. COURNU-REBEIX, C. GEORGOPOULOS, D. ANG *et al.*, 2002 Hereditary spastic paraplegia SPG13 is associated with a mutation in the gene encoding the mitochondrial chaperonin Hsp60. Am J Hum Genet **70:** 1328-1332.

HARLOW, E., L. V. CRAWFORD, D. C. PIM and N. M. WILLIAMSON, 1981 Monoclonal antibodies specific for simian virus 40 tumor antigens. J Virol **39:** 861-869.

HARRIS, S. F., A. K. SHIAU and D. A. AGARD, 2004 The crystal structure of the carboxy-terminal dimerization domain of htpG, the Escherichia coli Hsp90, reveals a potential substrate binding site. Structure **12:** 1087-1097.

HARRISON, C., 2003 GrpE, a nucleotide exchange factor for DnaK. Cell Stress Chaperones **8:** 218-224.

HARRISON, C. J., M. HAYER-HARTL, M. DI LIBERTO, F. HARTL and J. KURIYAN, 1997 Crystal structure of the nucleotide exchange factor GrpE bound to the ATPase domain of the molecular chaperone DnaK. Science **276:** 431-435.

HARRISON, J. C., T. R. ZYLA, E. S. BARDES and D. J. LEW, 2004 Stress-specific activation mechanisms for the "cell integrity" MAPK pathway. J Biol Chem **279:** 2616-2622.

HARTL, F. U., and M. HAYER-HARTL, 2002 Molecular chaperones in the cytosol: from nascent chain to folded protein. Science **295:** 1852-1858.

HATA, H., H. MITSUI, H. LIU, Y. BAI, C. L. DENIS *et al.*, 1998 Dhh1p, a putative RNA helicase, associates with the general transcription factors Pop2p and Ccr4p from Saccharomyces cerevisiae. Genetics **148:** 571-579.

HEINISCH, J. J., A. LORBERG, H. P. SCHMITZ and J. J. JACOBY, 1999 The protein kinase C-mediated MAP kinase pathway involved in the maintenance of cellular integrity in Saccharomyces cerevisiae. Mol Microbiol **32:** 671-680.

HENNESSY, F., M. E. CHEETHAM, H. W. DIRR and G. L. BLATCH, 2000 Analysis of the levels of conservation of the J domain among the various types of DnaJ-like proteins. Cell Stress Chaperones **5:** 347-358.

HENNESSY, F., W. S. NICOLL, R. ZIMMERMANN, M. E. CHEETHAM and G. L. BLATCH, 2005 Not all J domains are created equal: implications for the specificity of Hsp40-Hsp70 interactions. Protein Sci **14:** 1697-1709.

HERNANDEZ, M. P., A. CHADLI and D. O. TOFT, 2002 HSP40 binding is the first step in the HSP90 chaperoning pathway for the progesterone receptor. J Biol Chem **277:** 11873-11881.

HILL, J. E., A. M. MYERS, T. J. KOERNER and A. TZAGOLOFF, 1986 Yeast/E. coli shuttle vectors with multiple unique restriction sites. Yeast **2:** 163-167.

HILLEMAN, M. R., 1998 Discovery of simian virus 40 (SV40) and its relationship to poliomyelitis virus vaccines. Dev Biol Stand **94:** 183-190.

HJORTH-SORENSEN, B., E. R. HOFFMANN, N. M. LISSIN, A. K. SEWELL and B. K. JAKOBSEN, 2001 Activation of heat shock transcription factor in yeast is not influenced by the levels of expression of heat shock proteins. Mol Microbiol **39:** 914-923.

HO, A. K., G. A. RACZNIAK, E. B. IVES and S. R. WENTE, 1998 The integral membrane protein snl1p is genetically linked to yeast nuclear pore complex function. Mol Biol Cell **9:** 355-373.

HOHFELD, J., and S. JENTSCH, 1997 GrpE-like regulation of the hsc70 chaperone by the anti-apoptotic protein BAG-1. Embo J **16:** 6209-6216.

HUBER, A. H., W. J. NELSON and W. I. WEIS, 1997 Three-dimensional structure of the armadillo repeat region of beta-catenin. Cell **90:** 871-882.

HUGHES, S. E., and S. A. GRUBER, 1996 New immunosuppressive drugs in organ transplantation. J Clin Pharmacol **36:** 1081-1092.
HUNTER, T., and R. Y. C. POON, 1997 Cdc37: a protein kinase chaperone? Trends Cell Biol. **7:** 157-161.
HYMES, L. C., and B. L. WARSHAW, 2006 Polyomavirus (BK) in pediatric renal transplants: evaluation of viremic patients with and without BK associated nephritis. Pediatr Transplant **10:** 920-922.
IBARAKI, N., S. C. CHEN, L. R. LIN, H. OKAMOTO, J. M. PIPAS *et al.*, 1998 Human lens epithelial cell line. Exp Eye Res **67:** 577-585.
IGUAL, J. C., A. L. JOHNSON and L. H. JOHNSTON, 1996 Coordinated regulation of gene expression by the cell cycle transcription factor Swi4 and the protein kinase C MAP kinase pathway for yeast cell integrity. Embo J **15:** 5001-5013.
ISAACS, J. S., W. XU and L. NECKERS, 2003 Heat shock protein 90 as a molecular target for cancer therapeutics. Cancer Cell **3:** 213-217.
ISHIDA, H., N. MIYAMOTO, H. SHIRAKAWA, T. SHIMIZU, T. TOKUMOTO *et al.*, 2007 Evaluation of Immunosuppressive Regimens in ABO-Incompatible Living Kidney Transplantation-Single Center Analysis. Am J Transplant.
ITO, H., Y. FUKUDA, K. MURATA and A. KIMURA, 1983 Transformation of intact yeast cells treated with alkali cations. J Bacteriol **153:** 163-168.
ITO, T., T. CHIBA, R. OZAWA, M. YOSHIDA, M. HATTORI *et al.*, 2001 A comprehensive two-hybrid analysis to explore the yeast protein interactome. Proc Natl Acad Sci U S A **98:** 4569-4574.
JELENSKA, J., N. YAO, B. A. VINATZER, C. M. WRIGHT, J. L. BRODSKY *et al.*, 2007 A J Domain Virulence Effector of Pseudomonas syringae Remodels Host Chloroplasts and Suppresses Defenses. Curr Biol **17:** 499-508.
JIANG, J., K. PRASAD, E. M. LAFER and R. SOUSA, 2005 Structural basis of interdomain communication in the Hsc70 chaperone. Mol Cell **20:** 513-524.
JIANG, R., B. GAO, K. PRASAD, L. E. GREENE and E. EISENBERG, 2000 Hsc70 chaperones clathrin and primes it to interact with vesicle membranes. J Biol Chem **275:** 8439-8447.
JOHNE, R., D. ENDERLEIN, H. NIEPER and H. MULLER, 2005 Novel polyomavirus detected in the feces of a chimpanzee by nested broad-spectrum PCR. J Virol **79:** 3883-3887.
JOHNE, R., W. WITTIG, D. FERNANDEZ-DE-LUCO, U. HOFLE and H. MULLER, 2006 Characterization of two novel polyomaviruses of birds by using multiply primed rolling-circle amplification of their genomes. J Virol **80:** 3523-3531.
JOHNSON, B. D., R. J. SCHUMACHER, E. D. ROSS and D. O. TOFT, 1998 Hop modulates Hsp70/Hsp90 interactions in protein folding. J Biol Chem **273:** 3679-3686.
JOHNSON, J. L., and E. A. CRAIG, 2001 An essential role for the substrate-binding region of Hsp40s in Saccharomyces cerevisiae. J Cell Biol **152:** 851-856.
JOLLY, C., and R. I. MORIMOTO, 2000 Role of the heat shock response and molecular chaperones in oncogenesis and cell death. J Natl Cancer Inst **92:** 1564-1572.
JOO, W. S., H. Y. KIM, J. D. PURVIANCE, K. R. SREEKUMAR and P. A. BULLOCK, 1998 Assembly of T-antigen double hexamers on the simian virus 40 core origin requires only a subset of the available binding sites. Mol Cell Biol **18:** 2677-2687.
JOO, W. S., X. LUO, D. DENIS, H. Y. KIM, G. J. RAINEY *et al.*, 1997 Purification of the simian virus 40 (SV40) T antigen DNA-binding domain and characterization of its interactions with the SV40 origin. J Virol **71:** 3972-3985.

JORDAN, R., and R. MCMACKEN, 1995 Modulation of the ATPase activity of the molecular chaperone DnaK by peptides and the DnaJ and GrpE heat shock proteins. J Biol Chem **270:** 4563-4569.
JUNG, U. S., and D. E. LEVIN, 1999 Genome-wide analysis of gene expression regulated by the yeast cell wall integrity signalling pathway. Mol Microbiol **34:** 1049-1057.
KABANI, M., J. M. BECKERICH and J. L. BRODSKY, 2002a Nucleotide exchange factor for the yeast Hsp70 molecular chaperone Ssa1p. Mol Cell Biol **22:** 4677-4689.
KABANI, M., C. MCLELLAN, D. A. RAYNES, V. GUERRIERO and J. L. BRODSKY, 2002b HspBP1, a homologue of the yeast Fes1 and Sls1 proteins, is an Hsc70 nucleotide exchange factor. FEBS Lett **531:** 339-342.
KAISER, C. A., and R. SCHEKMAN, 1990 Distinct sets of SEC genes govern transport vesicle formation and fusion early in the secretory pathway. Cell **61:** 723-733.
KALDERON, D., B. L. ROBERTS, W. D. RICHARDSON and A. E. SMITH, 1984 A short amino acid sequence able to specify nuclear location. Cell **39:** 499-509.
KASPER, J. S., H. KUWABARA, T. ARAI, S. H. ALI and J. A. DECAPRIO, 2005 Simian virus 40 large T antigen's association with the CUL7 SCF complex contributes to cellular transformation. J Virol **79:** 11685-11692.
KELLEY, W. L., and C. GEORGOPOULOS, 1997 The T/t common exon of simian virus 40, JC, and BK polyomavirus T antigens can functionally replace the J-domain of the Escherichia coli DnaJ molecular chaperone. Proc Natl Acad Sci U S A **94:** 3679-3684.
KETELA, T., R. GREEN and H. BUSSEY, 1999 Saccharomyces cerevisiae mid2p is a potential cell wall stress sensor and upstream activator of the PKC1-MPK1 cell integrity pathway. J Bacteriol **181:** 3330-3340.
KHALILI, K., L. DEL VALLE, J. OTTE, M. WEAVER and J. GORDON, 2003 Human neurotropic polyomavirus, JCV, and its role in carcinogenesis. Oncogene **22:** 5181-5191.
KIERSTEAD, T. D., and M. J. TEVETHIA, 1993 Association of p53 binding and immortalization of primary C57BL/6 mouse embryo fibroblasts by using simian virus 40 T-antigen mutants bearing internal overlapping deletion mutations. J Virol **67:** 1817-1829.
KIM, H. Y., B. Y. AHN and Y. CHO, 2001 Structural basis for the inactivation of retinoblastoma tumor suppressor by SV40 large T antigen. Embo J **20:** 295-304.
KIM, K. K., T. J. JANG and J. R. KIM, 1998a HSP70 and ER expression in cervical intraepithelial neoplasia and cervical cancer. J Korean Med Sci **13:** 383-388.
KIM, S., B. SCHILKE, E. A. CRAIG and A. L. HORWICH, 1998b Folding in vivo of a newly translated yeast cytosolic enzyme is mediated by the SSA class of cytosolic yeast Hsp70 proteins. Proc Natl Acad Sci U S A **95:** 12860-12865.
KIMURA, Y., I. YAHARA and S. LINDQUIST, 1995 Role of the protein chaperone YDJ1 in establishing Hsp90-mediated signal transduction pathways. Science **268:** 1362-1365.
KING, C., E. EISENBERG and L. E. GREENE, 1999 Interaction between Hsc70 and DnaJ homologues: relationship between Hsc70 polymerization and ATPase activity. Biochemistry **38:** 12452-12459.
KNOWLES, W. A., and K. SASNAUSKAS, 2003 Comparison of cell culture-grown JC virus (primary human fetal glial cells and the JCI cell line) and recombinant JCV VP1 as antigen for the detection of anti-JCV antibody by haemagglutination inhibition. J Virol Methods **109:** 47-54.
KOHRMAN, D. C., and M. J. IMPERIALE, 1992 Simian virus 40 large T antigen stably complexes with a 185-kilodalton host protein. J Virol **66:** 1752-1760.

KOMAROVA, E. Y., E. A. AFANASYEVA, M. M. BULATOVA, M. E. CHEETHAM, B. A. MARGULIS *et al.*, 2004 Downstream caspases are novel targets for the antiapoptotic activity of the molecular chaperone hsp70. Cell Stress Chaperones **9:** 265-275.

LACHMANN, S., J. ROMMELEARE and J. P. NUESCH, 2003 Novel PKCeta is required to activate replicative functions of the major nonstructural protein NS1 of minute virus of mice. J Virol **77:** 8048-8060.

LANFORD, R. E., P. KANDA and R. C. KENNEDY, 1986 Induction of nuclear transport with a synthetic peptide homologous to the SV40 T antigen transport signal. Cell **46:** 575-582.

LANGER, T., C. LU, H. ECHOLS, J. FLANAGAN, M. K. HAYER *et al.*, 1992 Successive action of DnaK, DnaJ and GroEL along the pathway of chaperone-mediated protein folding. Nature **356:** 683-689.

LAUFEN, T., M. P. MAYER, C. BEISEL, D. KLOSTERMEIER, A. MOGK *et al.*, 1999 Mechanism of regulation of hsp70 chaperones by DnaJ cochaperones. Proc Natl Acad Sci U S A **96:** 5452-5457.

LEE, B. N., and E. A. ELION, 1999 The MAPKKK Ste11 regulates vegetative growth through a kinase cascade of shared signaling components. Proc Natl Acad Sci U S A **96:** 12679-12684.

LEE, H. C., T. HON and L. ZHANG, 2002 The molecular chaperone Hsp90 mediates heme activation of the yeast transcriptional activator Hap1. J Biol Chem **277:** 7430-7437.

LEE, K. S., and D. E. LEVIN, 1992 Dominant mutations in a gene encoding a putative protein kinase (BCK1) bypass the requirement for a Saccharomyces cerevisiae protein kinase C homolog. Mol Cell Biol **12:** 172-182.

LESAGE, G., and H. BUSSEY, 2006 Cell wall assembly in Saccharomyces cerevisiae. Microbiol Mol Biol Rev **70:** 317-343.

LEVIN, D. E., 2005 Cell wall integrity signaling in Saccharomyces cerevisiae. Microbiol Mol Biol Rev **69:** 262-291.

LEVIN, D. E., and E. BARTLETT-HEUBUSCH, 1992 Mutants in the S. cerevisiae PKC1 gene display a cell cycle-specific osmotic stability defect. J Cell Biol **116:** 1221-1229.

LI, D., R. ZHAO, W. LILYESTROM, D. GAI, R. ZHANG *et al.*, 2003a Structure of the replicative helicase of the oncoprotein SV40 large tumour antigen. Nature **423:** 512-518.

LI, J., X. QIAN and B. SHA, 2003b The crystal structure of the yeast Hsp40 Ydj1 complexed with its peptide substrate. Structure **11:** 1475-1483.

LIBEREK, K., J. MARSZALEK, D. ANG, C. GEORGOPOULOS and M. ZYLICZ, 1991 Escherichia coli DnaJ and GrpE heat shock proteins jointly stimulate ATPase activity of DnaK. Proc Natl Acad Sci U S A **88:** 2874-2878.

LIN, J. Y., and J. A. DECAPRIO, 2003 SV40 large T antigen promotes dephosphorylation of p130. J Biol Chem **278:** 46482-46487.

LIU, X. D., K. A. MORANO and D. J. THIELE, 1999 The yeast Hsp110 family member, Sse1, is an Hsp90 cochaperone. J Biol Chem **274:** 26654-26660.

LOEBER, G., R. PARSONS and P. TEGTMEYER, 1989 The zinc finger region of simian virus 40 large T antigen. J Virol **63:** 94-100.

LOMMEL, M., M. BAGNAT and S. STRAHL, 2004 Aberrant processing of the WSC family and Mid2p cell surface sensors results in cell death of Saccharomyces cerevisiae O-mannosylation mutants. Mol Cell Biol **24:** 46-57.

LU, Z., and D. M. CYR, 1998a The conserved carboxyl terminus and zinc finger-like domain of the co-chaperone Ydj1 assist Hsp70 in protein folding. J Biol Chem **273:** 5970-5978.

LU, Z., and D. M. CYR, 1998b Protein folding activity of Hsp70 is modified differentially by the hsp40 co-chaperones Sis1 and Ydj1. J Biol Chem **273:** 27824-27830.
LUSSIER, M., A. M. WHITE, J. SHERATON, T. DI PAOLO, J. TREADWELL *et al.*, 1997 Large scale identification of genes involved in cell surface biosynthesis and architecture in Saccharomyces cerevisiae. Genetics **147:** 435-450.
MACHI, K., M. AZUMA, K. IGARASHI, T. MATSUMOTO, H. FUKUDA *et al.*, 2004 Rot1p of Saccharomyces cerevisiae is a putative membrane protein required for normal levels of the cell wall 1,6-beta-glucan. Microbiology **150:** 3163-3173.
MADDEN, K., Y. J. SHEU, K. BAETZ, B. ANDREWS and M. SNYDER, 1997 SBF cell cycle regulator as a target of the yeast PKC-MAP kinase pathway. Science **275:** 1781-1784.
MAGER, W. H., and M. SIDERIUS, 2002 Novel insights into the osmotic stress response of yeast. FEMS Yeast Res **2:** 251-257.
MAIORANO, D., M. LUTZMANN and M. MECHALI, 2006 MCM proteins and DNA replication. Curr Opin Cell Biol **18:** 130-136.
MALLY, A., and S. N. WITT, 2001 GrpE accelerates peptide binding and release from the high affinity state of DnaK. Nat Struct Biol **8:** 254-257.
MANNING, B. D., R. PADMANABHA and M. SNYDER, 1997 The Rho-GEF Rom2p localizes to sites of polarized cell growth and participates in cytoskeletal functions in Saccharomyces cerevisiae. Mol Biol Cell **8:** 1829-1844.
MARCOUX, N., S. CLOUTIER, E. ZAKRZEWSKA, P. M. CHAREST, Y. BOURBONNAIS *et al.*, 2000 Suppression of the profilin-deficient phenotype by the RHO2 signaling pathway in Saccharomyces cerevisiae. Genetics **156:** 579-592.
MASTRANGELO, I. A., P. V. HOUGH, J. S. WALL, M. DODSON, F. B. DEAN *et al.*, 1989 ATP-dependent assembly of double hexamers of SV40 T antigen at the viral origin of DNA replication. Nature **338:** 658-662.
MAYER, M. P., and B. BUKAU, 2005 Hsp70 chaperones: cellular functions and molecular mechanism. Cell Mol Life Sci **62:** 670-684.
MAYER, M. P., H. SCHRODER, S. RUDIGER, K. PAAL, T. LAUFEN *et al.*, 2000 Multistep mechanism of substrate binding determines chaperone activity of Hsp70. Nat Struct Biol **7:** 586-593.
MAZUR, P., N. MORIN, W. BAGINSKY, M. EL-SHERBEINI, J. A. CLEMAS *et al.*, 1995 Differential expression and function of two homologous subunits of yeast 1,3-beta-D-glucan synthase. Mol Cell Biol **15:** 5671-5681.
MCCARTY, J. S., A. BUCHBERGER, J. REINSTEIN and B. BUKAU, 1995 The role of ATP in the functional cycle of the DnaK chaperone system. J Mol Biol **249:** 126-137.
MCCLELLAN, A. J., and J. L. BRODSKY, 2000 Mutation of the ATP-binding pocket of SSA1 indicates that a functional interaction between Ssa1p and Ydj1p is required for post-translational translocation into the yeast endoplasmic reticulum. Genetics **156:** 501-512.
MCCLELLAN, A. J., J. B. ENDRES, J. P. VOGEL, D. PALAZZI, M. D. ROSE *et al.*, 1998 Specific molecular chaperone interactions and an ATP-dependent conformational change are required during posttranslational protein translocation into the yeast ER. Mol Biol Cell **9:** 3533-3545.
MELENDEZ, K., E. S. WALLEN, B. S. EDWARDS, C. D. MOBARAK, D. G. BEAR *et al.*, 2006 Heat shock protein 70 and glycoprotein 96 are differentially expressed on the surface of malignant and nonmalignant breast cells. Cell Stress Chaperones **11:** 334-342.

MEYER, P., C. PRODROMOU, B. HU, C. VAUGHAN, S. M. ROE *et al.*, 2003 Structural and functional analysis of the middle segment of hsp90: implications for ATP hydrolysis and client protein and cochaperone interactions. Mol Cell **11:** 647-658.

MILLSON, S. H., A. W. TRUMAN, V. KING, C. PRODROMOU, L. H. PEARL *et al.*, 2005 A two-hybrid screen of the yeast proteome for Hsp90 interactors uncovers a novel Hsp90 chaperone requirement in the activity of a stress-activated mitogen-activated protein kinase, Slt2p (Mpk1p). Eukaryot Cell **4:** 849-860.

MINGUEZ, J. M., S. Y. KIM, K. A. GIULIANO, R. BALACHANDRAN, C. MADIRAJU *et al.*, 2003 Synthesis and biological assessment of simplified analogues of the potent microtubule stabilizer (+)-discodermolide. Bioorg Med Chem **11:** 3335-3357.

MIYATA, Y., and I. YAHARA, 2000 p53-independent association between SV40 large T antigen and the major cytosolic heat shock protein, HSP90. Oncogene **19:** 1477-1484.

MONTIJN, R. C., E. VINK, W. H. MULLER, A. J. VERKLEIJ, H. VAN DEN ENDE *et al.*, 1999 Localization of synthesis of beta1,6-glucan in Saccharomyces cerevisiae. J Bacteriol **181:** 7414-7420.

MUCHOWSKI, P. J., G. SCHAFFAR, A. SITTLER, E. E. WANKER, M. K. HAYER-HARTL *et al.*, 2000 Hsp70 and hsp40 chaperones can inhibit self-assembly of polyglutamine proteins into amyloid-like fibrils. Proc Natl Acad Sci U S A **97:** 7841-7846.

MUMBERG, D., R. MULLER and M. FUNK, 1995 Yeast vectors for the controlled expression of heterologous proteins in different genetic backgrounds. Gene **156:** 119-122.

MURPHY, P. J., Y. MORISHIMA, H. CHEN, M. D. GALIGNIANA, J. F. MANSFIELD *et al.*, 2003 Visualization and mechanism of assembly of a glucocorticoid receptor.Hsp70 complex that is primed for subsequent Hsp90-dependent opening of the steroid binding cleft. J Biol Chem **278:** 34764-34773.

MYUNG, J. K., L. AFJEHI-SADAT, M. FELIZARDO-CABATIC, I. SLAVC and G. LUBEC, 2004 Expressional patterns of chaperones in ten human tumor cell lines. Proteome Sci **2:** 8.

NADEAU, K., S. G. NADLER, M. SAULNIER, M. A. TEPPER and C. T. WALSH, 1994 Quantitation of the interaction of the immunosuppressant deoxyspergualin and analogs with Hsc70 and Hsp90. Biochemistry **33:** 2561-2567.

NADLER, S. G., M. A. TEPPER, B. SCHACTER and C. E. MAZZUCCO, 1992 Interaction of the immunosuppressant deoxyspergualin with a member of the Hsp70 family of heat shock proteins. Science **258:** 484-486.

NATHAN, D. F., and S. LINDQUIST, 1995 Mutational analysis of Hsp90 function: interactions with a steroid receptor and a protein kinase. Mol Cell Biol **15:** 3917-3925.

NECKERS, L., 2002 Hsp90 inhibitors as novel cancer chemotherapeutic agents. Trends Mol Med **8:** S55-61.

NEIMAN, A. M., V. MHAISKAR, V. MANUS, F. GALIBERT and N. DEAN, 1997 Saccharomyces cerevisiae HOC1, a suppressor of pkc1, encodes a putative glycosyltransferase. Genetics **145:** 637-645.

NGUYEN, T. H., G. H. FLEET and P. L. ROGERS, 1998 Composition of the cell walls of several yeast species. Appl Microbiol Biotechnol **50:** 206-212.

NICOLET, C. M., and E. A. CRAIG, 1989 Isolation and characterization of STI1, a stress-inducible gene from Saccharomyces cerevisiae. Mol Cell Biol **9:** 3638-3646.

NISHIKAWA, S. I., S. W. FEWELL, Y. KATO, J. L. BRODSKY and T. ENDO, 2001 Molecular chaperones in the yeast endoplasmic reticulum maintain the solubility of proteins for retrotranslocation and degradation. J Cell Biol **153:** 1061-1070.

NOMOTO, S., Y. WATANABE, J. NINOMIYA-TSUJI, L. X. YANG, Y. NAGAI *et al.*, 1997 Functional analyses of mammalian protein kinase C isozymes in budding yeast and mammalian fibroblasts. Genes Cells **2:** 601-614.

NOMURA, K., M. MELOTTO and S. Y. HE, 2005 Suppression of host defense in compatible plant-Pseudomonas syringae interactions. Curr Opin Plant Biol **8:** 361-368.

NYLANDSTED, J., M. ROHDE, K. BRAND, L. BASTHOLM, F. ELLING *et al.*, 2000 Selective depletion of heat shock protein 70 (Hsp70) activates a tumor-specific death program that is independent of caspases and bypasses Bcl-2. Proc Natl Acad Sci U S A **97:** 7871-7876.

O'ROURKE, S. M., and I. HERSKOWITZ, 1998 The Hog1 MAPK prevents cross talk between the HOG and pheromone response MAPK pathways in Saccharomyces cerevisiae. Genes Dev **12:** 2874-2886.

OBERMANN, W. M., H. SONDERMANN, A. A. RUSSO, N. P. PAVLETICH and F. U. HARTL, 1998 In vivo function of Hsp90 is dependent on ATP binding and ATP hydrolysis. J Cell Biol **143:** 901-910.

OCHEL, H. J., K. EICHHORN and G. GADEMANN, 2001 Geldanamycin: the prototype of a class of antitumor drugs targeting the heat shock protein 90 family of molecular chaperones. Cell Stress Chaperones **6:** 105-112.

OKA, M., M. NAKAI, T. ENDO, C. R. LIM, Y. KIMATA *et al.*, 1998 Loss of Hsp70-Hsp40 chaperone activity causes abnormal nuclear distribution and aberrant microtubule formation in M-phase of Saccharomyces cerevisiae. J Biol Chem **273:** 29727-29737.

OSUMI, M., 1998 The ultrastructure of yeast: cell wall structure and formation. Micron **29:** 207-233.

OTT, R. D., Y. WANG and E. FANNING, 2002 Mutational analysis of simian virus 40 T-antigen primosome activities in viral DNA replication. J Virol **76:** 5121-5130.

PACKSCHIES, L., H. THEYSSEN, A. BUCHBERGER, B. BUKAU, R. S. GOODY *et al.*, 1997 GrpE accelerates nucleotide exchange of the molecular chaperone DnaK with an associative displacement mechanism. Biochemistry **36:** 3417-3422.

PADGETT, B. L., D. L. WALKER, G. M. ZURHEIN, R. J. ECKROADE and B. H. DESSEL, 1971 Cultivation of papova-like virus from human brain with progressive multifocal leucoencephalopathy. Lancet **1:** 1257-1260.

PAGE, B. D., and M. SNYDER, 1992 CIK1: a developmentally regulated spindle pole body-associated protein important for microtubule functions in Saccharomyces cerevisiae. Genes Dev **6:** 1414-1429.

PANARETOU, B., C. PRODROMOU, S. M. ROE, R. O'BRIEN, J. E. LADBURY *et al.*, 1998 ATP binding and hydrolysis are essential to the function of the Hsp90 molecular chaperone in vivo. Embo J **17:** 4829-4836.

PARSONS, R. E., J. E. STENGER, S. RAY, R. WELKER, M. E. ANDERSON *et al.*, 1991 Cooperative assembly of simian virus 40 T-antigen hexamers on functional halves of the replication origin. J Virol **65:** 2798-2806.

PEARL, L. H., and C. PRODROMOU, 2006 Structure and mechanism of the Hsp90 molecular chaperone machinery. Annu Rev Biochem **75:** 271-294.

PEDEN, K. W., and J. M. PIPAS, 1992 Simian virus 40 mutants with amino-acid substitutions near the amino terminus of large T antigen. Virus Genes **6:** 107-118.

PHILIP, B., and D. E. LEVIN, 2001 Wsc1 and Mid2 are cell surface sensors for cell wall integrity signaling that act through Rom2, a guanine nucleotide exchange factor for Rho1. Mol Cell Biol **21:** 271-280.

PICARD, D., B. KHURSHEED, M. J. GARABEDIAN, M. G. FORTIN, S. LINDQUIST *et al.*, 1990 Reduced levels of hsp90 compromise steroid receptor action in vivo. Nature **348:** 166-168.

PIPAS, J. M., 1985 Mutations near the carboxyl terminus of the simian virus 40 large tumor antigen alter viral host range. J Virol **54:** 569-575.

PIPAS, J. M., 1992 Common and unique features of T antigens encoded by the polyomavirus group. J Virol **66:** 3979-3985.

PIPAS, J. M., K. W. PEDEN and D. NATHANS, 1983 Mutational analysis of simian virus 40 T antigen: isolation and characterization of mutants with deletions in the T-antigen gene. Mol Cell Biol **3:** 203-213.

PISHVAEE, B., G. COSTAGUTA, B. G. YEUNG, S. RYAZANTSEV, T. GREENER *et al.*, 2000 A yeast DNA J protein required for uncoating of clathrin-coated vesicles in vivo. Nat Cell Biol **2:** 958-963.

POULIN, D. L., and J. A. DECAPRIO, 2006a The carboxyl-terminal domain of large T antigen rescues SV40 host range activity in trans independent of acetylation. Virology **349:** 212-221.

POULIN, D. L., and J. A. DECAPRIO, 2006b Is there a role for SV40 in human cancer? J Clin Oncol **24:** 4356-4365.

PRATT, W. B., and D. O. TOFT, 2003 Regulation of signaling protein function and trafficking by the hsp90/hsp70-based chaperone machinery. Exp Biol Med (Maywood) **228:** 111-133.

PRODROMOU, C., B. PANARETOU, S. CHOHAN, G. SILIGARDI, R. O'BRIEN *et al.*, 2000 The ATPase cycle of Hsp90 drives a molecular 'clamp' via transient dimerization of the N-terminal domains. Embo J **19:** 4383-4392.

PRODROMOU, C., S. M. ROE, R. O'BRIEN, J. E. LADBURY, P. W. PIPER *et al.*, 1997 Identification and structural characterization of the ATP/ADP-binding site in the Hsp90 molecular chaperone. Cell **90:** 65-75.

PROFT, M., A. PASCUAL-AHUIR, E. DE NADAL, J. ARINO, R. SERRANO *et al.*, 2001 Regulation of the Sko1 transcriptional repressor by the Hog1 MAP kinase in response to osmotic stress. Embo J **20:** 1123-1133.

PROFT, M., and K. STRUHL, 2002 Hog1 kinase converts the Sko1-Cyc8-Tup1 repressor complex into an activator that recruits SAGA and SWI/SNF in response to osmotic stress. Mol Cell **9:** 1307-1317.

QADOTA, H., C. P. PYTHON, S. B. INOUE, M. ARISAWA, Y. ANRAKU *et al.*, 1996 Identification of yeast Rho1p GTPase as a regulatory subunit of 1,3-beta-glucan synthase. Science **272:** 279-281.

QIU, X. B., Y. M. SHAO, S. MIAO and L. WANG, 2006 The diversity of the DnaJ/Hsp40 family, the crucial partners for Hsp70 chaperones. Cell Mol Life Sci **63:** 2560-2570.

QUARTIN, R. S., C. N. COLE, J. M. PIPAS and A. J. LEVINE, 1994 The amino-terminal functions of the simian virus 40 large T antigen are required to overcome wild-type p53-mediated growth arrest of cells. J Virol **68:** 1334-1341.

RAJAVEL, M., B. PHILIP, B. M. BUEHRER, B. ERREDE and D. E. LEVIN, 1999 Mid2 is a putative sensor for cell integrity signaling in Saccharomyces cerevisiae. Mol Cell Biol **19:** 3969-3976.

RALHAN, R., and J. KAUR, 1995 Differential expression of Mr 70,000 heat shock protein in normal, premalignant, and malignant human uterine cervix. Clin Cancer Res **1:** 1217-1222.

RAMAN, B., T. BAN, M. SAKAI, S. Y. PASTA, T. RAMAKRISHNA *et al.*, 2005 AlphaB-crystallin, a small heat-shock protein, prevents the amyloid fibril growth of an amyloid beta-peptide and beta2-microglobulin. Biochem J **392:** 573-581.

RASHMI, R., S. KUMAR and D. KARUNAGARAN, 2004 Ectopic expression of Hsp70 confers resistance and silencing its expression sensitizes human colon cancer cells to curcumin-induced apoptosis. Carcinogenesis **25:** 179-187.

RAVIOL, H., H. SADLISH, F. RODRIGUEZ, M. P. MAYER and B. BUKAU, 2006 Chaperone network in the yeast cytosol: Hsp110 is revealed as an Hsp70 nucleotide exchange factor. Embo J **25:** 2510-2518.

RAYNES, D. A., and V. GUERRIERO, JR., 1998 Inhibition of Hsp70 ATPase activity and protein renaturation by a novel Hsp70-binding protein. J Biol Chem **273:** 32883-32888.

REVINGTON, M., T. M. HOLDER and E. R. ZUIDERWEG, 2004 NMR study of nucleotide-induced changes in the nucleotide binding domain of Thermus thermophilus Hsp70 chaperone DnaK: implications for the allosteric mechanism. J Biol Chem **279:** 33958-33967.

REVINGTON, M., Y. ZHANG, G. N. YIP, A. V. KUROCHKIN and E. R. ZUIDERWEG, 2005 NMR investigations of allosteric processes in a two-domain Thermus thermophilus Hsp70 molecular chaperone. J Mol Biol **349:** 163-183.

RICHTER, K., P. MUSCHLER, O. HAINZL, J. REINSTEIN and J. BUCHNER, 2003 Sti1 is a non-competitive inhibitor of the Hsp90 ATPase. Binding prevents the N-terminal dimerization reaction during the atpase cycle. J Biol Chem **278:** 10328-10333.

RODRIGUEZ-NAVARRO, S., T. FISCHER, M. J. LUO, O. ANTUNEZ, S. BRETTSCHNEIDER *et al.*, 2004 Sus1, a functional component of the SAGA histone acetylase complex and the nuclear pore-associated mRNA export machinery. Cell **116:** 75-86.

ROELANTS, F. M., P. D. TORRANCE and J. THORNER, 2004 Differential roles of PDK1- and PDK2-phosphorylation sites in the yeast AGC kinases Ypk1, Pkc1 and Sch9. Microbiology **150:** 3289-3304.

ROEMER, T., S. DELANEY and H. BUSSEY, 1993 SKN1 and KRE6 define a pair of functional homologs encoding putative membrane proteins involved in beta-glucan synthesis. Mol Cell Biol **13:** 4039-4048.

ROEMER, T., G. PARAVICINI, M. A. PAYTON and H. BUSSEY, 1994 Characterization of the yeast (1-->6)-beta-glucan biosynthetic components, Kre6p and Skn1p, and genetic interactions between the PKC1 pathway and extracellular matrix assembly. J Cell Biol **127:** 567-579.

ROTHBLATT, J. A., R. J. DESHAIES, S. L. SANDERS, G. DAUM and R. SCHEKMAN, 1989 Multiple genes are required for proper insertion of secretory proteins into the endoplasmic reticulum in yeast. J Cell Biol **109:** 2641-2652.

RUDIGER, S., L. GERMEROTH, J. SCHNEIDER-MERGENER and B. BUKAU, 1997 Substrate specificity of the DnaK chaperone determined by screening cellulose-bound peptide libraries. Embo J **16:** 1501-1507.

RUDIGER, S., J. SCHNEIDER-MERGENER and B. BUKAU, 2001 Its substrate specificity characterizes the DnaJ co-chaperone as a scanning factor for the DnaK chaperone. Embo J **20:** 1042-1050.

RUSHTON, J. J., D. JIANG, A. SRINIVASAN, J. M. PIPAS and P. D. ROBBINS, 1997 Simian virus 40 T antigen can regulate p53-mediated transcription independent of binding p53. J Virol **71:** 5620-5623.

RUSSELL, R., A. WALI KARZAI, A. F. MEHL and R. MCMACKEN, 1999 DnaJ dramatically stimulates ATP hydrolysis by DnaK: insight into targeting of Hsp70 proteins to polypeptide substrates. Biochemistry **38:** 4165-4176.

SAITO, H., and H. UCHIDA, 1977 Initiation of the DNA replication of bacteriophage lambda in Escherichia coli K12. J Mol Biol **113:** 1-25.

SANCHATJATE, S., and R. SCHEKMAN, 2006 Chs5/6 Complex: A Multi-Protein Complex That Interacts with and Conveys Chitin Synthase III from the Trans-Golgi Network to the Cell Surface. Mol Biol Cell.

SANTOS, B., and M. SNYDER, 1997 Targeting of chitin synthase 3 to polarized growth sites in yeast requires Chs5p and Myo2p. J Cell Biol **136:** 95-110.

SAWAI, E. T., and J. S. BUTEL, 1989 Association of a cellular heat shock protein with simian virus 40 large T antigen in transformed cells. J Virol **63:** 3961-3973.

SCHEUFLER, C., A. BRINKER, G. BOURENKOV, S. PEGORARO, L. MORODER *et al.*, 2000 Structure of TPR domain-peptide complexes: critical elements in the assembly of the Hsp70-Hsp90 multichaperone machine. Cell **101:** 199-210.

SCHLENSTEDT, G., S. HARRIS, B. RISSE, R. LILL and P. A. SILVER, 1995 A yeast DnaJ homologue, Scj1p, can function in the endoplasmic reticulum with BiP/Kar2p via a conserved domain that specifies interactions with Hsp70s. J Cell Biol **129:** 979-988.

SCHMITZ, H. P., J. JOCKEL, C. BLOCK and J. J. HEINISCH, 2001 Domain shuffling as a tool for investigation of protein function: substitution of the cysteine-rich region of Raf kinase and PKC eta for that of yeast Pkc1p. J Mol Biol **311:** 1-7.

SCHNEIDER, C., L. SEPP-LORENZINO, E. NIMMESGERN, O. OUERFELLI, S. DANISHEFSKY *et al.*, 1996 Pharmacologic shifting of a balance between protein refolding and degradation mediated by Hsp90. Proc Natl Acad Sci U S A **93:** 14536-14541.

SCHONFELD, H. J., D. SCHMIDT, H. SCHRODER and B. BUKAU, 1995 The DnaK chaperone system of Escherichia coli: quaternary structures and interactions of the DnaK and GrpE components. J Biol Chem **270:** 2183-2189.

SELKOE, D. J., 2003 Folding proteins in fatal ways. Nature **426:** 900-904.

SELKOE, D. J., 2004 Cell biology of protein misfolding: the examples of Alzheimer's and Parkinson's diseases. Nat Cell Biol **6:** 1054-1061.

SEO, J. S., Y. M. PARK, J. I. KIM, E. H. SHIM, C. W. KIM *et al.*, 1996 T cell lymphoma in transgenic mice expressing the human Hsp70 gene. Biochem Biophys Res Commun **218:** 582-587.

SETUBAL, J. C., L. M. MOREIRA and A. C. DA SILVA, 2005 Bacterial phytopathogens and genome science. Curr Opin Microbiol **8:** 595-600.

SHA, B., S. LEE and D. M. CYR, 2000 The crystal structure of the peptide-binding fragment from the yeast Hsp40 protein Sis1. Structure **8:** 799-807.

SHAHINIAN, S., and H. BUSSEY, 2000 beta-1,6-Glucan synthesis in Saccharomyces cerevisiae. Mol Microbiol **35:** 477-489.

SHANER, L., H. WEGELE, J. BUCHNER and K. A. MORANO, 2005 The yeast Hsp110 Sse1 functionally interacts with the Hsp70 chaperones Ssa and Ssb. J Biol Chem **280:** 41262-41269.

SHEN, S. H., P. CHRETIEN, L. BASTIEN and S. N. SLILATY, 1991 Primary sequence of the glucanase gene from Oerskovia xanthineolytica. Expression and purification of the enzyme from Escherichia coli. J Biol Chem **266:** 1058-1063.

SHOMURA, Y., Z. DRAGOVIC, H. C. CHANG, N. TZVETKOV, J. C. YOUNG *et al.*, 2005 Regulation of Hsp70 function by HspBP1: structural analysis reveals an alternate mechanism for Hsp70 nucleotide exchange. Mol Cell **17:** 367-379.

SIMMONS, D. T., R. UPSON, K. WUN-KIM and W. YOUNG, 1993 Biochemical analysis of mutants with changes in the origin-binding domain of simian virus 40 tumor antigen. J Virol **67:** 4227-4236.

SIMONS, J. F., M. EBERSOLD and A. HELENIUS, 1998 Cell wall 1,6-beta-glucan synthesis in Saccharomyces cerevisiae depends on ER glucosidases I and II, and the molecular chaperone BiP/Kar2p. Embo J **17:** 396-405.

SINGLETON, C. K., 1997 Identification and characterization of the thiamine transporter gene of Saccharomyces cerevisiae. Gene **199:** 111-121.

SLINSKEY, A., D. BARNES and J. M. PIPAS, 1999 Simian virus 40 large T antigen J domain and Rb-binding motif are sufficient to block apoptosis induced by growth factor withdrawal in a neural stem cell line. J Virol **73:** 6791-6799.

SMITH, D. F., B. A. STENSGARD, W. J. WELCH and D. O. TOFT, 1992 Assembly of progesterone receptor with heat shock proteins and receptor activation are ATP mediated events. J Biol Chem **267:** 1350-1356.

SMITH, R. C., K. M. ROSEN, R. POLA and J. MAGRANE, 2005 Stress proteins in Alzheimer's disease. Int J Hyperthermia **21:** 421-431.

SONDERMANN, H., A. K. HO, L. L. LISTENBERGER, K. SIEGERS, I. MOAREFI *et al.*, 2002 Prediction of novel Bag-1 homologs based on structure/function analysis identifies Snl1p as an Hsp70 co-chaperone in Saccharomyces cerevisiae. J Biol Chem **277:** 33220-33227.

SONDERMANN, H., C. SCHEUFLER, C. SCHNEIDER, J. HOHFELD, F. U. HARTL *et al.*, 2001 Structure of a Bag/Hsc70 complex: convergent functional evolution of Hsp70 nucleotide exchange factors. Science **291:** 1553-1557.

SPELLMAN, P. T., G. SHERLOCK, M. Q. ZHANG, V. R. IYER, K. ANDERS *et al.*, 1998 Comprehensive identification of cell cycle-regulated genes of the yeast Saccharomyces cerevisiae by microarray hybridization. Mol Biol Cell **9:** 3273-3297.

SPENCE, S. L., and J. M. PIPAS, 1994a Simian virus 40 large T antigen host range domain functions in virion assembly. J Virol **68:** 4227-4240.

SPENCE, S. L., and J. M. PIPAS, 1994b SV40 large T antigen functions at two distinct steps in virion assembly. Virology **204:** 200-209.

SRINIVASAN, A., A. J. MCCLELLAN, J. VARTIKAR, I. MARKS, P. CANTALUPO *et al.*, 1997 The amino-terminal transforming region of simian virus 40 large T and small t antigens functions as a J domain. Mol Cell Biol **17:** 4761-4773.

SRINIVASAN, A., K. W. PEDEN and J. M. PIPAS, 1989 The large tumor antigen of simian virus 40 encodes at least two distinct transforming functions. J Virol **63:** 5459-5463.

STEBBINS, C. E., A. A. RUSSO, C. SCHNEIDER, N. ROSEN, F. U. HARTL *et al.*, 1997 Crystal structure of an Hsp90-geldanamycin complex: targeting of a protein chaperone by an antitumor agent. Cell **89:** 239-250.

STIRLING, C. J., J. ROTHBLATT, M. HOSOBUCHI, R. DESHAIES and R. SCHEKMAN, 1992 Protein translocation mutants defective in the insertion of integral membrane proteins into the endoplasmic reticulum. Mol Biol Cell **3:** 129-142.

STONE, D. E., and E. A. CRAIG, 1990 Self-regulation of 70-kilodalton heat shock proteins in Saccharomyces cerevisiae. Mol Cell Biol **10:** 1622-1632.

STUBDAL, H., J. ZALVIDE, K. S. CAMPBELL, C. SCHWEITZER, T. M. ROBERTS *et al.*, 1997 Inactivation of pRB-related proteins p130 and p107 mediated by the J domain of simian virus 40 large T antigen. Mol Cell Biol **17:** 4979-4990.

STUBDAL, H., J. ZALVIDE and J. A. DECAPRIO, 1996 Simian virus 40 large T antigen alters the phosphorylation state of the RB-related proteins p130 and p107. J Virol **70:** 2781-2788.

SUH, W. C., W. F. BURKHOLDER, C. Z. LU, X. ZHAO, M. E. GOTTESMAN *et al.*, 1998 Interaction of the Hsp70 molecular chaperone, DnaK, with its cochaperone DnaJ. Proc Natl Acad Sci U S A **95:** 15223-15228.

SUH, W. C., C. Z. LU and C. A. GROSS, 1999 Structural features required for the interaction of the Hsp70 molecular chaperone DnaK with its cochaperone DnaJ. J Biol Chem **274:** 30534-30539.

SULLIVAN, C. S., A. E. BAKER and J. M. PIPAS, 2004 Simian virus 40 infection disrupts p130-E2F and p107-E2F complexes but does not perturb pRb-E2F complexes. Virology **320:** 218-228.

SULLIVAN, C. S., P. CANTALUPO and J. M. PIPAS, 2000a The molecular chaperone activity of simian virus 40 large T antigen is required to disrupt Rb-E2F family complexes by an ATP-dependent mechanism. Mol Cell Biol **20:** 6233-6243.

SULLIVAN, C. S., S. P. GILBERT and J. M. PIPAS, 2001 ATP-dependent simian virus 40 T-antigen-Hsc70 complex formation. J Virol **75:** 1601-1610.

SULLIVAN, C. S., and J. M. PIPAS, 2001 The virus-chaperone connection. Virology **287:** 1-8.

SULLIVAN, C. S., and J. M. PIPAS, 2002 T antigens of simian virus 40: molecular chaperones for viral replication and tumorigenesis. Microbiol Mol Biol Rev **66:** 179-202.

SULLIVAN, C. S., J. D. TREMBLAY, S. W. FEWELL, J. A. LEWIS, J. L. BRODSKY *et al.*, 2000b Species-specific elements in the large T-antigen J domain are required for cellular transformation and DNA replication by simian virus 40. Mol Cell Biol **20:** 5749-5757.

SZABO, A., R. KORSZUN, F. U. HARTL and J. FLANAGAN, 1996 A zinc finger-like domain of the molecular chaperone DnaJ is involved in binding to denatured protein substrates. Embo J **15:** 408-417.

SZABO, A., T. LANGER, H. SCHRODER, J. FLANAGAN, B. BUKAU *et al.*, 1994 The ATP hydrolysis-dependent reaction cycle of the Escherichia coli Hsp70 system DnaK, DnaJ, and GrpE. Proc Natl Acad Sci U S A **91:** 10345-10349.

TAKAYAMA, S., D. N. BIMSTON, S. MATSUZAWA, B. C. FREEMAN, C. AIME-SEMPE *et al.*, 1997 BAG-1 modulates the chaperone activity of Hsp70/Hsc70. Embo J **16:** 4887-4896.

TAKAYAMA, S., T. SATO, S. KRAJEWSKI, K. KOCHEL, S. IRIE *et al.*, 1995 Cloning and functional analysis of BAG-1: a novel Bcl-2-binding protein with anti-cell death activity. Cell **80:** 279-284.

TANABE, K., T. TOKUMOTO, N. ISHIKAWA, T. SHIMIZU, H. OKUDA *et al.*, 2000 Effect of Deoxyspergualin on the long-term outcome of renal transplantation. Transplant Proc **32:** 1745-1746.

TANG, X., Y. XIAO and J. M. ZHOU, 2006 Regulation of the type III secretion system in phytopathogenic bacteria. Mol Plant Microbe Interact **19:** 1159-1166.

TAYLOR, K., and G. WEGRZYN, 1995 Replication of coliphage lambda DNA. FEMS Microbiol Rev **17:** 109-119.

TEDESCO, D., J. LUKAS and S. I. REED, 2002 The pRb-related protein p130 is regulated by phosphorylation-dependent proteolysis via the protein-ubiquitin ligase SCF(Skp2). Genes Dev **16:** 2946-2957.

TERASAWA, K., M. MINAMI and Y. MINAMI, 2005 Constantly updated knowledge of Hsp90. J Biochem (Tokyo) **137:** 443-447.
THEYSSEN, H., H. P. SCHUSTER, L. PACKSCHIES, B. BUKAU and J. REINSTEIN, 1996 The second step of ATP binding to DnaK induces peptide release. J Mol Biol **263:** 657-670.
TREMBLAY, J. D., K. F. SACHSENMEIER and J. M. PIPAS, 2001 Propagation of wild-type and mutant SV40. Methods Mol Biol **165:** 1-7.
TSAI, J., and M. G. DOUGLAS, 1996 A conserved HPD sequence of the J-domain is necessary for YDJ1 stimulation of Hsp70 ATPase activity at a site distinct from substrate binding. J Biol Chem **271:** 9347-9354.
TSAI, S. C., K. B. PASUMARTHI, L. PAJAK, M. FRANKLIN, B. PATTON *et al.*, 2000 Simian virus 40 large T antigen binds a novel Bcl-2 homology domain 3-containing proapoptosis protein in the cytoplasm. J Biol Chem **275:** 3239-3246.
UNGEWICKELL, E., H. UNGEWICKELL, S. E. HOLSTEIN, R. LINDNER, K. PRASAD *et al.*, 1995 Role of auxilin in uncoating clathrin-coated vesicles. Nature **378:** 632-635.
VALDIVIA, R. H., and R. SCHEKMAN, 2003 The yeasts Rho1p and Pkc1p regulate the transport of chitin synthase III (Chs3p) from internal stores to the plasma membrane. Proc Natl Acad Sci U S A **100:** 10287-10292.
VALENTINE, M. T., and S. P. GILBERT, 2007 To step or not to step? How biochemistry and mechanics influence processivity in Kinesin and Eg5. Curr Opin Cell Biol **19:** 75-81.
VOGEL, J. P., L. M. MISRA and M. D. ROSE, 1990 Loss of BiP/GRP78 function blocks translocation of secretory proteins in yeast. J Cell Biol **110:** 1885-1895.
VOGEL, M., B. BUKAU and M. P. MAYER, 2006 Allosteric regulation of Hsp70 chaperones by a proline switch. Mol Cell **21:** 359-367.
VOLLOCH, V. Z., and M. Y. SHERMAN, 1999 Oncogenic potential of Hsp72. Oncogene **18:** 3648-3651.
VOLM, M., J. MATTERN and G. STAMMLER, 1995 Up-regulation of heat shock protein 70 in adenocarcinomas of the lung in smokers. Anticancer Res **15:** 2607-2609.
WALL, D., M. ZYLICZ and C. GEORGOPOULOS, 1994 The NH2-terminal 108 amino acids of the Escherichia coli DnaJ protein stimulate the ATPase activity of DnaK and are sufficient for lambda replication. J Biol Chem **269:** 5446-5451.
WALSH, P., D. BURSAC, Y. C. LAW, D. CYR and T. LITHGOW, 2004 The J-protein family: modulating protein assembly, disassembly and translocation. EMBO Rep **5:** 567-571.
WANG, T. F., J. H. CHANG and C. WANG, 1993 Identification of the peptide binding domain of hsc70. 18-Kilodalton fragment located immediately after ATPase domain is sufficient for high affinity binding. J Biol Chem **268:** 26049-26051.
WATANABE, Y., K. IRIE and K. MATSUMOTO, 1995 Yeast RLM1 encodes a serum response factor-like protein that may function downstream of the Mpk1 (Slt2) mitogen-activated protein kinase pathway. Mol Cell Biol **15:** 5740-5749.
WEGELE, H., M. HASLBECK, J. REINSTEIN and J. BUCHNER, 2003 Sti1 is a novel activator of the Ssa proteins. J Biol Chem **278:** 25970-25976.
WEGELE, H., S. K. WANDINGER, A. B. SCHMID, J. REINSTEIN and J. BUCHNER, 2006 Substrate transfer from the chaperone Hsp70 to Hsp90. J Mol Biol **356:** 802-811.
WEIBEZAHN, J., C. SCHLIEKER, P. TESSARZ, A. MOGK and B. BUKAU, 2005 Novel insights into the mechanism of chaperone-assisted protein disaggregation. Biol Chem **386:** 739-744.
WEISSHART, K., M. K. BRADLEY, B. M. WEINER, C. SCHNEIDER, I. MOAREFI *et al.*, 1996 An N-terminal deletion mutant of simian virus 40 (SV40) large T antigen oligomerizes

incorrectly on SV40 DNA but retains the ability to bind to DNA polymerase alpha and replicate SV40 DNA in vitro. J Virol **70:** 3509-3516.

WERNER, S., D. M. TURNER, M. A. LYON, D. M. HURYN and P. WIPF, 2006 A Focused Library of Tetrahydropyrimidinone Amides via a Tandem Biginelli-Ugi Multi-Component Process. SYNLETT **14:** 2334-2338.

WHITE, M. K., and K. KHALILI, 2004 Polyomaviruses and human cancer: molecular mechanisms underlying patterns of tumorigenesis. Virology **324:** 1-16.

WICKNER, S., J. HOSKINS and K. MCKENNEY, 1991 Function of DnaJ and DnaK as chaperones in origin-specific DNA binding by RepA. Nature **350:** 165-167.

WILLIAMS, F. E., and R. J. TRUMBLY, 1990 Characterization of TUP1, a mediator of glucose repression in Saccharomyces cerevisiae. Mol Cell Biol **10:** 6500-6511.

WINKLER, A., C. ARKIND, C. P. MATTISON, A. BURKHOLDER, K. KNOCHE *et al.*, 2002 Heat stress activates the yeast high-osmolarity glycerol mitogen-activated protein kinase pathway, and protein tyrosine phosphatases are essential under heat stress. Eukaryot Cell **1:** 163-173.

WRIGHT, C. M., S. W. FEWELL, M. L. SULLIVAN, J. M. PIPAS, S. C. WATKINS *et al.*, 2007 The Hsp40 Molecular Chaperone, Ydj1p, Along With the Protein Kinase C Pathway, Impact Cell Wall Integrity in the Yeast Saccharomyces cerevisiae. Genetics.

XIAO, J., L. S. KIM and T. R. GRAHAM, 2006 Dissection of Swa2p/auxilin domain requirements for cochaperoning Hsp70 clathrin-uncoating activity in vivo. Mol Biol Cell **17:** 3281-3290.

YAAKOV, G., M. BELL, S. HOHMANN and D. ENGELBERG, 2003 Combination of two activating mutations in one HOG1 gene forms hyperactive enzymes that induce growth arrest. Mol Cell Biol **23:** 4826-4840.

YAM, A. Y., V. ALBANESE, H. T. LIN and J. FRYDMAN, 2005 Hsp110 cooperates with different cytosolic HSP70 systems in a pathway for de novo folding. J Biol Chem **280:** 41252-41261.

YANG, X. X., K. C. MAURER, M. MOLANUS, W. H. MAGER, M. SIDERIUS *et al.*, 2006 The molecular chaperone Hsp90 is required for high osmotic stress response in Saccharomyces cerevisiae. FEMS Yeast Res **6:** 195-204.

YANO, M., Z. NAITO, S. TANAKA and G. ASANO, 1996 Expression and roles of heat shock proteins in human breast cancer. Jpn J Cancer Res **87:** 908-915.

YASHAR, B., K. IRIE, J. A. PRINTEN, B. J. STEVENSON, G. F. SPRAGUE, JR. *et al.*, 1995 Yeast MEK-dependent signal transduction: response thresholds and parameters affecting fidelity. Mol Cell Biol **15:** 6545-6553.

YOUKER, R. T., P. WALSH, T. BEILHARZ, T. LITHGOW and J. L. BRODSKY, 2004 Distinct roles for the Hsp40 and Hsp90 molecular chaperones during cystic fibrosis transmembrane conductance regulator degradation in yeast. Mol Biol Cell **15:** 4787-4797.

YUZHAKOV, A., Z. KELMAN, J. HURWITZ and M. O'DONNELL, 1999 Multiple competition reactions for RPA order the assembly of the DNA polymerase delta holoenzyme. Embo J **18:** 6189-6199.

ZHANG, Y., G. NIJBROEK, M. L. SULLIVAN, A. A. MCCRACKEN, S. C. WATKINS *et al.*, 2001 Hsp70 molecular chaperone facilitates endoplasmic reticulum-associated protein degradation of cystic fibrosis transmembrane conductance regulator in yeast. Mol Biol Cell **12:** 1303-1314.

ZHANG, Y., and E. R. ZUIDERWEG, 2004 The 70-kDa heat shock protein chaperone nucleotide-binding domain in solution unveiled as a molecular machine that can reorient its functional subdomains. Proc Natl Acad Sci U S A **101:** 10272-10277.

ZHAO, C., U. S. JUNG, P. GARRETT-ENGELE, T. ROE, M. S. CYERT *et al.*, 1998 Temperature-induced expression of yeast FKS2 is under the dual control of protein kinase C and calcineurin. Mol Cell Biol **18:** 1013-1022.

ZHAO, R., and W. A. HOURY, 2005 Hsp90: a chaperone for protein folding and gene regulation. Biochem Cell Biol **83:** 703-710.

ZHOU, Z., A. GARTNER, R. CADE, G. AMMERER and B. ERREDE, 1993 Pheromone-induced signal transduction in Saccharomyces cerevisiae requires the sequential function of three protein kinases. Mol Cell Biol **13:** 2069-2080.

ZHU, X., X. ZHAO, W. F. BURKHOLDER, A. GRAGEROV, C. M. OGATA *et al.*, 1996 Structural analysis of substrate binding by the molecular chaperone DnaK. Science **272:** 1606-1614.

ZYLICZ, M., D. ANG and C. GEORGOPOULOS, 1987 The grpE protein of Escherichia coli. Purification and properties. J Biol Chem **262:** 17437-17442.